

STRUCTURE OF ACID CASEIN GELS

A study of gels formed after acidification in the cold

CENTRALE LANDBOUWCATALOGUS



0000 0146 3088

Promotor: dr. A. Prins,  
hoogleraar in de fysica en de fysische chemie van  
levensmiddelen, met bijzondere aandacht voor de  
zuivel

Co-promotor: dr.ir. T. van Vliet,  
wetenschappelijk hoofdmedewerker

NN08201, 1076

Sebastianus P.F.M. Roefs

STRUCTURE OF ACID CASEIN GELS

A study of gels formed after acidification in the cold

Proefschrift

ter verkrijging van de graad van  
doctor in de landbouwwetenschappen,  
op gezag van de rector magnificus,  
dr. C.C. Oosterlee,  
in het openbaar te verdedigen  
op vrijdag 11 april 1986  
des namiddags te vier uur in de aula  
van de Landbouwhogeschool te Wageningen

ISW = 244947

BIBLIOTHEEK  
DER  
LANDBOUWVERSCHOLE  
WAGENINGEN

## STELLINGEN

1. Hoewel caseïne's macromoleculen zijn, gedraagt een zuur caseïne-gel zich fenomenologisch als een deeltjesgel.  
Dit proefschrift.
2. Rond pH=5,2 verandert het karakter van melkeiwitgelen aanzienlijk.  
Dit proefschrift.
3. Bij het onderzoek naar de microstructuur en de stevigheid van standyoghurt en op standyoghurt gelijkende systemen wordt te weinig aandacht geschonken aan fundamentele parameters als caseïneconcentratie, ionsterkte, ionsamenstelling en verouderingstijd.  
Tamime, A.Y., Kalab, M. and Davies, G. (1984). "Microstructure of set-style yoghurt manufactured from cow's milk fortified by various methods". Foodmicrostructure 3, 83-92.  
Harwalkar, V.R. and Kalab, M. (1981). "Effect of acidulants and temperature on microstructure, firmness and susceptibility to syneresis of skim-milk gels". Scanning Electron Microscopy, 1981; III, 503-513.
4. Bohlin et al. hebben ten onrechte geen rekening gehouden met de invloed van de pH op de grootte van de dynamische moduli van met stremsel bereide ondermelkgelen.  
Bohlin, L., Hegg, P.-O. and Ljusberg-Wahren, H. (1984). "Viscoelastic properties of coagulating milk". J. Dairy Sci. 67, 729-734.
5. Bij de interpretatie van het verloop van de drukval bij stroming door poreuze media gebruikt Ghoniem een kengetal, waarin hij de verblijftijd van het polymeer onjuist in rekening brengt.  
Ghoniem, S.A.-A. (1985). "Extensional flow of polymer solutions through porous media". Rheol. Acta 24, 588-595.

RECEIVED  
 1985  
 LANDBOUNIVERSITEIT  
 WAGENINGEN

6. De eigenschappen van bierschuim, zoals stabiliteit en hechtvermogen aan de glaswand, kunnen pas fysisch geïnterpreteerd worden als de relevante reologische oppervlakte-eigenschappen bekend zijn.  
Bamforth, C.W. (1985). "The foaming properties of beer". J. Inst. Brew. 91, 370-383.
7. Het nadenken over de betekenis van een zwichtspanning zonder dat de bijbehorende tijdschaal bekend is, is verloren tijd.
8. Veel levensmiddelen breken in rek als men erop drukt.
9. Het verschil tussen een goede en een slechte advocaat is af te lezen aan het gedrag onder geringe stress.
10. De langste polymeermoleculen trekken aan het kortste eindje.
11. Voor een verantwoord gebruik van medicijnen in de intensieve veehouderij is het van belang dat de honorering van de veeartsen wordt losgekoppeld van de verkoop van medicijnen.
12. Liever een goed dialect dan slecht Nederlands.

Sebastianus P.F.M. Roefs

STRUCTURE OF ACID CASEIN GELS

A study of gels formed after acidification in the cold  
Wageningen, 11 april 1986.

*Voor mijn ouders*

## ABSTRACT

Roefs, Sebastianus, P.F.M. (1985). "Structure of acid casein gels; a study of gels formed after acidification in the cold". Ph.D. Thesis, Laboratory of Dairying and Food Physics, Agricultural University, Wageningen. 209 + 9 pages, 68 figures, 11 tables. English and Dutch summaries.

The structure of acid casein gels was studied by rheology, permeametry, electron microscopy and pulse NMR. Gels were mainly formed by heating at rest of casein solutions acidified in the cold (0-2 °C). The structure of such gels involves both the spatial distribution of the structural elements and the interaction forces between them. An acid casein gel has an irregular particulate structure. Gelation results from the aggregation of casein particles, which themselves have a complex internal structure due to the association of numerous different casein molecules. Dense areas of coagulated particles are separated by large pores. Gelation at pH=4.6 appears to be subject to an activation Helmholtz energy, which is largely due to the stabilizing effect of the glycomacropeptide part of  $\kappa$ -casein. At ageing temperatures above 283 K, the dynamic moduli  $G'$  and  $G''$  linearly increase with the logarithm of time. Their absolute values primarily depend on the heterogeneity of the network. The moduli decrease with increasing time scale of measurement. From the effect of variation of experimental conditions (pH, ageing and measuring temperatures, ionic strength and ionic composition) it may be concluded that electrostatic interactions and hydrophobic bonding are involved in keeping the network together. Moreover, Van der Waals attraction, steric interactions and possibly hydrogen bonds may play a part. Differences in the internal structure of the casein particles appear to be paramount in determining differences in the number and character of the interparticle bonds; this was in agreement with results on the spin-spin relaxation time of water protons. Addition of rennet enables gel formation in a much broader range of temperature and pH; the character of the gels changes considerably around pH=5.2.

## CONTENTS

	Page
1 INTRODUCTION	1
1.1 Acid casein gels	1
1.2 Casein	3
1.3 Outline of this study	7
2 MATERIALS AND METHODS	9
2.1 Skimmilk powder	9
2.2 Sodium caseinate solutions	9
2.3 Acidification and gelation	11
2.4 Whey	13
2.5 Varying protein concentration by ultra filtration	13
2.6 Gel electrophoresis	13
2.7 Estimation of splitting of $\kappa$ -casein	14
2.8 Permeability measurements	14
2.8.1 General	14
2.8.2 The tube method	15
2.9 Pulse NMR measurements	17
2.10 Rheological measurements	18
2.10.1 Dynamic measurements	19
2.10.2 Measurement of acid casein gels	21
2.10.3 Stress relaxation measurements	22
2.10.4 Creep measurements	23
2.11 Electron microscopy	24
2.12 Solubility of casein	25
2.13 Particle size measurement	27
3 FORMATION OF ACID CASEIN GELS	29
3.1 Introduction	29
3.2 Formation and ageing of acid casein gels	30
3.2.1 Ageing of acid skimmilk gels	30
3.2.2 Irreversible character of gel formation	33
3.2.3 Skimmilk gels made by rapid heating	34
3.2.4 Different kinds of acid casein gels	35
3.3 Changes during cold acidification of casein	37
3.3.1 Introduction	37

3.3.2	Cold acidification of skimmilk	39
3.3.2.1	Solubility of casein at low temperature	40
3.3.2.2	Casein particle size	41
3.3.2.3	Electron micrographs of skimmilk	44
3.3.3	Cold acidification of sodium caseinate solution	46
3.3.4	Discussion	48
3.4	Network model for acid casein gels	50
3.4.1	General description of possible models	50
3.4.2	Experimental results	54
3.4.2.1	Storage modulus as a function of casein concentration	54
3.4.2.2	Electron micrographs of acid casein gels	57
3.4.2.3	Permeability of acid casein gels	60
3.4.3	Discussion	64
3.4.3.1	Schematic representation of an acid casein gel	65
3.4.3.2	Comparison of the measured permeability with that of some geometric models	67
4	RHEOLOGICAL CHARACTERIZATION OF ACID CASEIN GELS	72
4.1	Introduction	72
4.2	Rheological measurements	73
4.3	Interpretation of rheological data	76
4.3.1	Relaxation spectrum	79
4.4	Interaction forces in acid casein gels	80
4.4.1	Hydrophobic bonding	81
4.4.2	Van der Waals attraction	81
4.4.3	Electrostatic interactions	82
4.4.4	Hydrogen bonds	83
4.4.5	Steric interactions	84
4.5	Experimental results	84
4.5.1	Introduction	84
4.5.2	The dynamic moduli as a function of temperature	86

4.5.3	Variation with measuring temperature	88
4.5.4	Dynamic moduli of acid skimmilk gels as a function of pH	97
4.5.5	Variation with ionic composition	100
4.5.5.1	Rough estimate of ionic strength of acid skimmilk	100
4.5.5.2	The effect of added NaCl on acid skimmilk gels	103
4.5.5.3	The effect of NaCl and CaCl <sub>2</sub> on acid sodium caseinate gels	107
4.5.6	Relaxation spectra of acid skimmilk gels	111
4.5.6.1	Computation of the relaxation spectrum and of a semi-permanent network modulus	113
4.5.6.2	The value of a pseudo-stress relaxation modulus at long time scales	115
4.5.7	Creep measurements	118
4.6	Estimation of the modulus of a strand of particles	120
4.7	Discussion	123
5	THE STRUCTURE OF CASEIN GELS MADE BY ACIDIFICATION AND RENNET ACTION	128
5.1	Introduction	128
5.2	Proteolytic action	130
5.3	Results and discussion	132
5.3.1	The effect of rennet at pH=4.6	133
5.3.2	The effect of rennet at varying pH	143
5.3.2.1	Gel formation at different pH values	147
5.3.2.2	Influence of the time scale of the dynamic measurement	149
5.3.2.3	Effect of variation of measuring temperature	151
5.3.2.4	Proteolytic degradation	157
5.4	General discussion	160

6	PULSE NMR STUDY OF CASEIN SOLUTIONS	162
6.1	Introduction	162
6.2	Principles of pulse NMR	163
6.3	The effect of mobility of the nucleus on $T_2$	168
6.4	Experimental results	170
6.4.1	$T_2$ of skimmilk	171
6.4.2	$T_2$ of sodium caseinate	174
6.5	Discussion	176
7	CONCLUDING REMARKS	185
	Literature references	191
	List of symbols	197
	Summary	200
	Samenvatting	203
	Curriculum vitae	207
	Nawoord	208

## 1 INTRODUCTION

### 1.1 Acid casein gels

Milk is one of the most important foods in many countries all over the world. Besides being drunk in the liquid form, as secreted by the mammal, the nutritious substances of milk may be consumed in a series of derived milk products. Most of these products, now manufactured in highly equipped modern factories, are still prepared by empirical processes developed over tens of centuries from traditional methods already applied by ancient tribes. Examples are different types of cheese and a large variety of sour milk products such as yoghurts and quarg. All of these products were developed in olden times as a means of preserving the easy perishable fresh milk. Note that in this thesis the word milk is used for the mammary secretion of healthy cows excluding colostrum.

Milk is a complex fluid containing many components in several states of dispersion (e.g. Walstra and Jenness, 1984). Protein is a main constituent of many milk products, not only because of its nutritional value, but also because of its contribution to the physical structure of these milk products, this structure determining to a considerable extent the taste perception of the consumer. The two most important groups of milk proteins are the caseins (about 80% of total milk protein) and the whey or serum proteins.

Under the conditions of milk serum proteins are soluble, mainly separate molecules, whereas the caseins form aggregates of colloidal size (diameter may vary from 20 to 300 nm), the so called casein micelles, which may contain up to thousands of casein molecules (Walstra and Jenness, 1984). These casein micelles are the source of the colloidal blue white appearance of skimmilk. They are stabilized under normal conditions in milk (pH=6.7) by steric repulsion and a negative charge (Schmidt, 1982a, Payens, 1979, Walstra, 1979). Upon acidification the structure and composition of the casein micelles markedly alters; therefore the term casein micelles will be used here only for the casein aggregates in milk

or skimmilk under natural conditions. In all other cases we prefer to employ the term casein particles.

Due to rennet action (manufacture of cheese), acidification (manufacture of yoghurt) or a combination of both (manufacture of quarg) the casein particles become unstable and may coagulate to form a gel in an unstirred solution with casein as the main component of the gel network. Products like cheese, yoghurt, and quarg essentially are casein gels. However in spite of the economic importance the structure of casein gels has not been studied extensively. Only the spatial distribution of the basic elements of the casein gel network has been studied to any detailed extent by electron microscopy (e.g. Harwalkar and Kalab, 1981, Knoop and Peters, 1975, Glaser et al., 1980, and Kalab, 1981). With respect to the manufacture of cheese further attention has been paid to the structure and syneresis behaviour of rennet gels (e.g. Van Dijk, 1982, Walstra et al., 1985, Van Dijk et al., 1986) made at natural pH of milk. This relatively scanty knowledge of the structure of casein gels is somewhat surprising, because the method of manufacture and the ultimate taste perception of products like yoghurt, quarg and cheese depends not only on the chemical composition, but especially on the physical behaviour of the casein gels formed in the course of manufacture.

The aim of this work is to take a first step in a more thorough and fundamental characterization of the physical structure of milk gels made by acidification. Because casein is the main component determining the physical structure of this type of gels (Roefs and Van Vliet, 1984), we will denote them by the term acid casein gels. To characterize the structure of a gel we must consider two main features; namely the spatial distribution of the basic elements and the nature and the strength of the interaction forces between the basic elements. Due account must also be taken of the fact that the basic elements themselves have a certain physical structure, which can change with the environmental conditions. So in fact basic elements and interaction forces between them can be distinguished at different levels.

The spatial distribution of the basic elements of a gel network can be readily studied by means of a combination of permeability

measurements, electron microscopy and concentration dependent rheological measurements. The rheological properties and the effect of experimental conditions such as ionic strength, temperature, pH etc. on them provide information about the structure of and the interactions between the basic elements. The state of water (mobilized or immobilized) in a gel network, which depends on the structure and aggregation of the basic elements, may also be studied by pulse NMR.

## 1.2 Casein

As casein is the main component involved in the structure of gels made from milk by acidification (Roefs and Van Vliet, 1984), special attention will be paid to it in this section. The term casein includes a whole family of different casein molecules, whose common characteristic is that they are insoluble at pH=4.6. Under the natural conditions of milk they are aggregated in large spherical particles, the casein micelles. Casein micelles consist of water, casein, salts (mainly calcium and phosphate) and some minor components (Walstra and Jenness, 1984).

Four main groups of caseins may be distinguished:  $\alpha_{s1}$ -casein,  $\alpha_{s2}$ -casein,  $\beta$ -casein and  $\kappa$ -casein. Within each group small, but distinct variations may occur due either to small differences in amino acid sequence (very often constrained to a variation of only one amino acid) as a consequence of genetic variability or to differences in molecular residues attached to amino acid side groups (as e.g. a variable number of carbohydrate residues attached to  $\kappa$ -casein). Besides these four major caseins, some 2% of total casein exists as smaller minor caseins. These mostly result from the proteolytic breakdown of a major casein (e.g.  $\gamma$ -casein is a breakdown product of  $\beta$ -casein). In table 1.1 some data are given for one genetic variant of each group of caseins, except for the data in the last two lines, which apply generally to each group. The casein composition of milk varies with season, with lactation period, from cow to cow and even with the time of the day (Walstra and Jenness, 1984). However the overall casein composition of bulk milk, produced by a large number of cows is fairly constant.

None of the four groups of casein has a highly organized secondary structure. Their conformation appears to be much like that of denatured globular proteins, which is partly due to the rather high proline content. Caseins contain many hydrophobic amino acid residues (see table 1.1). In general, these residues are not distributed randomly along the peptide chain e.g.  $\alpha_{s1}$ -casein contains three predominantly hydrophobic regions (residues 1-44, 90-113, and 132-199, after Fox and Mulvihill, 1983), whereas  $\beta$ -casein has a soaplike character because of a hydrophilic N-terminal part and a hydrophobic C-terminal part. A significant feature of caseins is the number of ester bound phosphate residues, which varies considerably among the different caseins (see table 1.1).  $\alpha_{s2}$ -caseins contain 10 to 13 ester phosphate residues, whereas these figures are 8 or 9 for  $\alpha_{s1}$ -casein, 5 for  $\beta$ -casein and 1 or 2 for  $\kappa$ -casein. Since the ester phosphate groups of casein strongly bind divalent ions (presumably  $\text{Ca}^{2+}$ , which is the most abundant divalent ion in milk), especially at high pH, the number of ester phosphate groups determines the stability of the different caseins against  $\text{Ca}^{2+}$  induced precipitation. Thus  $\alpha_{s2}$ - and  $\alpha_{s1}$ -casein, but also  $\beta$ -casein aggregate and precipitate at very low  $\text{Ca}^{2+}$  concentration (table 1.1).  $\kappa$ -casein, however, is soluble over a wide range of  $\text{Ca}^{2+}$  concentrations.  $\kappa$ -casein is further characterized as the only casein carrying carbohydrate residues, linked to the threonine residues at position 131, 133, 135 and possibly 136 (Swaisgood, 1982). The carbohydrate content may vary from molecule to molecule.

All of the caseins tend to self-associate in solution in the absence of  $\text{Ca}^{2+}$ , to give a kind of "polymers" or soaplike micelles of fixed size ( $\kappa$ -casein, Payens and Vreeman, 1982) or of steadily increasing size ( $\alpha_{s1}$ -,  $\alpha_{s2}$ - and  $\beta$ -casein) as concentration is increased. The association behaviour of  $\beta$ -casein, however, is completely different from that of  $\alpha_{s1}$ - and  $\alpha_{s2}$ -casein, particularly in its temperature dependence.  $\alpha_{s1}$ - and  $\alpha_{s2}$ -casein associate in a series of consecutive steps, whereas  $\beta$ -casein associates more truly like soap molecules to form micellar aggregates. In the first step of  $\kappa$ -casein polymerization -S-S- linkages are involved. The final  $\kappa$ -casein "polymers" have a similar size as the  $\beta$ -casein "polymers" (Schmidt, 1982a). The degree of self association depends besides on concentration also on pH, temperature, ionic

Table 1.1 Properties of the main caseins<sup>a</sup>

	$\alpha_{s1}$ -casein B	$\alpha_{s2}$ -casein A	$\beta$ -casein A <sub>2</sub>	$\kappa$ -casein B
molecular weight	23,614	25,230	23,983	19,023 <sup>b</sup>
residues per molecule:				
amino acids	199	207	209	169
proline	17	10	35	20
ester phosphate	8	11	5	1
carbohydrate	-	-	-	+
hydrophobicity	4.9	4.7	5.6	5.1
% of total casein <sup>c</sup>	38	11	36	13
lowest Ca <sup>2+</sup> concentration of precipitation in mmol <sup>c</sup>	2	1	9	400

a. after various sources (Walstra and Jenness, 1984, Swaisgood, 1982, Schmidt, 1982a, Payens and Vreeman, 1982).

b. exclusive of carbohydrate residues

c. these are general figures, which refer to the whole group of caseins instead of the individual genetic variants.

strength and kind of ions in the medium (Payens and Vreeman, 1982, Schmidt, 1982a). In mixtures of two or more different caseins "polymers" (in fact aggregates) consisting of all available caseins will be formed. These aggregates generally are more stable than associations of any single casein. This is especially true for  $\kappa$ -casein, which will prevent precipitation of  $\alpha_{s1}$ - or  $\beta$ -casein aggregates by Ca<sup>2+</sup>, stabilizing up to ten times its own weight of  $\alpha_{s1}$ - or  $\beta$ -casein against precipitation (Walstra and Jenness, 1984).

Most of the casein appears in milk integrated into the casein micelles at or prior to secretion by the mammary glands of the cow. A great deal of work has been done on the structure of casein micelles. As we are only interested in the relative changes of ca-

sein micelle structure in the course of acidification, it is beyond the scope of this study to treat the structure and, particularly, stability of casein micelles in detail. In point of fact no conclusive model for the structure of casein micelles has yet been proposed. Schmidt (1982a) has discussed what is known of its structure extensively and has briefly reflected on several suggested models.

The diameter of casein micelles under natural conditions of milk (pH=6.7 and I~0.08 M) varies from 20 to 300 nm. They are comprised of some 40 to 150,000 casein molecules in a fairly constant distribution of the different kinds of casein. Casein micelles contain some 8 g of inorganic matter per 100 g casein, mainly calcium phosphate and some Mg, Na, K and citrate, together forming the so called colloidal calcium phosphate, which is indispensable for the micellar structure. The colloidal calcium phosphate is amorphous and occurs in small regions, dispersed throughout the entire micelle. Under natural conditions casein micelles are stable against coagulation. Stability is ascribed to electrostatic and steric effects. At pH=6.7 casein micelles contain a small, but significant negative charge i.e. the zeta potential is around -15 to -20 mV at 30 °C (Dalglish, 1984). Payens (1979) has argued that this value is too low to stabilize casein micelles in milk solely by electrostatic effects. Most of the  $\kappa$ -casein, having a very hydrophilic C-terminal part, is thought to be located at the outside of the casein micelles. These and other hydrophilic protein chains are thought to protrude from the casein micelle surface into solution, thus stabilizing the casein micelles by steric repulsion (Walstra, 1979).

Upon acidification all casein will coagulate at pH=4.6, being the isoelectric pH of the casein particles in milk. because of a loss of charge it is thought that the electrostatic and possibly the steric repulsion will decrease as pH decreases. The isoionic pH of individual isolated caseins may differ slightly from pH=4.6 (Swaisgood, 1982).

### 1.3 Outline of this study

To simplify the system, acid casein gels were made generally from skimmilk, but sometimes from a solution of sodium caseinate. Milk fat was omitted, because changes in its content or in the composition of the milk fat globule membrane may affect the structure of acid casein gels considerably (Van Vliet and Dentener-Kikkert, 1983). To reduce experimental error due to variation in composition, skimmilk was reconstituted from the same batch of low heat skimmilk powder. Sodium caseinate solutions, too, were always made from the same powder. Sodium caseinate powder merely contains purified caseins. HCl was used for acidification instead of bacterial enzymes, which are difficult to handle with respect to pH control. As gel formation only can occur in solution at rest, acidification by means of HCl was carried out at low temperature (0-4 °C), where a casein solution even at pH=4.6 (the isoelectrical pH) does not coagulate. After transferring the acidified solution to the measuring apparatus, gel formation was induced by heating at rest. In some experiments casein gels were formed by acidification at 30 °C using Glucono-Delta-Lactone (GDL), a slowly hydrolyzing acid precursor. This was done to simulate more closely acidification by bacteria.

The composition of the skimmilk and sodium caseinate powders is reported in chapter II. All experimental procedures and apparatus are described there, too.

In chapter III the effect of acidification on casein, especially at low temperature, is described first. Particle size and casein solubility in skimmilk were studied as a function of pH. In addition electron micrographs were made of skimmilk and sodium caseinate solutions at different pH's. Next the formation and ageing of different kinds of acid casein gels at different temperatures were studied by means of rheological measurements. The dynamic moduli  $G'$  and  $G''$  were determined. In the last part of this chapter a model is presented for the spatial distribution of the basic elements of an acid casein gel. This model is primarily based on the results of the concentration dependent rheological and permeability measurements, as well as on electron micrographs of acid casein gels.

Chapter IV deals with the rheological characterization of acid casein gels. The dynamic moduli were measured over a frequency range of three to four decades as a function of ionic composition, pH and measuring temperature at different ageing temperatures. Special attention was given to the 'permanent' network character of acid casein gels. The contribution of the different types of interaction forces, involved in acid casein gels, is discussed.

The structure of casein gels, made by acidification and rennet action in the pH range of 4.4 to 5.8, is the subject of chapter V. The rheological properties at constant ageing temperature (20 °C) were measured over the whole pH range, while ageing temperature was varied at pH=4.6.

In chapter VI the application of pulse NMR to elucidate the state of water in casein solutions is described. The spin-spin relaxation time,  $T_2$ , of water protons in skimmilk and sodium caseinate solutions was measured in the pH range of 6.7 to 4.6 at different temperatures.

The most important results of this study are summarized and discussed in chapter VII.

## 2 EXPERIMENTAL PART

All low molecular weight electrolytes used were analytical grade. Solutions were generally prepared with demineralized water though sometimes with distilled water. The rennet used was a commercial calf rennet (Leeuwarder kaasstremsel) with a strength of 10.000 units. This was diluted 1:4 before use.

### 2.1 Skimmilk powder

For all experiments reconstituted skimmilk was used. In general this was made from a commercial low-heat skimmilk powder (Krause, Heino). For some experiments skimmilk was prepared from a low-heat skimmilk powder, supplied by the Netherlands Institute for Dairy Research (NIZO). The composition of both powders is given in table 2.1. The two kinds of powder gave similar experimental results. The dry matter, casein, ash and fat content were respectively determined according to IDF standards 26(1964), 29(1964), 9A(1969) and 90(1979). Undenaturated whey protein nitrogen (W.P.N.) was determined according to the method of the American Dried Milk Institute (1971). The difference between the true protein fraction and the sum of the casein and serum protein fraction must be ascribed to the proteose-peptone components.

Standard skimmilk was prepared by dissolving 12 gr powder in 100 gr of demineralized water giving a somewhat higher total solids content (10.4%) than in normal bovine skimmilk. To allow equilibration the solutions were stirred at 30 °C overnight (16-20 hours) before use. To prevent bacterial growth 100 ppm thiomersal also called thimerosal ( $C_2H_5HgSC_6H_4COONa$ , BDH Chemicals LTD) was added as a preservative.

### 2.2 Caseinate solutions

Two different sodium caseinate powders were available. Both powders met the IDF standard 72(1974) for the composition of edible caseinate (extra grade), except for the fat content of one powder. The first was a spray dried powder made in the laboratory of the University. One batch of pasteurized (20 s at 72 °C) skim-

Tabel 2.1 Composition (in wt.%) of the low-heat non-fat dried milk powders employed in this study.

	powder A <sup>1)</sup>	powder B <sup>2)</sup>
dry matter	96.8	96.9
ash	6.1	6.5
fat	0.6	0.9
true protein <sup>3)</sup>	33.8	34.8
casein	28.3	28.6
serum protein	3.4	4.1
NPN	1.8	2.6
WPN	6.45	6.94

1) Obtained from Fa. Krause (Heino).

2) Obtained from the Netherlands Institute for Dairy Research.

3) Usually in literature one speaks about total protein. This includes true protein and NPN.

milk was acidified with 0.5 N HCl at 30 °C until pH=4.6. After separating the whey and pressing the curd three washing stages with demineralized water at respectively 40-50 °C, 60 °C and 30 °C followed. The washed curd was redispersed in demineralized water and passed through a colloid mill to give a fine ground dispersion. Under gentle stirring the pH was increased to pH=6.7 with 0.5 N NaOH. The dissolved caseinate was heated to 60-80 °C just before it was spray dried.

The second powder was kindly supplied by the Netherlands Institute for Dairy Research. Pasteurized (10 s at 72 °C) skim milk (Ottenhof, pers. communication) was mixed with 4 N HCl in a continuous flow process at relative low temperature (15-20 °C). At the end of this precipitation stage direct steam injection caused a rise of the temperature to 38-42 °C. The whey was separated from the curd with a decanter. Three washing stages each at 45 °C were carried out. The washed curd was redispersed in ordinary water and ground in a colloid mill, while 2-3 N NaOH was added to in-

Table 2.2 Composition (in wt.%) of sodium caseinate powders employed in this study.

	spray dried	freeze dried
dry matter	95.8	98.6
ash	3.7	3.9
fat	3.1	0.5
true protein	88.2	93.0
casein	87.3	92.0
serum protein	-	-
proteose-peptone	1.0	1.2
NPN	0.7	1.1

crease the pH to pH=6.7. The temperature during this process was kept below 70 °C. The sodium caseinate solution was freeze dried at 55 °C under low pressure. The composition of both powders is given in table 2.2. They will be distinguished by the terms spray dried (made at our laboratory) and freeze dried (made at the NIZO) powder. The fat content of the spray dried powder is relatively high and does not conform to the IDF standard 72(1974) for the composition of (extra grade) edible caseinate. Together with the higher moisture content this produces a lower value for the protein content of the spray dried powder. No serum (whey) proteins were detectable in either powder. The difference between the percentage of true protein and the sum of the casein and proteose-peptone percentage is due to experimental error.

Standard sodium caseinate solutions contained 3 gr sodium caseinate powder per 100 gr solution and some NaCl and/or CaCl<sub>2</sub>. Sodium caseinate did not dissolve as well as skimmilk powder and therefore caseinate solutions were stirred at least 20 hours at 30 °C before use.

### 2.3 Acidification and gelation

For acidification the caseinate and skimmilk solutions were cooled in ice water baths and transferred to a low temperature

(4 °C) room. The apparatus for automatic acidification consisted of an autoburette (type ABU 13e), coupled with a titrator (type TTT 60a) and a standard pH meter (type PHM 62a), all from Radiometer Copenhagen. The rate of acid addition was regulated by the titrator and slowed near the pH end-point. For skimmilk 3 N HCl was used, but in sodium caseinate solutions too many flocs will be formed with this acid concentration. By using 0.5 N HCl few or no flocs will be formed during acidification. Generally the solutions were titrated to a pH=4.6 end-point, though not in those experiments where the pH was the variable of interest. The acidified solutions (0-2 °C) were transferred to the apparatus making the experimental measurement of interest and heated at a rate of 0.5 °C per minute, unless otherwise stated. In time dependent experiments the time, at which the temperature rose above 4 °C, was chosen as zero time. Above 10 °C gelation started. The final ageing temperatures varied from 20 to 50 °C.

Heating rate and temperature was controlled (within  $\pm 0.1$  °C) by MGW LAUDA thermostatted baths (type K4RD and K2RD), coupled with a regulating unit (PTR Regler, type P20K or R20/3) and a so-called "programmgeber" (type P250/2 or P250).

In experiments where the combined effect of pH and rennet action was studied, 50  $\mu$ l of a diluted rennet solution was added to 50 ml of cold acidified skimmilk to give a final concentration of 250 ppm rennet. In these particular experiments the moment of mixing was taken as zero time.

#### GDL induced acidification

Glucono- $\delta$ -lactone (GDL) was used as an acid precursor to prepare acid casein gels (pH=4.6) with an acidification temperature of 30 °C. For gel preparation solid GDL (1.22 wt.% for standard skimmilk and 0.47 wt.% for standard sodium caseinate) was added to skimmilk or sodium caseinate at 30 °C. The solution was stirred thoroughly, before it was transferred to any measuring apparatus. In case of skimmilk the first flocculation was seen after  $1.8 \times 10^4$  s (~5hrs) at pH~4.90-4.95, followed by gel formation at lower pH. Finally after approximately  $9 \times 10^4$  s (24 hrs) the pH of skimmilk solution reached 4.60-4.62 and of sodium caseinate 4.64.

#### 2.4. Whey

Acid whey was prepared from fresh skimmilk, unless stated otherwise. For this preparation a gel was formed from fresh skimmilk in accordance with the procedure described in section 2.3. After an appropriate gelation time of about 16 hours the whey was separated from the curd by centrifugation (in a CHRIST UJ3 centrifuge) for 30 min at 3000 rpm (~2300g). The whey was filtered just before use. The kinematic viscosity  $\eta/\rho$  was determined with a KPG Ubbelohde viscometer (Schott-Geräte, BRD) at the desired measuring temperatures. The elution time was determined in the classical way.

#### 2.5 Varying protein concentration by ultrafiltration

Protein concentration was varied by ultrafiltrating standard skimmilk in an Amicon concentrator model CH3, equipped with a hollow fiber cartridge (type H1P10). All constituents with molecular mass above 10,000 Daltons were concentrated. The concentrate was used directly except in the case of low protein concentrations where standard skimmilk was diluted with the ultrafiltrate obtained. The extent to which the protein was concentrated or diluted as compared to standard skimmilk was determined by Kjehldahl analysis and/or by a rapid infrared absorption technique using a Milkoscan 104A/B (A/S N. Foss electric, Denmark). With this instrument the absorption of infrared radiation at  $\lambda=6.46 \mu\text{m}$  by the peptide bonds is measured. Results obtained with the two techniques were in good agreement.

#### 2.6 Gel electrophoresis

The proteolytic action of rennet on  $\alpha_s$ - and  $\beta$ -casein as a function of time after enzyme addition was studied by a quantitative variant of PolyAcrylamide gel Electrophoresis (PAE) according to the procedure described by De Jong (1975). Precooled glass tubes were filled with 0.5 ml of an acidified skimmilk solution, prepared according to section 2.3, immediately after the addition of 250 ppm rennet. Gel samples were obtained by heat treatment using

the standard procedure (section 2.3). After the appropriate time interval each sample (0.5 ml) was dissolved in 3.5 ml of a Tris-HCl buffer (pH=8.5), containing about 9 M urea, resulting in a 8 M urea solution. From this solution, with a protein concentration of approximately 0.5%, 50  $\mu$ l was taken for the gel electrophoresis. The optical density of the stained casein bands was determined with the aid of a Shimadzu dual-wavelength TLC scanner (model CS-910), coupled to a recorder (BBC Servogor 120). The densitometer operated in the single-wavelength (at 600 nm), double beam mode, using a tungsten lamp, with a scan speed of 20 mm/min. The transmission was measured with an illumination beam of 10 mm height and 0.2 mm width. Both the optical density and the integrated optical density were charted by the two pen recorder. From the integrated signal the decrease in protein content could be calculated.

## 2.7 Estimation of splitting of $\kappa$ -casein

With the aid of high-performance liquid chromatography the free GlycoMacroPeptide (GMP) content, resulting from rennet action on  $\kappa$ -casein, was determined according to the method described by Van Hooydonk and Olieman (1982). Glass tubes were filled with 2 ml acidified skimmilk, to which rennet was added. They were then warmed at a rate of 0.5  $^{\circ}$ C per min to three different gelation temperatures. At regular time intervals the reaction was quenched by adding 4 ml 12% (m/m) TriChloroacetic Acid (TCA) to the glass tubes. The rate of GMP splitting was analysed, partly with the apparatus of the Netherlands Institute for Dairy Research (kindly done by Van Hooydonk and Olieman), and partly at our laboratory with a Spectra Physics SP 1800 liquid chromatograph.

## 2.8 Permeability measurements

### 2.8.1. General

The resistance of a liquid flow through a porous medium depends on the spatial distribution of the solid phase. In case of a laminar flow through a homogeneous fixed matrix generally Darcy's law is obeyed. For a flow in one direction the liquid flux,  $v$ , can be read as:

$$v = - B/\eta \nabla P \quad (2.1)$$

$v$  = liquid flux (i.e. volume flow rate/cross-sectional area)( $m.s^{-1}$ )

$B$  = permeability coefficient ( $m^2$ )

$\eta$  = viscosity of the flowing liquid (Pa.s)

$\nabla P$  = pressure gradient. In our case  $\nabla P$  has only one component in the x-direction (i.e. parallel to the measuring tubes). So  $\nabla P = dP/dx$  ( $Pa.m^{-1}$ )

The permeability coefficient  $B$  depends on the geometry, scale and spatial distribution of the percolated matrix. For flow through a porous medium a Reynolds number  $Re$  can be defined (Scheidegger, 1960):

$$Re = v\rho\delta/\eta \quad (2.2)$$

$v$  = liquid flux ( $m.s^{-1}$ )

$\rho$  = density of the flowing liquid ( $Kg.m^{-3}$ )

$\eta$  = viscosity of the flowing liquid (Pa.s)

$\delta$  = a diameter associated with the porous medium, i.e some length corresponding to an average grain or pore diameter (m)

In case of laminar flow it is a prerequisite for applying Darcy's law that  $Re$  should not exceed a certain critical value, which varies from 0.1 to 75 depending on the porous medium (Scheidegger, 1960).

### 2.8.2 The tube method

By measuring the liquid flux,  $v$ , of usually whey through open glass tubes filled with casein gels, the permeability coefficient,  $B$ , could be calculated from the known pressure gradient,  $\nabla P$ , according to equation 2.1. The apparatus used was developed by Van Dijk (1982) for measurements on rennet gels. Glass tubes open at both ends with an inner diameter of 3.7 mm and a length of 25 cm were placed in a precooled vat. The tubes placed in a holder rested on a plexiglass base. Acidified skim milk or sodium caseinate

was added to the vat to such an extent that the tubes were filled over a length of about 10 cm. The gelation vat was heated according to the procedure given in section 2.3. After the required gelation time at the appropriate temperature the tubes were withdrawn from the gelation vat, cleaned at the outside and placed in a rack, which was placed in the measuring vat made of clear plexiglass. The level of the percolating liquid in the measuring vat (usually whey or a sodium phosphate solution) was adjusted in such

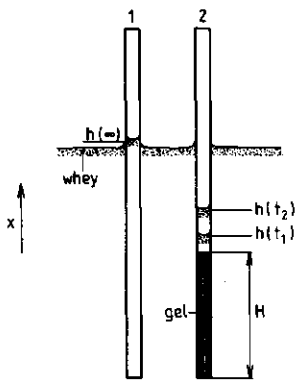


Fig. 2.1 Schematic representation of permeability measurement. For explanation see text.

a way that the initial pressure gradient was about  $4.5-6.0 \times 10^3 \text{ Pa.m}^{-1}$ . The whey level in the tubes was read at regular time intervals with the help of a travelling microscope. The length of the intervals depended on the permeability of the gel matrix. From the five readings usually made four permeability coefficients could be calculated. The order of magnitude of the flow velocity,  $v$ , varied from  $3 \times 10^{-6}$  to  $8 \times 10^{-8} \text{ ms}^{-1}$ . Assuming a value of  $10^{-7} \text{ m}$  for the parameter  $\delta$  (i.e. a low estimate of the approximate diameter of casein particles) in eq. 2.2, while  $\rho \sim 10^3 \text{ Kgm}^{-3}$  and  $\eta \sim 10^{-3} \text{ Pa.s}$ , the Reynolds number,  $Re$ , for the flow through casein gels varied from  $8 \times 10^{-9}$  to  $3 \times 10^{-7}$ . Taking for  $\delta$  a pore diameter of  $10^{-6}$  to  $10^{-5} \text{ m}$  instead of a particle diameter of  $10^{-7} \text{ m}$ ,  $Re$  will be 10 to 100 times larger, but still sufficiently small. There was therefore no risk for turbulent flow in our experiments. Variation of the pressure gradient from  $4.0 \times 10^3$  to  $11.0 \times 10^3 \text{ Pa.m}^{-1}$  did not influence the calculated permeability coefficients, so that the application of Darcy's law for flow through acid casein gels seems allowable.

The calculation of  $B$  from the experimental readings is somewhat complicated, because the pressure gradient is changing with time as the whey level in the glass tubes rises (see fig. 2.1). On the other hand because of the rather homogeneous character of

the flow through casein gels varied from  $8 \times 10^{-9}$  to  $3 \times 10^{-7}$ . Taking for  $\delta$  a pore diameter of  $10^{-6}$  to  $10^{-5} \text{ m}$  instead of a particle diameter of  $10^{-7} \text{ m}$ ,  $Re$  will be 10 to 100 times larger, but still sufficiently small. There was therefore no risk for turbulent flow in our experiments. Variation of the pressure gradient from  $4.0 \times 10^3$  to  $11.0 \times 10^3 \text{ Pa.m}^{-1}$  did not influence the calculated permeability coefficients, so that the application of Darcy's law for flow through acid casein gels seems allowable.

the gel and the one dimensional direction of flow (x-direction) the pressure gradient at a certain moment is constant and negative over the whole gel and is given by:

$$\frac{dP(t)}{dx} = - \rho g \frac{\{h(\infty)-h(t)\}}{H} \quad (2.3)$$

$h(\infty)$  = height of the whey level in the reference tube (m)

$h(t)$  = height of the whey level in the gel tube (m)

$H$  = length of the casein gel (m)

$g$  = gravitational acceleration  $\text{ms}^{-2}$

Because of the large volume outside the tubes  $h(\infty)$  is assumed to be constant. The liquid flux,  $v$ , also changes with time:

$$v(t) = \frac{dh(t)}{dt} \quad (2.4)$$

In this case the equation of Darcy (eq. 2.1) can be rewritten as:

$$v(t) = \frac{dh(t)}{dt} = \frac{B}{\eta} \frac{\rho g \{h(\infty)-h(t)\}}{H} \quad (2.5)$$

Integration, solving the integration constant and rewriting leads to an expression for  $B$ , depending on  $h(t)$  at  $t=t_1$  and  $t=t_2$  (Van Dijk, 1982).

$$B = - \frac{\frac{h(\infty)-h(t_2)}{\ln\left\{\frac{h(\infty)-h(t_2)}{h(\infty)-h(t_1)}\right\}} \eta H}{\rho g (t_2-t_1)} \quad (2.6)$$

Within the experimental accuracy the permeability coefficient,  $B$ , of acid casein gels did not change with time during the experiment.

## 2.9. Pulse NMR measurements

The spin-spin relaxation time  $T_2$  of several casein samples has been measured. Measurements have been carried out with a partly modified Bruker Minispec PC20 pulse NMR apparatus, operating at 20 MHz and equipped with a Newport 7-in. electromagnet. A Bruker Aspect 2000 computer and a Z17C pulseprogrammer were used for re-

gulation of the measurements and storage of experimental data. All  $T_2$  experiments involved the use of a Carr-Purcell-Meiboom-Gill pulse sequence. Each measurement consisted of one  $90^\circ$  pulse followed by a number of  $180^\circ$  pulses. The lengths of the  $90^\circ$  and  $180^\circ$  pulses were respectively 12.5 and 25  $\mu$ s. The time between the  $180^\circ$  pulses was 1.0 or 3.0 ms (for milk ultra filtrate samples). The delay time between two consecutive measurements was varied from 4 to 10 s depending on the  $T_2$  of the measured sample. This was sufficient to allow the nuclear magnetization to return to its equilibrium value. Each measurement resulted in a nuclear magnetization decay curve, characterized by one or more  $T_2$  relaxation times (see Chapter 6). For a suitable signal to noise ratio 8 to 16 decay curves were first summed and stored on disk in the computer. Each decay curve consisted of 2048, 3072 or 4096 sample points, depending on the length of the pulse sequence. Next the accumulated decay curve was fitted with a single exponential according to the method of McLachlan (1977). The inaccuracy in the calculated  $T_2$  values was estimated to be about 1%. This was determined by checking the computer fitting program with a generated decay curve. Previous fitting with sums of more than one exponential resulted in one single dominating exponential for the decay curve of skimmilk at different pH and temperature.

For thermostating a Varian ESR dewar coupled with a Varian temperature controller was used. The dewar was placed through the cavity, which was centered between two large electromagnets. A cold  $N_2$ -flow, created by heating liquid nitrogen in a dewar vat, which was connected directly to the ESR dewar, was used to regulate the temperature. The samples were held in tubes usually made of quartz but sometimes of glass, both with an outer diameter of 4 mm. The inner diameter was 3 mm and 2.2 mm for the quartz and glass tubes respectively. Notwithstanding the considerable reduction in volume the samples in the glass tubes still showed a reasonable signal to noise ratio.

## 2.10 Rheological measurements

Skimmilk gels, made by acidification and/or rennet action behave as visco-elastic materials (van Dijk, 1982, and Roefs and

Van Vliet, 1984). The number of techniques for studying the rheological properties of this type of gels is limited, because by transferring from one apparatus to another, e.g. from a beaker to a rheological apparatus, the gels will break and/or syneresis will begin. Thus the gels must be made in the apparatus itself.

In this study two different rheometers were used. The first was a dynamic viscometer developed by Den Otter (1967) and Duiser (1965) at TNO Delft. Except for dynamic measurements (section 2.10.1) it can also be used for a kind of stress relaxation measurements (section 2.10.3). The second rheometer was a constant stress apparatus from Deer LTD used for creep measurements (section 2.10.4).

### 2.10.1 Dynamic measurements

The rheometer used has been described extensively elsewhere by Duiser (1965), Den Otter (1967), Beltman (1975) and Te Nijenhuis (1977). Essentially the apparatus consists of two coaxial cylinders (see fig. 2.2) between which the sample is brought. The outer cylinder made of glass is fixed whereas the inner cylinder, made of stainless steel, is suspended between a torsion wire fixed to a

driving shaft and a strain wire. A sinusoidal rotational oscillation can be applied to the driving shaft. This movement is transferred to the inner cylinder by the torsion wire. When the sample behaves in a linear visco-elastic fashion, the inner cylinder also performs a sinusoidal oscillation, showing however a smaller amplitude than and a phase difference with that of the driving shaft. These differences depend on the visco-elastic properties of the sample, the elasticity of the torsion wire and the moment of inertia of the inner cylinder.

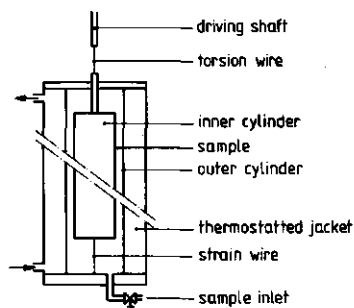


Fig. 2.2 Schematic representation of the dynamic rheometer. For explanation see text.

If the oscillation  $\varepsilon_a$  (rad) of the driving shaft is given by:

$$\varepsilon_a = \varepsilon_{a0} \sin (wt + \phi) \quad (2.7)$$

where  $\varepsilon_{a0}$  = the maximum amplitude (rad) of the oscillation of the driving shaft,  $\omega$  = the angular frequency ( $\text{rad.s}^{-1}$ ) of the oscillation,  $\phi$  = the phase difference (rad) between the oscillations of the driving shaft and the inner cylinder, and  $t$  = time (s), the oscillation  $\varepsilon_c$  (rad) of the inner cylinder can be written as:

$$\varepsilon_c = \varepsilon_{c0} \sin \omega t \quad (2.8)$$

$\varepsilon_{c0}$  is the maximum amplitude (rad) of the oscillation of the inner cylinder.

With  $I$  for the moment of inertia ( $\text{Nms}^2$ ) of the inner cylinder,  $D_1$  and  $D_2$  as the torsion constants of respectively the torsion wire (Nm) and the strain wire (Nm), and  $E$  ( $\text{m}^3$ ) as a characteristic cylinder constant, the equation of motion of the inner cylinder in this particular case is as follows:

$$\frac{D_1}{E}(\varepsilon_a - \varepsilon_c) - \frac{D_2}{E}\varepsilon_c - G'\varepsilon_c - \frac{G''}{\omega}\dot{\varepsilon}_c - \frac{I}{E}\ddot{\varepsilon}_c = 0 \quad (2.9)$$

Here  $\dot{\varepsilon}_c$  ( $\text{rad.s}^{-1}$ ) and  $\ddot{\varepsilon}_c$  ( $\text{rad.s}^{-2}$ ) are the first and second derivative of  $\varepsilon_c$  with respect to time  $t$ ,  $G'$  is the storage modulus ( $\text{Nm}^{-2}$ ) and  $G''$  is the loss modulus ( $\text{Nm}^{-2}$ ). In a more general description (Duiser, 1965) equations 2.7 and 2.8 are written as complex functions, while equation 2.9 must be rewritten using the complex shear modulus  $G^*$  ( $\text{Nm}^{-2}$ ), which is defined as:

$$G^* = G' + iG'' \quad (2.10)$$

Solving equation 2.9  $G'$  and  $G''$  can be calculated from the following equations:

$$G' = D_1/E \left( \frac{\varepsilon_{a0} \cos \phi}{\varepsilon_{c0}} - 1 \right) - D_2/E + I\omega^2/E \quad (2.11)$$

$$G'' = D_1/E \frac{\varepsilon_{a0} \sin \phi}{\varepsilon_{c0}} \quad (2.12)$$

$E =$  a cylinder constant  $= 4\pi h R_i^2 R_o^2 / (R_o^2 - R_i^2)$  ( $m^3$ ), where  $h$  is the length of inner cylinder (0.15 m),  $R_i$  is the radius of inner cylinder ( $3.75 \times 10^{-3}$  m) and  $R_o$  is the radius of outer cylinder ( $4.5 \times 10^{-3}$  m).

The angular frequency  $\omega$  was varied over the range  $10^{-3}$  to  $10^1$   $rad.s^{-1}$ . This range corresponded to a frequency range of  $1.6 \times 10^{-4}$  to  $1.6 s^{-1}$ . The amplitudes  $\epsilon_{ao}$ ,  $\epsilon_{co}$  and the phase difference  $\phi$  were measured by means of two light beams falling on a special mirror system fixed on inner cylinder and driving shaft (Beltman, 1975). The constants  $D_2$  and  $I$  were calculated as described by Beltman (1975) and Duiser (1965).  $D_1$  was determined with weights of exact known moment of inertia  $I_1$  ( $Nms^2$ ), which were suspended from the torsion wire and then brought into harmonic oscillation. From the observed frequency  $\nu$  ( $s^{-1}$ )  $D_1$  could be calculated as follows:

$$D_1 = 4\pi^2 I_1 \nu^2 \quad (2.13)$$

Temperature was controlled within 0.1 °C by a thermostating bath (MGM Lauda, see section 2.3), which was connected to the thermostatted jacket around the outer cylinder (see fig. 2.2).

### 2.10.2 Measurement of acid casein gels

After acidification and occasionally addition of rennet the skimmilk and caseinate solutions cooled on ice were transferred to the rheometer, which was precooled to approximately 2 °C. A funnel precooled in a refrigerator was used for filling. After filling the rheometer was warmed to the chosen gelation temperatures (see also section 2.3). In some experiments the measuring temperature was varied from 2 to 70 °C. To prevent evaporation gels were covered with paraffin oil. Sinusoidal deformations usually were not applied before a gel was formed to avoid disturbance in the first stage of gel formation. The amplitude of the driving shaft was kept sufficiently low to ensure linear behaviour of the sample, which appeared to exist if the maximum deformation  $\gamma < 0.04$ .

In the case of linear behaviour both the deformation  $\gamma$  and the shear stress  $\sigma$  depend on  $\epsilon_c$  and the distance  $R$  to the center of the inner cylinder, as follows:

$$\gamma = \frac{2 \varepsilon_c}{R^2 (R_i^{-2} - R_o^{-2})} \quad , \quad R_i < R < R_o \quad (2.14)$$

$$\sigma = \frac{2 \varepsilon_c |G^*|}{R^2 (R_i^{-2} - R_o^{-2})} \quad , \quad R_i < R < R_o \quad (2.15)$$

$\gamma$  varies from  $4.545 \cdot \varepsilon_c$  at the outercylinder to  $6.545 \cdot \varepsilon_c$  at the inner cylinder. The average value of  $\gamma$  over the whole sample equals  $5.545 \cdot \varepsilon_c$  and so an average maximum shear deformation  $\gamma_a$  can be defined as  $5.545 \cdot \varepsilon_{co}$ .

### 2.10.3 "Stress relaxation" measurements

Setting the driving shaft of the dynamic rheometer manually at a certain fixed position in such a way, that the gel is strained, offers the possibility of measuring a pseudo-stress relaxation modulus, which we will call  $G(t)^*$  ( $\text{Nm}^{-2}$ ). The problem is that in case of visco-elastic solids when  $\varepsilon_a$  is placed at a fixed position,  $\varepsilon_c$  will change with time and also both  $\gamma$  and  $\sigma$  (see eqs. 2.14 and 2.15). Therefore one cannot speak about a real stress relaxation experiment, nor about a creep experiment. For the deformation  $\gamma$  and the stress  $\sigma$  eqs. 2.14 and 2.15 still hold, except that  $\varepsilon_c$  and  $\varepsilon_a$  are no longer sinusoidal functions of time. Using  $\varepsilon'_c$  and  $\varepsilon'_a$  instead of  $\varepsilon_c$  and  $\varepsilon_a$  for the amplitude of respectively the inner cylinder and the driving shaft, the torsion moment  $M_1$  ( $\text{Nm} \cdot \text{rad}$ ) exerted by the torsion and the strain wire can be written as:

$$M_1 = D_1 (\varepsilon'_a - \varepsilon'_c) - D_2 \varepsilon'_c \quad (2.16)$$

Replacing the complex shear modulus  $G^*$  (eq. 2.9) by the pseudo-stress relaxation modulus  $G(t)^*$ , which has only a real value now, the total shear moment  $M_2$  ( $\text{Nm} \cdot \text{rad}$ ) exerted on the sample between inner and outer cylinder is given by:

$$M_2 = E G(t)^* \varepsilon'_c \quad (2.17)$$

In case of an applied harmonic oscillation the difference  $M_1 - M_2$  causes an angular acceleration  $\ddot{\epsilon}_C$  (see eq. 2.9), assuming  $G^*$  to be constant. When  $\epsilon'_a$  is fixed and  $G(t)^*$  is constant,  $M_1$  will be equal to  $M_2$  and  $\ddot{\epsilon}_C$  to zero and so  $\ddot{\epsilon}_C$  vanishes from eq. 2.9. A simple expression for  $G(t)^*$  can then be derived:

$$G(t)^* = D_1/E \left( \frac{\epsilon'_a}{\epsilon'_C} - 1 \right) - D_2/E \quad (2.18)$$

However in case of visco-elastic solids with very long relaxation times there is no steady-state situation and  $G(t)^*$  will decrease with time, whereas  $\epsilon_C$  and thus  $\gamma$  will increase causing  $\sigma$  to decrease. Equation 2.18 is no longer an exact solution, because  $\ddot{\epsilon}_C$  will have a small, although negligible value. Thus  $\epsilon'_C$  and though this  $G(t)^*$  should be written as time dependent functions. In that case eq. 2.18 is still an excellent approach for measuring a pseudo-stress relaxation modulus over longer time scales with the concentric cylinder apparatus, described above.

#### 2.10.4 Creep measurements

With this type of measurement the strain of a sample is monitored as a function of time during application of a constant stress. The experiments were carried out using a Deer PDR 81 Rheometer, fitted with a coaxial cylinder geometry machined from stainless steel and kept at the desired measuring temperature by immersion in a thermostating bath incorporated within the instrument. A constant stress was applied by means of an induction type electric motor. The rolling friction was reduced by using an air bearing support. Angular displacement was determined by a non-contacting electronic sensor, which measured the distance between a circular ramp and the sensor. The diameter of inner cylinder was 6 mm and that of the outer one 7.5 mm. The sample volume totalled 2 ml. Constant stress was applied to the inner cylinder at  $t=0$  and the resulting displacement measured as a function of time and monitored by means of a recorder. The applied stress was varied over the range 1 to 175 Pa. All measurements were carried out at 30 °C. To avoid interference of temperature gradients and air cur-

rents the apparatus was placed in a perspex cage. The instrument was adjusted at 30 °C, subsequently cooled to 2 °C and after filling with skim milk acidified in the cold, was heated again to 30 °C at a rate of 0.5 °C per minute (see section 2.3). After an ageing time of 18 to 20 hours each gel was subjected to only one creep measurement at one particular stress.

### 2.11 Electron microscopy

Transmission Electron Microscopy (TEM) using samples prepared by thin sectioning was applied to view the structural features of skim milk and sodium caseinate solutions in the liquid and gelled state in studies where temperature and pH were the variables. To minimize the disturbing influence of the preparation procedure on the structure of the casein solutions and gels, the micro-capsule method, introduced by Salyaev (1968) and adapted to milk by Hestra and Schmidt (1970a and b) was employed. Agar capsules, made by dipping glass rods with a diameter of ~1 mm in a hot 3% sterilized agar solution (Diftobacter), were filled with casein solutions by withdrawing the glass rods from the formed capsules, which were held in the solution at the other end, and then sealing both ends with hot agar. In case of liquid samples solutions of desired pH and temperature were prepared a few hours before fixation. After filling the capsules with a certain solution they were stored in the same solution. In the case of gelled samples the capsules were filled after acidification to pH=4.6 at ~2 °C and then heated in the same acidified solution to the desired gelation temperature (see also section 2.3).

After the appropriate ageing time the capsules were transferred for fixation to a 1% OsO<sub>4</sub> solution in a 0.1 M phosphate buffer of the corresponding pH and temperature. The samples were kept in the 1% OsO<sub>4</sub> solution for 16 hours. In some preliminary experiments the samples were first prefixed in 1.4% or 2% glutaraldehyde solutions for at least 6 hours and post fixed in 1% OsO<sub>4</sub> for two hours. This prefixing had no effect on the results. After rinsing with buffer and distilled water the capsules were dehydrated in a graded alcohol series from 20 to 100% ethanol. For embedding the samples were transferred to polyethylene capsules. Embedding was

carried out in three steps. Step 1 consisted of a treatment with a 1:1 mixture of alcohol and embedding medium (3 parts n-butylmethacrylate and 2 parts styrene), and then step 2 with pure embedding medium, both without initiator. The final step consisted of a treatment with embedding medium with 2% benzoyl peroxide as initiator. For adequate polymerization the polyethylene capsules were kept for at least 48 hours at 50 °C. After 24 hours more embedding medium was added to the polyethylene capsules, because shrinking and evaporation of the medium had taken place.

Thin sections (thickness about 60 nm) were cut with a LKB microtome and post stained with uranylacetate (7 min) and Reynolds leadacetate (7 min), and finally rinsed with 0.01 N NaOH to prevent lead carbonate precipitation, which causes artefacts. The samples were observed under a Philips Electronmicroscope (EM 400T), operating at 60 KV and micrographs were taken on 35 mm films.

## 2.12 Solubility of casein

Using the facilities put at our disposal by the Hannah Research Institute (Ayr, Scotland)<sup>1</sup> the solubility of casein at low temperature was determined as a function of pH. Casein was defined as soluble if it did not separate from a casein dispersion, when a centrifugal force of 60,000 g was applied for at least two hours. Fresh skimmilk was obtained from the bulk tank on the Institute farm. The skimmilk was cooled to 2-4 °C and the pH adjusted to a value in the range from 6.7 to 4.6 by adding HCl. After the skimmilk samples had been stored 44 hrs at 5 °C, they were centrifuged at 60,000 g for 2 hrs (temp. = 4 °C) in a Sorvall Superspeed RC 2-B centrifuge. The supernatants were carefully poured off from the pellets, which were drained and then redispersed in water. Both pellets and supernatants were raised to pH=6.7 by means of 1 M NaOH, treated with EDTA to remove Ca and warmed to room temperature. After dilution in a 20 mM imidazole, 50 mM NaCl buffer

1: The author wishes to thank the Hannah Research Institute for the facilities provided and Dr. Dalgleish and Dr. Horne for stimulating discussions.

(pH=7.0) the light absorption was measured at 320 nm and 280 nm. The light absorption at 280 nm ( $A_{280}$ ) arose from absorption by aromatic amino acids in the casein molecules plus a turbidity background, whereas the absorption at 320 nm ( $A_{320}$ ) was only due to solution turbidity. The  $A_{320}$  value was used to correct the  $A_{280}$  measurement using the equation:

$$A = A_{280} - 1.706 A_{320} \quad (2.19)$$

where A gave a rough measure of the casein concentration. The factor 1.706 stemmed from the assumption that turbidity was proportional to (wavelength)<sup>4</sup>. Ultimately the parameter, A, was recalculated in relative units of absorption per gram of original solution. Because the sum of light absorption of pellet and supernatant was equal for all pH's, the amount of casein in pellet and supernatant could be expressed as percentage of total casein. But as a correction for whey protein at each pH the total light absorption was reduced by the value of A of the supernatant at pH=4.6, which was entirely attributed to the whey protein fraction. The exact protein concentration could not be calculated, because the molar extinction coefficients of the individual caseins differ and the individual casein content of each fraction was not known.

In another experiment (kindly performed by Dr. Dalglish of the Hannah Research Institute) the fraction of the individual caseins in pellets and supernatants was determined. The samples were prepared as described above, except that the acidified skim milk solutions were only stored for 20 hrs at 5 °C. After the casein was isolated and purified from the supernatant and pellet, both pellet and supernatant were dissolved in a 8 M urea, 20 mM acetate buffer (pH=5.0), to which  $\beta$ -mercaptoethanol was added. The amount of individual caseins was estimated by means of column chromatography on a Pharmacia FPLC system. A MONO-S column with a solution of 20 mM acetate (pH=5.0) in 8 M urea as buffer A and a solution of buffer A + 1 M NaCl as buffer B were used (Dalglish, to be published). The  $\alpha_{s1}$ -casein and  $\alpha_{s2}$ -casein did not resolve properly and were therefore taken together. Estimates of errors are  $\pm 4\%$  for  $\alpha_s$ - and  $\beta$ -Casein and  $\pm 6\%$  for  $\kappa$ -casein.

### 2.13 Particle size measurement

The size of casein particles as a function of pH was investigated by means of Photon Correlation Spectroscopy (PCS) at the Hannah Research Institute (Ayr, Scotland). This method relies on the fact that the frequency of the laser light, which is scattered from a moving particle is Doppler-shifted by the motion of the particle relative to the observer. This property has been used to determine Brownian motion of particles in solution and hence to determine their translational diffusion coefficients. Detailed descriptions of the design and principle of the technique and its application to milk particles are given elsewhere (Horne, 1984, Chu, 1974, Berne and Pecora, 1976, and Holt et. al., 1973). The values of the diffusion coefficient,  $D$  ( $\text{m}^2\text{s}^{-1}$ ), for skimmilk, diluted in diffusate, were measured at different temperature and pH. In actual fact since the particles are polydisperse an average value of  $D$ , weighted by the intensity of the scattered light, was determined. This corresponded to a z-averaged  $D$ . The particle diameter,  $d$  (m), was calculated from the diffusion coefficient,  $D$  ( $\text{m}^2\text{s}^{-1}$ ), using the Stokes-Einstein equation

$$d = \frac{kT}{3\pi\eta D} \quad (2.20)$$

$\eta$  = solvent viscosity (Pa.s)

$T$  = absolute temperature (K)

$k$  = Boltzmann's constant ( $\text{Nm.K}^{-1}$ )

The photon correlator spectrometer (Horne, 1984) consisted of a scattering photometer with temperature-controlled water bath (within 0.1 °C) and variable scattering angle turntable, collection optics, and photomultiplier tube followed by pulse amplification and discriminator and a Malvern K7026 60 linear channels digital correlator. The correlator was operated in the single-clipped mode with clipping levels never greater than 3. The light source was a Spectra Physics He-Ne laser, model 124B. Experimental runs consisted of 1.67 to  $2.5 \times 10^6$  samples. Measurements were made at an angle of 90°. At low measuring temperature a flow of gaseous  $\text{N}_2$  was blown along the glass window of the index-matching bath,

in order to prevent condensation of water vapour on it. The correlator was interfaced to a DEC 11/02 computer. The computer data analysis was performed on-line within seconds of the completion of each run.

For sample preparation large amounts of standard skimmilk made from skimmilk powder A (see section 2.1) were acidified at 0-2°C to pH's varying from 6.7 to 4.6 (see section 2.3). Dialysis tubes filled with aliquots of standard skimmilk (10 ml) or a 4.5 wt.% lactose solution (25 ml) for the preparation of diffusate were added to beakers filled with 800 ml of the pH-adjusted skimmilk. For equilibration the samples were stored three days under gentle stirring at 5°C in a cold room.

For PCS measurements 5  $\mu$ l of dialysed skimmilk was diluted into 2 ml diffusate of corresponding pH. Before use diffusate was filtered through cellulose nitrate membrane filters (Millipore) of 0.22  $\mu$ m pore size.

### 3 FORMATION OF ACID CASEIN GELS

#### 3.1 Introduction

Whether a coagulating system forms a gel or a precipitate, is a very difficult question, largely unanswered by colloid chemists. It is known that factors like particle shape, volume fraction of particles and the ratio between the rate of aggregation and the rate of displacement of the particles, due to e.g. convection streaming, sedimentation or stirring, are important. The gel state, however, may be defined as one where both the dispersed component and the dispersion medium extend themselves continuously throughout the whole system. One can distinguish between gels with a reversible and gels with an irreversible character as function of e.g. temperature or pH. In fact a gel is usually a kind of metastable system being far from its absolute minimum of Helmholtz energy (see eq. 3.1), e.g. mostly a particle gel, disrupted by stirring, will not spontaneously reestablish in the same way.

This study is concerned with acid casein gels, made from skim-milk or sodium caseinate solutions acidified in the cold. As already implicitly mentioned in the title of this thesis and as will be shown further on, casein is the main constituent of the gel network. Gel formation by proteins in general and casein in particular depends on pH, temperature, ionic strength, ionic composition of the water phase, protein concentration and other more obscure and more difficult to define factors (such as temperature history and mechanical agitation).

Preliminary experiments showed that for gel formation by casein using the method described in section 2.3 a minimum casein concentration of about 1.0 wt.% is needed, whereas the ionic strength should exceed roughly estimated 0.08-0.09 M, both for skim milk diluted with ultra filtrate and sodium caseinate dissolved in a salt solution. The critical temperature for gel formation at pH=4.6 is about 8-10 °C. Below this temperature only part of the casein coagulates leading to a sediment. The rest of the casein is stable against coagulation or coagulates very slowly. With the method described in section 2.3 gel formation at 30 °C is restric-

ted to the pH range of 4.3 to 4.9. Above pH=4.9 casein doesnot coagulate at 30 °C and below pH=4.3 it coagulates during the acidification process at 0-2 °C. Possible gel formation during that stage of preparation would be disrupted immediately by stirring, which is needed for a homogeneous distribution of the added acid. For smooth gel formation it is essential that the system is not stirred, when it passes the coagulation point during heating leading to gel formation. Convection is largely diminished by slow, gradual heating.

Section 3.2 treats the formation and ageing of acid casein gels in general, monitored by measuring the storage modulus,  $G'$ , and loss modulus,  $G''$ , as a function of ageing time. As is known the structure of the casein particles, the basic elements of the gel network (section 3.4.2 and 3.4.3), drastically changes upon pH adjustment (e.g. Heertje et al., 1985). Therefore in section 3.3 special attention will be paid to the changes occuring in skimmilk with respect to the casein particles during acidification at low temperature. In section 3.4 a model for the acid casein gel network based on experimental evidence will be presented.

### 3.2 Formation and ageing of acid casein gels

#### 3.2.1 Ageing of acid skimmilk gels

In the first instance the formation and ageing of acid skimmilk gels was followed by measuring  $G'$  and  $G''$  (see section 2.10.1 and 2.10.2) as a function of time at different ageing temperatures (angular frequency  $\omega=1.0 \text{ rad.s}^{-1}$ ). Acidified standard skimmilk (section 2.3) was heated at a rate of 0.5 °C per min from 2 °C to the desired ageing temperature. Unless otherwise stated skimmilk in this chapter was made from skimmilk powder A (see section 2.1). The results are given in fig. 3.1a and b. Measurements were started after visible gel formation had occurred and the value of  $G'$  was at least larger than  $40 \text{ Nm}^{-2}$ . The deformation was kept sufficiently small (see also section 4.5.1) to prevent mechanical interference. Gel formation started above 10 °C (that means around  $t=720 \text{ s}$ , as  $t=0$  was chosen at the moment that temperature rises above 4 °C) and increased with temperature. The curves of  $G'$  and  $G''$  were largely similar. Experimentally  $G'$  could be determined more accu-

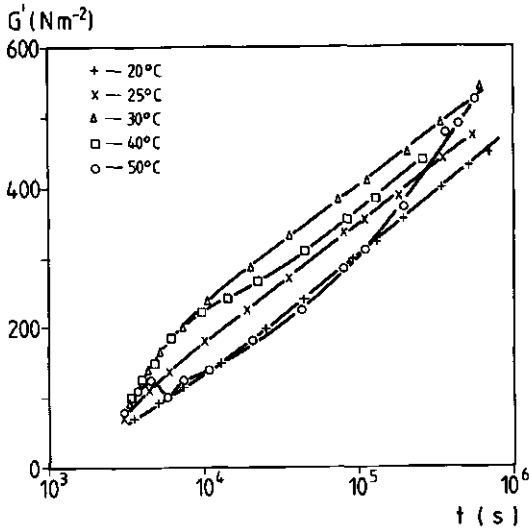
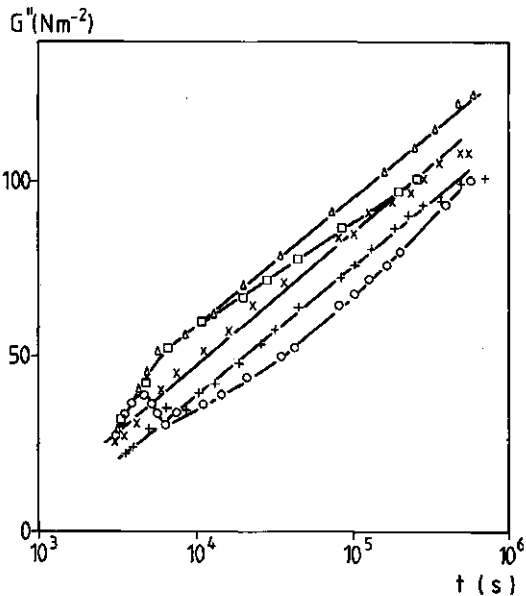


Fig. 3.1a. Storage modulus  $G'$  of acid skimmilk gels plotted as a function of the logarithm of the ageing time  $t$ (s) at different ageing temperatures. At  $t=0$  the heating of the acidified skimmilk solution (pH=4.6) at 4 °C commenced at a rate of 0.5 °C per min. Ageing temperatures: 20 °C (+), 25 °C (x), 30 °C ( $\Delta$ ), 40 °C ( $\square$ ) and 50 °C (o).  $\omega=1.0$  rad.s<sup>-1</sup>.

Fig. 3.1b. Loss modulus  $G''$  of the same gels as in fig. 3.1a plotted as a function of the logarithm of the ageing time. Conditions were the same as in fig. 3.1a.



rately. Between 10 and 20 °C a very strong temperature effect on the rate of gelation was found; after ageing at 10 °C for 16 hrs  $G'$  had a value of a mere 13 Nm<sup>-2</sup> in contrast with the value of 250 Nm<sup>-2</sup> after ageing for 16 hrs at 20 °C. After an initial pe-

riod, which included the time needed to heat the system from 4 °C to the measuring (and ageing) temperature,  $G'$  and  $G''$  tended to increase linearly with the logarithm of time, except for the gel aged at 50 °C. Even after 7 days ( $6 \times 10^5$  s) gelation still proceeded without any sign of reaching a plateau value. It is thought probable that the system needs an almost infinitely long time to reach the point of minimum Helmholtz energy inherent to the metastable state of the gel. The number of bonds between the casein particles, which most likely are physical protein-protein contacts, should increase with ageing time due to slow protein conformation rearrangements.

$\tan \delta$  (i.e. the ratio of  $G''/G'$ ) is depicted in fig. 3.2 as a function of ageing time. As can be seen  $\tan \delta$  decreased with ageing time, resulting in approximately the same value (0.23) after  $5 \times 10^5$  s for the gels aged at 20, 25 and 30 °C. In the beginning of gel formation the strongest decrease of  $\tan \delta$  was seen. This was to be expected, because  $\tan \delta$  of a solution is much larger than 1.0. The final value measured for  $\tan \delta$  for the gels aged at 40 and 50 °C was somewhat lower than 0.23. Apparently the elastic character of these gels increased in course of time. We will return to this point in section 4.5.3 and 4.5.4.

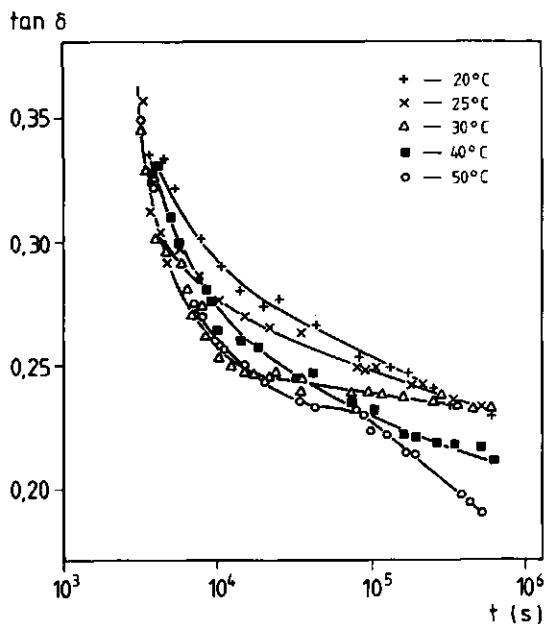


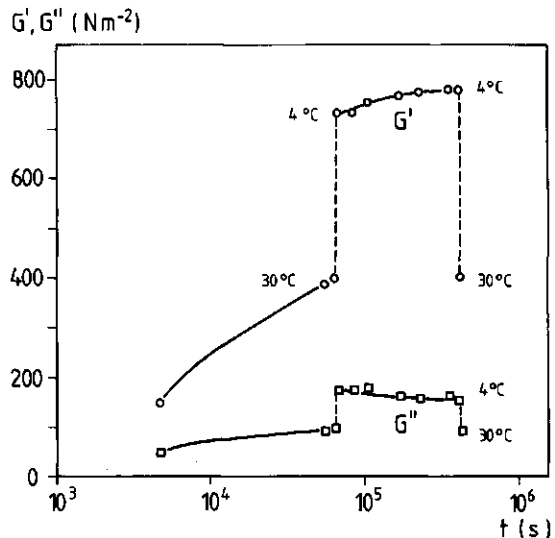
Fig. 3.2. The loss tangent,  $\tan \delta$ , of the acid skimmilk gels of fig. 3.1 plotted as a function of the logarithm of the ageing time  $t$ (s). Conditions and symbols are the same as in fig. 3.1, except for the curve of the gel aged at 40 °C, which was taken from a duplicate experiment.

The small maximum, occurring after  $4.5 \times 10^3$  s in the curve of the gel aged at 50 °C (fig. 3.1a and b), can be ascribed to a combined influence of heating and ageing. As we will see in section 4.5.3,  $G'$  and  $G''$  decrease with measuring temperature once a gel is formed. Thus during heating from 20 to 50 °C the moduli tended to increase due to ongoing gelation, but to decrease due to an increasing measuring temperature. This resulted in a small maximum after  $4.5 \times 10^3$  s, when temperature is 40 °C, and in a small minimum after  $5.8 \times 10^3$  s, when temperature had reached the ageing temperature of 50 °C. The strong increase in  $G'$  after  $10^5$  s was not seen for  $G''$  (compare fig. 3.1a and 3.1b). This is illustrated more explicitly in fig. 3.2, where at the moment that  $G'$  started to increase more strongly in fig. 3.1a, a dip in the curve of  $\tan \delta$  versus ageing time was found. We cannot explain this particular ageing behaviour for the gel at 50 °C.

### 3.2.2 Irreversible character of gel formation

Fig. 3.3 illustrates the irreversible character of gel formation of acid skimmilk gels. A skimmilk solution (pH adjusted to pH=4.6) was heated in the appropriate way (section 2.3) to 30 °C and aged at this temperature. After 18 hrs, when  $G'$  had reached a

Fig. 3.3. Storage modulus  $G'$  (o) and loss modulus  $G''$  (□) of an acid skimmilk gel plotted as a function of the logarithm of ageing time  $t$ (s). After heating in the standard manner the gel was aged for 18 hrs at 30 °C, before it was stored 4 days at 4 °C. Subsequently it was heated to 30 °C. The temperatures are indicated.  $\omega=1.0 \text{ rad.s}^{-1}$ .



value of  $400 \text{ Nm}^{-2}$ , temperature was lowered to  $4 \text{ }^\circ\text{C}$  and kept at that level for four days. Instead of a dissolution of the gel phase  $G'$  enormously increased, implying a drastic increase in the number or strength of the elastically effective bonds between the protein molecules of different casein particles. Apparently an acidified skimmilk solution at a temperature of  $0$  to  $4 \text{ }^\circ\text{C}$  must be regarded as a dispersion, which is stable in the colloid chemical sense, but thermodynamically unstable.

The strong increase of  $G'$  and  $G''$  upon temperature lowering will be discussed extensively in section 4.5.3. During the ageing at  $4 \text{ }^\circ\text{C}$   $G'$  tended to increase slightly, while  $G''$  slightly decreased, giving the gel a more elastic character. Bringing the system back to  $30 \text{ }^\circ\text{C}$  resulted in the same  $G'$  as before the cooling procedure, which suggests that the increase in  $G'$  at  $4 \text{ }^\circ\text{C}$  was not due to the same effect of ageing as found for the gels aged at temperatures varying from  $20$  to  $50 \text{ }^\circ\text{C}$  (described in section 3.2). Probably the observed slight increase of  $G'$  was due to some retarded temperature reversible protein rearrangements of the same kind as those which caused the observed increase and decrease of  $G'$  upon respectively lowering and raising the temperature.

Acidification was found to be reversible in that a skimmilk solution of  $\text{pH}=4.6$  after readjustment to  $\text{pH}=6.7$  by means of  $3\text{N NaOH}$  exhibited no visible coagulation and looked stable at  $4$  and  $30 \text{ }^\circ\text{C}$ , but of course it is questionable whether the original casein micelles were reformed by this procedure.

### 3.2.3 Skimmilk gels made by rapid heating

In a few experiments the rheometer filled with acidified skimmilk was heated within  $10$ - $15 \text{ s}$  in a temperature jump from  $4 \text{ }^\circ\text{C}$  to respectively  $30$ ,  $40$  and  $50 \text{ }^\circ\text{C}$ . In fig. 3.4 the measured values of  $G'$  are depicted as a function of ageing time. Again a rather linear increase of  $G'$  with the logarithm of the ageing time was found, which was in the case of ageing at  $30 \text{ }^\circ\text{C}$  very similar to the increase of  $G'$  found for a gel heated at a rate of  $0.5 \text{ }^\circ\text{C per min}$  (fig. 3.5a, curve 1 and 3). The smaller increases of  $G'$  with the logarithm of time for the gels at  $40$  and  $50 \text{ }^\circ\text{C}$  probably stem from the much coarser structure of the gel network in the sense of

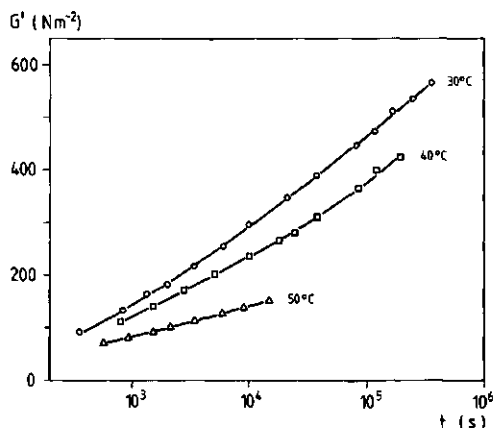


Fig. 3.4. Storage modulus  $G'$  of acid skimmilk gels heated in a single temperature jump plotted as a function of the logarithm of the ageing time  $t$ (s) at three different ageing temperatures. At  $t=0$  the skimmilk solution was heated within 10 s from 4 °C to the ageing temperature (indicated in graph).  $\omega=1.0 \text{ rad}\cdot\text{s}^{-1}$ .

very large conglomerates and pores, which were even macroscopically visible. Probably the large temperature gradient from thermostatted jacket to inner cylinder during the initial stage of gelation caused a more irregular coagulation, or perhaps convection streaming resulted in a more inhomogeneous network structure.

#### 3.2.4 Different kinds of acid casein gels

To highlight the influence of the method of preparation on acid casein gels  $G'$  is depicted as a function of ageing time for five different acid casein gels in fig. 3.5a. The ageing temperature was 30 °C and the final pH varied from 4.60 to 4.64.

The ageing curves for the gels made from standard skimmilk acidified in the cold and heated in a single jump (no. 1) or at a rate of 0.5 °C per minute (no. 3) are taken from fig. 3.4 and 3.1a respectively. A similar type of ageing curve (no. 2) was found for a sodium caseinate gel (casein conc. 2.8 wt.%) prepared according to the same procedure as gel no. 3. This similarity indicates that skimmilk gels are essentially casein gels (see also section 3.4.2 and 4.5.3). Curves 4 and 5 were measured on gels made by a direct slow acidification procedure at 30 °C, as is described in section 2.3. For this purpose the slowly hydrolyzing acid precursor Glucono- $\delta$ -Lactone (GDL) was used. For skimmilk (curve 5) coagulation was visible at  $1.8 \times 10^4$  s after the addition of GDL and for the sodium caseinate solution (curve 4) after  $3.0 \times 10^4$  s. Arbitrarily these times were chosen as zero time in fig. 3.5a. For skimmilk

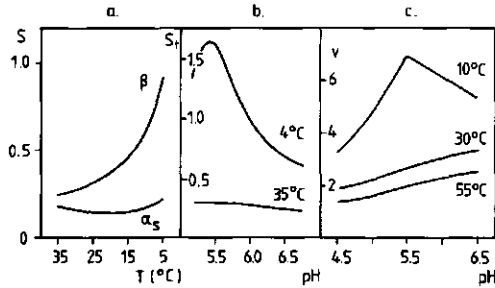


Fig. 3.6. a: the "solubility"  $S$  of  $\alpha_s$ - and  $\beta$ -Casein as function of temperature for fresh milk at physiological pH.  $S$  is expressed as fraction casein in the serum after centrifugation at 190.000 g (after Reimerdes and Klostermeyer, 1976). b: The total serum casein concentration  $S_t$  as function of pH at two different temperatures for fresh skimmilk after centrifugation at 78.000 g.  $S_t$  is expressed as mg casein N/ml (after Rose, 1968). c: the voluminosity,  $v$ , of casein as function of pH at three different temperatures for reconstituted skim-milk.  $v$  is expressed as gram water per gram protein in the pellet after centrifugation at 257.000 g (after Darling, 1982).

soluble total casein as function of pH at 4 and 35 °C (see fig. 3.6b). At pH=6.7 the solubility increased by a factor 2.8 as temperature was lowered from 35 °C to 4 °C. This agrees with the above mentioned results of Reimerdes and Klostermeyer. At 35 °C the serum casein concentration increased only very slowly over the pH range of 7.0 to 5.0. However at 4 °C a strong increase in serum casein concentration was found with decreasing pH until pH=5.4, where a clear maximum was observed. At this pH the solubility at 4 °C has increased by a factor 5.6 as compared to 35 °C. Another interesting feature is the voluminosity of casein particles as a function of pH. Voluminosity (g water per g casein) can be calculated from the water and casein content of the pellets left after centrifugation (centrifugation force  $\geq 70.000$  g for several hrs) of skimmilk samples at different pH and temperature (Tarodo de la Fuente et al., 1975, Darling, 1982 and Snoeren et al., 1984). As can be seen in fig. 3.6c (after Darling, 1982) at lower temperature a maximum in the voluminosity was also found around pH=5.4. According to Darling this maximum vanished at 30 °C or

higher, where a gradual increase with pH was observed, whereas Van Hooydonk (1986, to be published) still observed a small, but significant maximum in the voluminosity at 30 °C around pH=5.4. Further the voluminosity tended to decrease with temperature. Strikingly the pH, at which the maximum in voluminosity of casein at 10 °C was reached (Darling, 1982), coincides with the pH, at which the optimum in solubility at 4 °C was reached (Rose, 1968). However, at 30 °C Van Hooydonk observed the maximum in solubility to be at pH=5.6 as compared to the maximum in voluminosity, which he observed at pH=5.4. In this respect two main questions important for this study may be put forward; firstly, what happens to the structure of the casein particles during acidification to pH=4.6, and secondly, which caseins and how much of them dissolve from the casein particles around pH=5.4? We shall deal with these two questions in the next sections.

### 3.3.2 Cold acidification of skimmilk

In the standardized procedure for the preparation of the acid casein gels a skimmilk or a sodium caseinate solution was cooled down in a bath filled with ice and water to a temperature of 0-2 °C and kept thus around 20 to 60 minutes before the first acid was added (section 2.3). The subsequent pH-adjustment was carried out in 30 to 60 minutes. The acid addition was slowed down considerably near the allotted pH to ensure equilibrium. After acidification to pH=4.6 the pH sometimes increased a little, but normally by less than 0.05 unit of pH. One should remember that dissolution of colloidal calcium phosphate (CCP) and especially of casein are processes which take time. In the context of this section the same procedure was always followed. Skimmilk and sodium caseinate solutions were acidified to a pH in the range of 6.7 to 4.6. The solubility of total and individual casein (section 2.12), the casein particle size and the intensity of the scattered light (section 2.13) were studied for skimmilk samples stored at least 24 hrs at low temperature. The size and structure of casein particles in skimmilk and in sodium caseinate solutions at different stages of acidification were also studied by means of electron microscopy (section 2.11).

### 3.3.2.1 Solubility of casein at low temperature

The amount of non-centrifugable casein (centrifugal force 60.000g for 2 hrs) was determined in two ways (section 2.12): namely by measurement of the light absorption of supernatant and redispersed pellet, and by quantitative column chromatography. The last method also afforded the estimation of the soluble fraction of the individual caseins. Both methods were applied to fresh skim milk (section 2.12) and agreed well (compare curve 1 to curve 2 in fig. 3.7a). In this graph the fraction of non-centrifugable total casein is depicted as a function of pH after storage times of 20 hrs (curve 1) and 44 hrs (curve 2) at 5-8 °C. Whether the small differences between the curves are due to an effect of storage time is not known. Upon acidification the amount of soluble casein first increased gradually to a maximum of approx. 60% around pH=5.4 agreeing with the results of Rose (1968, see fig. 3.6b). Between pH=5.2 and 4.8 a very steep decrease of casein solubility was observed.

In fig. 3.7b the behaviour of the soluble fraction of the individual caseins after 20 hrs. storage is depicted as a function of pH (Roefs et al., 1985). The shape of the solubility curve of each individual casein was very similar to that of total casein with a maximum solubility around pH=5.4. At pH=6.7 the fraction of soluble total casein consisted mainly of  $\beta$ -casein (70%) with only 21% of  $\alpha_s$ -casein, which agreed with the results of Reimerdes et al. (1976, see fig. 3.6a). At pH=5.4 however only 51% of the soluble casein was  $\beta$ -casein, while the contribution of  $\alpha_s$ -casein had increased to 38%. This considerable increase of soluble  $\alpha_s$ -casein at pH=5.4 as compared to pH=6.7 (by a factor 5 overall) was the most remarkable result of this experiment. The  $\kappa$ -casein fraction of soluble total casein remained fairly constant (around 10%) over the whole pH-range. Below pH=5.4 the fastest decrease of solubility was seen for  $\alpha_s$ - and  $\kappa$ -casein.

It is probable that the dissolution of casein actually obtained during the acidification stage of acid casein gel preparation will be lower because this stage of lowering the pH from 6.7 to 5.0 takes place in only 10 to 20 min. However we assume that the observed trends will also hold for this situation.

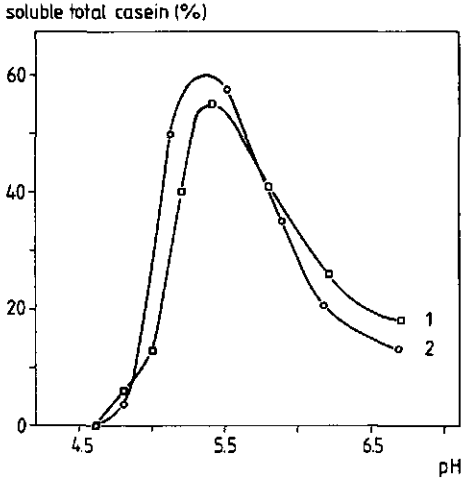
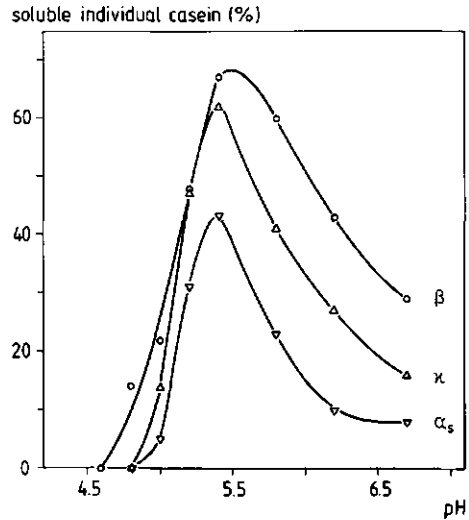


Fig. 3.7a. The fraction of total soluble casein as a function of pH at 5-8 °C. The amount of soluble casein was determined (see section 2.12) by means of column chromatography (curve 1) and light absorption measurements (curve 2). The samples were stored at 5-8 °C respectively 20 hrs (2) and 44 hrs (1).

Fig. 3.7b. The fraction of soluble individual caseins as a function of pH after 20 hrs of storage at 5-8 °C. The amount of soluble casein was determined by means of column chromatography. The total soluble casein curve for these samples is depicted as curve 1 of fig. 3.7a.



### 3.3.2.2 Casein particle size

In fig. 3.8a the casein particle diameter,  $\bar{d}$ , measured by means of photon correlation spectroscopy (section 2.13), is depicted as a function of pH at four different temperatures (see also Roefs et al., 1985). Samples were prepared by dialysing at 5-8 °C small amounts of skimmilk of natural pH against large amounts of skimmilk directly acidified in the cold. This bulk skimmilk was made

from the same skimmilk powder A (see section 2.1). A salt diffusate was simultaneously prepared by dialysing an appropriate lactose solution against the acidified skimmilk. For measurements at temperatures higher than 8 °C the dialysed skimmilk and salt diffusate were first incubated separately at the measuring temperature and mixed together (5  $\mu$ l of skimmilk into 2 ml of salt diffusate) just before use. Coagulation of casein (below pH=5.0) and precipitation of calcium phosphate (in the salt solutions of pH below 6.0 and above 6.3 at 35 °C) restricted the range of pH values, at which measurements were possible (see fig. 3.8a and b).

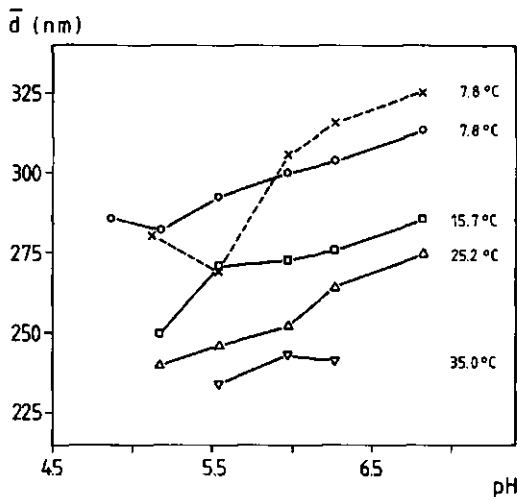
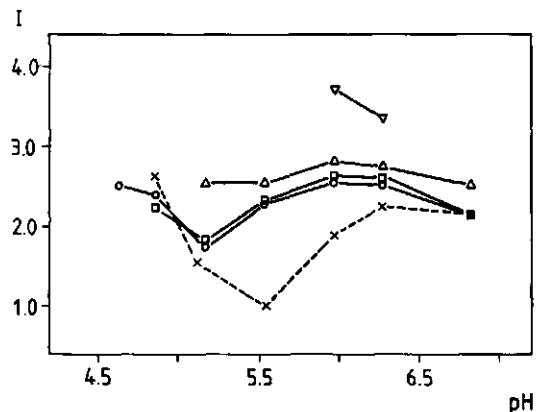


Fig. 3.8a. The average diameter,  $\bar{d}$ , measured by photon correlation spectroscopy, of casein particles in skimmilk as a function of pH. Temperatures are indicated. The samples were pH adjusted by means of dialysis for 40 hrs. The dashed curve refers to directly acidified bulk milk after storage for  $\leq 70$  hrs at 5-8 °C. The error in the measurements was  $\leq 10$  nm.

Fig. 3.8b. The intensity  $I$  of the scattered light as a function of pH for the samples of fig. 3.8a. Measuring temperatures are the same as in fig. 3.8a.



The particle diameter (fig. 3.8a) tended to increase slowly with pH and to decrease with temperature, which correlates with the voluminosity behaviour at higher temperatures (see fig. 3.6c). The differences found are relatively small, if one considers the extended scale on which  $\bar{d}$  is plotted. Clearly at all temperatures investigated no dip in the particle diameter was found around pH=5.5, which suggests that the dissolution of casein was not accompanied by complete disintegration of the casein particles. The corresponding intensity,  $I$ , of the scattered laser light, plotted as a function of pH (fig. 3.8b), showed only a small minimum around pH=5.1-5.2 at 7.8 and 15.7 °C. This minimum vanished at 25 °C. This almost constant particle diameter upon acidification in spite of the considerable dissolution of casein agrees with the optimum in voluminosity around pH=5.5 found by Darling (1982).

In contrast to the particle diameter the intensity of the scattered light is the same at 7.8 °C and 15.7 °C. The relatively strong increase of  $I$  at 35 °C must be ascribed to precipitation of CCP on the casein particles. Actually a larger minimum of  $I$  around pH=5.5 than found at  $T=7.8$  and 15.7 °C would be more in line with expectations, since a considerable amount of casein tends to dissolve from the casein particles at lower temperature (see fig. 3.7a). Surprisingly this was found for the scattered intensity of the bulk milk samples at 7.8 °C (fig. 3.8b). This minimum is relatively much deeper than the small but significant minimum in the particle diameter, which was also noticed around pH=5.5 for these samples (see fig. 3.8a). In this case probably some disintegration of particles had occurred, but the observed decrease in diameter of the casein particles in bulk milk at pH=5.5 is still too small to be correlated directly to the large amount of casein solubilized at that pH. On the other hand the large decrease in intensity of the scattered light at pH=5.5 seems to correlate directly to the large increase of soluble casein at that pH (see fig. 3.7a).

It is thought that the rate of acidification, which differs between direct acidification and dialysis regulated acidification, may be responsible for the observed differences between bulk milk and dialysed milk, since the dissolution of CCP and of casein, and the rearrangement of casein molecules are time dependent processes.

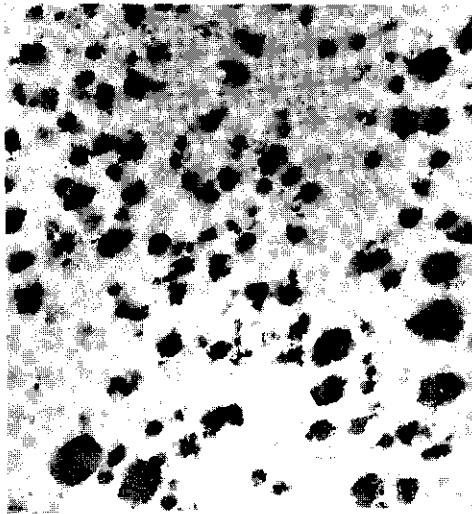
In summary it appears that the optimum in voluminosity of casein particles around pH=5.5 at low temperature is the result of a dissolving of casein and CCP from particles, the particles retaining approximately the same diameter.

### 3.3.2.3 *Electron micrographs of skimmilk*

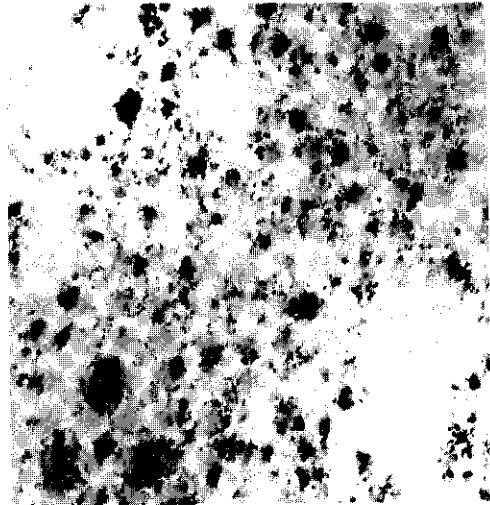
Electron microscopy is one of the most commonly used methods of studying the structure and size of all kinds of protein systems. It has often been applied to milk and milk products (e.g. Kalab, 1981 and Schmidt, 1982b). In this study Transmission Electron Microscopy (TEM) was used to study the casein particles in skimmilk (made from skimmilk powder A, section 2.1). Recently Schmidt (1982b) has discussed the problems and possibilities of applying TEM to milk and milk products. The dehydration and embedding steps may influence the observed protein structures. Particularly at low temperature some protein denaturation must be taken into account, because the hydrophobic and electrostatic bonds in proteins are sensitive to these preparation steps.

Fig. 3.9 shows electron micrographs of three different skimmilk samples, namely pH=6.7 at 30 °C, pH=5.3 at 4 °C and pH=4.6 at 4 °C. The samples were prepared according to section 2.11. At pH=6.7 free casein particles (approximate diameter varying from 70 to 250 nm) can be detected (fig. 3.9a), agreeing with results reported in literature (Henstra and Schmidt, 1970a and b and Davies et al., 1978). The observed particle diameter is an underestimate of the true value, because the embedding medium used (a mixture of styrene and n-butylmethacrylate) tends to shrink during polymerisation (Glauert, 1975).

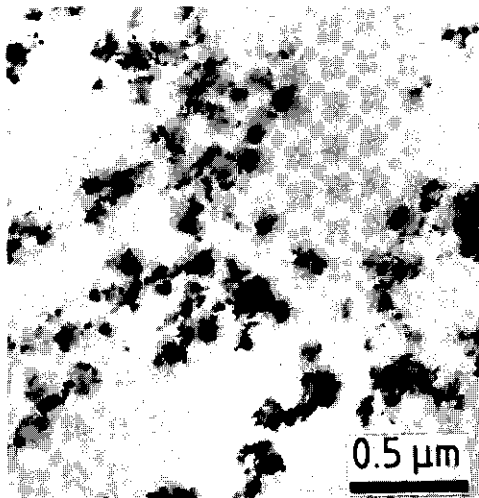
Apart from casein particles with a less compact structure a large amount of finely dispersed casein is seen at pH=5.3 and 4 °C (fig. 3.9b). The finely dispersed casein particles probably stem from dissolved casein molecules, which have reaggregated to a certain extent, and from more or less completely disaggregated casein particles. No apparent change was seen in the diameter of those larger particles still present. A similar effect was observed by Heertje et al. (1985) in electron micrographs of skimmilk acidified by means of GDL at 30 °C and 43 °C to a pH varying from 6.7



(a)



(b)



(c)

Fig. 3.9. Electron micrographs of standard skimmilk at different pH and temperature. a: pH=6.7, 30 °C. b: pH=5.3, 4 °C. c: pH=4.6, 4 °C. The magnification is indicated.

to 4.8. However they reported a disaggregation of casein particles around pH=5.2-5.4, which was even more pronounced than observed in this study.

At pH=4.6 the finely dispersed casein has reaggregated again (fig. 3.9c). When extrapolating these E.M. results to the standard

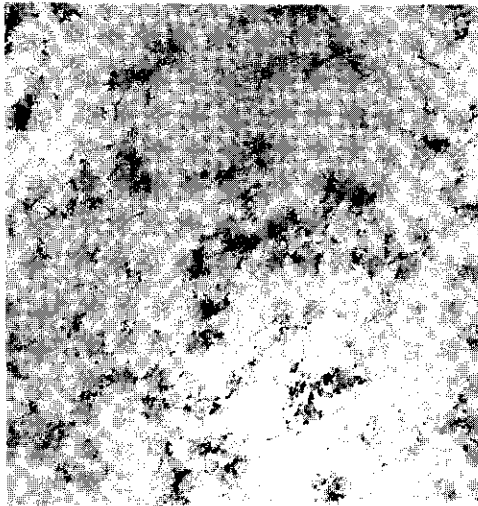
acidification procedure of skimmilk (section 2.3), which took only 30-60 min, it has to be considered that in the E.M. experiment the samples were kept several hours at pH=5.2 before the pH-endpoint of 4.6 was reached and fixation was started.

### 3.3.3 Cold acidification of sodium caseinate solutions

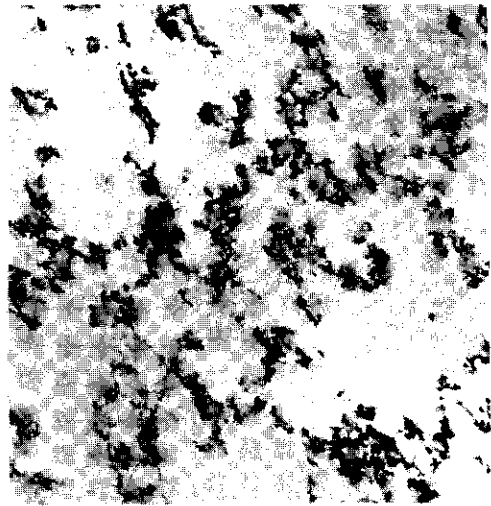
The appearance of a sodium caseinate solution changes, when its pH is lowered, from rather clear, greylike at pH=6.7 to colloidal white and turbid at pH=4.6, where it is no longer distinguishable from skimmilk. Hardly any visible coagulation occurs and the pH-adjusted solution is colloidally stable at 0 °C for several days at least. Obviously the transition from a rather transparent to a turbid casein solution is caused by the formation of casein aggregates of considerable size (diameter probably larger than 20 nm), in which probably individual casein molecules or smaller aggregates of the same size as the so called casein submicelles are involved.

This formation of aggregates was confirmed by electron micrographs of sodium caseinate solutions (in 0.16 M NaCl) at three stages of acidification (fig. 3.10). At pH=6.7 and 4 °C (fig. 3.10a) casein was visible as very finely dispersed, somewhat threadlike structures. It is possible that protein denaturation resulting in the threadlike structures has occurred during the preparation procedure, as was suggested by Schmidt (1982b). Using the same micrograph preparation procedure Schmidt obtained identical (threadlike) structures for disintegrated casein micelles. These he believed were casein submicelles. Applying a freeze-etching technique to specimens of spray-frozen solutions these submicelles were visible as small spherical particles (Schmidt, 1982b). Obviously considering fig. 3.10a and the clear grey appearance of sodium caseinate one may conclude that at pH=6.7 sodium caseinate molecules are present as individual molecules or as small aggregates.

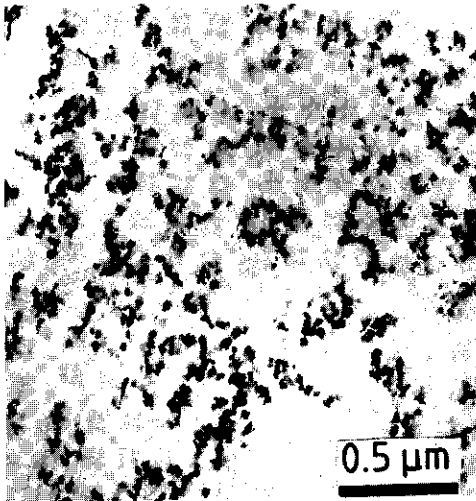
At pH=5.3 and 4 °C (fig. 3.10b) the casein is less finely dispersed and the first visible casein aggregates are formed. At pH=4.6 and 4 °C (fig. 3.10c) all casein is aggregated into small particles, as were also observed in skimmilk samples of that pH (fig. 3.9c). Based on the micrographs the diameter of the aggre-



(a)



(b)



(c)

Fig. 3.10. Electron micrographs of sodium caseinate at different pH a: pH=6.7, b: pH=5.3, c: pH=4.6. Temperature 4 °C. NaCl conc. 0.16 mol per kg dispersion. The magnification is indicated.

gates may be estimated to be 20 to 40 nm. The actual diameter will be larger because of the possible shrinkage during sample preparation mentioned in section 3.3.2.3. In fig. 3.10c some of the casein particles seem to have coagulated. Apparently at 4-5 °C the casein particles formed in sodium caseinate solutions at pH=4.6 are no longer colloiddally stable and tend to coagulate after a

longer storage time. Before fixation the sample at pH=4.6 was stored for several hours at 4-5 °C.

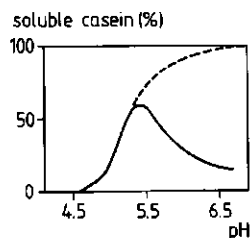
#### 3.3.4 Discussion

In regarding the aggregation of casein molecules leading ultimately to the formation of a gel one has to realize that different stages and levels of aggregation can be distinguished; namely, the aggregation of individual casein molecules leading to the formation of small aggregates, which probably quite often aggregate further to larger, under certain circumstances metastable particles; these particles may aggregate into strands and conglomerates, which ultimately will form a continuous gel network. The stability against coagulation of these metastable casein particles is directly related to their internal structure, which depends on the mutual interactions between the different casein molecules and above pH=5.4 also on the interactions of casein with CCP. Probably in both cases the casein particles formed are not completely homogeneous. Acidification and temperature variation will alter the internal structure. On acidification not only CCP will dissolve, but the extent of aggregation and probably the arrangement of the casein molecules inside the particles will change, too.

Different interactions as e.g. Van der Waals attractive forces, hydrogen bonding, hydrophobic bonding, electrostatic interactions, as well as steric factors, will be involved. Hydrophobic bonding may be of crucial importance, as it strongly increases with temperature between 0 and about 40 °C (e.g. Van Vliet, 1977). The interaction between charged areas depends on factors such as pH, ionic strength and salt composition, while the solvent quality strongly influences the steric terms.

In general the change in interaction between casein molecules inside casein particles during acidification is governed by two main mechanisms: a tendency to aggregate with decreasing pH (the protein is brought closer to its isoelectric point) and a tendency to disaggregate because of dissolution of CCP. In absence of CCP only the first mechanism plays a part. For sodium caseinate aggregation of casein molecules was found to start just below pH=6.0 and was complete at pH=4.6. This is schematically depicted in fig. 3.11.

Fig. 3.11. Schematical picture of the "solubility" of casein at low temperature (0-4 °C) as a function of pH for skimmilk (—) and sodium caseinate solution (---). Casein which cannot be pelleted by centrifugation at 60.000 g is regarded as soluble. The curve for skimmilk is derived from fig. 3.7a.



Disaggregation of casein molecules is observed in skimmilk between pH=6.7 and pH=5.5 at low temperature (section 3.3.2). All three kinds of casein investigated ( $\alpha_s$ -,  $\beta$ - and  $\kappa$ -casein) dissociate from the casein particles (see fig. 3.7b), while the particle diameter remains fairly constant (fig. 3.8). Some disintegration of casein particles cannot be excluded at pH=5.5 and 5 °C. However this will be far from complete, whereas dissolution of CCP at pH=6.7 leads to a complete disintegration of casein micelles.

The extent of casein dissociation at pH=5.5 could depend on the rate of acidification, as is suggested by the difference in intensity of the scattered light as function of pH between dialysed milk and bulk milk (fig. 3.8). Rapid acidification may lead to a faster dissolution of CCP, followed by a larger dissociation of casein. Perhaps then in the pH range around 5.5 the time for the individual casein molecules would be too short to compensate the loss of interaction with CCP by mutual casein-casein interactions, which might require protein conformational rearrangements. Casein dissociation possibly will be decreased, when the rate of acidification is decreased, since protein rearrangements may compensate the dissolution of CCP. At the other hand when rapid acidification is carried out until a pH below 5.0 casein dissociation might be decreased, too, since the loss of CCP may be compensated by an increased amount of +- ionic interactions. Such a dependency of the molecular structure and size of the casein particles on pH and perhaps their temperature history demands painstaking studies to reveal precisely what occurs.

Two possible mechanisms can be postulated to explain the fairly constant particle size during acidification to a pH around 5.4. Firstly and most likely, the dissolution of CCP and casein is ac-

accompanied by a swelling of the residual casein. Secondly, casein particles consist of a frame work of protein, which is mostly assumed to consist of one or two of the different kinds of casein (e.g. Lin et. al., 1972), filled with more loosely bound protein. In our view the results depicted in fig. 3.7 and 3.8 particularly favour the first mechanism. Below  $\text{pH}=5.5$  the amount of dissolved casein steeply decreases. Electron micrographs (fig. 3.9 and 3.10) suggest that soluble casein not only reassociates with already existing particles, but also may form new aggregates of the same size as found for sodium caseinate.

So the final result of the mechanisms described above is that, although the casein particles above  $\text{pH}=6.0$  and below  $\text{pH}=5.0$  are complete different entities, they have more or less the same diameter; this diameter is also found in the transition region.

### 3.4 Network model for acid casein gels

#### 3.4.1 General description of possible models

Continuity of structure and permanency of that structure is the general feature of a gel, apart from a relatively large volume fraction of the continuous liquid phase. Flory (1974) distinguishes four different types of gels: 1, ordered, lamellar gels (e.g. soap gels and phospholipids); 2, networks of covalent cross-linked flexible polymers (fig. 3.12a); 3, networks of flexible polymers with crosslinks formed by physical aggregation (see fig. 3.12b); 4, particulate disordered gels e.g. flocculated clays and

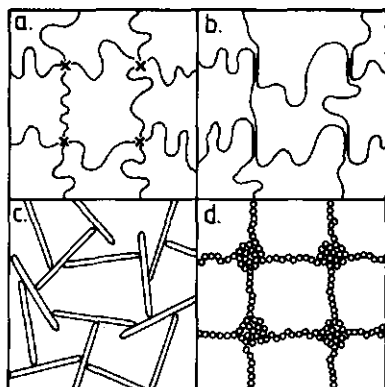


Fig. 3.12. Highly schematic representation of four different types of gels. a: a polymer network with permanent covalent crosslinks. b: a polymer network with semi-permanent crosslinks formed by physical aggregation. c: A particulate structure consisting of strongly anisotropic particles. d: a particulate structure consisting of identical hard spheres (after Papenhuizen, 1972).

most partly crystalized fats (fig. 3.12c and d). In reality the spatial arrangement of the basic elements in the last mentioned systems is much less regular than depicted in fig. 3.12c and d.

The nature, size, shape and spatial distribution of the basic elements forming the network, the permanent or non-permanent character of the junction points, and the entropic or enthalpic nature of the interaction forces are the main features for further classification of a gel. For a comprehensive theoretical description of protein gels, which is not achieved until now, elements of theories for both macromolecular gels (fig. 3.12a and b) and particle gels (fig. 3.12c and d) will be required.

Deformation of protein gels will lead to an increase in Helmholtz energy,  $A$ , arising from both a decrease of entropy and an increase of internal energy (van Vliet and Walstra, 1985). The change in Helmholtz energy,  $dA$ , at constant temperature,  $T$ , is written as:

$$dA = dU - TdS \quad (3.1)$$

where  $U$  is internal energy and  $S$  is entropy. Since both volume and pressure are constant in our experiments, the Helmholtz energy,  $A$ , equals the Gibbs energy,  $G$ , and the energy,  $U$ , will equal the enthalpy,  $H$ .

Deformation causes a stretching of the strands of the gel network. If one considers a network, to which an external force is applied in the direction  $x$ , one can according to van Vliet and Walstra (1985) derive the following equation for the modulus  $G$  of the network:

$$G = CN \frac{d^2A}{dx^2} \quad (3.2)$$

where  $N$  is the number of strands per unit area in a cross section perpendicular to  $x$  bearing the stress (i.e. the force per unit area).  $C$  is a characteristic length determining the geometry of the network. In the case of a network of particle strands  $dA$  is the change in Helmholtz energy (eq. 3.1), when the particles in the strands are moved apart over a distance  $dx$ .

Equation 3.2 is generally valid for small deformations (Van Vliet and Walstra, 1985), because the force exerted should be proportional to the deformation. From eq. 3.2 it is clear that the elastic or shear modulus  $G$  (and also the dynamic moduli  $G'$  and  $G''$ ) depends on the homogeneity of the gel network expressed in the number of stress carrying strands,  $N$ ; further it depends on the character and number of bonds between the basic elements inside the strands, as expressed in the change of the Helmholtz energy,  $dA$ . The character of the bonds will be determined by the nature of the interaction forces between the basic elements. In the case of a network of particles, which are homogeneously distributed over the available space, all particles will contribute to the network modulus  $G$  to the same extent.  $N$  will then be directly proportional to the volume fraction of particles,  $\phi$ . In the case of an inhomogeneous distribution only a fraction of the particles (see e.g. fig. 3.12d) will carry the stress and  $N$  will be no longer proportional to  $\phi$ . In such circumstances  $G$  will be proportional to  $\phi^x$ , where  $x > 1$  (Van den Tempel, 1979).

In a gel of aggregated particles (fig. 3.12c and d) such as margarine or flocculated clays the interaction forces are only of enthalpic nature. Then on deformation the increase of Helmholtz energy stems from an increase of internal energy rather than from a decrease of entropy.

This is not the situation with ideal polymer gels (fig. 3.12a and b) e.g. rubber gels which consist of long flexible macromolecules crosslinked at permanent or semi-permanent junction points. The chain segments between the crosslinks are so long that they have a very large number of possible conformations implying a substantial conformational entropy. They will behave as statistical coils and the energetic or enthalpic contributions to the increase of Helmholtz or Gibbs energy on deformation of these gels are negligible. Then the increase of Helmholtz energy stems only from a decrease of entropy.

Often protein molecules, although long chain molecules are folded into a compact and complicated structure, which can be classified as secondary, tertiary and even quaternary structure. Such compact folded protein molecules may be regarded as particles with a non-uniform structure and surface. Most denatured proteins, al-

though almost without secondary structure, are still constrained in their spatial arrangement by the diverse character of their amino acids and are far less flexible than ordinary homopolymers. Upon aggregation they, too, will behave to a large extent as particles and not as flexible macromolecules. Both a decrease of entropy and mostly a more important increase of enthalpy will contribute to an increase in Gibbs energy, when such protein gels are deformed. Only in a few protein gels as for example elastin (Norde et al., 1985) and gelatin (Te Nijenhuis, 1979) is the entropic contribution to  $\Delta A$  in equation 3.1 dominant.

A casein gel originates from the coagulation of particles consisting of at least several hundred of casein molecules. These particles, consisting of 70-80 wt.% of water, are probably not homogeneous in that the distribution of the different caseins may change from the outside to the core of the particles. They should probably also be regarded as easily penetrable and deformable, dynamic entities. After coagulation the formation of semi-permanent bonds between casein molecules at the boundary of adjacent particles will be very likely. The formation of entanglements as in the case of long flexible homopolymers seems less probable. It is unlikely that all coagulated particles will contribute equally to the macroscopical gel properties. Some of the particles may be incorporated in large non contributing conglomerates or aggregates, as illustrated schematically in fig. 3.12d for a gel of hard spheres. Indications of an aggregate-like structure of acid casein gels have been given e.g. by Harwalkar and Kalab (1981). Such inhomogeneity will drastically influence the mechanical properties of the gel formed (see above). To use an old Dutch saying: the strength of a whole chain equals the strength of the weakest link. Therefore the mechanical properties of acid casein gels depend not only on the number and nature of bonds between the particles, but also on the spatial distribution of the particles. The last factor determines that fraction of the total number of bonds which effectively contributes to the mechanical properties. To study the spatial distribution both permeability measurements and rheological measurements (measuring the dynamic moduli  $G'$  and  $G''$ ) as a function of concentration of the basic elements of the network were made. All particles, which possibly can take part in the

gel network are regarded as basic elements. Permeability measurements give information about the large inhomogeneities at the level of the gel network (Van Dijk, 1982). To these measurements an E.M. study of acid casein gels was added. To avoid confusion we will distinguish between heterogeneity at the level of the gel network and at the level of the structure of the protein particles. For a more extensive discussion see section 3.4.3 and section 4.6.

### 3.4.2 Experimental results

In order to obtain information about the basic elements of the network in an acid casein gel and about their spatial distribution the permeability and dynamic moduli ( $G'$  and  $G''$ ) of different types of acid casein gels were measured as a function of casein concentration. The size and shape of the basic elements was studied by means of electron microscopy.

#### 3.4.2.1 *Storage modulus as a function of casein concentration*

To study the role of different milk components, acid gels were made as a function of casein concentration following three different procedures. The results are shown in fig. 3.13, where  $G'$  is plotted as a function of casein concentration on a double logarithmic scale. All gels were aged for 16 hrs at 30 °C before measurement.

Curve 1 refers to gels made by dissolving skim milk powder B (section 2.1) in demineralized water. Along with the casein the concentration of all other milk components (e.g. salts) varied to the same extent. The result was a curved line exhibiting a strong dependence of  $G'$  on the casein concentration.

For curve 2 the casein concentration was varied by means of ultra filtration at pH=6.7 (section 2.5). This allowed the selective separation of casein micelles with bound CCP and whey proteins from lactose, salts and water. With this technique the casein in standard skim milk (casein conc. is 30 g per kg dispersion) was concentrated at 30 °C and the separated ultra filtrate was used to lower the casein concentration below that of standard skim milk by dilution. In this way primarily the concentration of

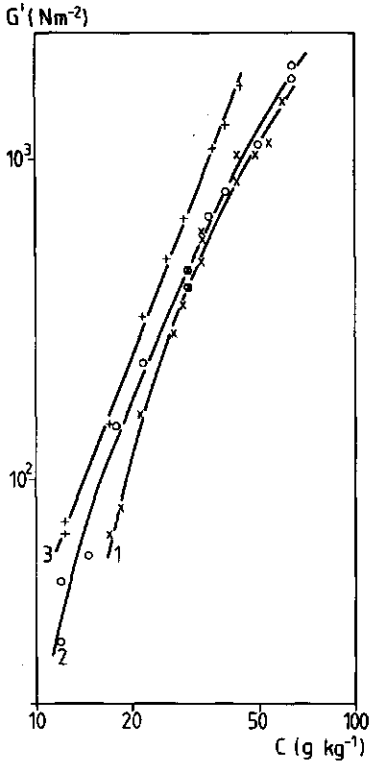


Fig. 3.13. Storage modulus  $G'$  as a function of casein concentration  $C$  (gram per kg dispersion) for three different types of acid casein gels. 1: skimmilk powder dissolved in demineralized water. 2: a standard skimmilk solution concentrated or diluted by means of ultra filtration. 3: sodium caseinate dissolved in 0.12 M NaCl. Gels were aged at 30 °C for 16 hrs.  $\omega=1.0 \text{ rad.s}^{-1}$ .

components with molecular mass greater than 10,000 was varied. Thus at pH=6.7 the ionic strength and composition could be kept almost constant with variation in protein content. However at pH=4.6 the ionic strength and composition still varied because of the CCP dissolving from the casein particles during acidification. This variation, however, was far less than in curve 1. As a consequence of the smaller variation of  $I$ , curve 2 is less bent than curve 1. Furthermore the minimum casein concentration at which a gel could be formed was lower for skimmilk gels made by dilution with ultra filtrate (curve 2, minimum casein concentration <12 g/kg) than for gels made by dissolving skimmilk powder in different amounts of water (curve 1, minimum casein concentration ~15 g/kg). These differences are probably due to a higher ionic strength at low casein concentration in the skimmilk diluted with ultra filtrate. Addition of NaCl to a skimmilk solution (according

to curve 1) with a low casein concentration so that the ionic strength was raised to the same value as of a solution made by diluting standard skimmilk with ultra filtrate, resulted in the same value for  $G'$  as for a gel of curve 2 at the same protein concentration. The ionic strength at the lowest casein concentration of curve 1 and 2 that a gel could be made was nearly the same (approximately 0.09 M and 0.1 M respectively), although these minimum casein concentrations ( $\sim 15$  g/kg and  $\sim 11$  g/kg respectively) differed significantly (see fig. 3.13). This indicates the relatively more important role of the ionic strength. An estimation of the ionic strength of standard skimmilk at pH=4.6 is given in section 4.5.5.1.

In the third procedure gels were made from pure sodium caseinate and as little salt as possible. No other milk components such as lactose and serum proteins were present. To obtain a gel a minimum level of NaCl ( $\sim 0.10$  M) was found necessary. For this experiment also a small amount of  $\text{CaCl}_2$  ( $\sim 0.007$  M, i.e. five times less Ca than the level in standard skimmilk) was added. Replacing this small amount of  $\text{CaCl}_2$  by NaCl and keeping the ionic strength constant did not influence significantly the values of the dynamic moduli obtained. The result for  $G'$  as a function of the casein concentration was a straight line (curve 3) with a slope of 2.6 falling slightly higher than the other curves (see fig. 3.13).

Similar results were obtained for  $G''$  as a function of the casein concentration. For gels prepared by all three methods  $\tan \delta$  varied between 0.21 and 0.24 over the whole casein concentration range.

From the similarity of the three curves may be concluded that the gel network was primarily built up of casein. Serum proteins and lactose were not important. The amount of salt played a prominent part, whereas the type of salt seemed to be less important. The difference in slope between the three curves could be due to different variations of ionic strength. This will be discussed more extensively in chapter IV (section 4.5.5.2).

From the strong exponential dependence of  $G'$  on the casein concentration ( $G' \sim c_{\text{cas}}^{2.6}$ ) it can be concluded that the number of stress carrying strands,  $N$  (see eq. 3.2), was not proportional to the volume fraction of casein particles, and so the network formed was

very heterogeneous. The heterogeneity of the spatial distribution of the basic elements forming the gel network will be investigated in more detail in the next two sections.

#### 3.4.2.2 *Electron micrographs of acid casein gels*

To study the spatial structure of the acid casein network, electron micrographs of gels made from acidified skimmilk and from acidified sodium caseinate solutions (section 2.3), were prepared as described in section 2.11. The gels were aged for at least 16 hrs at 30 °C before fixation. A few typical examples of the micrographs obtained are shown in fig. 3.14. The pictures of the acid skimmilk gels (fig. 3.14a and b) are very similar to those of the acid sodium caseinate gels (fig. 3.14c and d), which might be expected from the similarity in rheological properties (fig. 3.5a, fig. 3.13 and section 4.5.3 to 4.5.5) and supports the concept of casein as main constituent of the network in acid skimmilk gels (section 3.4.2.1). The electron micrographs are very similar to those reported by Harwalkar and Kalab (1981) for acid skimmilk gels, made by heating coldly acidified skimmilk to 40 °C, using HCl and citric acid as acidulants.

Both types of casein networks consist of coagulated particles, which have only partly fused. The coagulated particles are not homogeneously distributed over the available space. They tend to be grouped in dense areas, which can be considered as large aggregates and conglomerates. On the other hand the areas without casein represent the relatively large meshes of the gel network. Only a few particulate strands are seen, which is not surprising if one remembers the thickness of the thin sections (60-100 nm, see section 2.11).

The diameter of the particles of acid sodium caseinate gel ( $d=50-100$  nm) seems to be slightly smaller than in case of the acid skimmilk gel ( $d=80-300$  nm). In the acid skimmilk gel most particles have a diameter of around 100 nm. On micrographs taken from acid skimmilk gels with either half or double the casein concentration particles had roughly the same size. Comparing the gel situation with that existing prior to aggregation i.e. comparing the size of the partly fused particles in fig. 3.14 with that of

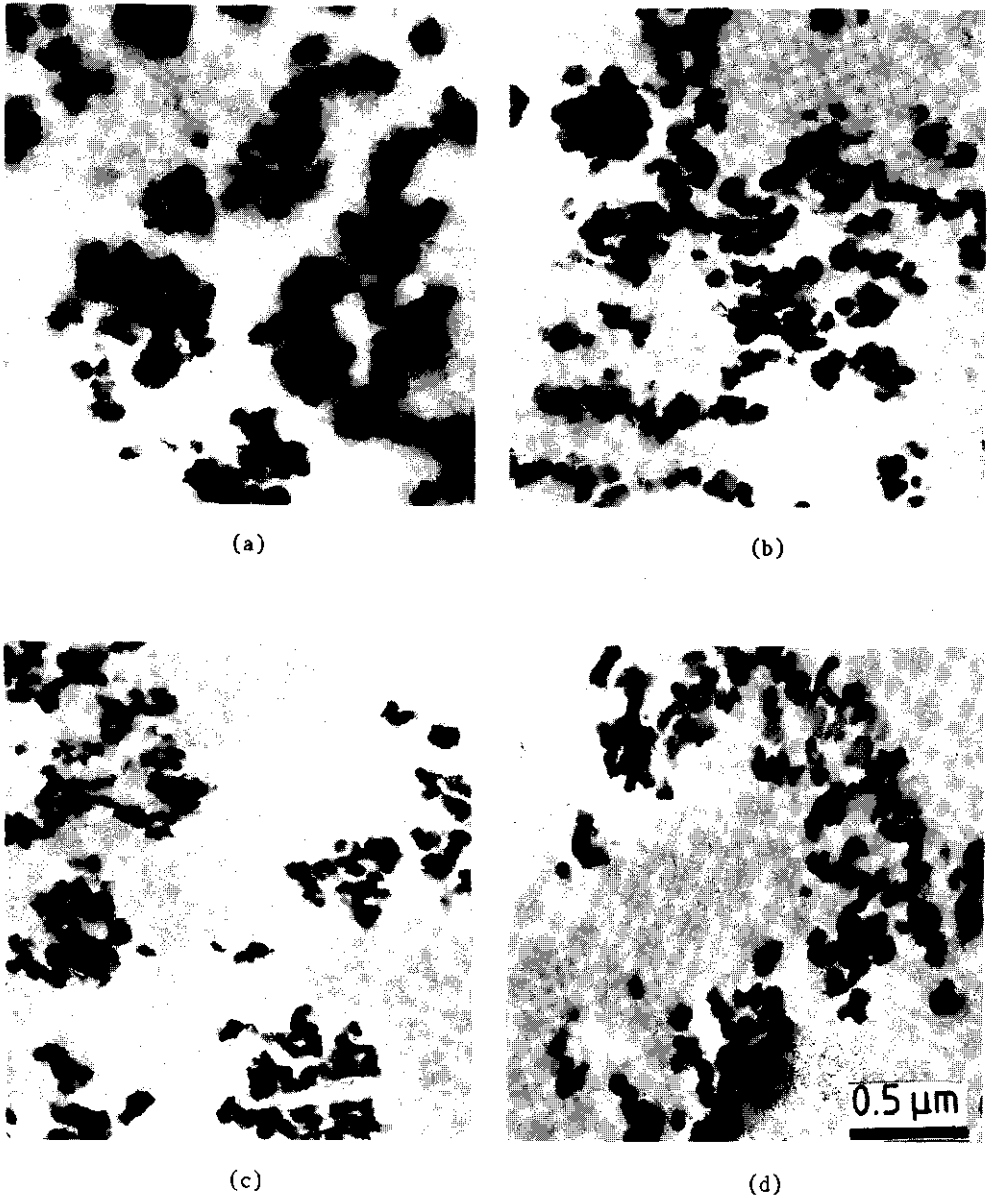


Fig. 3.14. Electron micrographs of acid skimmilk gels (a and b) and acid sodium caseinate gels (c and d). pH=4.6. The sodium caseinate gels were aged for 16 hrs at 30 °C. The skimmilk gels were aged for 25 hrs (a) and 170 hrs (b) at 30 °C.

the particles of fig. 3.9c (skimmilk at pH=4.6 and 4 °C) and fig. 3.10c (sodium caseinate solution at pH=4.6 and 4 °C) suggests, particularly for sodium caseinate, an increase in diameter of the protein particles during gelation induced by heating, whereas from voluminosity and particle size experiments (fig. 3.6c and fig. 3.8a) a decrease in particle diameter with increasing temperature would be expected, if one assumes the diameter of these particles to be changed reversibly with temperature. Bearing in mind possible experimental error involved in the preparation procedures, these results suggest that, particularly, for sodium caseinate, it is small casein particles which first coagulate to form larger particles. These subsequently take part in the formation of bigger aggregates and strands of particles ultimately resulting in the formation of a gel. To confirm this phenomenon many more electron micrographs will be necessary using other E.M. techniques. With the data presently available it is very difficult to give a reasonable explanation for the observed phenomenon. However an effect of acidification rate cannot be excluded. In the preparation of the E.M. samples the acidification rate was much higher for the gels (fig. 3.14) than for the samples of non-aggregated skimmilk at pH=4.6 and 4 °C (see fig. 3.9c). Because of the higher rate at which the pH range from 6.0 to 5.0 was passed, possibly less casein dissociated from the casein particles at a pH around 5.4 than suggested in fig. 3.9b and c (see also section 3.3.2.2), resulting in larger particles at pH=4.6 before and after heating. On the other hand one should remember that reaching a pH end-point in the range 5.2 to 6.0 at a higher acidification rate will possibly increase the amount of dissociated casein. It is however clear that casein aggregation occurs in steps and at different levels, depending on changing conditions such as temperature, pH etc.

In most of the electron micrographs a degree of anisotropy is seen. This is probably due to a slight sample deformation during the cutting of the thin sections with the microtome (section 2.11). At the margin of fig. 3.14c the contours of three small fat globules can be seen, their surface partly consisting of casein. These fat globules are incorporated in the gel network and in principle they should enlarge the rigidity of the gel (van Vliet

and Dentener, 1983). However because of the low fat content (around 0.1 wt.% or less) the effect on the dynamic moduli should be negligible.

### 3.4.2.3 *Permeability of acid casein gels*

The permeability coefficient,  $B$  ( $\text{m}^2$ ), of acid skimmilk and acid sodium caseinate gels was determined using Darcy's law for laminar flow through a porous medium (eq. 2.1, section 2.8). As  $B$  depends on the homogeneity and geometric structure of the porous medium, in principle information about these parameters can be obtained by measuring  $B$ . An equation for  $B$  as a function of the geometric parameters can be derived assuming a rather simple network model (see section 3.4.3.2).

In this section experimental results will be presented. In each experiment 10 to 14 tubes were used with 4 consecutive measurements of  $B$  per tube.

In fig. 3.15 the permeability coefficient  $B$  of acid skimmilk gels is depicted as a function of casein concentration, both on a logarithmic scale. The casein concentration was varied by means of ultra filtration (section 2.5). As can be seen the permeability exhibited a very strong dependence on the casein concentration. A straight line with a slope of  $-3.3$  was found, which implies that  $B$  is proportional to  $[\text{casein}]^{-3.3}$ . Thus the heterogeneity at the level of the gel network was very much concentration dependent.

In fig. 3.16 the permeability coefficient  $B$  of acid skimmilk gels is depicted as a function of the measuring temperature for gels aged for 16 hrs at respectively 20 °C, 30 °C and 40 °C. All experiments were carried out twice, except for the gel aged at 30 °C and measured at 40 °C, which was measured only once. The standard deviation in each experiment varied from 0.05 to  $0.25 \times 10^{-13} \text{ m}^2$ , while the difference between two duplicate experiments was  $0.04 \times 10^{-13} \text{ m}^2$  at most.

It is clear that ageing temperature affected  $B$  much more than the measuring temperature. The relatively small variation with measuring temperature may be ascribed to a decrease in voluminosity with increasing temperature (e.g. Darling, 1982 and see fig. 3.6c). The great influence of the ageing temperature on  $B$  shows

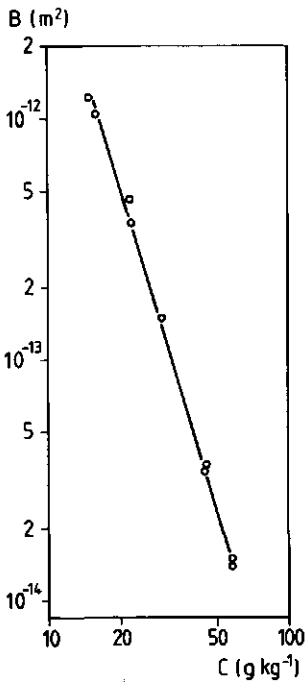
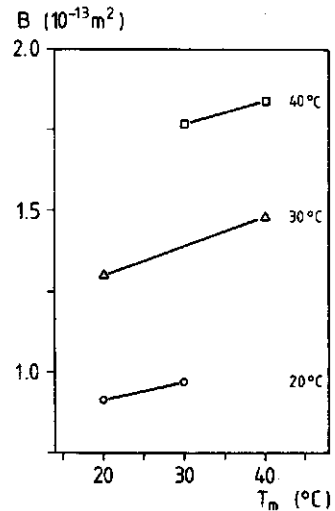


Fig. 3.15. Permeability coefficient,  $B$  ( $\text{m}^2$ ), as a function of casein conc.,  $C$  (g per kg dispersion), for acid skimmilk gels. The casein concentration was varied by means of ultra filtration (section 2.5). The gels were aged for 16 hrs at 30 °C, before measurement at 30 °C.

that the temperature at which initial gel formation takes place is of great importance for the spatial distribution of the basic elements. This was confirmed by measuring the permeability of acid skimmilk gels heated at different rates to 30 °C, followed by ageing at 30 °C (table 3.1). Coagulation and gel formation, which start above 10 °C, need a certain time for completion. Thus at the lowest heating rate gel formation should occur at lower temperature. In agreement with the results shown in fig. 3.16 a lower temperature during gel formation resulted in a lower permeability. Unfortunately the exact mechanism of how the coagulating particles form the network has not yet been elucidated. We will return to the effect of temperature on permeability in section 3.4.3.

All experiments on acid casein gels point to the fact that the permeability of these gels after initial gel formation hardly changed with ageing time in contrast to rennet gels (Van Dijk, 1982), indicating that possible rearrangements of the gelnetwork

Fig. 3.16. Permeability coefficient,  $B$  ( $m^2$ ), as a function of measuring temperature for acid skimmilk gels. The gels were aged for 16 hrs at the indicated temperatures.



after that stage were only very local and did not influence the overall structure. After 16 hrs ageing time acid casein gels did not show syneresis. Nor did  $B$  increase with time due to the pressure gradient (between  $4.5$  to  $6.0 \times 10^3 \text{ Pa} \cdot m^{-1}$ ), as found for rennet gels, which are sensitive to microsyreresis (see section 2.8). The heating of the gelation vat used in the permeability apparatus (section 2.8) always lagged behind that of the thermostatted bath because of a slow heat transfer. Therefore the actual heating rate in the vat was lower than the programmed one. This is probably the reason for the small difference in the values found for  $B$ , when acid skimmilk was heated at rates of  $30$  and  $12 \text{ }^{\circ}C/hr$  (table 3.1). However within each experiment this delay in temperature rise was always the same, so that the determined trends are real. However the absolute value of the measured permeability coefficients is probably too low because gel formation occurred at a lower temperature than the programmed one. Therefore for comparison  $B$  was measured for acid skimmilk gels made in tubes placed in a graduated cylinder. This cylinder was heated in direct contact with the liquid of the thermostatted bath (table 3.2). In agreement with the results given above a significant increase of  $B$  from  $1.5$  to  $2.0 \times 10^{-13} m^2$  was seen. Using another gelation vat with a faster heat transfer also resulted in higher values for  $B$ ; for gels, aged

Table 3.1 The effect of heating rate on the permeability coefficient,  $B$  ( $m^2$ ), of acid skimmilk gels. The skimmilk was made from powder B (section 2.1). After heating the gels were aged at 30 °C for 16 hrs. The number of experiments is given in brackets.

Heating rate (°C/hr)	$B$ ( $10^{-13} m^2$ )
30	1.47±0.18 (3)
12	1.43±0.16 (2)
4	1.15±0.09 (2)

at respectively 25 °C and 30 °C,  $B$  increased to  $1.37 \times 10^{-13} m^2$  (section 5.3.1) and  $1.78 \times 10^{-13} m^2$  (section 4.5.5.2) instead of approximately  $1.15 \times 10^{-13} m^2$  (estimated from fig. 3.16) and  $1.5 \times 10^{-13} m^2$ .

The permeability coefficients of acid sodium caseinate gels ( $1.06$  and  $1.04 \times 10^{-13} m^2$ , see table 3.2) are considerably lower than those of acid skimmilk gels of the same casein concentration ( $1.8 \times 10^{-13} m^2$  for 2.62 wt.% and  $2.0 \times 10^{-13} m^2$  for 2.76 wt.%, as derived from fig. 3.15). The fact that the two sodium caseinate samples had equal permeabilities, while they differed in casein concentration, may be due to experimental error. The explanation for these results is not clear. The tendency of a smaller  $B$  for acid sodium caseinate gels agrees with the slightly smaller particle diameter observed on the electron micrographs of these gels (fig. 3.14c and d), assuming that the total volume fraction of particles is more or less the same. Besides, the considerably smaller diameter observed at 4 °C after acidification (fig. 3.10c) and the fact that an acidified sodium caseinate solution tended to coagulate at lower temperature suggest that formation of a more homogeneous gel network should be possible.

Finally in table 3.2 two values are given for the permeability of acid skimmilk gels made at 30 °C with GDL. The permeability of GDL induced gels was slightly, but significantly higher than that of standard acid skimmilk gels. The difference may be due to the lower temperature at which gel formation starts in skimmilk acidi-

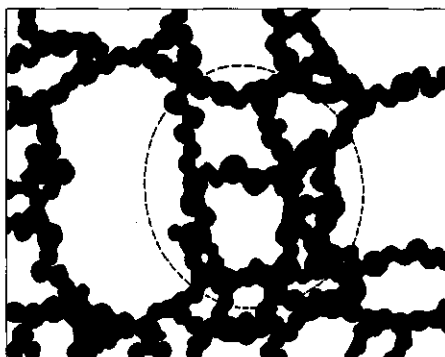


Fig. 3.17. Highly schematic two dimensional picture of the distribution of casein particles in an acid casein gel (pH=4.6). The casein particles have diameters of 80 to 200 nm. The dashed line surrounds a conglomerate of coagulated particles. The picture may be regarded as a projection of a thin section of the gel network (with a thickness of a few particles) on the horizontal plane. The cross sections of all strands in the direction perpendicular to the plane are omitted.

not showing the cross sections of all strands in the direction perpendicular to the horizontal plane.

The exact mechanism for gel formation in acid casein gels is not yet known. It is clear that it occurs in different steps, which depend particularly on temperature and pH. During acidification all individual casein molecules aggregate first into casein particles, which differ strongly from the casein micelles in milk of natural pH. Upon heating the casein particles will coagulate and small strands and small conglomerates will be formed. Out of these larger conglomerates with a less dense structure are formed. Subsequently the gel network consisting of the strands and of the small and large conglomerates of particles will be formed. That formation of a very open network structure is possible in this way, has been indicated by Sutherland and Goodarz-Nia (Sutherland, 1967, Sutherland and Goodarz-Nia, 1971, Goodarz-Nia and Sutherland, 1975), who simulated by means of computer calculations the floc structure in a system of coagulating particles.

The spatial structure with its large pores and thus the permeability of acid casein gels is determined by the ageing temperature in the first stage of gel formation. Different factors may be involved in the formation of the spatial structure, i.e. the diffusion rate of the coagulating particles, the activation energy for coagulation, the interaction energy after coagulation and for rearrangement of the gel network. At higher temperatures the activation Helmholtz energy for aggregation will decrease, which possibly will lead to a coarser network. As will be discussed in chapter V (section 5.4.3.2) rearrangement of a casein gel network as in the case of microsyreresis of rennet gels (Van Dijk, 1982) will only occur at high values of  $\tan \delta$ , which for acid casein gels are only found at the very beginning of gel formation (fig. 3.2). However, when only a few bonds or weak bonds exist between the particles of a strand, the chance that all bonds will break at the same time increases strongly. Then spontaneous rupture of gel strands despite a low value of  $\tan \delta$  may occur. So only at high temperatures, where the dynamic moduli have decreased significantly (section 4.5.3), can rearrangements occur to give a coarser gel network.

In the next chapter we shall discuss in more detail the different interaction forces responsible for aggregation of firstly individual casein molecules and secondly casein particles.

In the next section we shall compare the measured permeability values in relation to the built up of the acid casein gels as discussed in this section.

#### 3.4.3.2 *Comparison of the measured permeability with that of some geometric models*

Van Brakel (1975) and Scheidegger (1960) attempted to describe the structure of a porous medium using a geometrical model, having the same macroscopical properties as for example the permeability. Each geometric model is a simplification of the real spatial structure. We will compare the permeability coefficient of three models (Scheidegger, 1960) with the experimental values for acid casein gels.

The most widely used equation for the permeability of a porous medium is the so called Kozeny-Carman equation (Scheidegger, 1960). The void structure of the porous medium is represented by a bundle of tortuous, non-interconnecting channels of various cross-sections but of a definite length. The permeability is calculated from the flow through the channels and in the first instance expressed in terms of the specific surface area and the porosity ( $\epsilon$ ) of the porous medium. For a system of spheres the specific surface area may be converted into the volume surface average diameter,  $d_{vs}$ , which results in the following equation for B ( $m^2$ ) (Van Dijk, 1982):

$$B = \frac{\epsilon^3 d_{vs}^2}{180(1-\epsilon)^2} \quad (3.3)$$

However the porosity,  $\epsilon$ , should be smaller than 0.5 (Scheidegger, 1960). This condition is at first sight not met in an ideally homogeneously built up acid casein gel. From fig. 3.6c (after Darling, 1982) a total volume fraction of approximately 0.1 ( $\epsilon=0.9$ ) can be calculated for the acid casein particles at pH=4.6 and 30 °C in standard skimmilk. This is in the same range as found for unrenneted casein micelles at pH=6.7 and 30 °C (Walstra, 1979).

A refinement of this model may be found in the so called "cutting and joining model", recently proposed by Maghoub et al. (1982). In this model the bundle of channels is sliced perpendicular to their length and then the cut is rejoined after a random rotation. However this model requires a pore size distribution obtained from a capillary pressure curve and, because of this, is not applicable to acid casein gels.

The theory of Iberall, which may be called a "drag theory" (Scheidegger, 1960) and which holds only for dilute systems, appears more attractive at first sight. The porous medium is represented by a random distribution of circular cylindrical fibres of the same diameter,  $\delta$ . The permeability is calculated from the drag force needed to move liquid along the fibres. This is taken to be equal to the flow resistance of the porous medium. The separation between the fibres and the length of the individual fibres must

both be large compared to the fiber diameter,  $\delta$ . Also the disturbance due to adjacent fibres on the flow around any particular fiber must be negligible. B is given by:

$$B = 3/16 \frac{\varepsilon \delta^2}{1-\varepsilon} \frac{2-\ln Re}{4-\ln Re} \quad (3.4)$$

where Re is the Reynolds number (see eq. 2.2) as defined in section 2.8.1.

The theory of Brinkman also has its basis in the drag theory of permeability. The solid matrix is assumed to consist of spherical particles with radius, R, kept in position by external forces. The permeability coefficient, B, is calculated from the damping force exerted by the particles on the velocity of the liquid flow around them and can be written as:

$$B = \frac{R^2}{18} \left[ 3 + \frac{4}{1-\varepsilon} - 3\sqrt{\left(\frac{8}{1-\varepsilon} - 3\right)} \right] \quad (3.5)$$

A first refinement of this theory would be the incorporation of a particle size distribution. Equation 3.5 is applicable to media with both low and high volume fractions of particles.

If one estimates that the porosity,  $\varepsilon$ , of a homogeneous acid casein gel of standard casein concentration is 0.9 and that the average diameter of the particles or strands is roughly between 100 and 200 nm (fig. 3.14) B can be calculated with equations 3.3 to 3.5. These calculations give values for B which are far too low. This is clearly illustrated in fig. 3.18, where B is depicted as a function of the volume fraction,  $\phi$  ( $=1-\varepsilon$ ), of the casein particles (both on a logarithmic scale) for the three models mentioned. For particle diameter (eq. 3.3 and 3.5) or strand diameter (eq. 3.4) a value of 200 nm was chosen. Since B is proportional to the square of the diameter, it will strongly increase with particle size. At  $\phi=0.1$  the calculated B's, varying from  $9 \times 10^{-15} \text{ m}^2$  to  $6 \times 10^{-14} \text{ m}^2$ , are almost an order of magnitude smaller than the values for acid casein gels ( $1.0-2.0 \times 10^{-13} \text{ m}^2$ ). Moreover the concentration dependence at  $\phi=0.1$  (the slope of the curves here varies from -1.15 to -2.7, see fig. 3.18) is much smaller (except for the Kozeny-Carman model) than that found experimentally where the

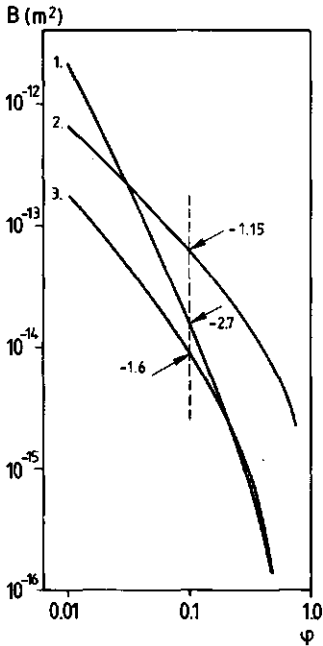


Fig. 3.18. Permeability coefficient,  $B$  ( $\text{m}^2$ ), as a function of volume fraction of the dispersed solid phase,  $\phi$ , calculated for three different model systems. The models used are: 1. Kozeny-Carman. 2. Iberall. 3. Brinkman. The slope of the tangent of the curves at  $\phi=0.1$  is indicated. The diameter of the particles (curve 1 and 3) or strands (2) was chosen to be 200 nm.

slope was  $-3.3$  (see fig. 3.15). Obviously the geometric models described above, represent a much more homogeneous system than the acid casein gel. Van Dijk (1982) proposed that the structurally very similar rennet gels can be considered as particle gels but with much larger particle diameters than those of the primary casein particles (whose diameter is around 100-200 nm). If these large particles (actually the product of aggregation of primary casein particles) are assumed to consist of densely packed casein, their permeability will be negligible compared to the large void spaces between the large particles, where no protein is found. An obvious choice is then to take the dense regions (large conglomerates) in fig. 3.17 as the permeability determining units. The dense regions are considered as spherical with at least a tenfold larger diameter (1-10  $\mu\text{m}$ ) than the primary casein particles. Since the diameter has increased, so must the effective volume fraction be increased, because the large conglomerates contain a lot of extra liquid. Recalculating the permeability coefficient,  $B$ , with a tenfold larger particle diameter (eq. 3.3. and 3.5) or strand dia-

meter (eq. 3.4) shows that the curves in fig. 3.18 will be shifted vertically to higher values of  $B$  over at least two decades. At a volume fraction of 0.4 to 0.5 the correct permeability is found according to the models of both Brinkman and Kozeny-Carman. Also at this value of  $\phi$ , the slope of both curves has decreased to even below -3.3, which confirms the applicability of both these models. Moreover, the minimum porosity requirement of the Kozeny-Carman model is also met.

Our general conclusion is that the acid casein gel can be represented by a porous medium, consisting of spherical aggregates of casein particles. The diameter of these aggregates is of order of micrometers and the effective porosity is approximately 0.5. The diameter of the pores will then approximately equal the diameter of the aggregates (see fig. 3.17).

## 4 RHEOLOGICAL CHARACTERIZATION OF ACID CASEIN GELS

### 4.1 Introduction

As discussed in the previous chapter a casein gel is built up of partly fused particles, which in their turn consist of aggregated casein molecules. Such a gel has a rather inhomogeneous structure, both at the level of the gel network and at the level of the particles themselves. It exhibits viscoelastic properties i.e. (Ferry, 1980) it exhibits both the viscous properties of a fluid and the elastic properties of a solid. Such properties are most fruitfully studied using rheological techniques. In rheology one studies the deformation of a material in relation to both the applied force and to the time scale over which that force is applied and the deformation is measured. Rheology is also concerned with those material properties which determine the deformation as a function of force and time (Darby, 1976).

The rheological properties of an acid casein gel will depend on the spatial distribution of the contributing particles and the kind and number of bonds between and within the particles (section 3.4.1 and 3.4.3). Different types of interaction forces may be involved in the formation of bonds between and within the casein particles. The type, number and magnitude of the different interaction forces largely influence the rheological behaviour of acid casein gels. In an equilibrium situation, the lifetime (the time of existence) of the bonds, whether stressed or not, is of particularly crucial importance for the ratio between the viscous and elastic character of the gel. Moreover, the spatial structure of a gel network, such as a casein gel made from skimmilk by rennet action at pH=6.7 (Van Dijk, 1982), may change with time, due to a constant breaking and reformation of bonds. In an ideally elastic solid all bonds have a permanent character, while ideally viscous behaviour indicates that all bonds have an ephemeral character, such that the lifetime of the bonds is several orders of magnitude smaller than the time scale of deformation. In relation to these aspects one has to realize that the measurement of rheological properties is always constrained to a certain limited time scale.

In this chapter acid casein gels are characterized mainly by one type of rheological measurements i.e. dynamic measurements. Special attention will be given to a rheological characterization of viscoelastic properties and to the different types of interaction forces involved in building up the gel structure.

#### 4.2 Rheological measurements

A sample may be deformed in various ways (such as elongation, bending, compression etc.). A particularly simple and commonly applied type of deformation is the so called simple shear, which is mathematically relatively easy to describe (Darby, 1976). The principle of simple shear is illustrated in figure 4.1a. A force is applied parallel to the surface of a rectangular body. The force per unit of surface area, called the shear stress,  $\sigma$  (Pa), causes a deformation expressed in the shear deformation,  $\gamma$ . For an ideally elastic body (a so-called Hookean body), where all bonds have a permanent character, one can write:

$$\sigma/\gamma = G \quad (4.1)$$

where  $G$  ( $\text{Nm}^{-2}$ ) is called the shear modulus or elastic modulus. After the shear stress  $\sigma$  is applied the body will deform instantaneously to a fixed deformation  $\gamma$ . The opposite behaviour is demonstrated by an ideally viscous fluid, where the lifetime of the bonds is several orders of magnitude smaller than the time scale of deformation. For an ideally viscous fluid Newton's law holds:

$$\sigma = \eta \, d\gamma/dt = \eta \dot{\gamma} \quad (4.2)$$

where  $\eta$  ( $\text{Nsm}^{-2}$ ) is the viscosity. As soon as a stress  $\sigma$  is applied, the liquid will start to flow at a constant rate ( $d\gamma/dt = \dot{\gamma}$ ). However for viscoelastic materials the relation between stress and deformation cannot be simply given by equations 4.1 or 4.2. Usually even a combination is not sufficient, because both  $G$  and  $\eta$  will depend on the applied stress and on the time scale of the measurement, as a result of breakage and formation of bonds (whether spontaneous or forced) in the time scale of deformation. In this context one can distinguish between static and dynamic experi-

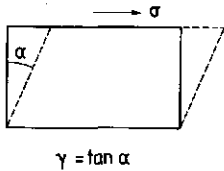


Fig. 4.1a Illustration of simple shear on a cross section of a rectangular body.  $\sigma$  (Pa) is the shear stress and  $\gamma = \tan \alpha$  is the shear deformation.

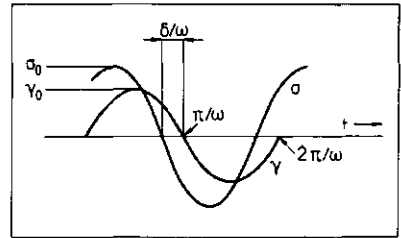


Fig. 4.1b Sinusoidal variation of strain and stress as a function of time for a viscoelastic material (for further explanation, see text).

ments. In static experiments the shear stress  $\sigma$ , the deformation  $\gamma$  or the deformation rate  $\dot{\gamma}$  are fixed at  $t=0$  and either  $\gamma(t)$  or  $\sigma(t)$  are monitored as a function of time. In dynamic experiments  $\sigma$  and  $\gamma$  are varied with time in an oscillatory, generally sinusoidal fashion. The deformation is usually kept sufficiently small to prevent disruption of the gel network and so ensure linear viscoelastic behaviour, which implies that  $\sigma$  is proportional to  $\gamma$  for all applied deformations. In terms of bonds, linear viscoelastic behaviour means that the measurement (i.e. the applied deformation) may in no way influence the spontaneous formation and breaking of bonds, or the strength of those bonds. Neither may formation or breaking of bonds be induced. The time scale of the deformations can be adjusted very easily by changing the frequency of deformation.

When a viscoelastic material is deformed sinusoidally at a frequency  $\omega$  ( $\text{rad.s}^{-1}$ ) according to:

$$\gamma(t) = \gamma_0 \sin \omega t \quad (4.3)$$

where  $\gamma_0$  is the maximum deformation (deformation amplitude), the shear stress  $\sigma$  is given by:

$$\sigma(t) = \sigma_0 \sin(\omega t + \delta) = \sigma_0 (\sin \omega t \cos \delta + \cos \omega t \sin \delta) \quad (4.4a)$$

where  $\sigma_0$  is the maximum stress (stress amplitude) and  $\delta$ , the phase difference between deformation and stress (see fig. 4.1b), originates from the viscous properties of the material. During a deformation cycle, stress carrying bonds will spontaneously break and new stress-free bonds will be formed. In this way part of the energy stored in the system will be dissipated as heat. When the deformation  $\gamma$  passes through  $\gamma=0$ , a number of bonds, which were formed in the preceding half of deformation cycle, have already been deformed in the opposite direction. Therefore  $\sigma(t)$  passes through  $\sigma=0$  at a time  $\delta/\omega$  prior to this point (see fig. 4.1b). The stress function  $\sigma(t)$  therefore runs ahead of the deformation  $\gamma(t)$  by a phase angle  $\delta$ .

In the case of an ideally elastic solid  $\delta$  equals zero and stress is exactly in phase with deformation. For an ideally viscous fluid  $\delta$  equals  $1/2\pi$  and stress is completely out of phase with the deformation, but in phase with the rate of deformation,  $d\gamma/dt$ . In this respect equation 4.4a may be split up into an elastic part and a viscous part. For linear viscoelastic materials  $\sigma_0$  will be proportional to  $\gamma_0$ . So 4.4a can be rewritten as:

$$\sigma(t) = \underbrace{\gamma_0(\sigma_0/\gamma_0 \cos\delta \sin\omega t)}_{\text{elastic}} + \underbrace{\sigma_0/\gamma_0 \sin\delta \cos\omega t}_{\text{viscous}} \quad (4.4b)$$

The first term at the right hand side of equation 4.4b contains the part of the stress in phase with the strain, i.e. the elastic part of the stress. This corresponds to the elastic or storage modulus  $G'$ , which is defined as

$$G'(\omega) = \sigma_0/\gamma_0 \cos \delta \quad (4.5a)$$

$G'$  is a measure of the energy stored and released per cycle of deformation. The second term at the right hand side of equation 4.4b contains the part out of phase with the strain, i.e. the viscous part of the stress. This corresponds to the loss modulus  $G''$ , which is defined as

$$G''(\omega) = \sigma_0/\gamma_0 \sin \delta \quad (4.5b)$$

$G''$  represents the viscous character of the material, it is a measure of the energy dissipated or lost as heat per cycle. The ratio of the maximum shear stress,  $\sigma_0$ , to the maximum shear strain,  $\gamma_0$ , equals the absolute value of the complex shear modulus  $G^*$ :

$$|G^*| = \sigma_0 / \gamma_0 \quad (4.6a)$$

where  $G^*$  can be written as:

$$G^* = G' + iG'' \quad (4.6b)$$

In this study special attention is given to the loss tangent  $\tan \delta$ , which is defined as:

$$\tan \delta(\omega) = G''(\omega) / G'(\omega) \quad (4.7)$$

### 4.3 Interpretation of rheological data

The way in which energy is stored or dissipated in a system during a periodic application of stress depends on the time scale of this process. For macromolecular gels a relation may be found for  $G'$  and  $G''$  as a function of  $\omega$  as shown schematically in fig. 4.2. The curves for three different types of polymer are depicted.

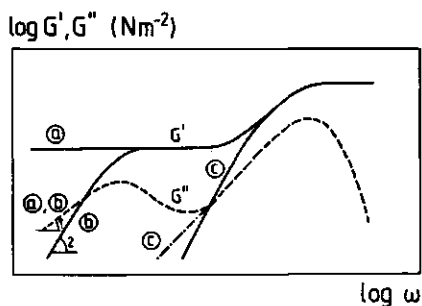


Fig. 4.2 Schematic picture of dynamic moduli  $G'$  (solid lines) and  $G''$  (dashed lines) as a function of  $\omega$ , both on a logarithmic scale, for not chemically crosslinked polymers of rather high (b) and low (c) molecular weight and for a slightly vulcanized rubber (a). The slope of  $G'$  and  $G''$  for curve (b) at small  $\omega$  is indicated.

Curves b and c refer to polymers of respectively rather high and low molecular weight both without chemical cross-linkages. Curve a refers to a slightly vulcanized rubber, which has a permanent character even at very small  $\omega$ . The curve of  $G'$  particularly for case a, may be characterized by two plateau regions: the rubber plateau, which is the lower, and the glassy region, which occurs at very high frequencies. These plateaus are linked by a glass transition area. The part of the curves at low  $\omega$  where  $G''$  exceeds  $G'$  (case b and c) is called the terminal zone. In this study we are interested in the time domain which corresponds to the so-called rubber plateau. In contrast with the ideal system b in fig. 4.2 the lifetime of the physical bonds in acid casein gels varies considerably, which causes an increase of the dynamic moduli as a function of  $\omega$  over the entire frequency range studied.

In the time scale considered in this study the magnitude of the storage modulus  $G'$  is approximately proportional to the elastic modulus  $G$  and so to the effective number of bonds (equation 3.2, section 3.4.1). In protein gels we can consider as bonds all protein-protein contacts whether of a permanent or a temporary character. These bonds will be both intramolecular and intermolecular. Moreover in acid casein gels, which in many respects have the features of a particle gel (section 3.4.3), intermolecular bonds between protein molecules in different particles determine certainly in the first stage of gelation the rheological properties to a large extent.

During a periodic application of stress (or strain) energy can be stored in a bond. The lifetime of a bond, whether it breaks spontaneously or by an applied stress, is usually called the relaxation time. Generally speaking strong bonds with a large energy content will have a long relaxation time. They will establish the permanent or elastic character of a gel. Weak bonds will generally break and reform spontaneously over much shorter time scales. They will contribute to the temporary character of the gel network. In acid casein gels bonds with a large variation in energy content will be present causing a wide variation in relaxation times.

In this respect the lifetime of a bond must be correlated with the oscillation time of the applied deformation. Therefore the

time scale (i.e. the frequency) of the dynamic measurements is of crucial importance. Non relaxing bonds only contribute to  $G'$ , whereas rapidly relaxing bonds only contribute to  $G''$ . Bonds with relaxation times in the time scale of the measurement will contribute to both  $G'$  and  $G''$ . Because at short time scales fewer bonds might relax than at longer time scales, an increase of  $G'$  with frequency can be expected (see e.g. fig. 4.2).

For polymers such as vulcanized or unvulcanized rubbers  $G''$  can be ascribed to the spontaneous formation and breaking of bonds caused by polymer backbone configurational changes (Ferry, 1980), e.g. rotation or translation of complete chains (at the beginning of the rubberplateau in fig. 4.2) or chain segments (in the glass transition area in fig. 4.2). For a protein gel with a high liquid content not only protein-protein but also protein-water bonds must be considered, since energy is also dissipated by liquid movement along the strands and conglomerates, and by liquid movement in and out of the strands and conglomerates. Water-water bonds do not have to be taken into account because of their very short lifetime ( $\sim 10^{-13}$ s). However the most important contribution probably stems from the dissipation of energy caused by the protein-protein bonds (Van Vliet, 1977) relaxing during a deformation cycle.

In an inhomogeneous gel network such as that of acid casein gels (fig. 3.17) many of the particles, incorporated into the large conglomerates, will not contribute effectively to the magnitude of the moduli and other rheological properties. Therefore the effective number of bonds, which depends on the particle concentration and spatial distribution (section 3.4), will be considerably smaller than the total actual number of bonds. The values of both moduli,  $G'$  and  $G''$  at a certain  $\omega$  will depend on the spatial distribution of the basic elements, this determining the effective number of bonds, and on the relaxation behaviour of those bonds, this being related to their energy content. It seems reasonable to assume that the dependence of  $G'$  and  $G''$  on the spatial distribution will be more or less the same. This causes the ratio  $G''/G' = \tan \delta$  to be almost independent of the spatial structure. Therefore  $\tan \delta$  will be more related to the nature of the bonds and the relative importance of the different types of bonds. So  $\tan \delta$  may be a much more sensitive parameter than  $G'$  and  $G''$  for indicating

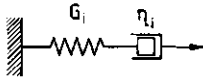


Fig. 4.3 The maxwell element.

changes in the nature of the bonds or in the contributions of the different types of bonds.

#### 4.3.1 Relaxation spectrum

Usually in rheology the distribution of all bonds with relaxation times,  $\tau$ , is described by means of the relaxation spectrum  $H(\tau)$  (Darby, 1976 and Ferry, 1980).  $H(\tau)$  indicates in each interval of  $\tau$  between  $\tau$  and  $\tau+d\tau$  the number of bonds with relaxation times in that interval, multiplied by the modulus belonging to those bonds. In principle  $H(\tau)$  can be derived partly or completely from all measured rheological parameters. Different rheological parameters in their turn can be expressed in each other using  $H(\tau)$  (Ferry, 1980). In such a theoretical approach bonds are mostly described by a mechanical analogue e.g. the most commonly used is the maxwell element, consisting of a spring and a dashpot in series (see fig. 4.3). The maxwell element, in which the applied stress is uniformly distributed, is characterized by a modulus  $G_i$  of the spring and a viscosity  $\eta_i$  of the dashpot. The relaxation time  $\tau_i$  is given by:

$$\tau_i = \eta_i / G_i \quad (4.8)$$

Based on this analogy, mathematical relations between  $H(\tau)$  and  $G'(\omega)$  resp.  $G''(\omega)$  can be derived for an experimental system (Ferry, 1980):

$$G'(\omega) = G_e + \int_{-\infty}^{+\infty} H(\tau) \frac{\omega^2 \tau^2}{1 + \omega^2 \tau^2} d \ln \tau \quad (4.9)$$

where  $G_e$  is the so called permanent network modulus, which represents the bonds which do not relax even at  $t = \infty$ . In this respect  $t = \infty$  does not correspond to infinity, but to extreme long times. Otherwise the definition of  $G_e$  would be redundant.

$$G''(\omega) = \int_{-\infty}^{+\infty} H(\tau) \frac{\omega\tau}{1+\omega^2\tau^2} d\ln \tau \quad (4.10)$$

It is clear that for a given  $H(\tau)$  both  $G'$  and  $G''$  depend on  $\omega$  and on  $\tau_i$ . At each frequency  $\omega$  the bonds relaxing at  $\tau \sim 1/\omega$  are of special interest. They are responsible for the increase of  $G'$  with increasing  $\omega$  in that particular time domain. So an increase of  $G'$  with  $\omega$  points to an increasing number of bonds, which are no longer able to relax during one deformation cycle. Bonds with a relaxation time close to  $1/\omega$  will also give the largest contribution to  $G''$  at that frequency  $\omega$ , because these bonds will be able to carry stress for a considerable time and to relax in the same deformation cycle, and so to dissipate a fair amount of energy.

#### 4.4 Interaction forces in acid casein gels

The conformation of an isolated protein molecule depends not only on intramolecular solute-solute interactions, but also on solvent-solute and solvent-solvent interactions. The presence of a second solute, e.g. low molecular weight electrolyte, also affects conformation. The structure and conformation of casein particles will also depend, in addition to the above-mentioned interactions, on intermolecular protein-protein interactions. Basically these intermolecular interactions are no different from the intramolecular ones. There will be a competition between them. The main interaction forces, which give rise to these interactions, are: hydrophobic bonding, formation of hydrogen bonds, Van der Waals attraction and electrostatic interaction. Steric interactions may also be involved. These types of interaction forces will briefly be discussed below. In the case of unfolded or random coil like protein molecules, bonds may also be formed by entanglements, which are the result of multiple interactions. Although similar in nature the mathematical formulation will be different for all interaction forces except hydrophobic bonding in the case of interaction between different casein particles. Interactions, in which  $\text{Ca}^{2+}$  bridges are involved, can be considered as a special case.

#### 4.4.1 Hydrophobic bonding

The term hydrophobic bonding refers to the tendency of non-polar groups to aggregate in water, thereby decreasing the extent of their interaction with the surrounding water. In fact, the hydrophobic effect arises primarily from the entropy gain of water molecules no longer surrounding a non-polar surface (Tanford, 1973). The attraction of the nonpolar groups for each other plays only a minor part.

Thermodynamically, hydrophobic bonding is characterized by a positive energetic or enthalpic effect (of the order of 1.5 kJ/mol at 25 °C) and a larger positive entropic effect (ca. 3 kJ/mol at 25 °C), which results in a negative Helmholtz or Gibbs energy of formation (see eq. 3.1) of the order of 1.5 kJ/mol at 25 °C (Némethy and Sheraga, 1962). The entropy gain is attributed to a decreased number of ordered water molecules after aggregation of the solutes, whereas the positive enthalpic term would arise from a decrease in hydrogen bonds between the water molecules. The free energy for the formation of hydrophobic bonds at moderate temperatures becomes more negative on raising the temperature. Némethy and Sheraga (1962) predicted an interaction maximum for hydrophobic bonding of aliphatic and aromatic groups at resp. 331 K and 315 K. Van Vliet (1977) found an interaction maximum for partially esterified polymethacrylic acid at ~325 K.

#### 4.4.2 Van der Waals attraction

The Van der Waals interaction between molecules arises from one or more of a family of generally attractive forces, namely: permanent dipole-permanent dipole interactions (described by the Keesom equation), permanent dipole-induced dipole interactions (described by the Debye equation) and induced dipole-induced dipole interactions (described by the London equation). The potential energy for all three types of interaction is related to the intermolecular distance  $x$  by an inverse sixth power dependence (Hiemenz, 1977). The potential energy of the van der Waals attraction between particles of molecular size is given by:

$$v_a = -\beta/x^6 \quad (4.11)$$

where  $\beta$  is a constant representing the various constants in the Deye, Keesom and London equations. For large particles at relatively small interparticle distances the London Van der Waals attraction energy can be calculated to a fair approximation by (Hiemenz, 1977):

$$V_a = - Ar/12H \quad (4.12)$$

where  $A$  is the Hamaker constant,  $r$  is the particle diameter and  $H$  is the shortest distance of separation between the particles. As can be seen the Van der Waals attraction for large particles has a long range character.

#### 4.4.3 Electrostatic interactions

Even at their isoelectric pH the caseins contain several residues carrying either positive or negative charge. In the case of simple coulombic interactions, which are of a long range nature, the potential energy (negative or positive) between such groups would be inversely proportional to their distance apart. However in a salt solution part of the charge will be screened by counter ions, which are partly mobile in the neighbourhood of the protein molecule or partly bound as ionic pairs (Oosawa, 1971). The distribution of counter-ions over both classes depends on charge density, ionic strength,  $I$ , and nature and valency of the salt ions. Oppositely-charged groups will attract each other and intramolecular and intermolecular salt bridges will be formed. In this context even originally equally charged groups may attract one another when the charge of one of them is altered by an association of a divalent counterion such as for example  $Ca^{2+}$  binding to a negatively charged phosphate residue. Because of the high  $Ca^{2+}$  concentration at pH=4.6 the formation of such  $Ca^{2+}$  bridges is very much a possibility.

When a protein molecule as a whole is positively or negatively charged, then, under certain conditions, the interaction between two protein molecules or aggregated protein particles can be described by the so-called DLVO-theory (Hiemenz, 1977). In this theory the attractive term arises from van der Waals attraction

(eq. 4.12). The generally repulsive electrostatic term is related among other things to the electrical potential at the surface of the charged species and to the thickness of the electrical double layer, i.e. the distance over which the electrical potential drops to  $1/e$  times its value at the surface. However, for valid application of the DLVO-theory, the distance between the individual surface charges should be much smaller than the thickness of the electrical double layer. This condition will not be met for casein at pH=4.6. For casein micelles at pH=6.7, where they carry a considerable negative zeta-potential (e.g. Dalgleish, 1984), Payens (1979) calculated a thickness of only 1.1 nm for the electrical double layer. This is a small value as compared to the irregular molecular structure at the boundaries of the casein micelles. Upon acidification the surface potential will decrease due to the decrease of charge and the ionic strength will increase (section 4.5.5.1). Both factors will diminish the double layer thickness, while the distance between individual charges will increase; thus at pH=4.6 the DLVO-theory is no longer valid. Probably most of the charges at pH=4.6 will occur separately or in small patches.

The ionic strength determines the extension of electrostatic interactions and thereby the decrease of potential with distance. At increasing ionic strength both electrical repulsion and attraction will be lowered; when the repulsive electrical effects dominate, this may lead to a more compact protein conformation; a less firm protein conformation is found when the attractive electrical forces dominate. During acidification of casein in skimmilk the number of negative charges will decrease, whereas the number of positive charges will hardly increase. At the same time the ionic strength will increase due to the dissolution of CCP. Thus during acidification the +- electrostatic attraction may possibly only increase as a result of rearrangement of protein molecules. At pH=4.6 the electrostatic interaction between and within casein particles will depend on the interaction between individual charged groups or small charged patches.

#### 4.4.4 Hydrogen bonds

Hydrogen bonds, although having a relatively large energy content, very often are of minor importance, because they require

fixed spatial positions for the contributing molecular groups. Moreover, there is always a competition with hydrogen bonding to water molecules in an aqueous environment. Therefore hydrogen bonds are probably only important in the apolar center of protein molecules or in structured proteins. Schmidt (1971) could only explain the formation of tightly bound dimers of  $\alpha_{s1}$ -casein at pH=2.5 by assuming a contribution from hydrogen bonds. One may therefore assume that for acid casein gels (pH=4.6) hydrogen bonds cannot be neglected.

#### 4.4.5 Steric interactions

Particles with flexible, hydrophilic macromolecules protruding from their surface into solution may be protected against coagulation by a repulsive mechanism due to these macromolecules. If the particles approach closely, the protruding chains will interpenetrate (Walstra and Jenness, 1984) or become compressed; this causes loss of conformational entropy and thus produces interparticle repulsion. Repulsion by hydration may also occur on close contact of the individual hydrophilic macromolecular chains. The total effect is called steric repulsion and its magnitude may be of the order of a few kT per molecular chain (Walstra and Jenness, 1984).

Steric stabilization, originating from all kinds of flexible, hydrophilic (charged or uncharged) casein fragments, will be involved in the stabilization of casein particles. At pH=6.7 steric repulsion may even be the main factor in the stabilization of casein micelles (Walstra, 1979). At pH=4.6 steric repulsion may still contribute considerably to the stability of the casein particles. Since its GMP-portion is negatively charged at pH=4.6 (see section 5.3.1),  $\kappa$ -casein may play a particular role in this stability, whilst the soap-like structure of  $\beta$ -casein may also play a part.

### 4.5 Experimental results

#### 4.5.1 Introduction

In this part of the study the properties of acid casein gels, prepared from skimmilk and sodium caseinate solutions (according

to section 2.1 to 2.3), were mainly tested with the dynamic rheometer, described in section 2.10.1 and 2.10.2. The effect of pH, measuring temperature and ionic strength on the dynamic moduli was studied in order to elucidate the role of the different interaction forces in the formation and structure of acid casein gels. The effect of ageing temperature has already been dealt with in section 3.2.

Gels were aged for at least 16 hrs at temperatures varying from 20 to 50 °C before the dynamic moduli were measured. These measurements involved a variation of measuring temperature from 5 to 50 °C, while the frequency  $\omega$  was kept constant at  $1.0 \text{ rad.s}^{-1}$ , or a variation of frequency from  $\omega=10^{-3}$  to  $10^1 \text{ rad.s}^{-1}$  at constant temperature (not necessarily the ageing temperature). When possible the results of the rheological measurements were related to permeability experiments in order to obtain independent information of the extent of inhomogeneities in the gel network.

The average maximum shear deformation  $\gamma_a$  (section 2.10.2) was kept sufficiently small to ensure linear behaviour.  $\gamma_a$  corresponds to an average value of  $\gamma_0$  (see equation 4.3), since  $\gamma_0$  varies a little from inner cylinder to outer cylinder (see section 2.10.2). For linear behaviour to hold, by definition the shear deformation  $\gamma$  should be proportional to the shear stress  $\sigma$  i.e.  $G'$  and  $G''$  may not change upon variation of  $\sigma$  and  $\gamma$ . Linearity was preserved by keeping  $\gamma_a$  smaller than or equal to 0.035, which is illustrated in fig. 4.4, where  $G'$  and  $G''$  are depicted on a logarithmic scale as a function of  $\gamma_a$  for two gels, one gel with relatively small moduli and one with moduli of common magnitude. It is clear that  $G'$  and  $G''$  tended to decrease only very slowly with increasing applied deformation even at large  $\gamma_a$ . The ratio  $G''/G'$  ( $=\tan \delta$ ) was constant over the whole range of  $\gamma_a$ . Remembering that results between identically prepared gels varied by up to 10%, it is obvious that even at  $\gamma=0.1$  reliable measurements could still be performed. Therefore a value for  $\gamma_a$  of 0.035 was regarded as a safe choice for all gels with  $G'$  varying from 50 to  $1000 \text{ Nm}^{-2}$ .

The experimental part was completed with some static measurements. Using a variant of ordinary stress relaxation measurements (see section 2.10.3) a kind of pseudo-stress relaxation modulus  $G(t)^*$  was determined. The value of this pseudo-stress relaxation

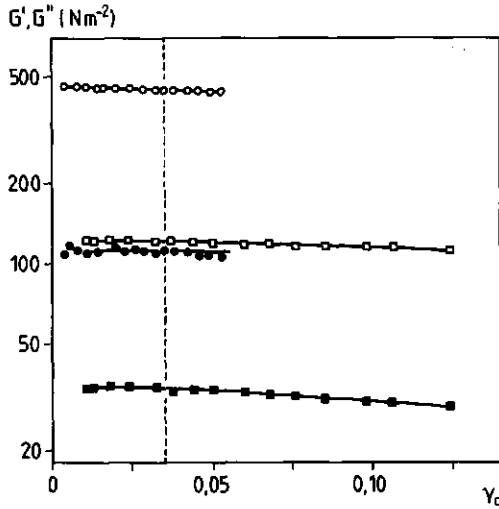


Fig. 4.4 Storage modulus  $G'$  (open symbols) and loss modulus  $G''$  (filled symbols) as a function of the average maximum shear deformation  $\gamma_a$  for two different acid skimmilk gels. The pH of the gels was resp. 4.6 (o,●) and 4.9 (□,■). The gels were aged for  $7.9 \times 10^4$  s (22 hrs) (o,●) and  $6.5 \times 10^4$  s (18.5 hrs) (□,■) hrs at 30 °C. Measuring temperature was 30 °C and  $\omega = 1.0 \text{ rad.s}^{-1}$ . The dashed vertical line indicates the maximum value of  $\gamma_a$  applied during the rheological measurements.

modulus agreed well with the values of the dynamic moduli measured in the same time scale. At long time scales ( $10^4$ - $10^5$  s) a kind of pseudo-permanent network modulus was found, which agreed well with predictions from theoretical computations carried out using the experimental values of the dynamic moduli.

The behaviour of acid casein gels at constant stress and large deformation was studied by employing of creep measurements (section 2.10.4). Assuming a simplified spatial distribution of the casein particles, it is possible to calculate the modulus  $G_s$  of an individual strand of casein particles.

#### 4.5.2 The dynamic moduli as a function of frequency

Strikingly the frequency dependence of the dynamic moduli was rather similar for all acid casein gels tested. Both  $G'$  and  $G''$  tended to increase with the angular frequency  $\omega$  over the whole

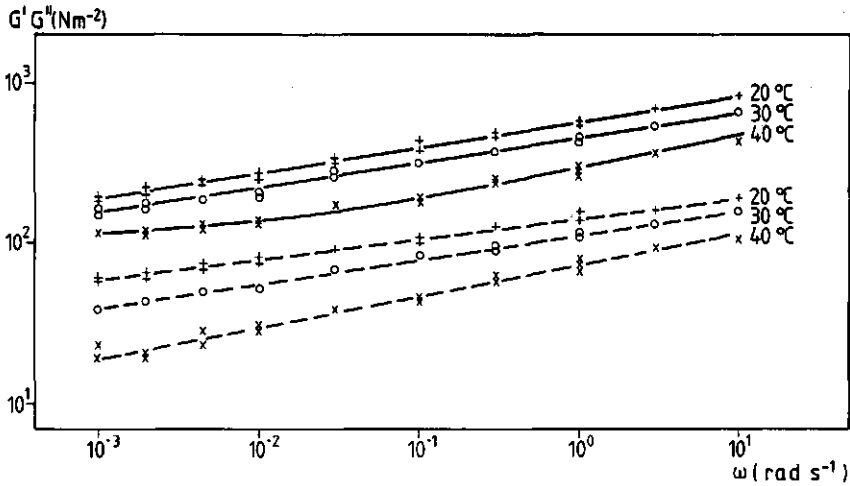


Fig. 4.5 Storage modulus  $G'$  and loss modulus  $G''$  of an acid skimmilk gel (pH=4.6) as a function of the angular frequency  $\omega$  ( $\text{rad}\cdot\text{s}^{-1}$ ). The gel was aged at  $30\text{ }^\circ\text{C}$  for  $5.6\times 10^4$  s (16 hrs) and subsequently tested at the temperatures indicated.

range tested from  $10^{-3}$  to  $10^1$   $\text{rad}\cdot\text{s}^{-1}$ . This is illustrated in fig. 4.5 and 4.6. In fig. 4.5  $G'$  and  $G''$  are shown as a function of  $\omega$  ( $\text{rad}\cdot\text{s}^{-1}$ ) on a double logarithmic scale for an acid skimmilk gel, aged at  $30\text{ }^\circ\text{C}$  for 16 hours and measured at respectively 20, 30 and  $40\text{ }^\circ\text{C}$ . In fig. 4.6 are shown the moduli of an acid skimmilk gel,

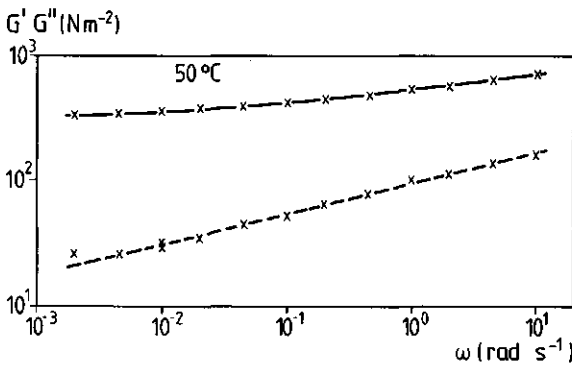


Fig. 4.6 Storage modulus  $G'$  and loss modulus  $G''$  of an acid skimmilk gel (pH=4.6) as a function of the angular frequency  $\omega$  ( $\text{rad}\cdot\text{s}^{-1}$ ). The gel was aged at  $50\text{ }^\circ\text{C}$  for  $5.3\times 10^5$  s (147 hrs) and subsequently tested at  $50\text{ }^\circ\text{C}$ .

which was first aged for 147 hrs at 50 °C and subsequently measured at the same temperature.

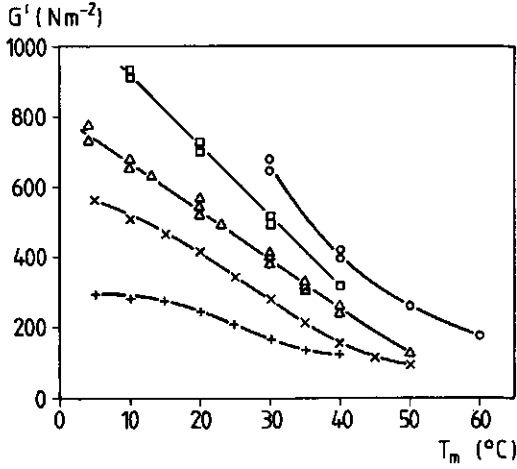
Acid skimmilk gels measured at 30 °C showed a linear relationship between both moduli and frequency, when plotted on a double logarithmic scale (see fig. 4.5). At 30 °C this linear relationship was always found for acid casein gels, whether they were made from skimmilk or sodium caseinate solutions, and whether they were acidified at 2 °C by means of HCl or at 30 °C by means of GDL (section 2.3). The slope of the linear curves at 30 °C was always around 0.15 for both  $G'$  and  $G''$ . As often as we have checked it, we have always found the shape of the  $G'$  and  $G''$  curves as a function of  $\omega$  to be independent of the manner, in which the acid casein gels were made; more or less straight lines were found with about the same slope, but with considerably different magnitudes for the moduli.

The increase of  $G'$  and  $G''$  with  $\omega$  pointed to a relaxation of bonds over the time scale of the measurements. Apparently at all temperatures a considerable number of effective bonds with relaxation times varying from  $\sim 0.6$  to  $6 \times 10^3$  s was present, because  $G'$  increased by a factor 2.5 to 4.5, when  $\omega$  was changed from  $10^{-3}$  to  $10^1$   $\text{rad.s}^{-1}$ .

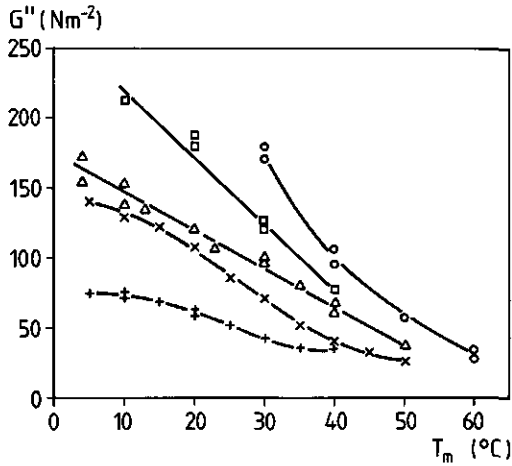
#### 4.5.3 Variation with measuring temperature

Acid casein gels show a peculiar temperature behaviour.  $G'$  and  $G''$  tend to vary very strongly with measuring and ageing temperature when measured at  $\omega = 1.0$   $\text{rad.s}^{-1}$ . Further the shape of the curve representing  $\tan \delta$  as a function of  $\omega$  changes considerably with the measuring temperature. Both aspects will be treated in detail in this section.

The effect of the measuring temperature ( $T_m$ ) on the dynamic moduli is shown in fig. 4.7a and b for acid skimmilk gels after ageing for a period of 16 to 20 hrs at constant temperature. The moduli were measured at  $\omega = 1.0$   $\text{rad.s}^{-1}$ . The gels were aged at temperatures from 20 to 50 °C. Reproducibility was good, except for gels aged at 20 °C, which showed a rather large variation in absolute values of the dynamic moduli; however the temperature dependence found was always the same. A gel was kept 15 to 30 min. at the desired temperature, while the dynamic moduli were mea-



(a)



(b)

Fig. 4.7a and b. Storage modulus  $G'$  (a) and loss modulus  $G''$  (b) of acid skimmilk gels (pH=4.6) as a function of the measuring temperature,  $T_m$ . The ageing temperatures of the gels were respectively 20  $^{\circ}\text{C}$  (+), 25  $^{\circ}\text{C}$  (x), 30  $^{\circ}\text{C}$  ( $\Delta$ ), 40  $^{\circ}\text{C}$  ( $\square$ ) and 50  $^{\circ}\text{C}$  (o).  $\omega=1.0 \text{ rad}\cdot\text{s}^{-1}$ . The ageing time varied between  $5.8 \times 10^4 \text{ s}$  (16 hrs) and  $7.2 \times 10^4 \text{ s}$  (20 hrs).

sured. The moduli did not change significantly during this time, except for the gels aged at 20 and 25 °C, when measured at 40 to 50 °C. In general a considerable decrease of the dynamic moduli with increasing  $T_m$  was found. However, a higher ageing temperature led to higher moduli, when measured at the same  $T_m$ . For  $G'$  and  $G''$  a similar temperature dependence was found. The decrease with measuring temperature tended to become stronger with longer ageing times and higher ageing temperatures. The curves were completely reversible, except for the gels aged at 20 and 25 °C. As soon as temperature was raised above 35 °C (for the gel aged at 20 °C) or 40 °C (for the gel aged at 25 °C) gelation was accelerated and, after the initial decrease of  $G'$  and  $G''$  caused by heating, a strong increase of the moduli was seen at these temperatures itself. Probably gelation as such i.e. the formation of effective bonds is subject to an activation Helmholtz energy, which sharply decreases with increasing temperature. At temperatures below 10 °C it prevents gel formation. This decrease in activation Helmholtz energy with increasing temperature may lead to a faster gelation at higher temperatures especially during the first hours. But even after some time, when the increase of  $G'$  and  $G''$  with  $\log t$  becomes nearly independent of ageing temperature for ageing temperatures between 20 and 40 °C (see fig. 3.1a and b), it is likely that the moduli of a gel aged at 40 °C would increase more strongly with time, when measured from time to time at 30 °C, than for a gel aged and measured at 30 °C.

The small maximum in the  $G'$  and  $G''$  versus  $\log t$  curves (fig. 3.1a and b) for the 50 °C gel at  $t=4.6 \times 10^3$  s (actual temperature at that moment was 40 °C) could be the resultant of an increase in dynamic moduli caused by ongoing gelation and a stronger decrease due to the continuing rise of the measuring temperature, as the system was heated from 2 to 50 °C. The small minimum was found after  $5.6 \times 10^3$  s, when the ultimate ageing temperature of 50 °C was reached.

As can be concluded from the behaviour of  $\tan \delta$  (see later in this section), the character of the interaction forces will probably not depend on ageing temperature, when the moduli are measured at the same temperature  $T_m$ . However, the contribution of the different interaction forces to the effective bonds possibly could

vary with ageing temperature, although the rheological properties measured at  $\omega=1.0 \text{ rad.s}^{-1}$  did not suggest this for the interaction forces dominating around the time scale corresponding to that frequency. The character of the bonds at the same  $T_m$  will not therefore change with ageing temperature. This implies that the increase of the moduli with ageing temperature will probably not be due to a change in the Helmholtz energy (equation 3.2), but to an increase in the number of effective bonds  $N$ .

From section 3.4.2.3 and fig. 3.16 it is clear that larger moduli at higher ageing temperatures are accompanied by a larger permeability. This means that the strongest gels are the most inhomogeneous at the level of the network. This seems contradictory to the general rule that gel strength and the dynamic moduli decrease with increasing inhomogeneity of the gel network. However, the magnitude of the moduli depends on both the number of effective bonds between the particles and the spatial distribution of those particles, whereas the permeability depends on the dimensions of the large pores between the dense areas of particles (see section 3.4.3). As described in chapter 3 inhomogeneity will occur not only at the level of the gel network, but also at the level of the casein particles themselves and at the level of the strands and the small conglomerates of casein particles. Apparently the number of effective bonds strongly increases at higher ageing temperatures. More contacts between the particles are formed, possibly involving previously useless particles (i.e. those not effectively contributing to the gel network), so that the proportion of such useless protein particles decreases. In this respect it would be worthwhile to investigate the possible increase of fusion of the aggregated casein particles with increasing ageing temperature.

$\tan \delta$  ( $G''/G'$ ) was found nearly constant ( $\omega=1.0 \text{ rad.s}^{-1}$ ) over the whole temperature range studied, except for the sample aged at 50 °C. for this sample  $\tan \delta$  significantly decreased at  $T_m > 50$  °C. This was also found for gels aged at higher temperatures (results not shown), but this range of  $T_m$  was not studied extensively. So there was no indication of a clear change in the character of the bonds in the time scale around 6 s ( $\omega=1.0 \text{ rad.s}^{-1}$ ), caused by rise of  $T_m$  from 2 to 50 °C. In any case, most interaction forces are

not so strongly temperature dependent. In the case of a direct effect involving hydrophobic interaction, an increase of  $G'$  and  $G''$  with  $T_m$  would have been expected instead of a decrease (Van Vliet and Lyklema, 1978). In the region between two particles there will always be a competition between intermolecular interactions between protein molecules belonging to different particles and those belonging to the same particle, and a competition between intermolecular and intramolecular interactions within a particle. Therefore it is difficult to give a straightforward explanation in terms of molecular interaction forces for the observed temperature behaviour, because a competition as indicated above depends on the balance between the different types of interaction forces. Moreover, the interaction forces may be effective not only in a direct way, but also in a more indirect manner via the conformation of protein molecules and the structure of casein particles. The resultant of the competition mentioned will largely determine  $G'$  and  $G''$ . But again, as said above most interaction forces in protein molecules are only slightly temperature dependent, that is, except for hydrophobic interactions which go the opposite way. A small shift in the balance of the interaction forces may have a large effect on the conformation of a protein molecule and so on the structure of particles of aggregated protein. Apparently the structure of the casein particles, which form the gel network is of crucial importance. This structure is probably not homogeneous (section 3.3.4 and 3.4.3). It seems justified to assume that it will change from the outside to the inside. The structure of these casein particles will depend strongly on the conformation of and the interactions between the individual casein molecules. A small change in interaction forces can cause large changes in conformation of casein molecules and so in the structure of the particles. Undoubtedly besides the others hydrophobic interactions are involved in determining the conformation of casein molecules. Our hypothesis is now that the observed temperature behaviour is not directly but indirectly caused by hydrophobic interactions, which probably induce a more compact conformation of the casein molecules with increasing  $T_m$  and thus a shrinking of the casein particles. This shrinking in its turn influences the balance between interparticle (only intermolecular) and intraparticle (both intra- and intermolecular) bonds. Probably the number

of interparticle bonds will decrease with  $T_m$ . Further the shrinking of casein particles will be reflected in the decreasing voluminosity of casein with increasing temperature (Darling, 1982, see fig. 3.6c). We will further elaborate this discussion in section 4.6.

The same temperature dependence was observed for acid casein gels whether, made from sodium caseinate solutions acidified in the cold, or from respectively a skimmilk or a sodium caseinate solution acidified at 30 °C by hydrolysis of GDL. This is illustrated in figure 4.8, where  $G'$  is depicted as a function of measuring temperature  $T_m$ . The sodium caseinate solutions acidified in the cold were aged at respectively 20, 30 and 40 °C. For the gel aged at 20 °C the decrease with measuring temperature (of the dynamic moduli) was partly neutralized by an accelerated gelation above 30 °C. This resulted in some irreversible behaviour so that, after cooling down again to 20 °C, the same value for  $G'$  was obtained as for the gel aged at 30 °C. The gels made with the help of GDL are those already shown in fig. 3.5a. They exhibited the same decreasing temperature dependence although at much lower absolute values. This is better seen when  $\log G'$  is plotted as a function of  $T_m$  (not shown).

As stated before  $\tan \delta$  is a parameter which is very sensitive to changes of  $G'$  and  $G''$  with respect to each other. A high value of  $\tan \delta$  ( $>1.0$ ) points to a more liquid like character in a system, while a low value of  $\tan \delta$  ( $<0.1$ ) points to a more elastic character. Moreover,  $\tan \delta$  is related more directly to the nature of the bonds than  $G'$  or  $G''$  (section 4.3). At higher frequencies ( $\omega=10^{-1}$  to  $10^1$  rad.s $^{-1}$ )  $\tan \delta$  did not change significantly either with ageing temperature or measuring temperature, as long as these temperatures were kept below 50 °C. At a measuring temperature of 60 °C and also after longer ageing times at 50 °C (see fig. 3.2)  $\tan \delta$  tended to decrease strongly. All values of  $\tan \delta$  calculated from the moduli depicted in fig. 4.7 and 4.8 ( $\omega=1.0$  rad.s $^{-1}$ ) ranged between  $\tan \delta = 0.20$  and  $0.30$  with the majority around  $\tan \delta = 0.25$ . This spreading was due to experimental error as can be seen in the following figures.

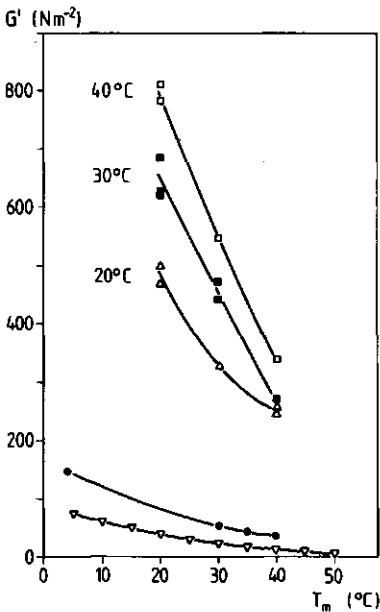


Fig. 4.8 Storage modulus  $G'$  as a function of measuring temperature  $T_m$  for acid casein gels, made from sodium caseinate solutions acidified in the cold ( $\square, \blacksquare, \blacktriangle$ ) and made from skimmilk ( $\nabla$ ) and sodium caseinate ( $\bullet$ ) acidified by means of GDL. The sodium caseinate solutions acidified in the cold (casein conc.=2.6 wt.% and  $C_{NaCl}=0.12$  mol per kg dispersion) were aged for  $6.5 \times 10^4$  s (18 hrs) at the indicated temperatures. The GDL gels (the same as in fig. 3.5a) were aged for resp.  $2.6 \times 10^5$  s (skimmilk) and  $2.3 \times 10^5$  s (sodium caseinate) at 30 °C.  $\omega=1.0 \text{ rad.s}^{-1}$ .

In fig. 4.9  $\tan \delta$  is shown as a function of the angular frequency  $\omega$  for acid skimmilk gels aged at 30 °C and measured at resp. 20, 30 and 40 °C. These are the same gels whose moduli are plotted in fig. 4.5. At low frequencies  $\tan \delta$  increased with decreasing measuring temperature  $T_m$ . Consequently the casein gels became more liquid-like at low temperature and more elastic (or solid-like) at high temperature. This effect of  $T_m$  on  $\tan \delta$  cannot be identical to that related to the temperature time superposition as described by Ferry (1980). Possibly it involves some form of interaction leading to bonds with relaxation times of the order of  $10^3$  s, which cause an increase in the ratio of  $G''$  over  $G'$  at  $\omega=10^{-3} \text{ rad.s}^{-1}$  upon a decrease of measuring temperature. Probably this difference in the effect of  $T_m$  on  $\tan \delta$  at low and high  $\omega$  and the fact that a temperature time superposition cannot be applied, indicate that at least two different interaction forces each with different time dependence are involved. Since the elastic character of acid casein gels increases with  $T_m$  it seems logical that hydrophobic bonding is one of them.

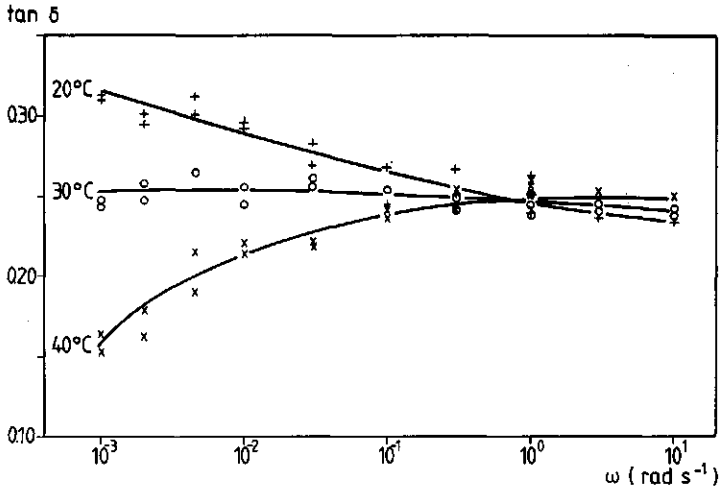


Fig. 4.9 The loss tangent,  $\tan \delta = G''/G'$ , as a function of the angular frequency  $\omega$  for the gels of fig. 4.5. Measuring temperature is indicated.

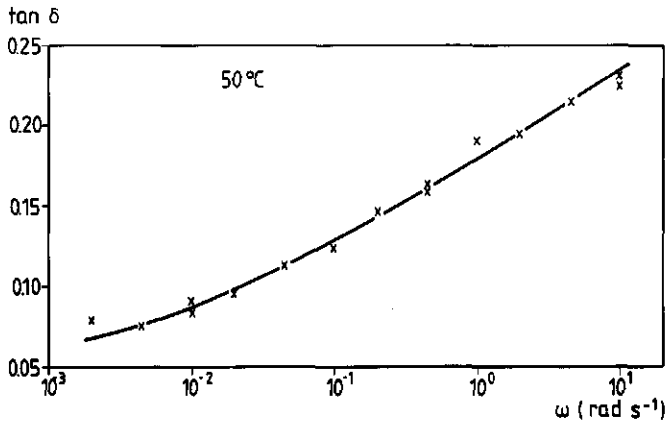


Fig. 4.10 The loss tangent,  $\tan \delta = G''/G'$ , as a function of the angular frequency  $\omega$  for the gel of fig. 4.6. Measuring temperature  $T_m$  was 50 °C.

For a gel aged for 147 hrs at 50 °C the decrease of  $\tan \delta$  at small  $\omega$  was much more pronounced (fig. 4.10). The dynamic moduli  $G'$  and  $G''$  of this gel are depicted in fig. 4.6.

#### 4.5.4 Dynamic moduli of acid skimmilk gels as a function of pH

The effect of pH on the dynamic moduli of acid skimmilk gels, made from skimmilk powder A (section 2.1), was studied. The gels were aged for 18 hrs at 30 °C, measured at the same temperature and tested at  $\omega=1.0 \text{ rad.s}^{-1}$ . Above pH=4.9 no gels were formed. This agrees with the results obtained by GDL induced gel formation, which started at pH=4.94 (section 3.2.4). At pH=4.9 a relative weak gel was formed (fig. 4.13). Between pH=4.8 and 4.3 only a slight variation in the value of the moduli was seen. At pH=4.5 a small maximum occurred. Almost an identical curve for  $G'$  was obtained by Van Dijk (1982), who used skimmilk powder B, although he did not find the small maximum around pH=4.5. In his case the moduli kept increasing from 4.8 to 4.3. This small difference could, however, be easily explained by a greater experimental inaccuracy at low pH. At pH=4.3 the permeability increased sharply (Van Dijk, 1982) pointing to a much coarser gel network. Experimentally it was found that at low pH casein particles were already tending to coagulate at lower temperature, just before the end of the acidification procedure ( $T \leq 2 \text{ }^\circ\text{C}$ ) or during the filling of the rheometer. Although at that moment stirring and streaming will prevent gel formation, the average particle size could increase sharply leading to a much coarser gel network after subsequent heating without stirring. From these experimental results one may conclude that at lower pH the number of effective bonds between two coagulated casein particles will increase. Particularly the

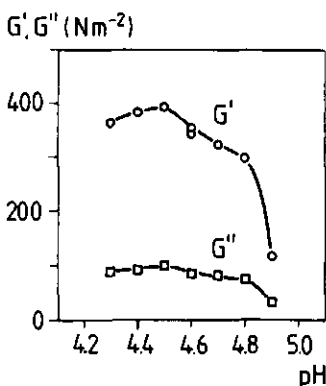


Fig. 4.13 Storage modulus  $G'$  (o) and loss Modulus  $G''$  ( $\square$ ) of acid skimmilk gels as a function of pH. The gels were aged for  $6.5 \times 10^4 \text{ s}$  (18 hrs) at 30 °C. Measuring temperature was 30 °C and  $\omega=1.0 \text{ rad.s}^{-1}$ .

repulsive forces due to negative charges will be decreased. However the more inhomogeneous character of the gel network will decrease the magnitude of the moduli, since the number of stress carrying particles will decrease. The balance between these two phenomena will determine the absolute value of  $G'$  and  $G''$ . Subtle differences in experimental performance may be responsible for the observed differences between the curve for  $G'$  of this study and that obtained by Van Dijk (1982). Probably the strong increase of  $G'$  for some samples at pH=4.3 as found by van Dijk was due to the formation of large dense flocs, which could reach from the inner to the outer cylinder of the measuring apparatus.

For all pH's the dynamic moduli  $G'$  and  $G''$  increased linearly with  $\omega$  ( $\omega$  varying from  $10^{-2}$  to  $10^1$  rad.s $^{-1}$ ) when depicted on a double logarithmic scale. The lines were parallel for all pH's and the slope was the same as in fig. 4.5 for the acid skim milk gel of pH=4.6 measured at 30 °C.

The values of  $\tan \delta$  at  $\omega=1.0$  rad.s $^{-1}$  ranged between 0.24 and 0.28 as the pH was varied from 4.3 to 4.9. This spread was within experimental error;  $\tan \delta$  as a function of  $\omega$  (from  $10^{-2}$  to  $10^1$  rad.s $^{-1}$ ) for pH's between 4.3 and 4.8 gave when measured at 30 °C straight horizontal lines. This behaviour is the same as that already found for all acid casein gels prepared (pH=4.6), however, when measured at 30 °C (see fig. 4.9, 4.11 and 4.12). Only at pH=4.9 was a slight increase in  $\tan \delta$  found at the lowest frequencies.

It is probable that the pH of the system affects the effective number of bonds rather than the nature of the interactions. In this context it should be repeated that we are concerned with bonds and interactions whose relaxations extend over a time scale of roughly 0.6 to  $6 \times 10^3$  s, since, except from the bonds with a more permanent character, these determine the values of the moduli. Typically at higher pH's (4.5 to 4.9) decreasing moduli are accompanied by a decreasing permeability (Van Dijk, 1982). The gel with the lowest permeability i.e. the fewest large pores appears to be the weakest one. It is probable that the pH affects the observed values of the moduli indirectly by modifying the structure of the participating particles (similar to the effect of the measuring temperature  $T_m$ , see last section) and directly by altering

the number of bonds between the particles. In this context electrostatic interactions between positive and negative charges seem to be involved. We will deal further with this in the next sections.

#### 4.5.5 Variation of ionic composition

The ionic strength of the water phase has a marked effect on the formation of acid casein gels (e.g. section 3.4.2.1, fig. 3.13). It was found that a minimum salt concentration of  $\sim 0.10$  mol NaCl per kg dispersion was required to make a gel from sodium caseinate solutions by acidifying in the cold and subsequently heating. Adding less salt causes casein precipitation at pH=4.6 even at 0 °C. Moreover it was found that adding too much salt ( $>0.24$  mol NaCl per kg dispersion) prevented gel formation even at elevated temperatures. Bivalent cations, particularly  $\text{Ca}^{2+}$ , strongly bind to casein (see section 1.2 and table 1.1). The turbidity of sodium caseinate solutions of pH=6.8 sharply increased upon the addition of  $\text{Ca}^{2+}$  ions, ionic strength being maintained constant. The presence of  $\text{Ca}^{2+}$  induces the formation of large aggregates of coagulated casein, sedimentable under gravity. Therefore it seems reasonable to assume that ionic strength and the type of salt ions are important parameters in the formation, stability and structure of casein particles at pH=4.6.

First of all in this section we make a rough estimate of the ionic strength in acid skimmilk at pH=4.6. The effect of the ionic strength on the properties of acid skimmilk gels was mainly studied by measuring the dynamic moduli and the permeability of these gels at different levels of extra added NaCl. However, the effect of salts on sodium caseinate gels was studied in two ways: firstly the total NaCl concentration with no other ions present was varied, and secondly both the NaCl and  $\text{CaCl}_2$  concentration were varied, while the ionic strength was kept constant.

##### 4.5.5.1 *Rough estimate of ionic strength of acid skimmilk*

The ionic strength is one of the conditions in skimmilk, which undoubtedly will change upon acidification. At pH=6.7 the effective ionic strength,  $I$ , for natural skimmilk is estimated to be

0.08 M (Walstra and Jenness, 1984). During acidification I will increase due particularly to the dissolution of Colloidal Calcium Phosphate (CCP). Because of the enormously complex composition of the water phase of skimmilk it is almost impossible to give an exact estimate of I at pH=4.6. Extensive computer computations taking into account all dissociation and association equilibria between the electrolytes present would be necessary. The result obtained would then only be applicable at the temperature imposed for that calculation, because all the equilibria involved are temperature dependent. Moreover, it would only apply to the analysis of a particular sample, since ionic composition is different for every milk sample due to natural variations.

Based on the average ionic composition of natural skimmilk (Walstra and Jenness, 1984) we shall attempt to give a rough indication of the effective ionic strength at pH=4.6 of the standard skimmilk used in this study (section 2.1 and 2.3). First the maximum possible I for the aqueous phase of standard skimmilk at pH=4.6 was calculated. The following assumptions and correction factors were applicable:

- in a first approach all ionic complexes were considered as split into anions and cations.
- all CCP was regarded as dissolved and split into  $\text{Ca}^{2+}$  and phosphate acid residues.
- the charge of the acidic residues was governed by their dissociation constants in the aqueous phase.
- all activity coefficients were taken equal to 1.0.
- of the HCl added during acidification the chloride ion was taken into account but the  $\text{H}^+$  was not. The added  $\text{H}^+$  was thought as being used to dissolve CCP and neutralize protein charge.
- a correction factor was introduced to account for the higher total solids concentration in the standard skimmilk of this study compared to natural skimmilk.
- another correction factor was introduced for the dilution brought about by acid addition.
- the association of ions to macromolecular species, presumably the proteins was not taken into account.
- no contribution of the protein to I was taken into account since we seek first an estimate of the ionic strength of the aqueous phase of skimmilk.

Table 4.1: Calculation of I of the salt solution in standard skimmilk at pH=4.6.

Conc. x valency (cz) of all positively charged ions at pH=4.6 in the aqueous phase of natural skimmilk <sup>a</sup>	0.139 M
idem, of negatively charged ions.	0.088 M
Cl <sup>-</sup> added during acidification	0.058 M
total solids correction factor	1.15
dilution factor due to acidification	1.02

a: all ionic complexes are thought to be split into ions. Charge of acid residues depends on dissociation constants. All ion concentrations are taken from Walstra and Jenness (1984).

- all ionic concentrations were expressed in molar concentrations.

When all values are summed and corrected for the concentration effects (see table 4.1), we obtain an estimated maximum ionic strength of 0.20 M for the salt solution i.e. salt dialysate of standard skimmilk. For the true I in the salt solution one also has to take into account the ion activity coefficients and the ionic complexes formed. Wood et al. (1981) have published computer calculations on the ionic composition, including all association and dissociation equilibria, of salt solutions with an overall composition very similar to that of our skimmilk dialysate. For one of their systems, containing slightly more Ca and phosphate and considerably less chloride than our system, but with about the same amount of citrate, sodium and potassium, Wood et al. calculated an effective ionic strength of 0.15 M, whereas with all ionic complexes now dissociated in this solution a maximum ionic strength of 0.22 M can be calculated. Their experimentally measured pH (=4.19) agreed well with their calculated pH (4.11). Assuming the same 30% reduction of I due to ionic complex association the effective ionic strength I would be estimated at 0.13 to 0.14 M in our salt solution. In standard skimmilk some of the divalent cations (Ca<sup>2+</sup> and Mg<sup>2+</sup>) may be associated with proteins. Therefore the rough estimate of I presented here will probably be a maximum value for standard skimmilk at pH=4.6.

#### 4.5.5.2 The effect of added NaCl on acid skimmilk gels

Standard skimmilk (powder A, 3.0 wt.% casein, section 2.1) was acidified to pH=4.6 at 0-2 °C (section 2.3). Subsequently different amounts of NaCl were added. After dissolving the NaCl by thorough stirring, the solutions were transferred to the rheometer and heated in the appropriate way (section 2.3) to 30 °C. As soon as gel formation had started, the dynamic moduli  $G'$  and  $G''$  were measured as a function of ageing time.

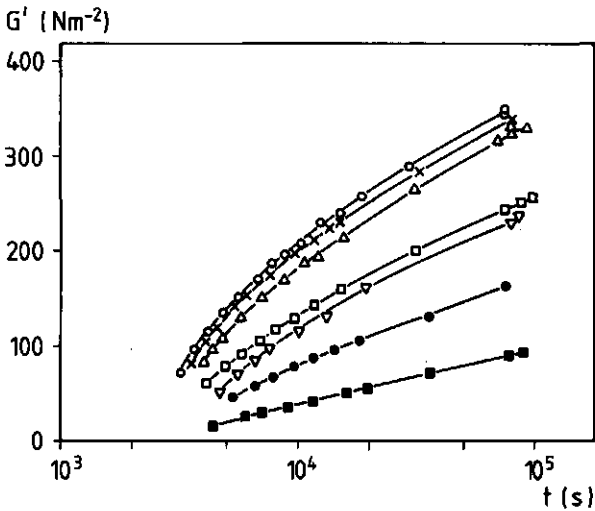


Fig. 4.14 Storage modulus  $G'$  as a function of the logarithm of the ageing time  $t$ (s) for acid skimmilk gels with different amounts of NaCl added. At  $t=0$  and 4 °C the heating of the skimmilk solution was begun. Amount of NaCl added: zero (o), 0.025 (x), 0.050 ( $\Delta$ ), 0.071 ( $\square$ ), 0.084 ( $\nabla$ ), 0.100 ( $\bullet$ ) and 0.125 ( $\blacksquare$ ) mol per kg dispersion.

In fig. 4.14 the storage modulus  $G'$  is depicted as a function of the logarithm of ageing time  $t$ (s) for different amounts of NaCl added (varying from 0.0 to 125 mmol of NaCl per kg dispersion). For  $G''$  the path of the curves was very similar. Addition of NaCl had a distinct effect on the values of the dynamic moduli of acid skimmilk gels. Although measurable gel formation began at approximately the same time (between  $2 \times 10^3$  and  $3 \times 10^3$  s, when the tempera-

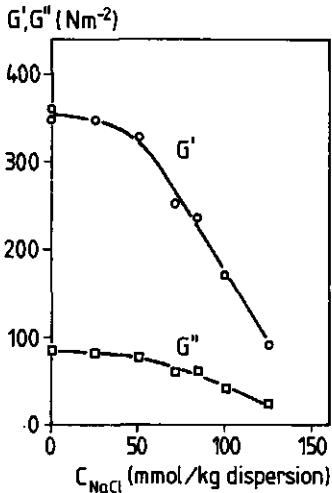


Fig. 4.15 Storage modulus  $G'$  and loss modulus  $G''$  after  $8.6 \times 10^4$  s (24 hrs) as a function of added amount of NaCl for the gels of Fig. 4.14.

ture approached 30 °C), the slope of the ageing curves decreased with increasing amount of NaCl added. However the value of the moduli after a fixed ageing time did not decrease linearly with the amount of NaCl added, as is illustrated more clearly in fig. 4.15. At low levels of added NaCl only a slow decrease of the moduli was seen, which on the addition of more salt passed into a steep decrease above 50 mmol NaCl added per kg dispersion. The upper limit for gel formation at 30 °C seemed to be around 150 mmol NaCl added per kg dispersion. By this level of added NaCl, the ionic strength of the system will have been, roughly, doubled.  $\tan \delta$  fluctuated between 0.23 and 0.26 independent of added salt concentration.

Significantly, the permeability of similarly prepared acid skimmilk gels also decreased as a function of the added amount of NaCl (see fig. 4.16). The permeability coefficient  $B$  was measured at 30 °C after an ageing time of 18 hrs at 30 °C. Again lower values of the dynamic moduli were accompanied by a lower permeability, i.e. a gel network with fewer and/or smaller large pores (section 3.4, see also section 4.5.3 and 5.3.1). Adding extra NaCl apparently decreased the effective number of bonds involved in  $G'$  and  $G''$  in the gel network formed. Since the overall tendency of the gel network is to become more homogeneous, the number of bonds

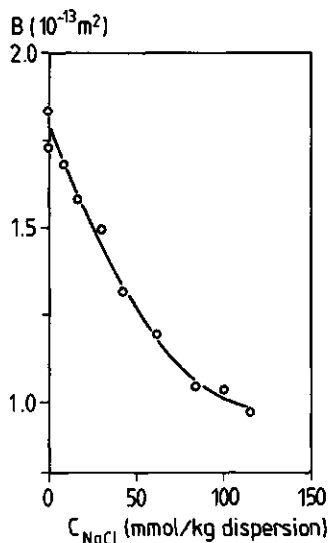


Fig. 4.16 Permeability coefficient  $B$  of acid skimmilk gels ( $\text{pH}=4.6$ ) as a function of added amount of  $\text{NaCl}$ . The gels were aged for  $6.5 \times 10^4$  s (18 hrs) at  $30^\circ \text{C}$  and measured at  $30^\circ \text{C}$ .

between two coagulated particles after a certain ageing time will probably decrease with the  $\text{NaCl}$  concentration. However, the effect of  $\text{NaCl}$  can be not only a direct effect causing fewer interparticle  $\pm$  interactions but also an indirect effect by influencing the structure of the casein particles.

The decrease of  $G'$  in fig. 4.15 and of  $B$  in fig. 4.16 occurs according to respectively a convex and a concave curve. A simple explanation can be given for this behaviour. At low amounts of  $\text{NaCl}$  added the decrease of the number of contacts between the particles is probably counterbalanced by an increasing number of particles contributing to the modulus  $G'$ , since the gel network is becoming more homogeneous. Above 50 mmol  $\text{NaCl}$  added per kg dispersion the gel network can become only slightly more homogeneous with increasing  $\text{NaCl}$  concentration. The decrease of the effective number of bonds is then no longer counterbalanced and  $G'$  decreases more rapidly.

From these results and from the  $\text{pH}$  influence it is clear that ionic interactions are very important in acid skimmilk gels. Whether they act directly via attraction between positively and negatively charged groups on different casein particles is less clear. Neither from the frequency dependence of  $\tan \delta$  at  $30^\circ \text{C}$

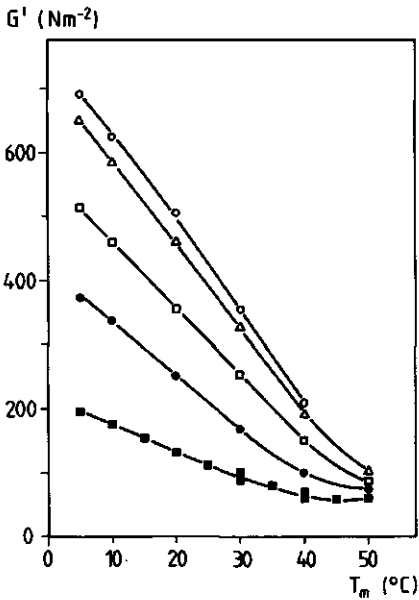


Fig. 4.17 Storage modulus  $G'$  as a function of measuring temperature for some of the gels of fig. 4.14. The symbols refer to the same gels as in fig. 4.14.  $\omega=1.0 \text{ rad.s}^{-1}$ . The measurement of the curve for the gel with 0.125 mol NaCl per kg dispersion added was interrupted during 15 hrs at 30 °C, while the sample was kept at this temperature (see text). Ageing time was respectively  $7.5 \times 10^4 \text{ s}$  (o),  $8.1 \times 10^4 \text{ s}$  ( $\Delta$ ),  $9 \times 10^4 \text{ s}$  ( $\square$ ),  $9.5 \times 10^4 \text{ s}$  ( $\bullet$ ) and  $9.1 \times 10^4 \text{ s}$  ( $\blacksquare$ ).

(not shown), nor from a variation of the dynamic moduli with the measuring temperature (fig. 4.17) was any indication found that the form of interactions determining the moduli had changed due to addition of NaCl.  $\tan \delta$  measured as a function of  $\omega$  ( $10^{-2}$  to  $10^1 \text{ rad.s}^{-1}$ ) gave straight horizontal lines around  $\tan \delta = 0.25$  for all gels. The lines of  $G'$  and  $G''$  ran parallel at different absolute values. The decrease of  $G'$  with the measuring temperature  $T_m$  for gels with different amounts of NaCl added (varying from 0.0 to 125 mmol NaCl per kg dispersion) is illustrated in fig. 4.17. The gels are those for which the ageing behaviour was shown in fig. 4.14. The decrease of  $G'$  as a function of  $T_m$  is very similar to that of ordinary acid skimmilk gels. The absolute slope of the curves decreased with increasing amount of NaCl added. However, the relative decrease of  $G'$  with  $T_m$ , which is apparently when  $G'$  is plotted as a function of  $T_m$  on a double logarithmic scale (not shown), was about the same for all gels. Above 40 °C the rate of gelation increased enormously, particularly at the highest amount of NaCl added. This also occurred with acid skimmilk gels with no added NaCl, when they were aged at 20 and 25 °C (section 4.3). Apparent-

ly the added NaCl increased the activation Helmholtz energy for the formation of interparticle bonds (section 4.5.3). This effect could be neutralized by raising temperature, which decreased the activation energy for gel formation. The values of  $\tan \delta$  fluctuated between 0.22 and 0.27 with no regularity and irrespective of  $T_m$  value or NaCl concentration. This variation was within experimental error.

#### 4.5.5.3 *The effect of NaCl and CaCl<sub>2</sub> on acid sodium caseinate gels*

As discussed in section 3.4.2.1 a minimum ionic strength and a minimum casein concentration are necessary for the formation of acid casein gels. For both acid skimmilk and sodium caseinate the minimum level of I after acidification to form a gel is approximately 0.11 M. It is also probable that gel formation depends on the type of ions present. NaCl will only affect I. However CaCl<sub>2</sub> (especially when present as Ca<sup>2+</sup>) not only affects the ionic strength, but also may react with negatively charged acid residues, mainly phosphate groups (pK=1.5 and 6.5 in unfolded peptide chains, after Walstra and Jenness, 1984), on the proteins and thereby affect protein conformation and casein particle structure.

In a first series of experiments sodium caseinate was dissolved in solutions containing only different amounts of NaCl. After acidification and heating gels were formed with added NaCl in the range of 0.10 to 0.24 M. In these systems acidification increased I by approximately 0.01 M because of the added 0.5 N HCl (see section 2.3), so that after acidification I varied approximately between 0.11 and 0.25 M. In fig. 4.18 G' and G'' of sodium caseinate gels, aged for 16 to 20 hrs at 30 °C before measurement at 30 °C, are depicted as a function of the NaCl concentration.

The same trend is seen as for acid skimmilk gels (fig. 4.15). The dynamic moduli decreased with increasing NaCl conc., while  $\tan \delta$  (not shown) had a constant value of ~0.25. Again the permeability coefficient B decreased with increasing NaCl conc. (see table 4.2).

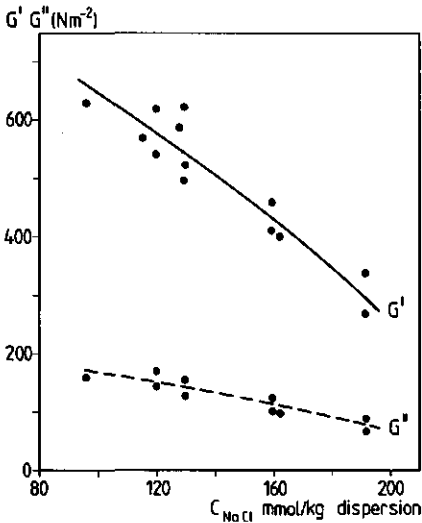


Fig. 4.18 The dynamic moduli  $G'$  (solid line) and  $G''$  (dashed line) of acid sodium caseinate gels as a function of total NaCl concentration. The gels were aged for  $5.8$  to  $7.2 \times 10^4$  s (16 to 20 hrs) at  $30^\circ C$ .  $\omega = 1.0 \text{ rad} \cdot s^{-1}$ .

Figs. 4.15 and 4.18 suggest an optimum ionic strength or salt concentration for gel formation, since no gels can be formed at low  $I$ . Such an optimum salt concentration will depend on pH and casein concentration. For skimmilk this optimum seems to be approximately at the concentration found in standard skimmilk ( $I \sim 0.13$  to  $0.14$  M) with no added salts. A further indication of the existence of an optimum salt concentration for acid skimmilk gels was found in fig. 3.13 (section 3.4.2.1). Adding extra NaCl ( $0.07$  M) to skimmilk solutions of half the casein concentration ( $1.69$  wt.%) of standard skimmilk (curve 1), implying that  $I$  is also lower, increased the dynamic moduli considerably. Under these conditions (lower casein concentration and lower ionic strength) the system was at the other side (left side) of the optimum suggested in fig. 4.15. The bending of curves 1 and 2 in fig. 3.13 can be explained by an increasing ionic strength over the whole casein concentration range. Curve 3 suggests a straight line in the case of constant ionic strength. The variation of  $I$  with casein concentration for the gels measured for curve 1 is obvious. For the gels measured to give curve 2,  $I$  at  $pH=4.6$  still increased with casein concentration because of the dissolution of CCP from the increasing amount of casein particles dispersed in the milk ul-

Table 4.2. Permeability coefficient B of acid sodium caseinate gels as a function of NaCl concentration. The gels were aged for 16 hrs at 30 °C. Spray dried sodium caseinate (section 2.2) was used. The standard deviation is indicated.

B ( $10^{-13} \text{ m}^2$ )	$C_{\text{NaCl}}$ mmol per kg dispersion
1.64 ± 0.08	0.095
1.04 ± 0.06	0.12
0.79 ± 0.02	0.19

tra filtrate. For the gels of curve 1 and 2 at low casein concentrations (at the left side of the salt optimum) an increase in I caused a relatively stronger increase in  $G'$  than expected from the casein concentration alone at constant I. The slopes of  $G'$  versus the casein concentration from curves 1 and 2 were therefore steeper than that of curve 3 at low casein concentrations. At high casein concentrations the salt concentration lay to the right-hand side of the salt optimum, so that depending on the exact conditions a relatively smaller increase of  $G'$  with casein concentration was found, compared to that expected from the casein concentration dependence alone.

For sodium caseinate with only NaCl present the optimum salt concentration was smaller than 0.10 M NaCl. However at this salt level the attraction between casein particles was so strong, that they were already coagulated at 0-2 °C during the acidification procedure. The reason for this difference in behaviour between the acid skimmilk gels and the sodium caseinate gels is not known. As shown in section 3.3.3 the size of the casein particles at pH=4.6 and 0-2 °C was also different. Maybe these effects were related to differences in the ionic composition, which could be of particular importance in the formation of the casein particles during the acidification process.

In a second series of experiments sodium caseinate was dissolved in solutions containing both NaCl and  $\text{CaCl}_2$ . Gel formation was possible when I varied between 0.11 and 0.17 M. However the effects of  $\text{CaCl}_2$  and NaCl were not complementary. This is illustrated in fig. 4.19, where the dynamic moduli  $G'$  and  $G''$  are depicted.

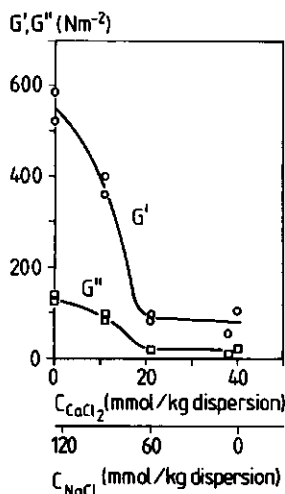


Fig. 4.19 Storage modulus  $G'$  (o) and loss modulus  $G''$  ( $\square$ ) as a function of the concentration of added  $CaCl_2$  and  $NaCl$  for acid sodium caseinate gels (casein conc. 2.76 wt.%). The ionic strength after acidification only varied between 0.13 and 0.14 mol per kg dispersion. The gels were aged for  $6.1 \times 10^4$  s (17 hrs) at 30 °C. Measuring temperature was 30 °C and  $\omega = 1.0 \text{ rad.s}^{-1}$ .

ted as a function of the ionic composition. The ionic strength was maintained approximately constant between 0.13 and 0.14 M, whereas the ratio between  $NaCl$  and  $CaCl_2$  varied from 0.0 to 1.0. Between a  $CaCl_2$  concentration of 10 mmol/kg dispersion and 20 mmol/kg dispersion a strong decrease of the moduli was seen, pointing to a specific effect of  $CaCl_2$ . Such an effect has already been seen, when the casein was dissolved at around  $pH=6.8$ . There, above a  $CaCl_2$  concentration of 10 mmol per kg dispersion the casein molecules tended to aggregate strongly and large particles of colloidal dimensions were formed. At those  $CaCl_2$  concentrations the sodium caseinate solution had a colloidal white, milklike appearance (even at  $pH=6.7$ ) and the largest particles formed tended to sediment. These particles were much larger than the casein particles in skimmilk. It is probable that they were disrupted only partially, if at all, by acidification, resulting in a very coarse gel network on heating, as was confirmed by permeability measurements (table 4.3).

Above a certain critical  $CaCl_2$  concentration ( $\sim 20$  mmol per kg dispersion) it is probable that addition of more  $CaCl_2$  no longer affected the formation of large casein aggregates at  $pH=6.8$ . Consequently there was no further variation in the structure of the casein particles at  $pH=4.6$  and with that no further changes in the values of the moduli and the permeability of the resulting gels.

Table 4.3. Permeability coefficient  $B$  ( $m^2$ ) of acid casein gels made from sodium caseinate dispersed in different salt solutions with the same ionic strength ( $I=0.13-0.14$  M). The samples were aged for 17 hrs at 30 °C. The standard deviation is indicated.

$B$ ( $10^{-13} m^2$ )	salt solution
$1.06 \pm 0.09$	NaCl: 0.12 mol per kg dispersion
$9.22 \pm 0.42$	NaCl: 0.063 mol per kg dispersion and CaCl <sub>2</sub> : 0.021 mol per kg dispersion

The replacement of NaCl by CaCl<sub>2</sub> had no effect on  $\tan \delta$ . This fluctuated between 0.22 and 0.24 for all the gels whose values of  $G'$  and  $G''$  are given in fig. 4.19.

Summarizing the specific Ca effect may be explained by its influence on the size and structure of the casein particles formed before and during acidification. In the subsequent gel formation and ageing these properties are more or less frozen. From the experiments described it is not clear whether there was also a specific Ca effect at pH=4.6 on the casein particles already formed. In order to obtain this information the CaCl<sub>2</sub> should be added after acidification.

#### 4.5.6 Relaxation spectra of acid skimmilk gels

For a complete characterization of the rheological behaviour of acid casein gels various other rheological techniques in addition to dynamic measurements such as constant stress and constant strain measurements would be needed, unless one is able to recalculate the different rheological parameters as a function of the time scale into one another. In principle this can be done quite easily by using the relaxation spectrum,  $H(\tau)$ , calculated from one type of rheological parameters. However, such a spectrum can only be calculated completely, when the time scale is known at which the so-called terminal zone (fig. 4.2) is reached. In this region theory predicts that  $G'$  and  $G''$  should approach zero at a slope of

respectively 2 and 1 with decreasing  $\omega$ , this when  $G'$ ,  $G''$  and  $\omega$  are plotted on a double logarithmic scale (fig. 4.2). For linear viscoelastic materials, such as a physically cross-linked gel, this in principle occurs always as  $\omega$  approaches zero. Such a linear viscoelastic system may be simulated by a system of maxwell elements (fig. 4.3) with different relaxation times. However quite often physically cross-linked gels show over longer time scales a semi-solid-like or permanent character i.e.  $G'$  approaches some constant value  $G_e$  at the lowest measurable  $\omega$  (see fig. 4.2, curve a). In fact the presence of a permanent modulus  $G_e$  depends in principle on the longest time scale taken into consideration; i.e. it depends on the ratio of the longest time scale of the measurement with respect to the longest lifetime of the bonds in the gel network. In such case it might be much more difficult to calculate the relaxation spectrum in an unequivocal manner. One way to derive  $H(\tau)$  then is by calculating it from  $G''$  using eq. 4.10. Subsequently  $G'$  is recalculated from  $H(\tau)$  using eq. 4.9. The calculated and experimental values of  $G'$  should agree then, when the possibility of a permanent network modulus  $G_e$  is taken into consideration. Permanent refers in this case to the longest experimental time.

Since the time/temperature superposition principle could not be applied to acid casein gels and since experimental limitations always constrained the computed relaxation spectrum to a relatively small range of  $\omega$  (4 decades at most in this study), at best, only a semi-permanent network modulus could be calculated.

In the context of this study we were interested in the possible presence of a so-called permanent network character in acid skim-milk gels over time scales between  $10^3$  to  $10^5$  s (0.25 to 25 hrs). It is, however, also possible that over these time scales  $G'$  and  $G''$  keep decreasing at more or less the same slope or that the gel behaves as a liquid,  $G'$  and  $G''$  approaching zero at a slope of respectively 2 and 1.

The presence of a permanent network character can be tested experimentally by measurements over very long time scales. Different methods are available, but stress relaxation measurements are most convenient for this purpose. At  $t=0$  a certain constant deformation  $\gamma$  is applied suddenly and the shear stress  $\sigma(t)$  is monitored as a

function of time. The shear stress will decrease with time and eventually it will relax to  $\sigma=0$  or to a constant value  $\sigma=\sigma_\infty$ . The permanent network modulus is defined as:

$$G_e = \sigma_\infty/\gamma \quad (4.14)$$

By means of this type of experiment it can be checked whether the value of  $G_e$  derived from the experimental dynamic moduli by applying eqs. 4.9 and 4.10 is a reasonable one. In this section some results of computer simulations on the dynamic moduli of acid skimmilk gels (kindly performed by Prof. B. de Cindio, Università degli studi di Napoli) will first be presented. These theoretical calculations suggested the possibility that a semi-permanent network modulus was present beyond the time scale of  $6 \times 10^3$  s. Therefore acid skimmilk gels were tested over longer time scales by means of a variant of a stress relaxation experiment. This variant however had some disadvantages, because both  $\sigma(t)$  and  $\gamma(t)$  changed with time.

#### 4.5.6.1 Computation of the relaxation spectrum and of a semi-permanent network modulus

Acid casein gels were considered as a system of parallel Maxwell elements. As a first step the relaxation spectrum  $H(\tau)$  was derived from the loss modulus  $G''$  by means of an iterative method (de Cindio et al., 1977), using eq. 4.10 over a truncated frequency range:

$$G''(\omega) = \int_{\ln(\tau_1=1/\omega_1)}^{\ln(\tau_2=1/\omega_2)} H(\tau) \frac{\omega\tau}{1+\omega^2\tau^2} d\ln \tau \quad (4.15)$$

where  $\omega_1$  ( $=10^1/2\pi$  s $^{-1}$ ) and  $\omega_2$  ( $=10^{-3}/2\pi$  s $^{-1}$ ) are the maximum and minimum experimental value of  $\omega$ . The calculations begin from the experimental values of  $G''$  and  $H(\tau)$  is calculated in a first approach. Subsequently  $G''$  is recomputed from  $H(\tau)$ , which is continually adjusted to obtain the best fit between the experimental  $G''$  and its recomputed value. In fig. 4.20 an example of a calculated

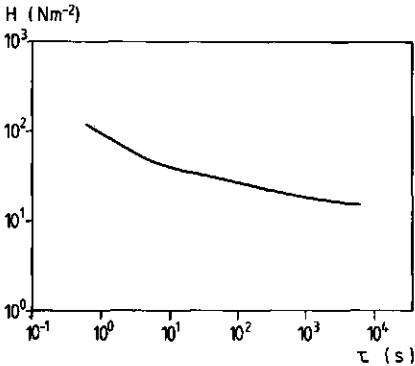


Fig. 4.20 The relaxation spectrum  $H(\tau)$  calculated from the loss modulus  $G''$  (see text) for the acid skimmilk gel of fig. 4.5, which was tested at 40 °C.

relaxation spectrum is shown. In the situation where  $H(\tau)$  is completely known and  $G_e$  is zero,  $G'$  and  $G''$  can be converted directly into each other. However, in this study  $H(\tau)$  was truncated at the lowest measurable frequency, which implies that the curve of  $\log G''$  versus  $\log \omega$  was assumed to have a slope of 1 in the frequency range below the truncated frequency. Therefore  $G_e$  would be due to all bonds having a relaxation time greater than  $\sim 10^4$  s. For many macroscopical properties, which are of interest for manufacture on a factory scale, this is equivalent to an infinitely long time.

$G'$  may be derived then from  $H(\tau)$  according to the integral term in eq. 4.9 (for the truncated frequency range) and the difference between calculated and experimental values of  $G'$  ascribed to  $G_e^*$ :

$$G'_{\text{exp}} = G_e^* + \int_{\ln(\tau_1=1/\omega_1)}^{\ln(\tau_2=1/\omega_2)} H(\tau) \frac{\omega^2 \tau^2}{1 + \omega^2 \tau^2} d \ln \tau \quad (4.16)$$

where  $G_e^*$  is a semi-permanent network modulus. The word semi is used to indicate among other reasons that  $G_e^*$  was obtained from only a very limited frequency range. For acid casein gels a substantial value for  $G_e^*$  was found. This value showed little variation over the experimental range of  $\omega$  as opposed to the variations of  $G'$  and  $G''$  (fig. 4.21), which favours the validity of the calculation. The constant value of  $G_e^*$  as a function of  $\omega$  implies an increase in the proportional contribution of  $G_e^*$  to the experimental values of  $G'$  at small values of  $\omega$ , as is illustrated in fig.

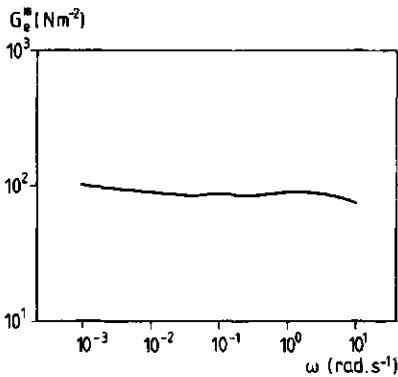


Fig. 4.21 The semi-permanent network modulus  $G_e^*$  as a function of angular frequency  $\omega$ , calculated from the storage modulus  $G'$  and the relaxation spectrum  $H(\tau)$  (see text) for the acid skimmilk gel of fig. 4.5, which was tested at 40 °C.

4.22. In this figure the ratio of the calculated value of  $G_e^*$  to experimental value of  $G'$  is depicted as a function of  $\omega$  for four different acid skimmilk gels. Curve 1 refers to an acid skimmilk gel, which was aged for 147 hrs at 50 °C and subsequently measured at 50 °C (for dynamic moduli, see fig. 4.6). Curves 2 to 4 refer to acid skimmilk gels, which were aged for approximately 18 hrs at 30 °C and subsequently measured at resp. 40 °C, 20 °C and 30 °C (for dynamic moduli see fig. 4.5). For the gels aged at 30 °C (curves 2 to 4)  $G_e^*$  varied between 80 and 150  $\text{Nm}^{-2}$  (see fig. 4.21 for the gel measured at 40 °C), while for the gel aged at 50 °C a straight line at  $G_e^*=300 \text{Nm}^{-2}$  was found. Of course the value obtained for  $G_e^*$  will be very sensitive to the smallest  $\omega$ , where the range was truncated. It appears that at the time scales considered the gel aged at 50 °C showed a more pronounced solid-like behaviour than the three gels aged at 30 °C, which all showed a similar more liquid-like behaviour with a tendency to be more liquid-like at low  $T_m$ . This conclusion was also obtained more qualitatively from the behaviour of  $\tan \delta$  as a function of measuring temperature at low frequency (section 4.5.3).

#### 4.5.6.2 The value of a pseudo-stress relaxation modulus at long time scales

The dynamic viscometer was used to roughly test the permanent character of acid skimmilk gels (section 2.10.3) at long time scales. For this purpose the driving shaft was set at its maximum displacement. This corresponded to the maximum amplitude used for

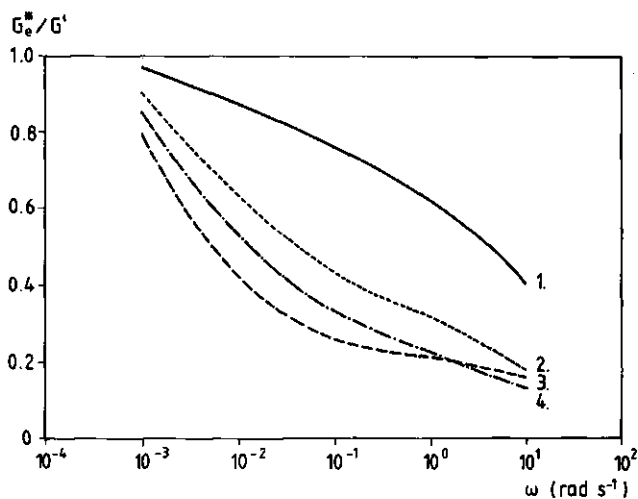


Fig. 4.22 The ratio  $G_e^*/G'$  as a function of angular frequency  $\omega$  ( $\text{rad}\cdot\text{s}^{-1}$ ). Curve 1 refers to the gel of fig. 4.6, which was aged for  $5.3 \times 10^5$  s (147 hrs) at  $50^\circ\text{C}$  and subsequently tested at  $50^\circ\text{C}$ . Curves 2 to 4 refer to the gels of fig. 4.5, which were aged for  $5.8 \times 10^4$  s (16 hrs) at  $30^\circ\text{C}$  and subsequently tested at resp.  $40^\circ\text{C}$ ,  $20^\circ\text{C}$  and  $30^\circ\text{C}$ .

dynamic measurements within the linear region. The displacement of the inner-cylinder was measured as a function of time. Because of the visco-elastic character of the gel both  $\gamma(t)$  and  $\sigma(t)$  will change with time. As the amplitude of the inner-cylinder increases,  $\sigma(t)$  will decrease and  $\gamma(t)$  will increase. Therefore we define a pseudo-stress relaxation modulus  $G(t)^*$  as:

$$G(t)^* = \sigma(t)/\gamma(t) \quad (4.17)$$

Ultimately  $G(t)^*$  will reach a limit value  $G_\infty^*$ , which may be regarded as a parameter characteristic of the permanent character of a gel network. For that reason we will call  $G_\infty^*$  a pseudo-permanent network modulus.

In fig. 4.23  $G(t)^*$  is depicted as a function of the logarithm of time for different acid skimmilk gels (made from skimmilk powder A, section 2.1). One series of gels were aged for 19 to 25 hrs at  $30^\circ\text{C}$  and subsequently tested at resp. 10, 20, 30 and  $40^\circ\text{C}$ . One gel was aged for 175 hrs at  $40^\circ\text{C}$  and subsequently tested at  $40^\circ\text{C}$ .

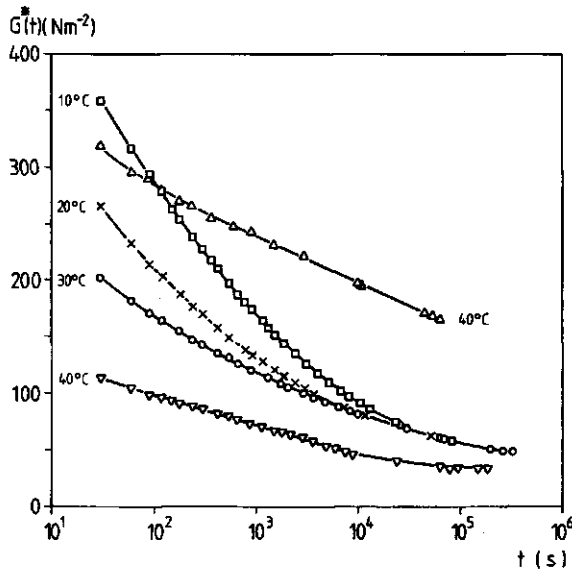


Fig. 4.23 The pseudo-stress relaxation modulus  $G(t)^*$  as a function of the logarithm of measuring time for five different acid skimmilk gels. Four gels ( $\square, \times, \circ, \nabla$ ) were aged for  $6.8 \times 10^4$  s to  $9.0 \times 10^4$  s (19 to 25 hrs) at  $30^\circ\text{C}$ , before  $G(t)^*$  was measured (measuring temperatures indicated at the left handside of the figure). The remaining gel (measuring temperature indicated at the right handside of the figure) was aged for  $7.3 \times 10^5$  s (175 hrs) at  $40^\circ\text{C}$ , before  $G(t)^*$  was measured.

$G(t)^*$  decreased with time for all gels tested, but even after  $10^5$  s (30 hrs) a considerable value of  $G(t)^*$  remained, confirming a kind of permanent character in these acid skimmilk gels. The computed values of  $G_e^*$  at  $\omega = 10^{-3}$  rad.s $^{-1}$  (varying from  $100 \text{ Nm}^{-2}$  at  $40^\circ\text{C}$  (fig. 4.21) to  $150 \text{ Nm}^{-2}$  at  $20^\circ\text{C}$ ) were of the same order of magnitude as the values of  $G(t)^*$  after  $6 \times 10^3$  s. However at longer times  $G(t)^*$  decreased further indicating that for the calculation of  $G_e^*$  the frequency range had been truncated at values of  $\omega$  which were too large. In this context it would be interesting to compute  $G_e$  and  $H(\tau)$  from fig. 4.23 and compare these results with the data calculated from the dynamic moduli according to eqs. 4.15 and 4.16. Clearly more research in this field is necessary.

The rather gradual decrease of  $G(t)^*$  with the logarithm of

time (fig. 4.23) for the gels aged at 30 °C was halted at longer times probably partly because of an ongoing gelation, which tended to increase the modulus  $G(t)^*$ . The gel aged for  $7.3 \times 10^5$  s (175 hrs) at 40 °C showed a substantially higher  $G(t)^*$  and an almost linear decrease of  $G(t)^*$  with the logarithm of time. In this case  $G'$  hardly increased during the  $G(t)^*$  experiment, whereas for the gels, aged for  $6.8$  to  $9.0 \times 10^4$  s at 30 °C, the increase of  $G'$  during the  $G(t)^*$  experiment ran from 15% at 10 °C to 60% at 40 °C. Apparently  $G(t)^*$  increased at higher ageing temperatures and longer ageing times; this agreed with the theoretical calculation of  $G_e^*$  from the dynamic modulus for the gel aged for 147 hrs at 50 °C with respect to  $G_e^*$  for the gels aged at 30 °C (see fig. 4.22).

Significantly the decrease of  $G(t)^*$  with the logarithm of time for the gels aged at 30 °C (fig. 4.23) was more pronounced at lower temperature. However the dynamic modulus  $G'$  of these gels after ageing was equal to  $355 \text{ Nm}^{-2}$  at 30 °C except for the one tested at 20 °C, where  $G'$  was equal to  $310 \text{ Nm}^{-2}$  at 30 °C. The tendency of the storage moduli to decrease faster with decreasing frequency at longer time scales for lower  $T_m$  was already seen in fig. 4.5. Obviously more bonds relaxed faster in the time scale below roughly  $10^4$  s at lower temperature, which agreed with the more liquid-like character at lower measuring temperatures as indicated by the higher values of  $\tan \delta$  at lower angular frequency (section 4.5.3). After  $10^4$  s  $G(t)^*$  seemed to be almost independent of measuring temperature.

#### 4.5.7 Creep measurements

The behaviour of acid skimmilk gels prepared from skimmilk powder B at large deformations was studied by constant stress measurements (section 2.10.1). Before the measurement the gels were aged for 16 hrs at 30 °C and subsequently tested at the same temperature. At  $t=0$  a constant stress  $\sigma$ , varying from 10 to 175 Pa, was applied. The shear deformation  $\gamma(t)$  was measured as a function of time for loading times up to 900 s (15 min). These results were the so-called creep curves. A fast initial increase of  $\gamma$ , due to the elastic character of the gel, was followed by a slow gradual increase of  $\gamma$ , due to its viscous character, until fracture occurred. Each gel was used only once. In fig. 4.24 the shear deforma-

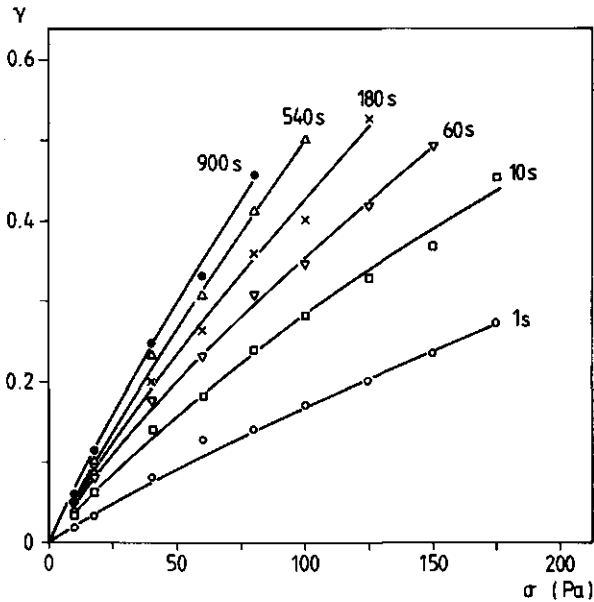


Fig. 4.24 The shear deformation  $\gamma$  as a function of the shear stress  $\sigma$  derived from creep measurements for acid skimmilk gels (pH=4.6). Each gel, aged for  $5.8 \times 10^4$  s (16 hrs), at 30 °C, was measured only once at 30 °C at one constant shear stress  $\sigma$ . The loading time is indicated.

tion  $\gamma(t)$  is shown as a function of the applied constant stress at different time intervals.  $\gamma(t)$  tended to increase gradually but less than linearly with  $\sigma$  until the network was broken. Independently of the loading time macroscopic fracture occurred at a  $\gamma$  of 0.5-0.6. In contrast to  $\gamma$ ,  $\sigma$  at the point of fracture strongly depended on the loading time. Below a  $\sigma$  of  $80 \text{ Nm}^{-2}$  the gel network remained macroscopically intact for at least 900 s, while the highest applied  $\sigma$  of  $175 \text{ Nm}^{-2}$  caused fracture after ca. 20 s. Qualitatively this picture was the same as that found by Van Dijk (1982) for rennet gels. However quantitatively there was a large difference. The deformation at fracture for rennet gels was much larger namely ca. 1.5, while the stress at fracture was much lower e.g.  $10 \text{ Nm}^{-2}$  for a loading time of 900 s. Significantly this difference in stress at fracture ( $90 \text{ Nm}^{-2}$  in contrast to  $10 \text{ Nm}^{-2}$ )

after loading times of 900 s was larger than the difference in the storage modulus, which equalled approx.  $400 \text{ Nm}^{-2}$  for the acid skimmilk gels and approx.  $110 \text{ Nm}^{-2}$  for rennet gels, indicating that these parameters were not directly related. Rennet skimmilk gels probably have a much less permanent network character than acid skimmilk gels; this conclusion is supported by the very low value of  $G_e^*$ , which can be calculated according to section 4.5.6.1 from the dynamic moduli of rennet gels (Van Vliet and de Cindio, unpublished results).

The maximum deformation of 0.5 to 0.6 found in these constant stress measurements agreed well with a maximum deformation varying from 0.5 to 0.8 found in stress overshoot experiments (not presented in this study). In those experiments the shear stress  $\sigma(t)$  was measured as a function of the shear deformation  $\gamma(t)$  on applying a constant shear rate  $\dot{\gamma}$ .

The less-than-linear increase of  $\gamma$  with  $\sigma$  indicates that with higher applied  $\sigma$  the shear modulus  $G$  should increase. At first sight this seems to be in contradiction with fig. 4.4, where the dynamic moduli  $G'$  and  $G''$  slightly decreased with  $\gamma$ . However in the constant stress experiments not enough data in the low  $\gamma$  region were obtained to check whether a sigmoid shaped curve was found at low  $\gamma$ . In fact the very limited data obtained do not exclude such a shape. The increase of  $G$  with  $\gamma$  might be due to bent strands, which only contribute at larger deformations, when they are stretched. At increasing  $\gamma$  the number of stress-carrying strands will increase, although the strands already stretched at  $t=0$  will break.

From the slope of the  $\gamma$  versus  $\sigma$  curve after 1 s, extrapolated to  $\gamma=0$  and  $\sigma=0$ , a shear modulus  $G$  of approximately  $500 \text{ Nm}^{-2}$  was calculated. This is of the same order of magnitude as  $G'$  for acid skimmilk gels at high  $\omega$ . In this calculation the already mentioned possibility of a sigmoid shape of the  $\gamma$  versus  $\sigma$  curve at small  $\gamma$  was not taken into account.

#### 4.6 Estimation of the modulus of a strand of particles

The modulus of an inhomogeneous acid casein gel will depend on the number and the strength of the strands, connecting the large

aggregates of casein particles. Assuming a very simplified spatial distribution it is possible to estimate the order of magnitude of the modulus of a strand of particles.

The gel network is thought to be built up of a cubic array of strands, which extend in three perpendicular directions. Each strand reaches from one side of the network to the other. At regular distances, i.e. at the angular points of the cubic array, the strands of particles will intersect each other forming crosslinks. Only a fraction  $f'$  of the total number of available casein particles will be built into the strands. The remainder of the casein particles are thought to be accumulated at the crosslinks and thus forming large aggregates. A very schematic two-dimensional picture of such a network is given in fig. 3.12d. The segment of a strand between two crosslinks may be represented by a cylinder of length  $L$  and diameter  $d$ . This  $d$  is the actual diameter of the segments of the strand between the large aggregates of casein particles. This implies that only part of the aggregates at the crosslinks is thought to be effective in controlling the mechanical properties of the gel. The volume of such a segment of strand will be given by  $\pi d^2 L/4$ . Suppose we have  $N$  cylinders per  $m^3$ , then the volume fraction  $\phi'$  of segments and so of all strands can be written as:

$$\phi' = 1/4 N \pi d^2 L \quad (4.18)$$

The total length of stress carrying segments of strands amounts  $NL$  per  $m^3$  of total gel volume. Remembering that the strands extend in three perpendicular directions, the number of segments of strands carrying a tensile stress across one  $m^2$  is as a first approximation, given by:

$$1/3 NL = \frac{4\phi'}{3\pi d^2} \quad (4.19)$$

When the gel network is sheared strands carrying a tensile force will be elongated. The elongation force  $f$  for a segment of strand, when it is elongated from  $L$  to  $L+dL$ , can be written as (Van Vliet, 1977)

$$f = 3G_s A \frac{dL}{L} \quad (4.20)$$

where  $A$  is the cross section area ( $=\pi d^2/4$ ) and  $G_s$  the modulus of a strand.  $G_s$  is considered to have the same value over the whole strand and for all strands. Macroscopically the shear stress  $\sigma$  may be coupled to the elongation force  $f$  by (Van Vliet, 1977):

$$\sigma = \frac{4f'\phi}{3\pi d^2} f \quad (4.21)$$

where  $\phi$  is the total volume fraction of casein particles and  $f'$  is a correction factor for the fraction of particles not contributing to the strands. In fact  $f'\phi$ , which equals  $\phi'$  in eqs. 4.18 and 4.19, is the volume fraction of particles, which form the strands. At small deformations a simple relation between the macroscopical shear deformation  $\gamma$  and the elongation  $dL/L$  may be derived (Van Vliet, 1977):

$$\gamma = 2 \frac{dL}{L} \quad (4.22)$$

Using equation 4.20 to 4.22 the shear modulus  $G$  can be written as:

$$G = \sigma/\gamma = f'G_s \phi/2 \quad (4.23)$$

or

$$G_s = \frac{2G}{f'\phi} \quad (4.24)$$

Thus a simple relationship between the shear modulus  $G$  and the modulus of a strand  $G_s$  is found. The factor 2 may be somewhat variable, in that it depends on the arbitrary assumptions made regarding the geometrical structure assumed in the model. Kamphuis (personal communication, and Kamphuis, 1984) derived a similar relationship to equation 4.24 with a factor 5 instead of 2, when he assumed a more random distribution of strands. Equation 4.24 seems to be only valid for calculating the order of magnitude of  $G_s$ .

To apply equation 4.24 to acid skimmilk gels requires a rough estimate of  $f'$ . From e.g. permeability measurements and the relationship found between  $G'$  and the casein concentration (chapter 3) it follows that acid casein gels are very inhomogeneous; this implies that only a relatively small part of the casein actually contributes to the mechanical properties of the gel. If we say that  $f'$  is around 0.1, i.e. effectively 90% of the particles do not carry an applied stress, that  $\phi$  is also  $\sim 0.1$  and  $G$  is  $\sim 500 \text{ Nm}^{-2}$  (see previous section), then  $G_s$  will be approximately  $10^5 \text{ Nm}^{-2}$ . Thus  $G_s$  will be at least two orders of magnitude larger than  $G$ , which seems reasonable. Inside the strands the protein concentration will be at least around 25 wt.%. Almost no data are available for the moduli of such concentrated protein gels. Protein gels of 10% heat denatured lysozyme or ovalbumin exhibit moduli of approximately  $10^4 \text{ Nm}^{-2}$  (Graham, 1976). The difference in modulus of a factor 10 seems reasonable since the concentration is around a factor 2.5 lower (see also section 3.4.2). Van Kleef (personal communication) and Van Kleef et al. (1978) found dynamic moduli of  $2 \times 10^3$  to  $7 \times 10^3 \text{ Nm}^{-2}$  for 10wt.% and  $10^5$ - $4 \times 10^5 \text{ Nm}^{-2}$  for 25 wt.% heat-set ovalbumin gels and of  $1.5 \times 10^4$ - $5 \times 10^4 \text{ Nm}^{-2}$  for 25 wt.% soya protein gels.

#### 4.7 Discussion

The rheological properties of acid casein gels will depend on the interactions between the particles and their spatial distribution throughout the gel network. The spatial distribution of strands of particles and especially the effect of inhomogeneities in this distribution has been discussed in section 3.4.3.1. In this section we will discuss the different interaction forces involved in the formation of a casein gel network and the consequences for the structure of the strands.

The interactions between the particles i.e. the formation of interparticle bonds strongly depends on the structure and state of aggregation of the individual casein molecules. In this context a hierarchy of protein aggregation can be distinguished at three levels i.e. intramolecular leading to the secondary structure and tertiary structure of protein molecules, intermolecular

inside the casein particles leading to the structure of these casein particles and intermolecular between distinct particles leading to coagulation. As discussed in chapter 3 and section 4.5.5.3 the structure of the particles and probably the extent of fusion between them after gel formation depends on the conditions (pH, temperature, kind of salt ions present and I) during their formation.

Different interaction forces both at molecular and at colloidal level will be involved. Hydrophobic bonding, electrostatic interactions, van der Waals attraction and probably hydrogen bonds will contribute to the conformation of the casein molecules.

The contribution of hydrogen bonds to the spatial structure of the casein particles is very difficult to estimate. In principle their contribution can increase as pH is lowered from 6.7 to 4.6, since the number of protonated carboxylic groups will increase; because of their large energy content only a few hydrogen bonds can have a large effect. However, in the relatively random structure, as caseins have, there will also be a competition of hydrogen bonds formed with water molecules. Because of the varying charge distribution and different hydrophobic character of the various caseins the relative importance of the other mentioned interactions on the spatial structure of the casein particles will vary with the type of casein. Further one has to take into account the possible formation of Ca-bridges, as  $\alpha_{s1}$ -,  $\alpha_{s2}$ - and  $\beta$ -casein, all of which contain serinephosphate rich amino acid sequences, are very sensitive to  $\text{Ca}^{2+}$  (Dalgleish and Parker, 1980, Parker and Dalgleish, 1981). It is probable that these Ca-bridges are mainly involved in determining the size and structure of the casein particles and not directly in the interparticle interactions, because the rheological properties of acid sodium caseinate gels prepared in the absence of Ca are very similar to those of acid skimmilk gels. The much weaker dynamic moduli of acid sodium caseinate gels prepared with  $\text{CaCl}_2$  as compared to those prepared with NaCl at the same I are probably due to the much larger particles already formed at higher pH (pH=5.0-6.8), while  $\tan \delta$ , which is insensitive to variations in the spatial distribution, remains the same. Electrostatic interactions are very important in controlling the structure of the casein particles. This can be concluded from behaviour

seen during acidification of skimmilk where casein molecules first tend to dissolve from the casein particles, but close to the isoelectrical pH all dissolved casein disappeared from the serum once more. The same aggregation effect occurs in sodium caseinate solutions, where casein tends to aggregate between pH=6.0 and 5.0 to form casein particles. Of course part of this aggregation will be due to a decrease of electrostatic repulsion between the protein molecules, since the net negative charge of the caseins decreases, when pH is being decreased to pH~4.6. Without doubt hydrophobic interactions are also involved. Casein molecules are fairly hydrophobic (Walstra and Jenness, 1984) and the decrease in voluminosity with increasing temperature can be accounted for by simply a change in hydrophobic interactions. In addition to these interaction forces the ever-present van der Waals interaction forces and steric interactions are also involved in the intra- and intermolecular protein-protein interactions.

All these types of interaction forces will be involved in the formation of bonds between casein particles. However the results of this study are not conclusive enough to give an estimation of the contribution of each type of interaction forces. The formation and character of the bonds will depend on the balance between the interaction forces. Each change in the conformation of the casein molecules will affect the particle structure and so its possibilities for the formation of interparticle bonds. However the experimental results clearly offer the possibility of some simple speculations. The formation of direct electrostatic bonds between oppositely charged groups on different casein particles is strongly suggested by the specific pH dependence and the large effect of extra NaCl, added after acidification, on the magnitude of the dynamic moduli. The ever-present van der Waals attraction may enhance the formation of these bonds. There are no clear indications of the presence of direct interparticle bonds due to hydrophobic bonding, since the dynamic moduli decrease with increasing measuring temperature in the temperature range from 0 to 50 °C. However in some preliminary experiments at large deformations and long loading times a positive temperature effect was found. In these experiments, which were carried out according to section 4.5.6.2, at a large constant deformation ( $\gamma \gg 0.04$ ) applied for

several hours  $G(t)^*$  did increase with temperature. However no conclusion can be drawn as to whether this positive temperature effect is due to entropic contributions or hydrophobic bonding or both. Another temperature effect was seen with  $\tan \delta$  at low frequency ( $10^{-3}$  to  $10^{-1}$  rad.s $^{-1}$ ). The more liquid-like character at low temperature expressed in the higher values of  $\tan \delta$  (see fig. 4.9, 4.11 and 4.12) and in a faster decrease of  $G(t)^*$  (see fig. 4.23) is probably simply due to relatively faster relaxing hydrophobic bonds at low temperature. As discussed in section 4.5.3 we assume that the large effect of  $T_m$  on the values of the dynamic moduli is at least partly due to an indirect effect of hydrophobic interactions. An important contribution from hydrogen bonds is not obviously expected since they need specific spatial orientations of carboxylic groups on different casein particles. Steric interactions still play an important part at pH=4.6, as will be shown in the next chapter. Splitting off the glycomacropeptide part of  $\kappa$ -casein considerably reduces the stability of casein particles at pH=4.6 (see next chapter).

It should be emphasized that most probably, the nature and number of interparticle bonds depends in the first instance on the conformation of the individual casein molecules and the structure of the casein particles. This structure will probably change from the outside to the inside of these particles. Changing a system parameter such as pH, I,  $T_m$  and type of ions, will first affect the casein particles and subsequently the nature and number of interparticle bonds. For example: as discussed in section 4.5.3 changes in protein conformation upon temperature rise, leading to a more compact protein molecule, may then produce a more compact casein particle. This could ultimately result in fewer interparticle bonds.

If we consider, the amino acid sequences of the individual caseins,  $\beta$ -casein probably will be involved relatively more in hydrophobic bonds, whereas  $\alpha_s$ -caseins will be involved more in electrostatic bonds. Perhaps,  $\beta$ -casein in particular may be able to migrate reversibly from the outside of the casein particles to the core as temperature is raised, thereby decreasing the particle voluminosity and particle stability due to a decrease of steric repulsion.  $\kappa$ -casein will still be located at the outside of the

casein particles at pH=4.6 and contribute to the steric stabilization of the casein particles. It is doubtful whether it contributes more than the other caseins to the formation of interparticle bonds, as long as GMP is not released.



## 5 THE STRUCTURE OF CASEIN GELS MADE BY ACIDIFICATION AND RENNET ACTION

### 5.1 Introduction

Rennet is used in the manufacture of many kinds of dairy products. Several of them are acidified to a pH between 5.0 and 6.0 before rennet action takes place, e.g. quarg and some types of cheddar cheese.

Steric repulsion is expected to be involved in the stabilization of casein particles, even at pH=4.6. The hydrophilic glycomacropeptide (GMP) part of  $\kappa$ -casein will especially contribute to the stabilization of casein particles. Addition of rennet offers the possibility of studying the stabilizing effect of GMP at low pH, since the rate of scission of GMP is much faster than other proteolytic reactions of rennet, even at low pH.

Ordinary commercial rennet samples contain primarily the enzyme chymosin and some pepsin. Both these enzymes are so-called endopeptidases. Bovine pepsin is roughly similar in action to chymosin. The most noteworthy property of rennet is the rapid and specific manner in which it splits  $\kappa$ -casein between the amino acid residues Phe (no. 105) and Met (no. 106) (Walstra and Jenness, 1984). This reaction is highly temperature dependent. The  $Q_{10}$  is about 3. The chain of amino acid residues 106-169, resulting from proteolysis, is called GMP, because it contains all of the glycosyl residues found in  $\kappa$ -casein. These are attached to threonine residues, particularly those found in position 131, 133, 135 and possibly 136 (Swaisgood, 1982).

It is well documented that GMP plays a key role in the stability of casein micelles at pH=6.7, but very little is known about its role at low pH (below 5.2). It is generally accepted that the coagulation of casein micelles in the first stage of cheese making is induced by rennet action on  $\kappa$ -casein, resulting in para  $\kappa$ -casein and GMP. The stabilizing effect of GMP at pH=6.7 can be attributed to two mechanisms: steric stabilization and charge stabilization. GMP has a strong hydrophilic character and a negative charge, which depends on the number of bound sialic acid residues

(Walstra and Jenness, 1984). Renneting causes a drop in Zeta potential of casein micelles at natural pH to about two thirds of its original value (Dalglish, 1984). At this pH a charge of  $\sim -10.5$  or  $\sim -9.5$  (depending on the genetic variant A or B of the  $\kappa$ -casein) can be attributed to the peptide backbone of GMP (Swaisgood, 1982, Walstra and Jenness, 1984). For each sialic acid residue one negative charge must be added. Taking an average of one sialic acid per  $\kappa$ -casein molecule (Walstra and Jenness, 1984) this would give a charge of  $\sim -11$  for the GMP part of  $\kappa$ -casein at pH=6.7. A similar calculation at pH=4.6, using the pK-values for the acidic and hydroxylic side groups, the serine phosphate and the N-acetylneuraminic acid (sialic acid) as given by Walstra and Jenness (1984) and Swaisgood (1982), results in a negative charge of approximately -4 for the GMP part of  $\kappa$ -casein.

In passing we note that the overall Zeta potential of the casein particles at pH=4.6 ( $T=2$  °C) is found to be zero (Darling and Dickson, 1979), but these particles are of a rather complicated, indeterminate structure.

In this particular study we were interested in the stabilizing effect of GMP on the casein particles formed after acidification at low temperature (0-2 °C) to a pH between 4.4 and 5.8. This effect was studied with the help of rheological and permeability measurements of gels formed after (successively) acidification to the desired pH, addition of rennet and heating at a rate of 0.5 °C per minute to the desired temperature. Gels can be made over a much broader range of pH's and temperatures by the mentioned combined effect of acidification and rennet action than by acidification alone (see section 4.5.4). The rheological properties of acid casein gels differ little in the pH range between 4.3 and 4.9, over which acid casein gels can be formed at 30 °C (see section 4.5.4). However these properties differ significantly from those of casein gels made by rennet action on skimmilk at natural pH (Zoon, 1984). Therefore the effect of pH in combination with rennet addition was investigated to seek a transition in rheological properties between acid casein gels (around pH=4.6) and rennet gels (natural pH). This transition was not expected to be due to the release of GMP, but to the properties of the casein particles in which Ca was involved either in ionic form or as colloidal

calcium phosphate (CCP).

In general, rennet action on milk proteins includes two stages: a fast first stage in which GMP is split off and a second slow stage in which proteolytic cleavage of only  $\alpha_{s1}$ - and  $\beta$ -casein occurs (see next section). This slow proteolysis will only influence gel properties at longer time scales, while the influence of GMP splitting will be seen at the beginning of gel formation. According to Pierre (1983) at 32 °C the proportion of GMP, which was released at the moment of milk clotting, decreased from 92% to 43% as pH was decreased from 6.7 to 5.0. Although in the experiment of Pierre, milk was acidified at elevated temperatures, it is probable that a similar trend may be expected for milk acidified at 2 °C, but the absolute percentages hydrolysed will depend on temperature.

## 5.2 Proteolytic action

After the rapid cleavage of the protein bond between Phe 105 and Met 106 of  $\kappa$ -casein rennet action does not stop.  $\alpha_{s1}$ - and  $\beta$ -casein are hydrolysed in a slow process which continues over weeks in normal cheesemaking practice, but para  $\kappa$ -casein and  $\alpha_{s2}$ -casein suffer no further degradation.

Recently Visser (1981), Pélissier (1984) and Grappin et al. (1985) have reviewed the proteolysis of the caseins. They paid detailed attention to the rennet-induced hydrolysis. The degradation of  $\alpha_{s1}$ - and  $\beta$ -casein is quite complicated. The rate of degradation and the type of products formed depend very much on pH, ionic strength and temperature. These factors not only affect the enzyme activity, but predominantly the conformation and state of aggregation of the casein molecules and thereby the accessibility of bonds for proteolytic cleavage. For example soluble casein is hydrolysed much faster than micellar casein (Ledford et al., 1968). Above 40 °C rennet is rapidly inactivated, the  $Q_{10}$  of the inactivation reaction being about 2.5 (Walstra and Jenness, 1984).

A suitable technique to trace the degradation of  $\alpha_{s1}$ - and  $\beta$ -casein is polyacrylamide gel electrophoresis (Ledford et al., 1966, De Jong, 1975 and Grappin et al., 1985). Most experiments described in the literature have been carried out with solutions

of isolated caseins (Mulvihill and Fox, 1977, 1979a, 1979b, Creamer, 1976, Creamer et al., 1971, Visser and Slangen, 1977), with sodium caseinate (Fox, 1969) or with cheese-like substrates (De Jong and De Groot-Mostert, 1977, and Noomen, 1978). From these results it is clear that the accessibility of the proteins and therefore their state of aggregation play a key role in the proteolytic action of rennet. Both  $\alpha_{s1}$ - and  $\beta$ -casein are not hydrolysed into many small peptides in a one step process, but in a multi step process. At every step a small peptide is split off to give macro-peptides of decreasing length, ultimately resulting in a series of small peptides.

The degradation of  $\alpha_{s1}$ - and  $\beta$ -casein and the hydrolysis products formed are schematically depicted in figure 5.1.  $\alpha_{s1}$ -casein is first cleaved at the N-terminal end of its peptide chain to give  $\alpha_{s1}$ -I casein (residue 24 or 25 to 199, Pélissier, 1984). At least six other protein bonds are known to be sensitive to rennet. According to Mulvihill and Fox (1977 and 1979a)  $\alpha_{s1}$ -II casein is split off from  $\alpha_{s1}$ -I casein at pH=5.8 in a 2%  $\alpha_{s1}$ -casein solution and in the next stage  $\alpha_{s1}$ -II casein is further hydrolysed to  $\alpha_{s1}$ -III and  $\alpha_{s1}$ -IV casein. At pH=4.6 on the other hand, where the substrate is aggregated,  $\alpha_{s1}$ -I casein is hydrolysed to  $\alpha_{s1}$ -V casein only (see fig. 5.1) and small peptides which cannot be detected with polyacrylamide gelelectrophoresis. In this case (a 2%  $\alpha_{s1}$ -casein solution after 12 hrs incubation time at T=30 °C)  $\alpha_{s1}$ -casein breakdown is optimal at pH=5.8 and minimal at pH=4.6.

$\beta$ -casein is degraded from its C-terminal end to give successively  $\beta$ -I casein (residue 1-189 or 192),  $\beta$ -II casein (residue 1-165 or 166) and  $\beta$ -III casein (residue 1-139). Detection of the  $\beta$ -II and  $\beta$ -III casein bands in the electrophoretic patterns of milk products is hampered because of the position of these bands just before and after the band of  $\alpha_{s1}$ -casein (see figure 5.1). The rate of hydrolysis of both  $\alpha_{s1}$ - and  $\beta$ -casein (Fox, 1969, Creamer et al., 1971, and Creamer, 1976) increases with temperature,  $\alpha_{s1}$  hydrolysis faster than  $\beta$  so that at increasing temperatures relatively more  $\alpha_{s1}$ -casein is degraded. At 10 °C (Creamer et al., 1971) the degradation product  $\beta$ -I is hydrolysed much slower than at 37 °C.

Proteolysis of  $\alpha_{s1}$ - and  $\beta$ -casein in a sodium caseinate solution

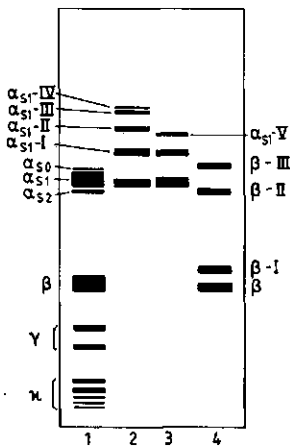


Fig. 5.1 Schematic picture of polyacrylamide gel electrophoretic patterns of different casein samples, whether hydrolysed by rennet or not.

1. total casein without rennet.
2.  $\alpha_{s1}$ -casein hydrolysed by rennet at pH=5.8.
3.  $\alpha_{s1}$ -casein hydrolysed by rennet at pH=4.6.
4.  $\beta$ -casein hydrolysed by rennet (no specific pH).

(Fox, 1969) shows an optimum at pH=5.8. This was also found by de Jong et al. (1977) for sodium paracaseinate.

### 5.3 Results and discussion

This section is divided in two parts. The first part describes experiments with skimmilk gels made at pH=4.6 and varying gelation temperatures. The second part deals with experiments in which gels were made at 20 °C, but with a pH varying from 4.4 to 5.8.

All gels were prepared according to the standard procedure as explained in section 2.3. Skimmilk, reconstituted from skimmilk powder A (section 2.1), was cooled down to 0-2 °C and subsequently acidified to the desired pH in the range of 4.4 to 5.8. The rate of acidification was made slow enough to assure a stable pH. At  $t=0$  rennet was added to the cold, acidified skimmilk to a final concentration of 250 ppm. Immediately the measuring apparatus was filled as quickly as possible and heated to the desired gelation temperature at a rate of 0.5 °C per min. The delay time between the moment of rennet addition and the moment of temperature rise above 4 °C varied from 4 to 16 minutes.

In preliminary experiments a rough test was performed to find the pH and temperature at which stable, intact gels could be formed using the procedure described above. In contrast with acid skimmilk gels made without rennet addition (section 4.5.4) the

combined use of acidification and rennet allowed gel formation over the entire range of pH tested, from 4.4 to 5.8. At  $\text{pH} > 5.0$  a minimum temperature of approximately  $8\text{ }^{\circ}\text{C}$  was necessary, while at temperatures above  $20\text{ }^{\circ}\text{C}$  a severe breakdown of the gel network (especially around  $\text{pH}=5.2$ ) was noticed, starting within a few hours after gel formation. At  $\text{pH}=5.2$  and at a temperature of  $30\text{ }^{\circ}\text{C}$  the gel network first collapsed and after 30 hours had completely disappeared. Syneresis, i.e. mainly microsyreresis, and proteolytic breakdown of casein were most probably responsible for these effects. At a pH of around 6.7 Zoon (1984) found that relatively stable gels could also be made at higher temperatures ( $T < 40\text{ }^{\circ}\text{C}$ ). At pH values from 4.4 to 5.0 gels were formed at temperatures from 0 to  $30\text{ }^{\circ}\text{C}$ .

#### 5.3.1 The effect of rennet at $\text{pH}=4.6$

The results of the measurements of  $G'$  of skimmilk gels at  $\text{pH}=4.6$  and in the presence of 250 ppm rennet as a function of the ageing time  $t(\text{s})$  are shown in figure 5.2 for six different ageing temperatures (2,5,10,15,20 and  $25\text{ }^{\circ}\text{C}$ ). For comparison we also show (dashed line) the ageing curve of an acid skimmilk gel made at  $30\text{ }^{\circ}\text{C}$  without rennet. This had the largest moduli for this kind of gels (see also figure 3.1a). Two gels aged at  $30\text{ }^{\circ}\text{C}$  (not shown) initially showed an ageing curve very similar to the curve obtained at  $25\text{ }^{\circ}\text{C}$ , but collapsed after approximately  $10^4\text{ s}$ .

The apparent discrepancy between the early portions of the curves at  $25\text{ }^{\circ}\text{C}$  and  $20\text{ }^{\circ}\text{C}$  was due to a shorter delay time of  $3 \times 10^2\text{ s}$  between rennet addition and the start of the heating for the gel aged at  $20\text{ }^{\circ}\text{C}$ . Rennet action at  $\text{pH}=4.6$  has a marked effect on formation and ageing of acid skimmilk gels as can be seen from a comparison of figure 5.2 with figure 3.1a. Two pronounced features can be noticed due to the presence of rennet: firstly, gel formation can take place below  $10\text{ }^{\circ}\text{C}$  (even at  $2\text{ }^{\circ}\text{C}$ ) and secondly, the gels formed at higher temperatures (15 to  $25\text{ }^{\circ}\text{C}$ ) have a much larger value of  $G'$ . Moreover, the linear relationship between  $G'$  and  $\log t$  was not found apart from a limited range of low temperatures. In the presence of rennet the shape of the ( $G'$  versus ageing time) curve changes with temperature. Below we will discuss the shape of the curve in more detail in relation to the cleavage

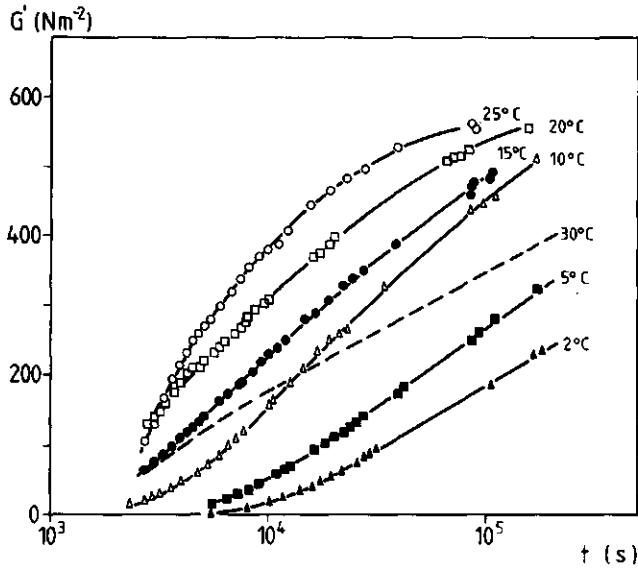


Fig. 5.2 The storage modulus  $G'$  as a function of ageing time  $t$  for acid skim-milk gels ( $\text{pH}=4.6$ ) made with 250 ppm rennet and aged at different temperatures. Ageing temperature varied as indicated. Rennet was added at  $t=0$  s. The dashed curve refers to an acid skimmilk gel made without rennet and aged at  $30^\circ\text{C}$  (derived from fig. 3.1a).  $\omega=1.0\text{ rad}\cdot\text{s}^{-1}$ . Measurements were made at the ageing temperature.

of GMP and the hydrolysis of  $\beta$ -casein and  $\alpha_{s1}$ -casein.

Below  $15^\circ\text{C}$  gel formation showed a kind of lag phase (figure 5.2). It began only when a critical minimum proportion of GMP had been freed as can be seen from a comparison of fig. 5.2 with 5.3. In figure 5.3 the percentage of GMP released is depicted as a function of time after rennet addition (see section 2.7). Experimental conditions were the same as for figure 5.2. At  $25^\circ\text{C}$  the heating was retarded in the early stages. This produced the initial slow increase of GMP released. At  $5^\circ\text{C}$  gel formation had already started after  $5 \times 10^3$  s, when 60% of the  $\kappa$ -casein was cleaved. From a comparison of figure 5.2 with 5.3 it also follows that at low temperatures the  $G'$  versus  $\log t$  curves became linear, when at least 90% of the GMP was released. For the  $5^\circ\text{C}$  curve e.g. this

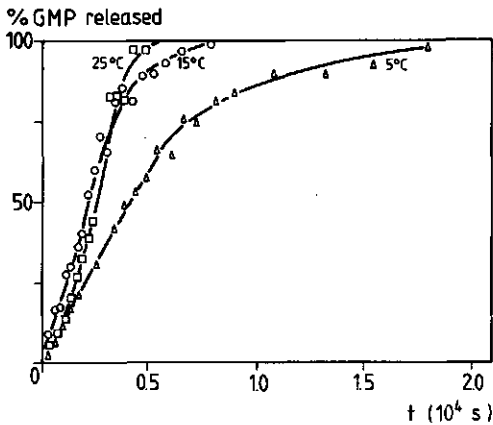


Fig. 5.3 The percentage of GMP, split off from  $\kappa$ -casein, as a function of time for acid skimmilk gels (pH=4.6) aged at three different temperatures. At  $t=0$  250 ppm rennet was added to the acidified skimmilk solutions.

occurred at a time of about  $1.2$  to  $1.5 \times 10^4$  s, when 90 to 95% had been hydrolysed.

Apparently GMP still has a considerable effect on the stability of casein particles at pH=4.6. This must be due to its small, but significant negative charge at this pH and to its overall hydrophilic character which probably at pH=4.6 also gives rise to a small but significant steric repulsion.

The slope of the linear increase of  $G'$  with  $\log t$  increased as the ageing temperature was increased from 2 to 10 °C. This increase of slope cannot be related directly to the loss of stability caused by GMP cleavage, because the change in slope occurred after all GMP had been split off. Apparently the rate of ageing of gels formed from the para casein particles increased much more strongly with temperature than in case of acid skimmilk gels formed from ordinary casein particles without rennet action (see fig. 3.1). A highly speculative explanation can be given for this phenomenon. After the GMP is released, the activation Helmholtz energy for aggregation of casein particles is possibly largely due to the stabilizing effect of  $\beta$ -casein chains protruding from the surface of the particles. These chains, causing a certain, but insufficient steric repulsion, are moved to the interior of the casein particles, when temperature is raised and so the activation Helmholtz energy for aggregation is lowered.

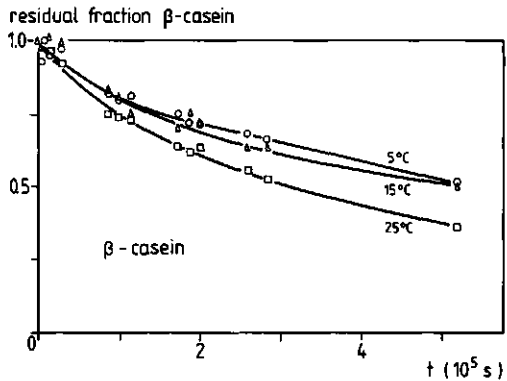
Above and at 15 °C the situation was somewhat different. GMP splitting was no longer a prerequisite for gel formation, as we

have already found that acid skimmilk starts to gel as soon as the temperature is raised above 10 °C. At that moment (after about  $1.3 \times 10^3$  s) only a small proportion of GMP, approximately 25%, has been split off (fig. 5.3). During heating the casein particles will become increasingly more unstable because of both the acidity of the solution and the continuing rennet action; when  $G'$  was measured at 15 and 25 °C for the first time at least 60 to 70% of GMP had been released (after  $2.7 \times 10^3$  s). As can be seen in fig. 5.2 rennet action still had a significant effect on the ageing curves of the gels at 15 °C and higher. The loss of GMP led to a large increase in the initial value of the dynamic moduli (compare figure 5.2 to figure 3.1a) and to a much steeper increase of  $G'$  with  $\log t$ . However except for the gel at 15 °C for ageing time below  $3 \times 10^4$  s there was no longer a linear increase of  $G'$  with  $\log t$ . The lines were curved, especially at 25 °C. Permeability measurements (see below) on these gels gave permeability coefficients which did not increase with measuring time, indicating an absence of microsineresis. This contrasts with the behaviour of rennet gels, as found by Van Dijk (1982). These were subject to microsineresis and  $B$  increased with time.

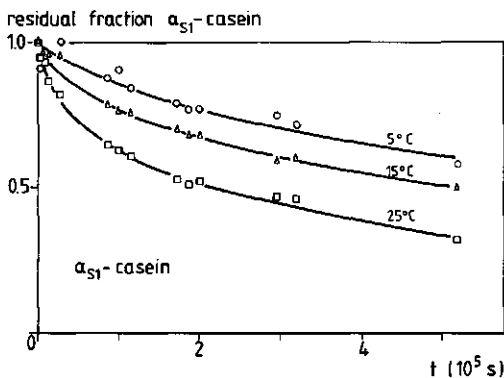
A more obvious cause for the curvature in  $G'$  versus  $\log t$  plots could be proteolytic cleavage of  $\alpha_{s1}$ - and  $\beta$ -casein. In figure 5.4a and b the residual protein concentration of  $\alpha_{s1}$ - and  $\beta$ -casein is depicted as a function of time after rennet addition for three different temperatures (5, 15 and 25 °C). The proteolysis (see section 2.6) was followed for up to  $5 \times 10^5$  s, whereas all rheological measurements (fig. 5.2 and 5.5) were carried out within  $2 \times 10^5$  s. Therefore only the hydrolysis of the caseins within  $2 \times 10^5$  s can be important for the curvature of the lines in fig. 5.2. In this period of time a moderate, but significant proteolysis of  $\alpha_{s1}$ - and  $\beta$ -casein had occurred. The degradation of  $\beta$ -casein showed little temperature dependence (fig. 5.4a): there was hardly difference between measured levels at 5 °C and 15 °C and the hydrolysis was only a little higher at 25 °C. A stronger temperature dependence was found for  $\alpha_{s1}$ -casein (fig. 5.4b): at 5 °C less  $\alpha_{s1}$ - than  $\beta$ -casein was hydrolysed, while at 25 °C relatively more  $\alpha_{s1}$ -casein was degraded. After  $2 \times 10^5$  s (55 hrs) at 25 °C 50% of the initial  $\alpha_{s1}$ -casein concentration and 60% of the initial  $\beta$ -casein

concentration remained. The base line for the residual casein concentration in figure 5.4a and b was approximately 8% for  $\beta$ -casein and 18% for  $\alpha_{S1}$ -casein. A relative increase in the breakdown of  $\alpha_{S1}$ -casein in relation to the breakdown of  $\beta$ -casein, as temperature was raised, was also found by Fox (1969) for sodium caseinate at pH=4.6. The pattern of degradation products also changed with temperature (not shown). At 5 °C more  $\beta$ -I casein was left uncleaved, whereas at 15 and 25 °C less  $\beta$ -I casein and more  $\beta$ -II casein and  $\beta$ -III casein were found. The same effect was found by Creamer et al. (1971) in a solution of pure  $\beta$ -casein at pH=6.5.  $\beta$ -III casein was difficult to detect in the electrophoretic pattern.

Fig. 5.4 The residual concentration of  $\beta$ -casein (a) and  $\alpha_{S1}$ -casein (b) in acid skimmilk gels (pH=4.6) made with rennet as a function of time for three different ageing temperatures. Ageing temperatures are indicated. 250 ppm rennet was added at  $t=0$  s.



(a)



(b)

From the degradation products of  $\alpha_{s1}$ -casein only  $\alpha_{s1}$ -I casein was clearly visible. Above the  $\alpha_{s1}$ -I casein band two minor bands could be detected, one of which might be ascribed to  $\alpha_{s1}$ -V casein (Mulvihill et al., 1977). At 25 °C  $\alpha_{s1}$ -I casein was more rapidly hydrolysed than at lower temperatures.

In view of the significant casein degradation during the ageing of the gels one could conclude that the bending of the  $G'$  versus  $\log t$  curves after longer ageing times at  $T \geq 15$  °C might be due at least partly to casein hydrolysis. The fact that the line at 25 °C was curved from the beginning, when degradation was at most a few percent, shows that other effects must also be involved. Maybe at this temperature the bending of the curve at shorter ageing times was caused by changes in the properties of the aggregated casein particles due to the on-going release of GMP, while at longer ageing times it was caused by protein breakdown. A possible positive role of the very hydrophobic para  $\kappa$ -casein (Walstra and Jenness, 1984), left after release of GMP, must also be considered. Moreover, at pH=4.6 para  $\kappa$ -casein will be positively charged, since its isoelectric pH is around pH=9-9.5 (Vreeman personal communication).

As the bending of the  $G'$  versus  $\log t$  curves increased with temperature in parallel with the breakdown of  $\alpha_{s1}$ -casein (compare fig. 5.2 to fig. 5.4b), it suggests that  $\alpha_{s1}$ -casein is a main component of the casein gel network. In this respect no conclusion, positive or negative, can be drawn about a possible role of  $\beta$ -casein, because  $\beta$ -casein breakdown showed a very slight temperature dependence (fig. 5.4a).

The rheological properties of the acid skimmilk gels made in the present of rennet were further characterised by calculating  $\tan \delta$  as a function of ageing time, and by measuring the dynamic moduli  $G'$  and  $G''$  and calculating  $\tan \delta$  both as a function of angular frequency  $\omega$  and of measuring temperature  $T_m$ .

A rapid decrease of  $\tan \delta$  in the early stages of ageing was found. This passed into a slow decrease after  $5 \times 10^3$  s resulting in  $\tan \delta$  values varying from 0.24 to 0.28 after  $10^5$  s (see table 5.1). Similar behaviour was found for acid skimmilk gels made without rennet (see fig. 3.2, section 3.2).

Table 5.1 Tan  $\delta$  of acid skimmilk gels (pH=4.6) made in the presence of 250 ppm rennet as a function of ageing temperature after an ageing time of  $10^5$  s.  $\omega=1.0$  rad.s $^{-1}$ .

T(°C)	tan $\delta$
2	0.24
5	0.26
10	0.24
15	0.27
20	0.27
25	0.28

The dynamic moduli  $G'$  and  $G''$  showed a virtually linear increase with the angular frequency  $\omega$  on a double logarithmic scale with the same slope (around 0.15) as was found for acid casein gels made without rennet. For tan  $\delta$  as a function of  $\omega$  straight horizontal lines were found at 30 °C while at lower temperatures a slight increase at small  $\omega$  was observed.

Once a gel was formed the dynamic moduli  $G'$  and  $G''$  strongly decreased, when the measuring temperature was increased (see fig. 5.5, where  $G'$  is depicted as a function of measuring temperature for gels aged at least 25 hours at different ageing temperatures). This behaviour was similar to that found for normal acid casein gels (see fig. 4.7, section 4.5.3). Although  $G'$  was measured after different ageing times, the picture remains clear. The smaller decrease with measuring temperature found at 25 and 30 °C for the 5 °C curve was thought to be due to an accelerated gelation during the measurement. This started above 20 °C and is thought to arise from a faster rearrangement of protein molecules in the casein particles forming the strands and aggregates of the gel network. Probably these protein rearrangements take place at the outer region of the casein particles. These rearrangements which cause an increase of the dynamic moduli at higher measuring temperatures obviously only occur for gels aged at low ageing temperature (see also section 4.5.3).

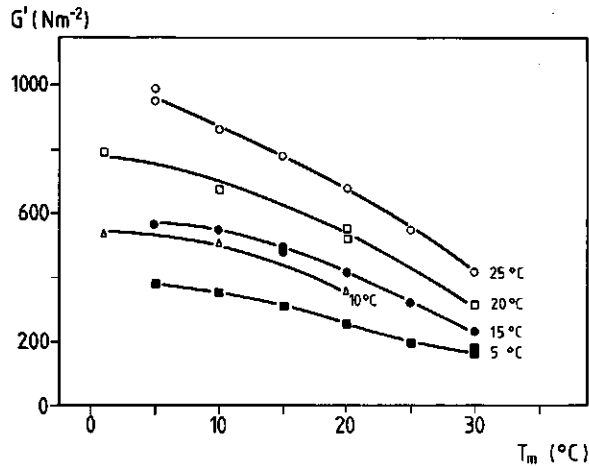


Fig. 5.5 The storage modulus  $G'$  as a function of measuring temperature,  $T_m$ , for acid skimmilk gels (pH=4.6) made with 250 ppm rennet and aged at different temperatures. Ageing temperature was varied as indicated. The ageing times were respectively: 5 °C,  $1.9 \times 10^5$  s; 10 °C,  $1.7 \times 10^5$  s; 15 °C,  $1.05 \times 10^5$  s; 20 °C,  $1.2 \times 10^5$  s; 25 °C,  $9 \times 10^4$  s. Angular frequency  $\omega = 1.0 \text{ rad} \cdot \text{s}^{-1}$ .

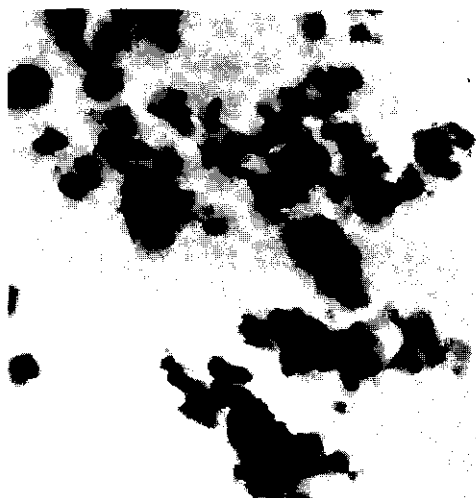
To explain the difference in the absolute values of  $G'$  and  $G''$  and in the  $G'$  versus  $\log t$  curves between acid skimmilk gels made with and without rennet, information concerning possible changes in the spatial distribution of the basic elements (i.e. the casein particles) upon rennet action at pH=4.6 is very relevant. Therefore at 25 °C the permeability coefficient of acid skimmilk gels with and without rennet was measured simultaneously. The permeability increased by a factor of two in the presence of rennet (see table 5.2). This suggests that a much more inhomogeneous gel network was formed. The value of the dynamic moduli also increased significantly. This is again a remarkable result, which can only be explained by an increase in the number of bonds between the casein particles; since in general a more inhomogeneous distribution of the basic elements of a gel network results in lower network moduli (see section 3.4). This feature, that a coarser gel network is formed in the case of probably a higher number of interparticle bonds, was noticed before for acid casein gels (see e.g. section 4.5.3, and section 3.4 and figure 3.15). Part of the

Table 5.2 The permeability coefficient B of acid skimmilk gels (pH=4.6) made with (+) and without (-) rennet (250 ppm) at 25 and 10 °C. The gels, made at 25 °C with and without rennet, were measured simultaneously at 25 °C. The ageing time was respectively 19 hours (25 °C) and 20 hours (10 °C). The values of column 1 are the average values of several experiments, the number of which is given in column 4. In each experiment at least 8 tubes (see section 2.9) were used. The variation between the average values in each experiment is indicated.

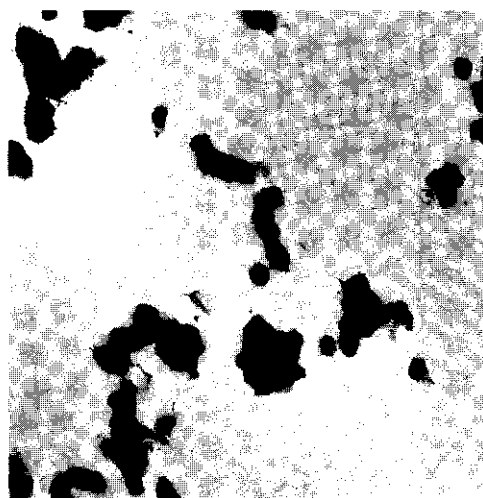
T(°C)	$B(10^{-13} \frac{m^2}{m})$	rennet	number of experiments
25	1.37±0.05	-	3
25	2.76±0.03	+	3
10	1.78±0.04	+	2

increase of permeability may however be due to a decrease of voluminosity of the casein particles as a result of GMP cleavage. It is possible for inhomogeneity to increase at the level of the gel network, while at the level of the particle strands homogeneity may increase due to a more extensive fusion of the casein particles, when GMP is released. Electron micrographs (fig. 5.6) support this suggestion. In figure 5.6 micrographs (see section 2.11) of three different casein gels are depicted: an acid skimmilk gel without (fig. 5.6a) and with rennet (fig. 5.6b), and a rennet gel (fig. 5.6c). The samples for electron microscopy were all prepared in the same way (see section 2.11). At pH=6.7 thick strands consisting of completely fused para-casein micelles are found, while at pH=4.6 without rennet individual particles are still recognizable and are only partly fused. The strands of the acid casein gels are also much thinner. In the sample with rennet present at pH=4.6 (compare fig. 5.6a and b) particle fusion increases, the strands seem to be more compact and moreover fewer free particles, not contributing to a strand, seem to be present.

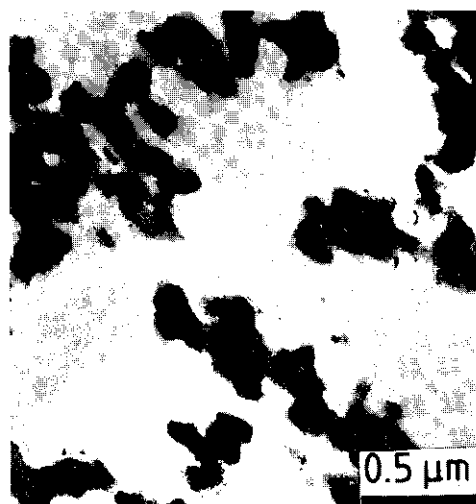
The permeability of an acid skimmilk gel prepared at 10 °C with rennet was also measured at 10 °C. This permeability was signific-



(a)



(b)



(c)

Fig. 5.6. Electron micrographs of three different skimmilk gels. The E.M. samples were prepared as described in section 2.11. The magnification is given in the graphs. a: acid skimmilk gel, pH=4.6, made without rennet, aged at 30 °C for  $7.2 \times 10^4$  s (20 hrs); b: acid skimmilk gel, pH=4.6, made with 250 ppm rennet and aged for  $5.5 \times 10^4$  s (16 hrs) at 25 °C; c: rennet gel made from skimmilk (pH=6.7) by rennet action at 30 °C. Ageing time is  $2.2 \times 10^4$  s (ca 6 hrs).

antly lower than that of a similarly prepared sample at 25 °C (see table 5.2), but still higher than the permeability of acid skimmilk gels made without rennet at 25 °C. A decrease in B with decreasing ageing temperature was also found for acid casein gels made without rennet addition (see section 3.4.2.3).

### 5.3.2 The effect of rennet at varying pH

The rheological properties of acid skimmilk gels prepared in the presence of rennet were studied at different pH values in the range of 4.4 to 5.8. To ensure that the chosen pH was constant during the measurement, sufficient time was taken for acidification. Particularly around pH=5.2 acidification was a time consuming process, because of the retarded dissolution of colloidal calcium phosphate and the formation of all kinds of soluble Calcium phosphate complexes. A final check of the pH at 20 °C after the gels had been aged for at least two days showed a maximum rise in pH of less than 0.1 unit. In all cases ageing temperature was kept constant at 20 °C. To trace gel formation, the dynamic moduli were measured as a function of ageing time and pH. For further rheological characterization, measuring temperature and measuring frequency were varied. The effect of proteolytic activity was tested by following the degradation of  $\alpha_{s1}$ - and  $\beta$ -casein.

In table 5.3 a summary is given of the measurements made on these gels. For sake of clarity only a selection of the available experimental data will be depicted in the figures 5.7 to 5.13.

#### 5.3.2.1 *Gel formation at different pH values*

The development of  $G'$  as a function of ageing time at different pH's is shown in fig. 5.7. As can be seen the pH of the solution had a large effect. Both the shape of the ageing curves and the magnitude of  $G'$  strongly depended on pH. Below pH=5.0 the shape of the ageing curves resembled that found for pH=4.6 at 20 °C (figure 5.2). Above pH=5.0 not only the value of  $G'$  but also the shape of the ageing curves markedly altered. Instead of a more or less parallel shift to lower values of  $G'$ , the curves had a more convex shape. At pH=5.2 and 5.4 a maximum was found after  $10^4$  s, after which  $G'$  decreased slightly.

For clarity,  $G'$  after an ageing time of respectively  $10^4$  s (ca. 3 hrs) and  $10^5$  s (ca. 28 hrs) is depicted as a function of pH in figure 5.8 (see also table 5.3). A maximum in  $G'$  was found between pH=4.7 and 4.8 in contrast to acid skimmilk gels made without rennet, where the optimum was found around pH=4.5 (fig. 4.13, section

Table 5.3 A summary of the rheological properties of all gels made by the combined action of acidification and rennet proteolysis in the pH range from 4.4 to 5.8. The rennet concentration was 250 ppm. Ageing temperature was 20 °C and angular frequency  $\omega$  was 1.0 rad.s<sup>-1</sup>.

gel no.	pH	G' (Nm <sup>-2</sup> ) after 10 <sup>4</sup> s	tan $\delta$ after 10 <sup>4</sup> s	G' (Nm <sup>-2</sup> ) after 10 <sup>5</sup> s	tan $\delta$ after 10 <sup>5</sup> s
1	4.40	240	0.26	433	0.24
2a	4.59	290	0.27	512	0.24
2b <sup>1</sup>	4.60	310	0.30	538	0.27
3	4.70	362	0.27	613	0.24
4	4.83	316	0.29	572	0.26
5	4.92	248	0.32	490	0.25
6	5.01	150	0.37	330	0.28
7a	5.10	102	0.43	222	0.30
7b	5.16	70	0.49	98	0.34
8a	5.20	63	0.47	61	0.39
8b	5.20	73	0.42	38	0.42
8c <sup>2</sup>	5.20	-	-	50	0.41
8d	5.20	63	-	82	0.39
9	5.40	82	0.38	60	0.36
10	5.60	124	0.31	140	0.29
11	5.83	136	0.28	188	0.27

1: data taken from section 5.3.1

2: this gel, after ageing at 20 °C for  $6.5 \times 10^4$  s (18 hrs), was only used for measurement of tan  $\delta$  and G' as a function of  $\omega$ . The given values of G' and tan  $\delta$  were measured after  $6.5 \times 10^4$  s.

4.5.4). Moreover, without rennet the pH dependence around the optimum was much less pronounced. Obviously this small shift of optimum pH was due to the cleavage of the slightly negatively charged GMP, which results in a small shift of the isoelectric pH of the para-casein particles remaining. It is probable that the maximum size of the dynamic moduli still coincides with charge

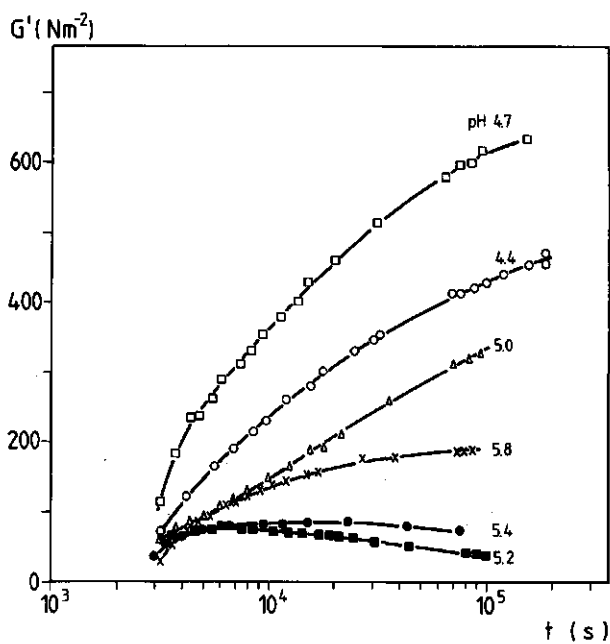


Fig. 5.7 The storage modulus  $G'$  as a function of ageing time  $t$  (s) for skim-milk gels made by the combined action of acidification and 250 ppm rennet. The gels were aged at 20 °C. pH was varied as indicated.  $\omega=1.0 \text{ rad}\cdot\text{s}^{-1}$ .

neutrality in the aggregating particles as was found for acid casein gels prepared without rennet (see section 4.5.4). Comparing the pH dependence of  $G'$  of acid skimmilk gels made without rennet at 30 °C (fig. 4.13, section 4.5.4) with that of gels made with rennet at 20 °C (fig. 5.8) and remembering that at an ageing temperature of 20 °C much weaker gels were formed than at 30 °C (see e.g. fig. 4.7, 5.2 or 5.5), it is clear that over the whole range of pH=4.4 to 5.0 rennet action caused much stronger gels to be formed. The same conclusion has already been reached for gels made with rennet at different ageing temperatures at pH=4.6 in section 5.3.1.

At the beginning of the ageing process the curves of  $G'$  became measurable at the same time and had approximately the same value for  $G'$ , independent of pH. However  $\tan \delta$  ( $=G''/G'$ ) depended strongly on the pH (fig. 5.9 and table 5.3) indicating a pH-dependent

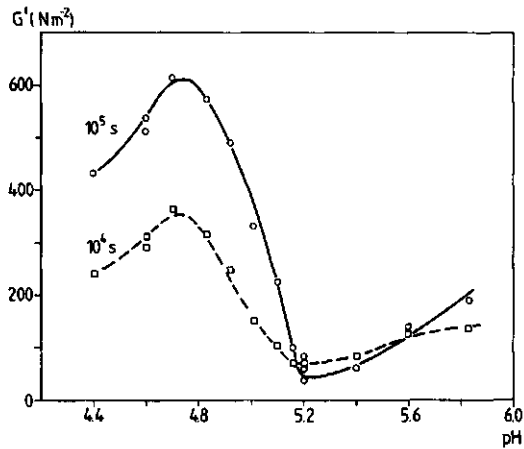


Fig. 5.8 The storage modulus  $G'$  after ageing times of respectively  $10^4$  s (---) and  $10^5$  s (—) as a function of pH for skimmilk gels made by combined acidification and rennet (250 ppm) action. Ageing temperature was 20 °C and  $\omega=1.0$  rad.s<sup>-1</sup>.

relaxation behaviour of the bonds in the gel network ( $\omega=1.0$  rad.s<sup>-1</sup>).

The data presented in fig. 5.8 and 5.9 show that around pH=5.2 a minimum in  $G'$  and a maximum in  $\tan \delta$  was found. Between pH=4.9 and 5.2  $G'$  decreased dramatically with increasing pH, while  $\tan \delta$  showed a drastic increase. After a longer ageing time this increase was shifted to between pH=5.1 and 5.2. Hence the ageing curves for  $G'$  and  $\tan \delta$  at pH=5.10 (sample 7a, see table 5.3) had a shape much more like that for pH=5.0, while the curves found at pH=5.16 (sample 7b) resembled those found at pH=5.2. Significantly the increase in  $G'$  and the decrease in  $\tan \delta$ , found with increasing pH at pH above 5.2, occurred much more gradually.

As can be seen from fig. 5.9 not only the value of  $\tan \delta$  after a specified ageing time but also the shape of the ageing curves of  $\tan \delta$  versus  $\log t$  varied strongly with pH. All curves have to begin at  $\tan \delta$  above 1.0 because in every case the starting point was a skimmilk solution at  $t=0$  s. The latter behaves as a newtonian liquid (Van Vliet and Walstra, 1980). At the boundaries of the pH range studied (pH=4.4 and 5.8)  $\tan \delta$  already has decreased

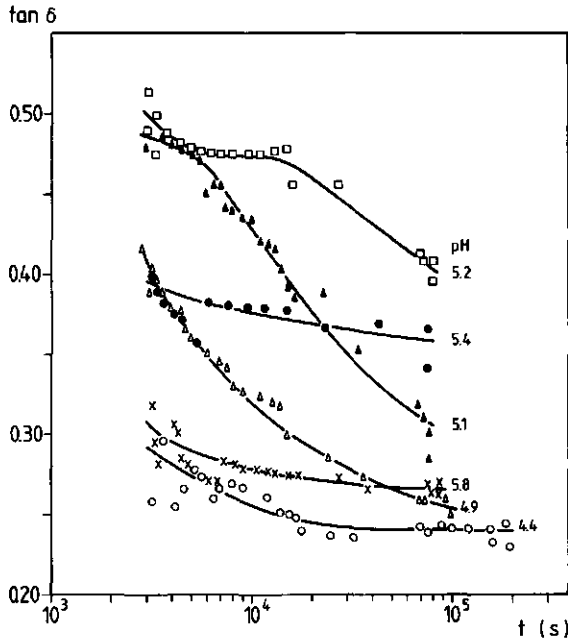


Fig. 5.9 The loss tangent  $\tan \delta$  ( $=G''/G'$ ) as a function of ageing time  $t$ (s) for skimmilk gels under the same conditions as in fig. 5.7. pH was varied as indicated.

to substantially low values ( $\leq 0.30$ ) at the moment the rheological measurements were begun ( $t$  then had a value of around  $3 \times 10^3$  s). In the course of ageing only a slight further decrease in  $\tan \delta$  was seen. When pH was lowered from 5.8 to 5.4 the horizontal character remained, but the curves were shifted to higher values. At pH=5.2 a horizontal curve in the early stages (until  $1.5 \times 10^4$  s) was followed by a significant decrease. At pH=5.1 the horizontal domain was shorter and the subsequent decrease steeper. In the pH range from 4.6 to 5.1 a transition in the rheological character of the gels as expressed in  $\tan \delta$  occurred over the time span of the measurements.  $\tan \delta$  strongly decreased over the entire time range, e.g. at pH=5.0 from approx. 0.50 after  $3 \times 10^3$  s to 0.28 after  $10^5$  s. The above observation implies that in the pH range from 4.6 to 5.1 the elastic character of the gels increased significantly with time, whereas below pH=4.6 and above pH=5.4 the change from a

net and measured at 20 °C (see fig. 4.9, 4.11 and 4.12). A slight increase, which was hardly if at all significant, was observed in the final frequency decade ( $1.0$  to  $10^1$   $\text{rad.s}^{-1}$ ). At higher pH the curves shifted to higher values for  $\tan \delta$  and the decrease of  $\tan \delta$  with increasing  $\omega$  at lower frequencies became more pronounced with a maximum effect at pH=5.2. At this pH the viscous character of the gel strongly increased at low rates of deformation. Further pH rise caused again a decrease in the magnitude of  $\tan \delta$  but the shape of the curves remained the same. The curve of pH=5.8 resembled very closely the  $\tan \delta$  versus  $\omega$  curve, found by Zoon (1984) for skimmilk gels, made from skimmilk of natural pH(=6.7) by rennet action at 25 °C. It will be shown below that the small difference in the shape of  $\tan \delta$  versus  $\omega$  curve between pH=4.9 and 5.8 for  $\omega$  below  $10^{-1}$   $\text{rad.s}^{-1}$  is of significance for the difference between acid casein gels and renneted casein gels. The transition again took place at a pH of around 5.2. The increase of  $\tan \delta$  with decreasing  $\omega$  began for all pH's at  $\omega=10^{-1}$   $\text{rad.s}^{-1}$ . As already suggested in section 4.5.3 for acid casein gels, it is possible that this involves some form of interactions leading to interparticle bonds with relaxation times in the order of  $10^3$  s. It is also possible that these interactions are more or less pH independent.

### 5.3.2.3 *Effect of variation of measuring temperature*

As indicated previously (section 4.5.3) the measuring temperature may be a very valuable parameter for characterizing acid casein gels, once formed and after a certain ageing time. The value of the dynamic moduli of such formed acid casein gels (pH=4.6) tended to decrease strongly as temperature was raised (see section 4.5.3). There is one prerequisite: the gels must have a considerable age, so that  $G'$  only increases slowly during the measurement because of further ageing.

In all experiments temperature was varied in the following manner: after ageing at 20 °C for approximately  $10^5$  s the gels were cooled down first in steps of 5 °C to a lowest temperature of 5 °C. The rate of cooling and heating was always 0.5 °C per minute. After each temperature change a waiting time of 20-30 min was allowed, before  $G'$  and  $\tan \delta$  were measured. Subsequently the

Table 5.4  $G'$  and  $\tan \delta$  of a number of gels with varying pH, before and after the measuring temperature experiment.  $T=20\text{ }^\circ\text{C}$  and  $\omega=1.0\text{ rad.s}^{-1}$ . The age at the beginning of the temperature experiment is given in s.

gel no.	pH	age $10^5$ s	$G'$ ( $\text{Nm}^{-2}$ )		$\tan \delta$	
			before	after	before	after
1	4.40	1.85	456	386	0.24	0.28
4	4.83	1.85	550	391	0.25	0.32
6	5.01	0.85	319	262	0.28	0.31
7a	5.10	0.77	209	170	0.30	0.30
7b	5.16	0.85	94	40	0.36	0.39
8a	5.20	0.80	61	8	0.40	0.42
9	5.40	0.80	68	2	0.36	0.36
10	5.60	0.85	137	11	0.30	0.29
11	5.83	0.85	189	18	0.26	0.27

system was heated in steps of  $5\text{ }^\circ\text{C}$  first to  $20\text{ }^\circ\text{C}$  and then ultimately to  $40\text{ }^\circ\text{C}$ . At the end the gels were cooled down to  $20\text{ }^\circ\text{C}$  in a single step and the residual value of the moduli was determined (see table 5.4).

In fig. 5.11a and 5.11b  $G'$  is depicted as a function of measuring temperature first on a linear and then on a logarithmic scale. At low pH, i.e. 4.4-4.8, the same temperature dependence was found as for acid casein gels made without rennet (compare these results and fig. 5.5 with fig. 4.7 and 4.8): a fairly linear decrease of  $G'$  with measuring temperature  $T_m$  was noted especially above  $20\text{ }^\circ\text{C}$ . No explanation can be given for the relative increase at pH=4.4 between  $35\text{ }^\circ\text{C}$  and  $40\text{ }^\circ\text{C}$ . It is probably not due to increased gelation, because  $G'$  was lower after the temperature experiment (table 5.4). Above pH=4.8 the temperature behaviour changed drastically. A maximum value of the dynamic modulus was seen between  $15$  and  $20\text{ }^\circ\text{C}$  and  $G'$  tended to decrease as temperature was lowered below  $15\text{ }^\circ\text{C}$ . In the range of pH=4.9 to 5.1  $G'$  decreased above  $20\text{ }^\circ\text{C}$  as expected for acid casein gels. Although the moduli of the gels lost a considerable part (about 20%) of their value after being heated from  $20\text{ }^\circ\text{C}$  to  $40\text{ }^\circ\text{C}$  (table 5.4), they were still character-

creased hydrolysis with temperature may be expected to occur at each pH, probably with a small optimum around pH=5.2-5.4 (see next section), but certainly not with such a strong transition as observed in this experiment. Thus it may be expected that increased hydrolysis could only explain a small part in the sharp drop  $G'$ .

The lack of microsineresis is one of the characteristics of acid casein gels at pH=4.6 (see chapter 3 and 4). On the other hand from cheese making practice it is known that syneresis is stimulated by heating and acidification. Van Vliet and Van Dijk (to be published) pointed out that for rennet gels (pH=6.7) there is possibly a relation between the value of  $\tan \delta$  and the susceptibility to microsineresis. Gels with a higher  $\tan \delta$  value over the frequency range of  $10^{-2}$  to  $10^1$  rad.s<sup>-1</sup> tended to show an increase in rate of microsineresis. Microsineresis leads to a coarsening of the gel network (Van Dijk, 1982). For the gels formed at pH values >5.1 this was ultimately visible macroscopically, as the colloidal white appearance of the gels had changed into a grey appearance after the temperature experiment.

The behaviour of  $\tan \delta$  as a function of measuring temperature at five different pH's ( $\omega=1.0$  rad.s<sup>-1</sup>) is shown in fig. 5.12. The values of  $\tan \delta$  and  $G'$  before and after the temperature experiments are given in table 5.4. The results at 20 °C before and after cooling to 5 °C were equal within experimental error. This also applied to the  $\tan \delta$  values after the heating cycle. The seemingly large deviations at pH=4.4 and 4.8 are still within experimental error limits.

Fig. 5.12 shows that at 5 °C there was little variation in  $\tan \delta$  (from 0.25 to 0.30 for all pH's), as pH was varied, while at 40 °C a dramatic effect of pH was registered. At low pH (4.4 to 4.9) horizontal curves ( $0.20 < \tan \delta < 0.30$ ) were found for  $\tan \delta$  as a function of measuring temperature. At higher pH  $\tan \delta$  gradually increased with temperature with a maximal increase at pH=5.2. After a further increase in the pH to 5.8 the increase in  $\tan \delta$  became smaller again especially at  $T_m$  below 30 °C. Above 30 °C there was still a relatively strong increase. This effect was also found by Zoon (1984) for rennet gels. From table 5.4 and fig. 5.11b one can conclude that the relatively strong decrease in  $G'$  with temperature and the concurrent increased lack of reversibil-

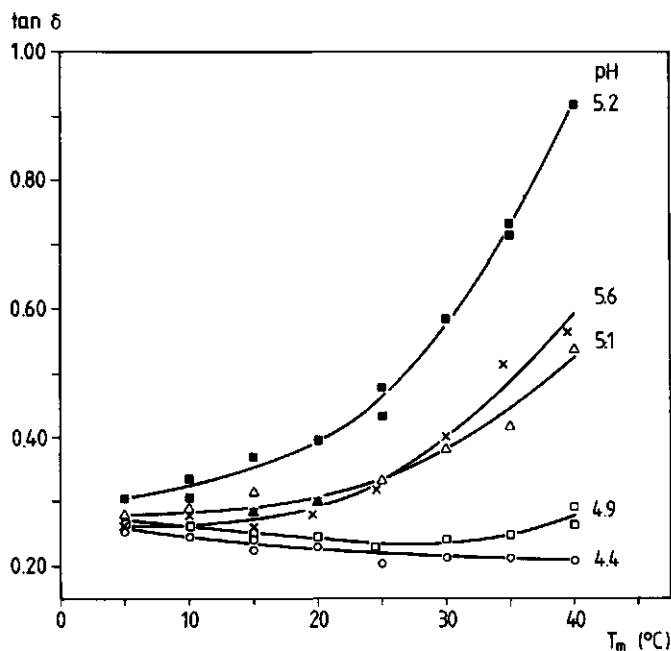


Fig. 5.12 The loss tangent  $\tan \delta$  as a function of measuring temperature  $T_m$  for the gels of fig. 5.11b. pH values are indicated.  $\omega=1.0 \text{ rad.s}^{-1}$ .

ity in the value of  $G'$  after the temperature experiment, began at a pH of around 5.16. At pH=5.16 a value of 0.75 for  $\tan \delta$  at 40 °C was found. Comparing fig. 5.11b and fig. 5.12 with table 5.4 shows that a high value of  $\tan \delta$  at high temperature correlates with the above-mentioned decrease of  $G'$  and the increased lack of reversibility in  $G'$ . In general the decrease of  $G'$  occurred when  $\tan \delta$  was greater than 0.45-0.50, whereas microsineresis should result in a coarsening of the gel network. Therefore probably the fall in  $G'$  during the temperature experiment was accompanied more by a decrease in the number of interactions i.e. the number of interparticle bonds, which would correspond to a coarsening of the gel network, than to a change in the nature of the interactions.

The resemblance of the curves for pH=5.1 and 5.6 (fig. 5.12) showed that the correlation between enhanced microsineresis and value of  $\tan \delta$  at  $\omega=1.0 \text{ rad.s}^{-1}$  as a function of measuring tempe-

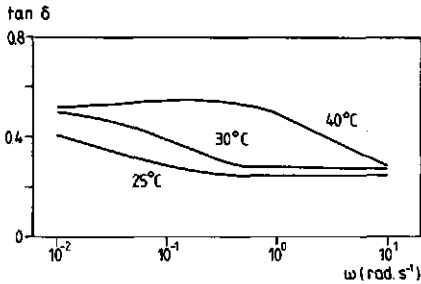


Fig. 5.13 The loss tangent  $\tan \delta$  as a function of frequency  $\omega$  (rad.s<sup>-1</sup>) for renneted skimmilk gels (pH=6.7) at three different measuring temperatures (after Zoon, 1984). The observed effect is independent of ageing temperature.

perature was not complete. Although they had a similar  $\tan \delta$  curve they largely differed in the observed decrease of  $G'$ . In the first instance it is questionable whether it is permissible to correlate microsineresis only with the  $\tan \delta$  value at  $\omega=1.0$  rad.s<sup>-1</sup>, because one may also expect syneresis processes to occur over longer time scales. Rennet gels (pH=6.7) for example had approximately the same value for  $\tan \delta$  at  $\omega=1.0$  rad.s<sup>-1</sup> in the temperature range of 20 to 30 °C, while at lower  $\omega$  the values of  $\tan \delta$  differed significantly (see fig. 5.13, after Zoon, 1984). The microsineresis of rennet gels is enhanced considerably when their temperature is raised from 20 to 30 °C. Moreover at pH=5.6 the colloidal calcium phosphate will be only partially dissolved. Therefore the composition of the casein particles and probably the type of interaction forces between them will differ between pH=5.1 and 5.6.

In general it is clear from the results of this section that enhanced microsineresis upon heating depends on the  $\tan \delta$  value of the preformed gel at elevated temperatures and perhaps also on the pH-determined composition of the basic elements (casein particles). The small decrease in  $G'$  found at pH<5.1 after the heating cycle was possibly not due to microsineresis. This will be discussed further in the next section.

A final remark not directly related to the discussion above, is that none of the gels demonstrated a temperature behaviour characteristic of an ideal rubber gel. Acid casein gels therefore do not behave as ideal elastic gels and both energetic and entropic effects contribute to the Helmholtz energy (see eq. 3.1).

### 5.3.2.4 Proteolytic degradation

The amount of residual  $\beta$ - and  $\alpha_{s1}$ -casein was determined according to section 2.6. The gel samples were prepared by the procedure used in the rheological experiments. The pH of the samples varied from 4.5 to 5.9. At each pH the degradation was followed as function of time over  $5 \times 10^5$  s (~140 hrs).

In fig. 5.14a and b, respectively, the residual amount of  $\beta$ - and  $\alpha_{s1}$ -casein is depicted as a function of pH. pH was measured at 20 °C. The baseline for the residual casein concentration in fig. 5.14a and b was approximately about 8% for  $\beta$ -casein and 18% for  $\alpha_{s1}$ -casein.

Both  $\alpha_{s1}$ - and  $\beta$ -casein were hydrolysed to a considerable extent. It is probable that the initial degradation products ( $\alpha_{s1}$ -I,  $\beta$ -I,  $\beta$ -II casein, etc.) still contributed considerably to the structure of the gel network, but it is also possible that casein molecules not involved in network bonds were more readily attacked by rennet and so were degraded more rapidly. Both  $\alpha_{s1}$ - and  $\beta$ -ca-

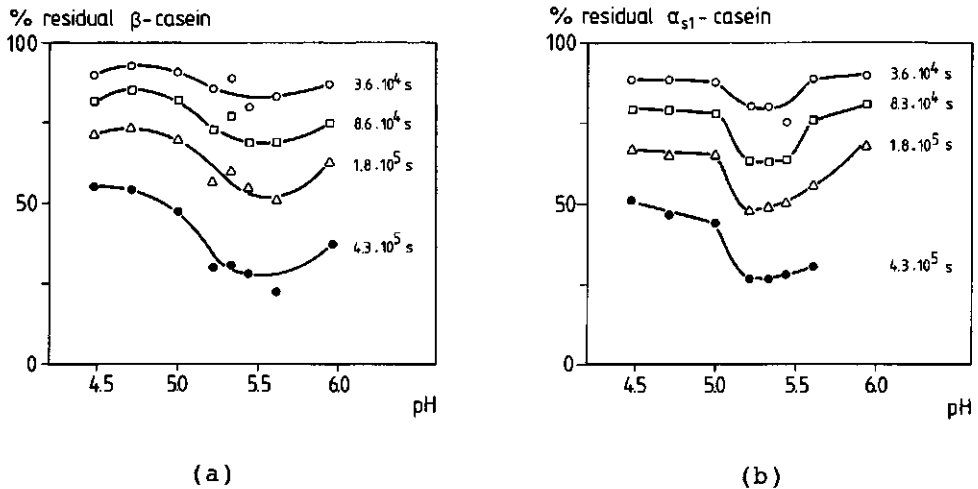


Fig. 5.14 The percentage of residual  $\beta$ -casein (a) and  $\alpha_{s1}$ -casein (b) concentration in skimmilk gels made by the combined action of acidification and 250 ppm rennet reaction as a function of pH at four different ageing times. Rennet was added at  $t=0$ . Ageing times are indicated.

sein showed about the same pH-dependence of protein breakdown, although  $\alpha_{s1}$ -casein was hydrolysed somewhat faster (fig. 5.14). A maximum degree of proteolysis occurred around pH=5.2-5.4 for  $\alpha_{s1}$ -casein and around pH=5.4-5.6 for  $\beta$ -casein, which was somewhat different from the results of Fox (1969) who used sodium caseinate, Fox and Mulvihill (1977 and 1979a) who used a pure  $\alpha_{s1}$ -casein solution or De Jong (1977) who used sodium paracaseinate. All of these workers reported a maximum degree of proteolysis around pH=5.8.

For comparison with the measurements shown in fig. 5.7 one has to restrict oneself to the proteolysis occurring during the first  $2 \times 10^5$  s. As argued already in section 5.3.1 the deviation from a linear increase of  $G'$  with  $\log t$  found at pH=4.6 upon rennet action was probably partly due to casein hydrolysis. The same arguments may be applied to the bending of the other  $G'$  versus  $\log t$  curves at a pH  $\leq 5.1$ . However the bending of the gelation curves at pH values greater than 5.1, which was already underway within  $4 \times 10^3$  s, cannot be due to increased hydrolysis alone. Nor can hydrolysis explain the large effect of pH on  $G'$ , e.g. after  $10^4$  and  $10^5$  s (fig. 5.8), as hydrolysis varies relatively little with pH. Besides for all samples the protein hydrolysis after  $10^4$  s was still very small. It is more probable that the significant increase of  $\alpha_{s1}$ -casein hydrolysis, when pH was raised from 5.0 to 5.2 had the same root cause as the large decrease in  $G'$  around these pH's: i.e. a change in the structure and properties of the casein particles, which form the gel network, and thus an alteration in the availability of the caseins for proteolytic activity. This change would enhance microsyreresis and cause the large bending and lowering of the  $G'$  versus  $\log t$  curves.

The electrophoretic pattern varied with pH. At pH=4.5  $\beta$ -I casein was only visible as a small band, which meant that  $\beta$ -I casein in its turn was hydrolysed relatively rapidly. The  $\beta$ -II casein band was clearly visible, whereas the  $\beta$ -III casein band could hardly be detected. Of the  $\alpha_{s1}$ -casein degradation products only  $\alpha_{s1}$ -I casein was clearly visible. At this pH only traces of one or two other degradation products of  $\alpha_{s1}$ -casein could be seen. At pH=5.2 to 5.4 more  $\beta$ -I and relatively less  $\beta$ -II casein was detected, even a trace of  $\beta$ -III casein could be seen. Probably the

degradation of  $\beta$ -I casein was slowed relative to the other processes. A more intense  $\alpha_{s1}$ -I casein band but again hardly any traces of other  $\alpha_{s1}$ -casein degradation products were seen. As pH increased to pH=5.9 the level of  $\beta$ -II casein was reduced to a trace, while  $\beta$ -I casein appeared as an intense band.  $\alpha_{s1}$ -I casein was again the single detectable degradation product of  $\alpha_{s1}$ -casein. Within experimental error, it was not possible to detect any correlation between the pattern of degradation products and the rheological properties of the gels at any pH.

#### 5.4 General remarks

The number and strength of bonds between casein particles and the spatial distribution of the particle strands determine the value of the dynamic modulus  $G'$  (chapter 4). The loss tangent,  $\tan \delta$ , depends much more on the relative number and the character of the different bonds between the casein particles than on the spatial distribution of the strands. The shape and magnitude of the  $G'$  versus  $\log t$  curves and the (ageing and measuring) temperature dependence of  $G'$  are determined by five factors:

1. The molecular conformation of the individual casein molecules and the molecular structure of the casein particles consisting of aggregated casein molecules.
2. The spatial distribution of the stress carrying strands and the large conglomerates, both consisting of coagulated casein particles.
3. The ratio of the rates of protein-protein bond formation and cleavage in the region between the coagulated casein particles.
4. The rates of hydrolysis of  $\alpha_{s1}$ - and  $\beta$ -casein molecules, which effectively contribute (directly or indirectly) to the interparticle bonds.
5. The occurrence of microsineresis, which is very much temperature and pH dependent, depending as it does on the structure of the casein particles and the relaxation behaviour of the interparticle bonds.

From the results of this chapter it can be concluded that GMP has a large effect on the stability of casein particles over the entire pH range from 4.4 to 6.7. The character of the skimmilk

gels made by the combined action of acidification and rennet changed abruptly around  $\text{pH}=5.2$ .

Below  $\text{pH}=5.2$  the gels formed were subject only to proteolytic hydrolysis and not to microsineresis. At and around the isoelectric  $\text{pH}$  of casein particles the values of the dynamic moduli increased considerably (fig. 5.2 and 5.8) as GMP was released and skimmilk gels could be formed even at low temperatures ( $<10^\circ\text{C}$ ). However, these gels consisted of a much coarser gel network than in case of acid skimmilk gels made without rennet. Therefore the number of bonds between the casein particles must have increased drastically, because the character of the bonds remained the same, as  $\tan \delta$  did not change upon rennet action. Particle fusion will be enhanced and more homogeneous gel network strands will be formed.

Above  $\text{pH}=5.1$  the skimmilk gels became subject to both proteolytic hydrolysis and microsineresis. Microsineresis may occur because of a sharp change in casein particle structure and relaxation behaviour of the interparticle bonds around  $\text{pH}=5.2$ . Particularly at higher temperatures ( $>30^\circ\text{C}$ ) the relaxation behaviour of the interparticle bonds altered as indicated by higher values of  $\tan \delta$ . It is suggested that this is due to a change in the contribution rather than the nature of the different types of inter-

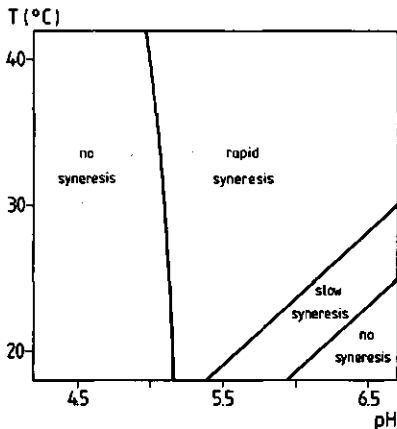


Fig. 5.15 Schematic picture of syneresis behaviour of skimmilk gels made by combined action of acidification and rennet as a function of  $\text{pH}$  and temperature.

action forces. The occurrence of microsineresis may be coupled to the behaviour of  $\tan \delta$ , although not at the angular frequency of  $1.0 \text{ rad.s}^{-1}$  applied in this study.

Based on the results of this chapter a schematical picture of the occurrence of microsineresis in skimmilk gels can be drawn. This is done in figure 5.15 with temperature and pH as variables. In this graph we have made no distinction between syneresis and microsineresis. The most remarkable feature is the sharp transition from the region of rapid microsineresis to that of no microsineresis at  $\text{pH}=5.2$ , a transition which is hardly temperature dependent.

## 6 PULSE NMR STUDY OF CASEIN SOLUTIONS

### 6.1 Introduction

Nuclear Magnetic Resonance (NMR) spectroscopy is a widely used non-invasive, relatively rapid, spectroscopical technique. In NMR measurements one makes use of the specific magnetic properties of the nuclei of certain atoms. Hydrogen nuclei are the most abundant and appropriate nuclei for this purpose, but recently much attention has been given to carbon-13, phosphorous-31, nitrogen-14, deuterium-2, fluorine-19 and oxygen-17. The NMR technique nowadays is employed in many variations, of which ordinary wide line and pulse NMR are the most familiar.

In this study only pulse NMR is applied to hydrogen nuclei. Two characteristic relaxation times, which depend on the environment and mobility of the nuclei, are determined: the spin-lattice relaxation time,  $T_1$ , and the spin-spin relaxation time,  $T_2$ . The large difference in  $T_2$  between mobile and immobile nuclei offers the possibility of monitoring the behaviour of hydrogen nuclei in all kinds of heterogeneous systems. Because water molecules i.e. the main constituent of all biological species consists of two hydrogen nuclei and one oxygen nucleus, pulse NMR can be a very suitable technique for determining the amount and mobility of those water molecules. Special interest has been focused on the physical state of water in biological systems such as protein solutions, or cellular suspensions and tissues (e.g. Packer, 1977, Lynch, 1983, Fullerton et al., 1982). In such systems more than one type of water can be distinguished on the basis of their mobility (e.g. bound and free water). Sometimes this distinction can be extended to three or even more different fractions (Fullerton et al., 1982). Even the flow of water through the vessels of plants may be measured (van As and Schaafsma, 1984). Furthermore the solid/liquid ratio or the solid fat content in systems containing oils and fats such as margarine, butter or oil in water emulsions (van Boekel, 1980) can be determined very easily using pulse NMR.

Recently Brosio et al. (1983, 1984) and Leung et al. (1976) studied water-binding to powdered milk and to three different dried milk protein species i.e. casein, albumin and  $\gamma$ -globulin. Brosio et al. divided the water content into a bound water and a free water fraction, the amount of which they were able to calculate. Each fraction was characterized by its own  $T_2$ -value, which changed in a different way for each protein species, as moisture content was raised. At the lowest moisture content the values obtained for powdered milk were very close to those obtained for albumin and only at higher moisture content were the values closer to those obtained for casein. In other experiments on milk systems Lelievre and Creamer (1978) observed no changes in relaxation times, when liquid skim milk was changed into a rigid gel by rennet action, as long as no visible syneresis occurred.

This study focuses on the effect of pH and temperature on the spin-spin relaxation time ( $T_2$ ) of hydrogen nuclei of the water molecules of casein solutions and skim milk. The behaviour of these water molecules strongly depends on the protein-water interactions. Therefore pulse NMR can provide a great deal of information concerning the properties of casein molecules. An additional advantage of pulse NMR arises from the large signal response from the abundant water protons in contrast to wide line NMR, where the less abundant protein protons are studied.

## 6.2 Principles of pulse NMR

A treatment of the basic principles of NMR has been given by Dwek (1973), and Farrar and Becker (1971). Many atomic nuclei possess a spin and thereby, an associated spin angular momentum. The possession of both spin and charge confers a magnetic moment on the nucleus. As only hydrogen nuclei are of interest in this study, we will limit this treatment to hydrogen nuclei and protons.

A number of electromagnetic properties of nuclei, although based on quantum mechanical restrictions, can be very easily visualized by a classical approach. When a nucleus and its spin is placed in a strong external (homogeneous) magnetic field,  $H_0$ , only two possible orientations for its magnetic moment,  $\mu_{up}$  and  $\mu_{down}$

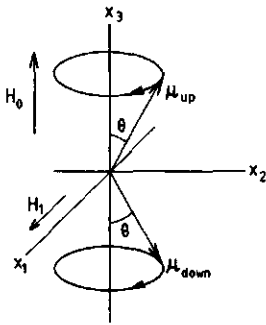


Fig. 6.1 Schematic picture of the magnetic moment vectors of hydrogen nuclei in the two spin states (spin-up and spin-down) inclined at an angle  $\theta$  relative to the direction  $x_3$  of an applied magnetic field  $H_0$ . The magnetic moment vector will precess around the direction  $x_3$  at the Larmor frequency  $\omega_0$ . To induce transitions between the two states  $H_1$  must be perpendicular to  $H_0$  and also rotating at the Larmor frequency  $\omega_0$ .

(see fig. 6.1), are allowed by quantum mechanical theory. The magnetic moment  $\mu$  will incline at a fixed angle  $\theta$  parallel or anti-parallel to  $H_0$ . Popular terms for these orientations are commonly termed the spin-up and spin-down positions. The torque exerted by the magnetic field,  $H_0$ , causes the nuclear magnetic moment to precess about  $H_0$  (in Tesla) at the so called Larmor precession frequency,  $\omega_0$  ( $\text{rad.s}^{-1}$ ):

$$\omega_0 = \gamma H_0 \quad (6.1)$$

where  $\gamma$  is the magnetogyric ratio ( $\text{rad.s}^{-1}.\text{Tesla}^{-1}$ ), a fixed constant for a given nucleus. The two permitted orientations differ in energy, each orientation being characterized by a fixed energy level. The difference between the energy levels,  $\Delta U(\text{J})$ , depends on the experimentally fixed field-parameter  $H_0$  and is given by:

$$\Delta U = \gamma \hbar H_0 \quad (6.2)$$

in which  $\hbar$  is  $h/2\pi$ , where  $h$  is Planck's constant ( $6.6256 \times 10^{-34}$  Js). The spin-up position, which is parallel to the magnetic field  $H_0$ , has the lower energy. In practical systems, there is always an ensemble of a large number of nuclei, possessing magnetic moments, all precessing at the same or nearly the same  $\omega_0$  (see fig. 6.2). The small energy difference (eq. 6.2) between the two energy levels results in a very small difference in population. The ratio

of energy level populations is governed by Boltzmann's distribution law:

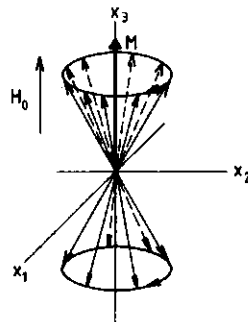
$$N_u/N_d = \exp (\gamma \hbar H_0 / kT) \quad (6.3)$$

where  $N_d$  and  $N_u$  are respectively the number of spins in the spin-down and the more populated spin-up position,  $k$  being the Boltzmann's constant ( $1.3807 \times 10^{-23} \text{ JK}^{-1}$ ) and  $T$  is absolute temperature (K). The slightly larger number of spins, aligned in the direction of the external magnetic field (along the  $x_3$ -axis of the coordinate system of figure 6.2) causes a net magnetization  $M_0$ , which is also orientated along the  $x_3$ -axis of the coordinate system. From equation 6.3 an expression for  $M_0$  can be derived (Abragam, 1961):

$$M_0 = N \gamma^2 \hbar^2 H_0 / 4kT \quad (6.4)$$

where  $N = N_u + N_d$  is the total number of spins in the system. Because the system is in thermal equilibrium transitions between the two energy levels continuously occur. These transitions are induced by interactions with the surrounding medium, interactions which are generated by local dipolar magnetic fields. These magnetic fields are fluctuating, since they mostly originate from other nuclei, both intramolecular and intermolecular. They disturb to a small extent the large external field  $H_0$  to which the nucleus is subjec-

Fig. 6.2 Precession of an ensemble of magnetic moments of hydrogen nuclei. The net macroscopic magnetization  $M$  is oriented along the  $x_3$  axis, the direction of the applied magnetic field  $H_0$



ted. These disturbances are responsible for the continuously occurring transitions between the spin levels, and they are the reason why the magnetic moments of an ensemble of nuclei do not precess in phase and at exactly the same frequency. If all magnetic moments did precess in phase and at the same frequency, this would imply that in fig. 6.2 the position of all magnetic moments could be visualized classically by two arrows, one representing the magnetic moments in the spin-up position and one for those in the spin-down position, both rotating around the  $x_3$ -axis. This would result in a net magnetic moment with a component rotating in the  $x_1x_2$  plane. However, in reality, the spins will be out of phase and in the case of an ensemble of spins at thermal equilibrium no net magnetization can be detected in the  $x_1x_2$ -plane perpendicular to the direction of the external field (see fig. 6.2).

Transitions between the two energy levels can also be induced by a radio frequency field,  $H_1$ , which is applied perpendicular to  $H_0$  in the  $x_2x_3$ -plane of the coordinate system (see figure 6.1). Energy is absorbed from this radio frequency field,  $H_1$ , only when the frequency of this field equals the Larmor precession frequency,  $\omega_0$ , of the nuclei. Upon energy absorption the population of the two energy levels is changed. When the  $H_1$  field is switched off, the spin system relaxes back to the equilibrium Boltzmann distribution. Two different relaxation processes may be distinguished, characterized by two different relaxation times: the spin-lattice relaxation time,  $T_1$ , and the spin-spin relaxation time,  $T_2$ . These relaxation times can be determined separately by means of two different pulse techniques. In both techniques the distribution of the magnetic moments over the two energy levels is disturbed, but in a different way. The difference between a  $T_1$  and  $T_2$  measurement can be partly classically visualized. In both cases a large  $H_1$  field is applied suddenly and for a short time i.e. a pulse of radiation is given.

In a so called  $T_1$  experiment the population of the energy levels is exactly inverted by a pulse of definite length and strength. Classically this can be visualized (fig. 6.2) by a net magnetization  $M_{x_3}(t)$  pointing along the  $-x_3$ -axis immediately after the  $H_1$  field is switched off. The relaxation of  $M_{x_3}(t)$  back to the equilibrium situation is characterized by the spin-lattice relaxation time,  $T_1$ :

$$M_{x_3}(t) = M_0(1-2\exp(-t/T_1)) \quad (6.5)$$

where  $M_0$  is the original equilibrium magnetization along the  $+x_3$ -axis. Thus at  $t=0$   $M_{x_3}(t)$  is  $-M_0$ . During this relaxation process, which is caused by interactions with the small local fluctuating magnetic fields, energy is transferred from the spin system to the surrounding medium, which is also termed the lattice.  $T_1$  is then measured by monitoring the amplitude and sign of  $M_{x_3}(t)$  using an additional special pulse sequence.  $T_1$  is also called the longitudinal relaxation time.

In a  $T_2$  experiment a shorter pulse is given. This leads to an equal occupation of both energy levels. Besides the fact that the magnetic moments are thereby all fixed in the same phase, as described above, this creates a net magnetization  $M_{x_1x_2}(t)$  at  $t=0$  in the  $x_1x_2$ -plane of figure 6.2. When the  $H_1$  field is switched off, two processes will occur, both caused by interactions with small local fields. First the spins will lose phase coherence partly because of spin-spin interactions between like nuclei and so the net magnetization in the  $x_1x_2$ -plane will vanish. In solid materials the loss of phase coherence is almost completely due to direct spin-spin interactions. The characteristic time  $T_2$  for this relaxation process is therefore mostly called the spin-spin relaxation time, but the term transverse relaxation time is also used. It is defined by the equation:

$$M_{x_1x_2}(t) = M_{x_1x_2,0} \exp(-t/T_2) \quad (6.6)$$

where  $M_{x_1x_2,0}$  is the net magnetization in the  $x_1x_2$  plane at  $t=0$  at the moment  $H_1$  is switched off.

$T_2$  is measured by monitoring the net magnetization in the  $x_1x_2$ -plane. The population of the two energy levels does not change because of the relaxation mechanisms involved only in the  $T_2$  processes and the loss of phase coherence is not attended by a transfer of energy from the spin system to the surrounding medium. However, simultaneously with the relaxation mechanisms just described transitions will occur from the higher to the lower energy level to restore the equilibrium Boltzmann distribution, governed

by the relaxation time  $T_1$ . These transitions also decrease the phase coherence (second process) and, on the contrary, are attended by a transfer of energy from the spin system to the surrounding medium. Thus any process, which is involved in the spin-lattice relaxation ( $T_1$ ) processes, will also be involved in transverse relaxation ( $T_2$ ) processes. Consequently  $T_2$  always will be smaller than or equal to  $T_1$ .

### 6.3 The effect of mobility of the nucleus on $T_2$

$T_1$  and  $T_2$  directly depend on the mobility of the molecules containing the hydrogen nuclei. This mobility is usually expressed in a correlation time  $\tau_c$ . The general relationship between  $T_1$ ,  $T_2$  and  $\tau_c$  for a homogeneous and isotropic nuclear spin system is shown schematically in figure 6.3. The parameter  $\tau_c$  is a characteristic time to describe the motion of a molecule and, depending on the state of the molecule, it can be regarded as either the time needed to move translationally over a distance equal to its own diameter, to rotate through an angle of one radian or as the average time between molecular collisions. The  $T_2$  of hydrogen nuclei in aqueous systems varies very strongly with the mobility of the water molecules. It is also strongly influenced by the ability of hydrogen nuclei on different water molecules to participate in

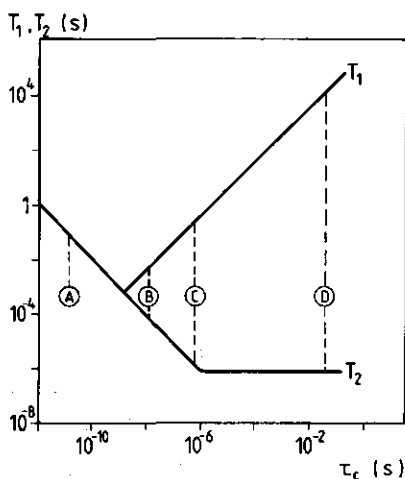


Fig. 6.3. Schematic dependence of relaxation times  $T_1$  and  $T_2$  on molecular correlation time,  $\tau_c$ , for a homogeneous and isotropic nuclear spin system. Ordinate and abscissa values are only approximate. (A): non viscous liquid,  $T_1 = T_2$ . (B): viscous liquid,  $T_1 > T_2$ . (C): non rigid solid,  $T_1 \gg T_2$ . (D): rigid lattice,  $T_1 \gg T_2$ .

spin-spin exchange processes. In this study we will focus our attention on the  $T_2$  of water protons in solutions of casein. No attention is paid to the hydrogen nuclei of proteins or other macromolecules, because not only do they possess very short  $T_2$  values but also they make only a small contribution to the total number of hydrogen nuclei present in a casein solution (viz. 10.4 wt.% dry matter for skimmilk and 3 wt.% casein for skimmilk and sodium caseinate solutions). It is widely accepted that the mobility of water decreases sharply in the vicinity of protein molecules or other macromolecules. The correlation time  $\tau_C$  may increase by some orders of magnitude, when a water molecule is transferred from a bulk solution to a water layer close to the surface of the protein, so that this is generally denoted as bound water (Berendsen, 1975). However, these water molecules still possess a considerable mobility and particularly the hydrogen nuclei rapidly exchange with the bulk solution. In fact water in a macromolecular solution should be regarded as a multi-phase system. It is then dependent on the exchange rate between these phases whether one or more  $T_2$  processes can be detected. This means that the curve of the decreasing transverse magnetization measured as a function of time can be fitted with one or more exponentials.

In the case of rapid exchange i.e. when the interchange time between phases is short in comparison to the relaxation time, the spin system will display a single relaxation rate:

$$1/T_2 = \sum_i P_i/T_{2i} \quad (6.7)$$

where  $P_i$  is the fraction of spins in the  $i^{\text{th}}$  phase and  $T_{2i}$  the relaxation time of the  $i^{\text{th}}$  phase. The transverse decay curve can be fitted with a single exponential, whose characteristic decay time is a weighted average of relative spin populations  $P_i$  and relaxation times  $T_{2i}$ . In the case of slow exchange the transverse decay curve becomes multiexponential and is built up of separate contributions from each phase:

$$M_{x1x2}(t) = \sum_i M_{x1x2,oi} \exp(-t/T_{2i}) \quad (6.8)$$

where  $M_{x1x2}(t)$  is the total transverse magnetization relaxing to zero and  $M_{x1x2,0i}$  is the transverse magnetization of the  $i^{\text{th}}$  phase at  $t=0$  after applying the pulse.

In practice, however, the exchange rate between the water phases very often will be intermediate relative to the decay rates of the phases. In that situation, fitting the decay curve becomes very complicated and the  $T_{2i}$  values found often vary as protein concentration is varied. Brosio et al. (1983 and 1984) distinguished two water phases in their study of water-binding to milk proteins resulting in a biphasic transverse decay curve. But there the relaxation time  $T_2$  of both bound and free water also tended to increase with water content.

#### 6.4 Experimental results

All skimmilk (standard concentration) and sodium caseinate solutions, respectively reconstituted from skimmilk powder A (section 2.1) and freeze-dried sodium caseinate (section 2.2) were acidified to pH's varying from 6.7 to 4.6 according to section 2.3. The highest pH among the sodium caseinate solutions was 6.9. All pH values given were measured at 0-2 °C after the acidification step was completed. Some solutions later showed increased pH values (see later). Milk ultra filtrate was obtained as described in section 2.5. The measurements were carried out with the apparatus described in section 2.9.

Using extensive curve-fitting calculations, preliminary experiments with skimmilk (pH=6.7) and acid skimmilk gels (pH=4.6) revealed only one dominant exponential ( $\geq 96\%$  of total amplitude), except when a small layer of condensed water or syneresis fluid had developed. All later measurements were fitted with one exponential, which could be adequately corrected for the small overlying liquid layer.

The measuring tubes were filled immediately after acidification and for any particular gel, the same tube was used at all temperatures. Temperature inaccuracy was within 0.5 °C at lower temperatures and about 0.5 °C at higher temperatures. Repeat measurements of  $T_2$  for a sample in the same tube varied by at most 0.5%. Different tubes containing the same gel sample sometimes showed devi-

ations of a few percent. All samples were first equilibrated for at least one hour at the measuring temperature, unless stated otherwise. If not used for longer times they were stored at 4° C.

#### 6.4.1 $T_2$ of skimmilk

After acidification the skimmilk samples were stored at 0-4 °C overnight. Experiments were carried out at the rate of two temperatures per day. Figure 6.4 shows the  $T_2$  of skimmilk as a function of pH measured at respectively 4, 10.5, 20, 30, 40 and 49.5 °C. In the sample of pH=5.2 at 49.5 °C the milk protein had flocculated and too much syneresis fluid was formed to give a reliable value for  $T_2$ .

There was a very strong effect of pH on  $T_2$  at every temperature investigated. A maximum in  $T_2$  is found between pH=5.0 and pH=5.2. These pH values were somewhat arbitrary, because the dissolution of colloidal calcium phosphate was a time consuming process at pH's above 5.0 (see section 3.3). If we had waited a longer time before measuring the pH after acidification the pH-value obtained would have been shifted upward by approximately 0.1 to 0.3 units depending on the temperature.

An increase of  $T_2$  with temperature as found was expected as the correlation time  $\tau_c$  of the hydrogen nuclei decreases with temperature (see fig. 6.3).

The maximum found in the  $T_2$  value when pH of the skimmilk was varied (fig 6.4), must be ascribed to the skimmilk proteins and perhaps to the CCP, but not to the salt solution. This follows when we compare the results shown in figure 6.5 for milk ultrafiltrate with those of figure 6.4 for skimmilk. This milk ultrafiltrate, obtained at room temperature from standard skimmilk, was acidified at 0-2 °C according to section 2.3. As a check, we also used ultrafiltrate obtained at 4 °C from skimmilk which had been first acidified to the range pH=5.0 to 5.2. The  $T_2$  values for the ultra filtrates were about five times higher than for the corresponding skimmilk and are very close to the  $T_2$  value of pure water. No clear influence of pH on  $T_2$  was found. The  $T_2$  values of ultrafiltrate obtained from skimmilk acidified to pH=5.2 and 5.0 agreed well with those of ultrafiltrate made from skimmilk of pH=6.8 and acidified to the same pH (see fig. 6.5).

The ultrafiltrate sample of pH=6.8 showed a remarkable decrease in  $T_2$  during the measurement at 49.5 °C. This must have been due to the formation of a calcium phosphate precipitate (see also section 3.3.2.2). Prolonged heating at 50 °C enlarged the decrease, which after extended waiting time led to a  $T_2$  value of about 1.6 s. The temperature dependence was almost the same for all pH's.

At low pH the decrease in the value of  $T_2$  of skimmilk with decreasing pH might be related to an increasing gelation of these skimmilk solutions, especially at higher temperatures, since gelation tends to decrease the  $T_2$ . This is illustrated in fig. 6.4 for pH=4.6, where the filled symbols belong to a skimmilk sample, which was aged 10 hrs at 30 °C before the first measurement (see text).

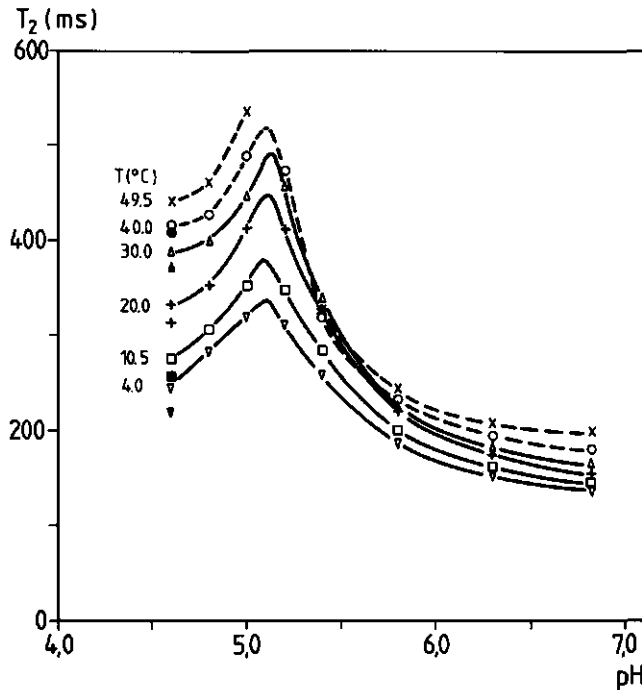


Fig. 6.4. The  $T_2$  (ms) of acidified skimmilk as a function of pH. The temperature was varied as indicated. The filled symbols at pH=4.6 belong to a skimmilk solution, which was aged 10 hrs at 30 °C before the first measurement (see text).

was gelled at 30 °C over 10 hrs and then cooled for the first measurement at 4 °C. It shows that there was a small but noticeable difference in  $T_2$  between gel and solution of skimmilk at pH=4.6, especially at low temperature. The  $T_2$  of the gel was significantly smaller. The difference vanished as the solution became a gel during the measurements at 20 °C and higher. At 49.5 °C there was no difference anymore. However, as we shall show later it is more likely that the observed pH dependence is due to aggregation of casein molecules inside the casein particles rather than to aggregation of these particles themselves (see for further discussion chapter 3 and section 6.5).

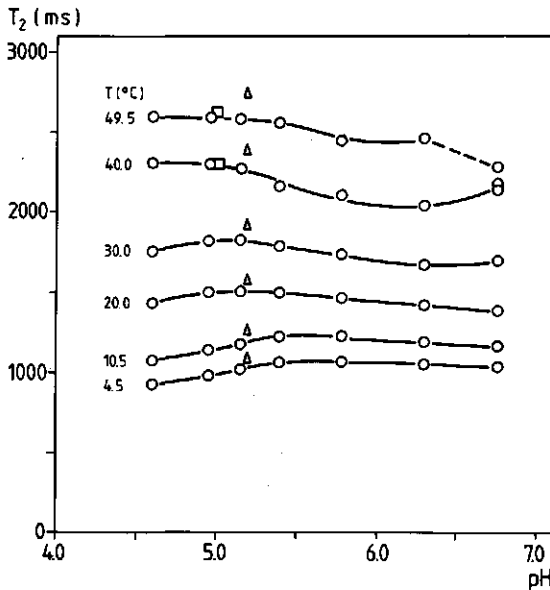


Fig. 6.5 The  $T_2$  (ms) as a function of pH for milk ultrafiltrate obtained at room temperature from standard skimmilk of natural pH and subsequently acidified (o). Also included are the  $T_2$  values of milk ultrafiltrate, gained from skimmilk acidified to pH=5.2 ( $\Delta$ ) and pH=5.0 ( $\square$ ). Temperature was varied as indicated. For the sample with pH=6.76 at 49.5 °C, where  $T_2$  strongly decreased during the measurement, the highest value obtained is given (see text).

### 6.4.2 $T_2$ of sodium caseinate

In order to study the influence of the casein on the  $T_2$  values in absence of colloidal calcium phosphate and serum proteins the same experiments were repeated with solutions of sodium caseinate in water (see section 2.2 and 2.3). The casein concentration varied slightly from 2.8 to 2.9 wt.%, depending on the volume of acid added. Figure 6.6 shows the results for sodium caseinate dissolved in a solution of 0.13 mol NaCl per kg dispersion. The  $T_2$  value diminished with decreasing pH. No maximum with pH was found, unlike the behaviour of skimmilk. The drop in  $T_2$  with decreasing pH became more pronounced at higher temperatures especially in the pH region between 5.0 to 6.0. At low pH the  $T_2$  value was only slightly larger than for skimmilk, while at higher pH the  $T_2$  value of

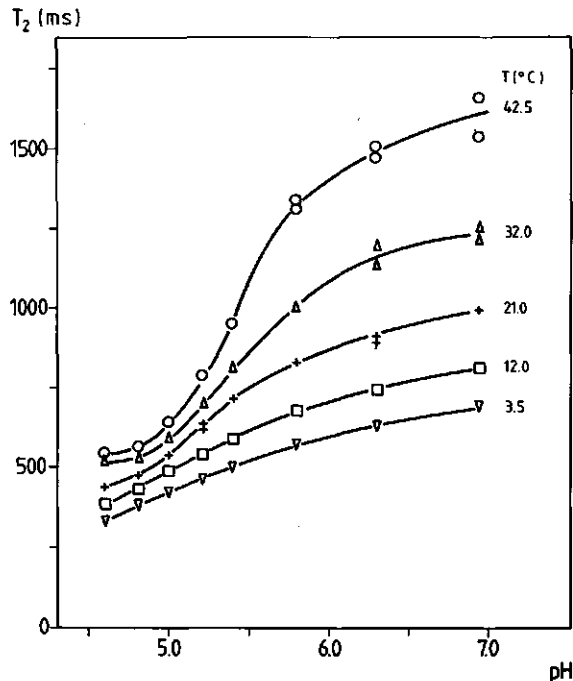


Fig. 6.6 The  $T_2$  (ms) of acidified sodium caseinate solutions as a function of pH. Temperature was varied as indicated. The casein concentration was 2.8-2.9 g per kg dispersion. The caseinate was dissolved in a solution of approximately 0.13 mol NaCl per kg dispersion.

sodium caseinate solutions was much larger. Part of the difference, especially at low pH, will be due to the absence of serum proteins and all other smaller milk components.

$T_2$  again increased with temperature. At low pH ( $\leq 5.1$ ) the increase was more or less identical to that shown by skimmilk. However, at higher pH's the rise in  $T_2$  as a function of temperature was much larger than at low pH's, in contrast to the behaviour of skimmilk solutions.

Upon acidification at 0-2 °C the appearance of the sodium caseinate solutions changed from a rather clear, greyish colour to colloidal white and turbid (just like milk) at pH=4.6 (see section 3.3.3). This must have been caused by the aggregation of casein, and could also be observed on electron micrographs (fig. 3.10, section 3.3.3). The transition from smaller to larger casein aggregates, which took place between pH=5.8 and 5.2, is paralleled only at higher temperatures by a steep decline in  $T_2$  value.

When sodium caseinate was dissolved in a solution of 0.066 mol NaCl and 0.022 mol  $\text{CaCl}_2$  per kg dispersion ( $I \sim 0.13 \text{ M}$ ), large protein aggregates were already present at pH=6.6. These tended to sediment when stirring was stopped. The solution had the same colloidal white appearance as skimmilk (see also section 4.5.5.3). Figure 6.7 shows the  $T_2$  value of sodium caseinate dispersed in the above mentioned mixture of NaCl and  $\text{CaCl}_2$  as a function of pH at three different temperatures. These results are less absolute than those given previously, because some sediment was present in every tube. No attempts at curve fitting were applied to distinguish a

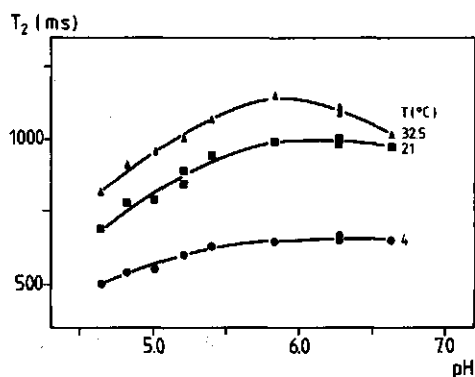


Fig. 6.7. The  $T_2$  (ms) as a function of pH for sodium caseinate; dispersed in a solution of 0.066 mol NaCl and 0.022 mol  $\text{CaCl}_2$  per kg dispersion and then acidified. Temperature was varied as indicated.

separate  $T_2$  value for the hydrogen nuclei of the water molecules trapped in the sediment. The  $T_2$  value shown probably belongs to the supernatant caseinate solution, this solution obviously at a lower protein concentration than the corresponding caseinate solutions dissolved in pure NaCl.  $T_2$  again generally decreased with decreasing pH but showed a small maximum around pH=6.0 at 32.5 °C. Although absolute values cannot be compared there is a striking difference in pH dependence caused by the presence of calcium ions.

### 6.5 Discussion

The large effect of pH on the  $T_2$  value of skimmilk and sodium caseinate solutions proves that the  $T_2$  value of hydrogen nuclei of water is a very useful parameter for monitoring the protein-water interactions in these systems. The large difference in  $T_2$  between milk ultrafiltrate and skimmilk or sodium caseinate solutions proves the presence of at least two water phases: free water and so called bound water. The bound water must be situated on the casein (or casein micelles), serum proteins and perhaps on the amorphous colloidal calcium phosphate (CCP). Rapid or at least moderate exchange must be responsible for the  $T_2$  values obtained for skimmilk.

Brosio et al. (1983 and 1984) distinguished a bound and a free water fraction with a multiphasic transverse decay curve for powdered milk and milk proteins. However the  $T_2$  values of both phases increased with water content, which points to exchange processes within the time scale of the NMR measurements. The change of  $T_2$  value upon acidification could be due to a change in the amount of bound water, but could also be the result of a change in the rate of exchange between bound and free water or to a change in  $T_2$  value itself of that bound water. According to Berlin et al. (1970) the amount of bound water should be 0.55 g/g casein and 0.50 g/g total whey protein as estimated by a DSC technique. In the same way Rüegg et al. (1974) estimated the amount of bound water to be 0.44 g/g casein for casein micelles, para casein, and acid precipitated casein also. Using NMR techniques, the amount of non-freezable water was estimated to be 0.3 g/g dried casein

micelles (Lelievre and Creamer, 1978) and 0.26 g/g purified casein (Leung et al., 1976). Thus the amount of water very tightly bound to individual casein molecules may vary from 0.25 to 0.55 gram per gram casein depending on the measuring method. Based on the above literature data it is difficult to say whether the amount of tightly bound water changes with the state of casein; nor is it possible to say what will be the size of the total bound water fraction in casein solutions. Concentration dependent experiments will be necessary to reveal the state of water more explicitly. In this way it may be possible to correlate the measured  $T_2$  values with the hydration and voluminosity of casein.

Recently Fullerton et al. (1982) proposed a model with three water phases to explain results on tissue and cellular suspensions. The bound water fraction was split up into a hydration water phase and a crystalline water phase. A large hydration water layer will slow the exchange between crystalline water and free water, this exchange determining the  $T_2$  of the free water. According to the model an increasing hydration fraction would lead to an increasing  $T_2$  value. Concentration dependent experiments will be necessary to check the applicability of this model to skimmilk solutions.

Therefore with the results presented in the previous section it is not yet possible to give a conclusive model which will use the measured  $T_2$  parameter, the spin-spin relaxation time, to describe the behaviour of water in casein systems in terms of bound, free or even more water phases. Thus we will try to explain our own results in more general terms.

Skimmilk is a complicated system containing mainly proteins (chiefly casein and serum proteins) and lactose dissolved in a mixture of several kinds of salts. The composition of the salt mixture will change upon acidification, when CCP dissolves from the casein micelles. The  $T_2$  value of the salt solution however was hardly affected by pH or by dissolution of CCP (fig. 6.5) As discussed in section 3.3 the structure of the casein particles changes drastically during acidification from pH=6.7 to 4.6. Roughly speaking above pH=5.2 the casein is present in the form of casein micelles or the relics of casein micelles, these both con-

sisting of aggregated casein molecules and amorphous CCP. Below pH=5.2 the casein particles no longer contain CCP. As discussed in chapters 3 and 4, casein aggregation is accompanied by the formation of protein-protein bonds at three levels: intramolecular, leading to the secondary and tertiary structure of the proteins, intermolecular inside the casein particles and governing the structure of those casein particles, and intermolecular between different particles. The latter reaction is in fact coagulation and may be followed by gel formation. CCP is mainly involved at the second level. All of the different components of skimmilk will influence the state of water, but all to different extents.

Lelievre and Creamer (1978) determined the  $T_2$  values of skimmilk and rennet whey at natural pH ( $T=34^\circ\text{C}$ ) at the same frequency of the magnetic field ( $\approx 20$  MHz, see section 2.9) as we used in this study. For skimmilk they found an identical value for  $T_2$  ( $\approx 0.17$  s) as can be derived from fig. 6.9 for reconstituted skimmilk (pH=6.8) at  $34^\circ\text{C}$ . The value they found for whey ( $T_2=1.3$  s) was smaller than the  $T_2$  of our corresponding milk ultrafiltrate (containing lactose and all dissolved salts), which we estimate to be 1.9 s (fig. 6.5). The difference between those two values must be ascribed to the presence of serum proteins and glycomacropetides in the whey. However, the difference in  $T_2$  between whey and milk ultrafiltrate (1.3 and 1.9 s., respectively) is small when compared to the difference between skimmilk and whey (0.17 s. and 1.3 s. respectively). This implies that, certainly at natural pH, the  $T_2$  of skimmilk depends to a large extent on the casein and maybe on the CCP. Moreover it must certainly also depend on their mutual interaction as reflected in their interaction with water. For at pH=6.7 a higher value of  $T_2$  was found for the sodium caseinate solutions (fig. 6.6) than for skimmilk. It seems reasonable to suppose that at other pH's, too, the  $T_2$  of skimmilk and sodium caseinate solutions will (largely) depend on the interaction of water molecules with casein and for the skimmilk at higher pH's also directly or indirectly on the CCP. Supporting evidence for this statement is found by comparing the small change of  $T_2$  with pH for milk ultrafiltrate (fig. 6.5) with the strong pH dependency of  $T_2$  found for sodium caseinate solutions (fig. 6.6) and the peculiar effect of pH on  $T_2$  for skimmilk (fig. 6.4). Further the

curves of  $T_2$  versus pH for pure sodium caseinate (fig. 6.6) show a great similarity to the curves of skim milk at low pH, but a striking difference at higher pH's (above pH=5.2). This difference must be due to the absence of CCP in the sodium caseinate solutions. The strong increase of  $T_2$  with decreasing pH for skim milk at pH>5.2 runs parallel to the dissolution of CCP from the casein micelles. The question remains unanswered, whether this increase in  $T_2$  stems directly from a change in the interactions between amorphous CCP and water, or whether it depends indirectly on the dissolution of CCP, because of a change of the casein aggregation induced by it, or whether it depends on both processes. Dissolution of CCP probably results in a partial unfolding of the casein particles accompanied at least at low temperature by a partial dissolution of casein molecules (section 3.3). Such a change in casein aggregation from within the casein particles will also be manifest in the voluminosity of casein as a function of pH and temperature (section 3.3).

The maximum around pH=5.1 in fig. 6.4 became more obvious as temperature was raised. This implies that the changes in  $T_2$  of skim milk as function of pH and temperature do not correlate directly with changes in the voluminosity of casein micelles (fig. 3.6, section 3.2). According to Darling (1982), Snoeren et al. (1984) and Tarodo de la Fuente et al. (1975) a maximum in the voluminosity of casein micelles was found around pH=5.4, particularly at temperatures below 30 °C. However in contrast to the maximum in  $T_2$  this one disappeared at temperatures above 30 °C (see fig. 3.6a after Darling, 1982), or became smaller (Van Hooydonk, 1986). At each pH above pH=5.2 an equilibrium exists between dissolved and undissolved CCP at all temperatures. Temperature rise will enhance the reformation of amorphous CCP, as it shifts the balance between dissolved and undissolved to the undissolved species. Therefore temperature will affect  $T_2$  not only via the water-protein interaction, but also via the water-CCP interaction, which vanishes below pH=5.2. No guess can be made about the contribution of the direct water-CCP interaction. More research will be necessary, before more definite conclusions can be drawn. The sharp drop in  $T_2$  value caused by the formation of calcium phosphate precipitates in the milk ultrafiltrate sample of pH=6.7 at

49.5 °C (fig. 6.5) also indicates a possible direct effect of CCP on the  $T_2$  of skimmilk.

Below pH=5.0, when all CCP is dissolved, all of the dissolved casein reagggregates once more and casein particles of distinct structure are formed, leading to lower  $T_2$  values. In fact casein aggregation can be distinguished at different levels i.e. at the level of individual casein molecules, at the level of the particles and the level of the strands and conglomerates forming the gel network (see also chapter 3 and 4). The internal structure of the casein particles rather than coagulation or gel formation will determine  $T_2$ , since Lelievre and Creamer (1978) found the same value for  $T_2$  of skimmilk at natural pH, whether or not it had been gelled by rennet action. As long as no syneresis had occurred gel formation did not change  $T_2$ . The  $T_2$  of skimmilk acidified to pH=4.6 and measured at 4 °C was slightly, but significantly higher than that of the corresponding skimmilk gel aged first for 10 hrs at 30 °C and then also measured at 4 °C. The difference, however, is probably caused by irreversible changes in the internal structure of the casein particles caused by heating and subsequent gel formation and not to gelation as such; since casein particles at pH=4.6 after acidification at 2 °C are thermodynamically unstable as shown by the irreversible character of gel formation (section 3.3.2).

Since protein aggregation and dissolution of CCP will be temperature dependent, it may be enlightening to consider the temperature dependence of  $T_2$  for sodium caseinate and skimmilk in more detail. Fig. 6.3 suggests a linear relationship between  $T_2$  and  $\tau_c$  (plotted on a double logarithmic scale) for fast moving molecules such as water molecules in the bulk water phase. In that case  $T_2$  will be proportional to  $\eta/T$  (Carrington and Mclauchlan, 1969), where  $\eta$  is the viscosity of the medium and  $T$  absolute temperature. This proportionality stems from contributions to  $T_2$  from rotational and translational motions, these together resulting in Brownian motion. The correlation time  $\tau_c$  will also be proportional to  $\eta/T$ . However, for water molecules bound to a surface, molecular motion will be constrained and only rotational motions will be allowed. Thus  $\tau_c$  should be written as (Dwek, 1973, Lynch, 1983):

$$\tau_c = \tau_c^0 \exp(-U_a/kT) \quad (6.9)$$

where  $U_a$  is the activation energy for rotational motion. According to eq. 6.9  $\log \tau_c$  will be proportional to  $1/T$ . In heterogeneous systems with at least one bound water phase  $T_2$  of the bulk phase will depend on the bound phase. For that reason  $T_2$  of biological systems (Lynch, 1983, Bryant and Shirley, 1980) is generally depicted on a logarithmic scale as a function of  $1/T$  on a linear scale. In the case of fast exchange between bulk water and bound water (Lynch, 1983)  $\log T_2$  of the bulk phase will decrease linearly with  $1/T$ . This linearity may be lost when an intermediate exchange rate exists or when the fraction of bound water changes with temperature. If the bulk solution can be considered as a viscous liquid (region A, fig. 6.3), theory then predicts a linear decrease of  $T_2$  with increasing  $\eta/T$ , both depicted on a double logarithmic scale.

Except for the sample at pH=6.76 (particularly at 49.5°C) straight lines (not shown) were found for milk ultra filtrate, when  $T_2$  was depicted on a linear scale as a function of  $\eta/T$ . The  $T_2$  values were close to those of pure, free water.

For sodium caseinate solutions and skim milk it is unrealistic to expect a linear decrease of  $\log T_2$  with increasing  $1/T$  for all samples. Several phenomena will be involved as temperature is raised. Firstly, as mentioned above the correlation time  $\tau_c$  of the hydrogen nuclei will decrease leading to higher values of  $T_2$  for all water phases present, but the exchange rate between the different water phases may also change. Secondly the calcium phosphate equilibria will shift towards the undissolved species resulting directly, or indirectly through a change in protein aggregation, in a lower  $T_2$ . This effect will only play a part in skim milk at pH values above 5.2. Thirdly the aggregation of casein molecules will increase with temperature leading to a firmer internal structure of the casein particles. Upon increased casein aggregation one may also expect the amount of bound water to increase; so that  $T_2$  will decrease. This latter effect was especially seen with sodium caseinate, when pH was varied at constant

temperature (fig. 6.6). Below pH=5.8 the formation of casein particles in a sodium caseinate solution was accompanied by a huge drop in  $T_2$ . The sum of all the phenomena mentioned determines the change in  $T_2$  with temperature.

In fig. 6.8  $T_2$  is depicted logarithmically as a function of the inverse temperature,  $1/T$ , for sodium caseinate solutions at seven different pH's. These values were derived from fig. 6.6. Since we have only sodium caseinate present only the first and third effect plays a part. A more or less linear decrease of  $\log T_2$  with  $1/T$  was found for the samples of pH=5.4 and above. Here it is possible that the amount of bound water and the exchange rate remain constant. The deviation from linearity for these samples at the lowest value of  $1/T$  (pH=6.94 and 5.80) was probably due to an inaccuracy in the measurement of the experimental temperature. At lower pH values only over a portion of the depicted curves is there a linear decrease. Here the deviation from linearity will be due to an increased aggregation of casein molecules inside the casein particles as temperature is raised. This increased aggregation may cause an increase of the fraction of bound water leading to lower  $T_2$ -values, but the drop in  $T_2$  may also be due to a dif-

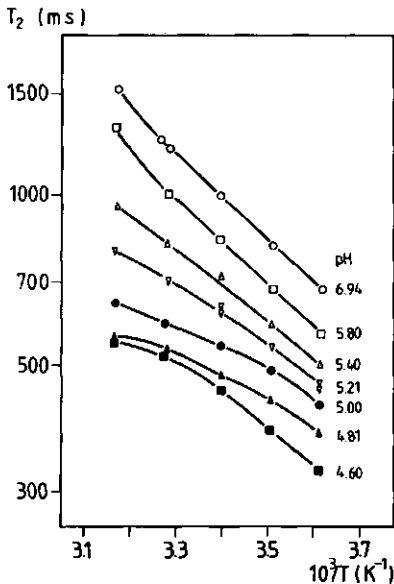
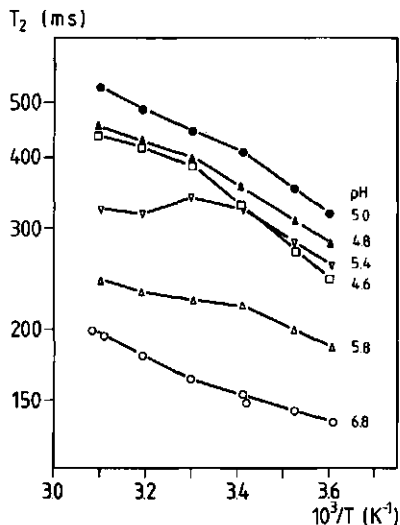


Fig. 6.8. The  $T_2$  (ms) of sodium caseinate solutions depicted on a logarithmic scale as a function of  $1/T$  ( $K^{-1}$ ). The pH of the samples is indicated. The values are derived from the data of fig. 6.6.

ferent exchange rate between bulk water and bound water. In this context it should be mentioned that as a general trend the slope of the curves also tends to decrease with decreasing pH; possibly the rate of casein aggregation inside the casein particles at low pH increases with temperature.

In fig. 6.9  $T_2$  of skimmilk is depicted logarithmically as a function of the inverse temperature,  $1/T$ , for six different pH's. These values were derived from fig. 6.4. Except for pH=5.4 more or less parallel curves decreasing with the inverse temperature are found. For all samples a linear decrease is lacking and at pH>5.0 the slope of the curves is much smaller than in case of the sodium caseinate solutions. Significantly at pH=4.6, where CCP is no longer present, the curves of skimmilk and sodium caseinate have almost identical slopes. At pH=5.4, which is close to the pH limit for the dissolution of CCP, the curve of  $T_2$  versus  $1/T$  levels off above 20 °C. At this and higher pH not only increased casein aggregation, but also reformation of amorphous CCP must be involved on raising the temperature, resulting in a large deviation from linearity and less steep curves. At all pH's a change with temperature in the extent of casein aggregation inside the casein particles may be expected. At moderate pH values and low temperatures this may stem partly from a migration of the casein, dissolved

Fig. 6.9. The  $T_2$  (ms) of skimmilk depicted on a logarithmic scale as a function of  $1/T$  ( $K^{-1}$ ). The pH of the samples is indicated. The values are derived from the data of fig. 6.4.



during acidification at 2 °C, back to the casein particles, or from the formation of new particles out of that dissolved casein. The voluminosity of the casein particles decreases with temperature for all pH's (fig. 3.6, section 3.3). In so far as this decrease reflects an increase in casein aggregation this will cause a reduced increase of  $T_2$  with temperature.

However the observed temperature effects are small compared to the observed pH-effects. Gel formation hardly affects  $T_2$ . Therefore it can be concluded that  $T_2$  and probably the amount of bound water depend to a large extent on intermolecular electrostatic interactions between casein molecules inside the casein particles, in which CCP may be involved at higher pH. pH affects  $T_2$  much more than temperature. The effect of temperature on  $T_2$  will probably be due more to hydrophobic interactions inside the casein particles. This agrees with the speculations of section 4.6 that electrostatic interactions, whether repulsive or attractive, are of primary interest in controlling the structure of casein particles, while hydrophobic interactions are involved in alterations of that particle structure on temperature rise.

## 7 CONCLUDING REMARKS

This study focuses on the structure of acid casein gels, which involves the spatial distribution of and the interaction forces between the structural elements. It is mainly concerned with gels formed by heating at rest of casein solutions, which were acidified chemically in the cold. Gel formation caused by heating an acidified casein solution is an irreversible process (section 3.2.2). It was found that not only casein concentration, pH, ionic strength, type of ions in the water phase, ageing time and ageing temperature, but also the conditions during acidification are the main factors determining the structure of acid casein gels. Essentially the same kind of gels are formed from skimmilk and from sodium caseinate solutions (see e.g. section 3.2.4, 3.4.2.1, 4.5.3 and 4.5.5.3), which points to casein being the basic element of acid casein gels.

Whey proteins did not affect the formation of acid casein gels (section 3.4.2.1); however, the skimmilk and sodium caseinate solutions (reconstituted from the corresponding powders) were not heat-treated prior to use, in contrast to industrial practice where milk is mostly preheated to invoke denaturation of whey proteins.

Acid casein gels could only be formed over a limited pH range (4.3-4.9, see section 4.5.4) and at temperatures above 10 °C (pH=4.6, see section 3.2.1). Addition of rennet, however, enabled gel formation in the entire pH range from 4.4 to 6.7 at 20 °C and also in the temperature range from 0 and 10 °C at pH=4.6 (Chapter V).

In fact acid casein gels can be considered to be particulate gels (Chapter 3), originating from the coagulation of casein particles. The diameter of particles eventually forming the strands and conglomerates of the gel network may vary from 50 to 300 nm (section 3.4.2.2). In the case of sodium caseinate gels the constituting casein particles are not "casein micelles", but arise from the aggregation of casein molecules or oligomers during acidification (section 3.3.3). In skimmilk the situation is much more complicated: starting at pH=6.7, acidification causes the

dissolution of colloidal calcium phosphate (CCP) while part of the casein molecules dissociate from the casein micelles (section 3.3.2.1), whereas the diameter of the casein particles appears to stay about constant (section 3.3.2.2 and 3.3.2.3) and few particles seem to disintegrate completely (section 3.3.2.3). Maximum solubility of casein is seen around  $\text{pH}=5.4-5.5$ , whereas close to  $\text{pH}=4.6$  all casein has disappeared from the serum (section 3.3.2.1). Although having approximately the same size as casein micelles in skimmilk of natural pH, the internal structure of (not yet aggregated) casein particles at  $\text{pH}=4.6$  must be different (section 3.3.4). Both the similarity in internal structure between casein particles in an acidified skimmilk and in a sodium caseinate solution, and the change of that internal structure during acidification were confirmed by the results of pulse NMR measurements (section 6.4.1, 6.4.2 and 6.5). The spin-spin relaxation time,  $T_2$ , of the hydrogen nuclei of the water molecules in the serum appears to depend (certainly at low pH) primarily on the interaction of the water molecules with casein inside the casein particles, and thereby also on the internal structure of the casein particles.

An acid casein gel may be characterized as a heterogeneous gel network. Heterogeneity may be distinguished at different levels, since it results from linkages at different levels: intramolecular bonds in individual casein molecules, aggregation of casein molecules inside the casein particles and bonds between casein molecules of different particles, the latter leading to coagulation of casein particles. In the first step of coagulation strands and small conglomerates of particles will be formed. Subsequently these will aggregate to form a network of large conglomerates connected by strands and separated by large pores. In fig. 3.17 a highly schematic representation is given. This description is supported by concentration dependent rheological (section 3.4.2.1) and permeability measurements (section 3.4.2.3), and by electron micrographs of acid casein gels (section 3.4.2.2). The permeability coefficient,  $B$ , will particularly depend on the size of the large pores, whereas the dynamic moduli,  $G'$  and  $G''$ , will depend on the character (relaxation time) and effective number of bonds. The effective number of bonds is determined by the number of bonds

between adjacent particles and the number of particles which come under stress if the network is deformed. The latter number highly depends on the spatial distribution of these stress carrying particles and is much smaller than the total particle number, because of network inhomogeneity. The spatial distribution as reflected in the permeability of an acid casein gel seems to be more or less fixed in the first stage of gel formation, hardly changing with time or measuring temperature (section 3.4.2.3 and 4.5.3).

If other factors, such as pH and ionic strength, are constant the temperature during the earlier stages of gel formation predominantly determines the permeability of the gel network. Considering the large conglomerates (being actually dense areas of casein particles) as spheres of approximately the same diameter (in the order of a few  $\mu\text{m}$ ) as the large pores, the measured permeabilities roughly agree with calculations according to models for the random packing of spheres (section 3.4.3.2).

After initial gel formation, the dynamic moduli of all gels studied tended to increase with time for periods even longer than a week (section 3.2.1, 4.5.4, 4.5.5 and 5.3.1). Aggregation as such is probably subject to an activation Helmholtz energy (section 3.4.1), which decreases with increasing ageing temperature (section 3.2.1 and 4.5.3), since the increase of the dynamic moduli (particularly occurring during the first stage of gelation) increases with ageing temperature, when measured at the same temperature. This activation Helmholtz energy tends to increase with ionic strength at pH=4.6 (section 4.5.5.2) and with pH in the pH range of 4.5 to 5.0, if no rennet is added (section 4.5.4). It must at least partly be due to a steric stabilization effect of the GMP part of  $\kappa$ -casein, since even at 2 °C acid skimmilk gels may be formed after release of GMP (section 5.1 and 5.3.1). The other factors determining this activation Helmholtz energy are less obvious. Possibly, there is a much smaller temperature dependent steric stabilization contribution of  $\beta$ -casein, which decreases at higher temperature, where  $\beta$ -casein tends to move to the interior of the casein particles (section 5.3.1). Different acid casein gels had in common that higher dynamic moduli went along with higher permeabilities (section 3.4.2.3, 4.5.3, 4.5.4 and 5.3.1). Probably, a decrease of the activation Helmholtz energy results in

larger pores, whereas the effective number of interparticle bonds between adjacent particles must increase. Anyhow more research, particularly on the kinetics of the aggregation and subsequent gelation process, are necessary to be able to draw more definite conclusions.

Part of the bonds in an acid casein gel have a relaxation time in the range from 0.6 to  $6 \times 10^3$  s (section 4.5.2). Another characteristic feature of acid casein gels is the rather permanent character over longer time scales ( $>10^4$  s). The existence of a pseudo-permanent network modulus, which resulted from the calculation of the relaxation spectrum (section 4.5.6.2), could be experimentally verified (section 4.5.6.1). The calculated pseudo-permanent network modulus and the measured pseudo-stress relaxation modulus (time scale  $>10^4$  s) formed a considerable part of the dynamic moduli in the time scale of 0.6 to  $6 \times 10^3$  s. Possibly, the more permanent network character of acid casein gels as compared to rennet gels is the reason that rupture of acid casein gels occurs at a smaller deformation and a larger stress than do rennet gels (section 4.5.7).

The parameter  $\tan \delta$  ( $=G''/G'$ ) may be a very useful parameter in further rheological characterization of acid casein gels, since it hardly depends on the spatial distribution of the gel network, but almost exclusively on the character of the interparticle bonds (section 4.3). It is concluded (section 4.7) that the character and number of bonds between two particles is determined by the internal structure of the casein particles involved. The internal structure of casein particles results from a balance between different interaction forces (section 3.3.4) i.e. hydrophobic bonding, electrostatic interactions, hydrogen bonds, Van der Waals attraction and steric interactions. The behaviour of  $\tan \delta$  at longer time scales differs from that at shorter time scales.  $\tan \delta$  in the range of 0.1 to  $10 \text{ rad.s}^{-1}$  does not change with ageing temperature ( $T < 50^\circ \text{C}$ , section 3.2.1), measuring temperature ( $T$  also  $< 50^\circ \text{C}$ , section 4.5.3),  $I$  (section 4.5.5), type of ions (section 4.5.5) and pH (section 4.5.4), as long as  $\text{pH} \leq 5.1$  (section 5.3.2), i.e. as long as the gel has the character of acid casein gels. This implies that there is no indication of a drastic change in the character of the bonds with relaxation times in the range of 0.6 to

60 s as a function of the mentioned parameters. At longer time scales (60 to  $6.0 \times 10^3$  s)  $\tan \delta$  tended to decrease with decreasing measuring temperature,  $T_m$ , this decrease being the strongest in the longest time range (section 4.5.3). At lower measuring temperature probably more bonds are formed with a relaxation time in the order of  $10^3$  s, since the value of the dynamic moduli increases with decreasing measuring temperature (section 4.5.3).

The decrease of the moduli with increasing  $T_m$  can only be explained from a shift in the balance between the different interaction forces governing the internal structure of the casein particles. Conformational rearrangements, particularly at the boundaries of the casein particles, are held responsible for an increase in the number of interparticle bonds. At least electrostatic  $\pm$  interactions (salt bridges) and hydrophobic interactions are involved in both the intra- and interparticle bonds. When temperature is lowered, hydrophobic bonding inside the casein particles is expected to decrease, causing conformational rearrangements of the protein molecules, ultimately resulting in an increase in particle voluminosity (section 3.3.2) and possibly an increase in the number of interparticle bonds, thus suggesting an explanation for the observed opposite temperature behaviour of the dynamic moduli. Increasing temperature leading to a stronger hydrophobic bonding inside the casein particles, is also the most obvious explanation for the effects noticed in the temperature dependent  $T_2$  measurements (section 6.5). An increasing ionic strength, which lowers the values of the dynamic moduli, would decrease the number of attractive interparticle electrostatic interactions (section 4.5.5.2). It is put forward that attractive electrostatic interactions may be responsible for the rather permanent character of acid casein gels (section 4.5.6 and 4.7).

The rheological parameters of skimmilk gels, made by the combined action of acidification and rennet in the pH range of 4.4 to 5.8, indicated a clear transition in character around pH=5.2 (section 5.3.2). Above pH=5.1 the gels are subject to microsineresis and a rise of measuring temperature causes an irreversible decrease of the dynamic moduli. The occurrence of microsineresis may possibly be related directly to the value of  $\tan \delta$  (section 5.3.2.3 and 5.4), since both depend on the relaxation behaviour of

the protein-protein bonds. At and below pH=5.1 skimmilk gels made by combined acidification and rennet action behave like ordinary acid casein gels with, however, considerably higher values of the moduli. Even at pH=4.6, the glycomacropeptide part of  $\kappa$ -casein considerably contributes to the stability of casein particles. Proteolytic degradation of  $\alpha_{s1}$ - and  $\beta$ -casein affects the ageing curves at longer time scales, but does not affect significantly other rheological properties.

The interaction of water protons with the casein particles, as studied in the pulse NMR experiments, could not be described by a simple two phase model. Certainly more than one kind of bound or immobilized water phase should be taken into account. It is clear (section 6.4.1, 6.4.2 and 6.5) that the  $T_2$  of skimmilk and sodium caseinate solutions depends on water-protein interactions inside the casein particles. In skimmilk above pH=5.2 CCP plays a special role, but whether direct or indirect is not clear. Casein particle aggregation leading to gel formation hardly affected the  $T_2$  (section 6.4.1), whereas casein aggregation leading to the formation of casein particles (section 6.4.2) considerably lowered the  $T_2$ .

## LITERATURE REFERENCES

- Abragam, A. (1961). "The principles of nuclear magnetism". Oxford University Press, Oxford.
- American Dry Milk Institute, inc., 1971. Standards for grades of dry milk. Bull. 916.
- As, H. van and Schaafsma, T.J. (1984). *Biophys. J.* 45, 469-472.
- As, H. van (1982). Doctoral Thesis Agricultural University Wageningen, the Netherlands.
- Beltman, H. (1975). Doctoral thesis Agricultural University Wageningen, the Netherlands.
- Berendsen, H.J.C. (1975). In "Water-a comprehensive Treatise", 5, Franks, F. ed., Plenum Press, New York-London. Chapter 6, p. 293-330.
- Berlin, E., Klimann, P.G. and Pallansch, M.J. (1970). *J. Colloid Interf. Sci.* 34, 488.
- Berne, B.J. and Pecora, R. (1976). "Dynamic Light Scattering". John Wiley & Sons, New York.
- Bloomfield, V.A. (1979). *J. Dairy Res.* 46, 241-252.
- Boekel, M.A.J.S. van (1980). Doctoral thesis Agricultural University Wageningen, the Netherlands.
- Brakel, J. van (1975). "Capillary liquid transport in porous media". Doctoral thesis Technical University Delft, the Netherlands.
- Brosio, E., Altobelli, G., Shi Yun Yu and Nola, A. di (1983). *J. Fd. Technol.* 18, 219-226.
- Brosio, E., Altobelli, G. and Nola, A. di (1984). *J. Fd. Technol.* 19, 103-108.
- Bryant, R.G. and Shirley, W.M. (1980). *Biophys. J.* 32, 3-16.
- Carrington, A. and McLachlan, A.D. (1969). "Introduction to Magnetic Resonance", sec. ed. Harper & Row, New York, and John Weatherhill, Tokyo.
- Chu, B. (1974). "Laser Light Scattering". Academic Press, New York.
- Cindio, B. de, Acierno, D., Gortemaker, F.H. and Janeschitz-Kriegl, H. (1977). *Rheol. Acta* 16, 484-489.
- Creamer, L.K., Mills, O.E. and Richards, E.L. (1971). *J. Dairy Res.* 38, 269-281.

- Creamer, L.K. (1976). *N.Z. J. Dairy Sci. & Technol.* 11, 30-39.
- Dalgleish, D.G. and Parker, T.G. (1980). *J. Dairy Res.* 47, 113-122.
- Dalgleish, D.G. (1984). *J. Dairy Res.* 51, 425-438.
- Darby, R. (1976). "Viscoelastic Fluids. An Introduction to Their Properties and Behavior". Marcel Dekker Inc., New York and Basel.
- Darling, D.F. and Dickson, J. (1979). *J. Dairy Res.* 46, 441-451.
- Darling, D.F. (1982). In "The effect of polymers on dispersion properties". Tadros, Th.F. ed., Acad. Press London.
- Davies, D.T. and White, J.C.D. (1960). *J. Dairy Res.* 27, 171-190.
- Davies, E.M., Shankar, P.A., Brooker, B.E. and Hobbs, D.G. (1978). *J. Dairy Res.* 45, 53-58.
- Dijk, H.J.M. van (1982). Doctoral thesis Agricultural University Wageningen, the Netherlands.
- Dijk, H.J.M. van and Walstra, P. (1986). *Neth. Milk Dairy J.* 40.
- Duiser, J.A. (1965). Doctoral thesis State University Leiden, the Netherlands.
- Dwek, R.A. (1973). "Nuclear magnetic resonance in biochemistry. Applications to enzyme systems". Clarendon Press, Oxford.
- Farrar, Th. C. and Becker, E.D. (1971). "Pulse and Fourier transform NMR. Introduction to theory and methods". Academ. Press, New York-London. 115 p.
- Ferry, J.D. (1980). "Viscoelastic properties of polymers". 3th ed. John Wiley & Sons, New York-London.
- FIL-IDF, international standard. 26: 1964.
- FIL-IDF, international standard. 29: 1964.
- FIL-IDF, international standard. 9A: 1969.
- FIL-IDF, international standard. 72: 1974.
- FIL-IDF, international standard. 90: 1979.
- Flory, P.J. (1953). "Principles of polymer chemistry". Cornell University Press, Ithaca.
- Flory, P.J. (1974). *Faraday Disc. Chem. Soc.* 57, 7-18.
- Fox, P.F. (1969). *J. Dairy Sci.* 52, 1214-1218.
- Fox, P.F. and Mulvihill, D.M. (1983). IDF symp. 17-19th may, Helsingør, Denmark.
- Fullerton, G.D., Potter, J.L. and Dornbluth, N.C. (1982). *Magn. Res. Imaging I*, 209-228.
- Gels and Gelling Processes, *Faraday Disc.* 75, 1974.

- Geurts, T.J., Walstra, P. and Mulder, H. (1974). *Neth. Milk Dairy J.* 28, 46-72.
- Glaser, J., Carroad, P.A. and Dunkley, W.L. (1980). *J. Dairy Sci.* 63, 37-48.
- Glauert, A.M. (1975). "Fixation, Dehydration and Embedding of Biological specimens". Elsevier North-Holland Biomedical Press, Amsterdam-New York.
- Goodarz-Nia, I and Sutherland, D.N. (1975). *Chem. Engng. Sci.* 30, 407-412.
- Graham, D.E. (1976). PhD Thesis Unilever Research, Colworth/Welwyn, Hertfordshire, England.
- Grappin, R., Rank, T.C. and Olson, N.F. (1985). *J. Dairy Sci.* 68, 531-540.
- Harwalkar, V.R. and Kalab, M. (1980). *J. Texture Studies* 11, 35-49.
- Harwalkar, V.R. and Kalab, M. (1981). *Scanning Electron Microscopy* III, 503-513.
- Heertje, I., Visser, J. and Smits, P. (to be published).
- Henstra, S. and Schmidt, D.G. (1970a). *Naturwissenschaften* 57, 247.
- Henstra, S. and Schmidt, D.G. (1970b). *Proc. 7th Intern. Congr. Electr. Microsc., Grenoble, 1*, Favard, P. ed., p. 389-390.
- Hiemenz, P.C. (1977). "Principles of Colloid and Surface Chemistry". Marcel Dekker Inc., New York and Basel.
- Holt, C. Dalglish, D.G. and Parker, T.G. (1973). *Biochim. et Biophys. Acta* 328, 428-432.
- Horne, D.S. (1984). *J. Colloid Interf. Sci.* 98, 537-548.
- Hooydonk, A.C.M. van (1986). *Neth. Milk Dairy J.* to be published.
- Hooydonk, A.C.M. van and Olieman, C. (1982). *Neth. Milk and Dairy J.* 36, 153-158.
- Jong, L. de (1975). *Neth. Milk Dairy J.* 29, 162-168.
- Jong, L. de and Groot-Mostert, A.E.A. de (1977). *Neth. Milk Dairy J.* 31, 296-313.
- Kalab, M. (1979). *Scanning Electron Microsc.* 1979; III, 261-272.
- Kalab, M. (1981). *Scanning Electron Microsc.* 1981; III, 453-472.
- Kamphuis, H. (1984). Doctoral thesis Twente University of Technology Enschede, the Netherlands.
- Kamphuis, H. (1985). Personal communication.

- Kleef, F.S.M. van, Boskamp, J.V. and Tempel, M. van den (1978). *Biopolymers* 17, 225-235.
- Knoop, A.M. and Peters, K.H. (1975). *Kieler Milchw. Forsch. Ber.* 27, 227.
- Ledford, R.A., O'Sullivan, A.C. and Nath, K.R. (1966). *J. Dairy Sci.* 49, 1098.
- Ledford, R.A., Chen, J.K. and Nath, K.R. (1968). *J. Dairy Sci.* 51, 792.
- Lelievre, J. and Creamer, L.K. (1978). *Milchwissenschaft* 33, 73-76.
- Leung, H.K., Steinberg, M.P., Wei, L.S. and Nelson, A.I. (1976). *J. Food Sci.* 41, 297-300.
- Lin, S.H.C., Dewan, R.K., Bloomfield, V.A. and Morr, C.V. (1972). *Biochemistry* 11, 1818-1821.
- Lynch, L.J. (1983). In "Magnetic Resonance in Biology". Cohen, J.S. ed., John Wiley & Sons. Chapter 5, 248-304.
- Maghoub, I., Prost, C. and Dodds, J.A. (1982). *Powder Technology* 31, 143-151.
- McLachlan, L.A. (1977). *J. Magn. Res.* 26, 223-228.
- McMahon, D.J. and Brown, R.J. (1984). *J. Dairy Sci.* 67, 499-512.
- Mulvihill, D.M. and Fox, P.F. (1977). *J. Dairy Res.* 44, 533-540.
- Mulvihill, D.M. and Fox, P.F. (1979a). *J. Dairy Res.* 46, 641-651.
- Mulvihill, D.M. and Fox, P.F. (1979b). *Milchwissenschaft* 34, 680-683.
- Némethy, G. and Sheraga, H.A. (1962). *J. Phys. Chem.* 66, 1773.
- Nola, A. di and Brosio, E. (1983). *J. Fd. Technol.* 18, 125-128.
- Noomen A. (1978). *Neth. Milk Dairy J.* 32, 49-68.
- Norde, W., Bosgoed, H.M.M. and Vries, P. de (1985). *Biophysical Chem.* 21, 115-126.
- Nijenhuis, K. te (1979). Doctoral Thesis Technical University Delft, the Netherlands.
- Nijenhuis, K. te (1979). *Colloid & Polymer Sci.* 25, 522-535, 1017-1026.
- Oosawa, F. (1971). "Polyelectrolytes". Marcel Dekker, Inc., New York.
- Ottenhof, H. (1984). Personal communication.
- Otter, J.L. den (1967). Doctoral thesis State University Leiden, the Netherlands.
- Packer, K.J. (1977). *Phil. Trans. R. Soc. London B* 278, 59-87.

- Papenhuizen, J.M.P. (1972). *Rheol. Acta* 11, 73-88.
- Parker, T.G. and Dalgleish, D.G. (1981). *J. Dairy Res.* 48, 71-76.
- Payens, T.A.J. (1979). *J. Dairy Res.* 46, 291.
- Payens, T.A.J. and Vreeman, H.J. (1982). In "Solution Behaviour of Surfactants", I. Mittal, K.L. and Fendler, E.J. eds., Plenum Publ. Corp., New York. P. 543-571.
- Pélissier, J.P. (1984). *Sci. Aliments* 4, 1-35.
- Pierre, A. (1983). *Le Lait* 63, 217-229.
- Reimerdes, E.H. and Klostermeyer, H. (1976). *Kieler Milchw. Forsch. Ber.* 28, 17.
- Roefs, S.P.F.M. and Vliet, T. van (1984). In "Advances in Rheology", 4, "Applications". Mena, B., Garcia-Rejon, A. and Rangel-Nafaile, C., eds., 249-256.
- Roefs, S.P.F.M., Walstra, P., Dalgleish, D.G. and Horne, D.S. (1985). *Neth. Milk Dairy J.* 39, 119-122.
- Rose, D. (1968). *J. Dairy Sci.* 51, 897.
- Rüegg, M., Lüscher, M. and Blanc, B. (1974). *J. Dairy Sci.* 57, 387.
- Salyaev, R.K. (1968). *Proc. 4th Eur. Reg. Conf. Electr. Microsc.*, Rome, p. 151.
- Scheidegger, A.E. (1960). "The physics of flow through porous media". Chapter VI and VII, p. 112-193. Oxford University Press London.
- Schmidt, D.G. (1982a). In "Developments in Dairy Chemistry", vol 1, "Proteins". Fox, P.F., ed., Appl. Sci. Publ., London. Ch. 2, 61-86.
- Schmidt, D.G. (1982b). *Food Microstructure* 1, 151-165.
- Schmidt, D.G. (1971). In "Protides of the biological fluids". Peeters, H., ed., Pergamon Press Oxford-New York, Ch. 1, 337-340.
- Shirley, W.M. and Bryant, R.G. (1982). *J. Am. Chem. Soc.* 104, 2910-2918.
- Snoeren, T.H.M., Klok, H.J., Hooydonk, A.C.M. van and Damman, A.J. (1984). *Milchwissenschaft* 39, 461-463.
- Sutherland, D.N. (1967). *J. Colloid Interf. Sci.* 22, 373.
- Sutherland, D.N. and Goodarz-Nia, I. (1971). *Chem. Engng. Sci.* 26, 2071-2085.

- Swaisgood, H.E. (1982). In "Developments in Dairy Chemistry", vol. 1, "Proteins". Fox, P.F., ed., Appl. Sci. Publ., London. Ch. 1, 1-59.
- Tamime, A.Y., Kalab, M. and Davies, G. (1984). Food Microstructure 3, 83-92.
- Tanford, C. (1973). "The hydrophobic effect". John Wiley & Sons, New York.
- Tarodo de la Fuente, B. and Alais, C. (1975). J. Dairy Sci. 58, 293-300.
- Tempel, M. van den (1979). J. Coll. Interf. Sci. 71, 18-20.
- Treolar, (1975). "The physics of rubber elasticity". Oxford.
- Visser, S. and Slangen, K.J. (1977). Neth. Milk Dairy J. 31, 16-30.
- Visser, S. (1981). Neth. Milk Dairy J. 35, 65-88.
- Vliet, T. van (1977). Doctoral thesis Agricultural University Wageningen, the Netherlands.
- Vliet, T. van and Lyklema, J. (1978). J. Coll. Interf. Sci. 63, 97.
- Vliet, T. van and Walstra, P. (1980). J. Texture Studies 11, 65-68.
- Vliet, T. van and Dentener-Kikkert, A. (1982). Neth. Milk Dairy J. 36, 261-265.
- Vliet, T. van and Walstra, P. (1985). Neth. Milk dairy J. 39, 115-118.
- Vliet, T. van and Dijk, H.J. van (1986). To be published.
- Vreeman, H.J. (1985). Personal communication.
- Walstra, P. (1979). J. Dairy Res. 46, 317.
- Walstra, P. and Jenness, R. (1984). "Dairy Chemistry and Physics". John Wiley & Sons, New York.
- Walstra, P., Dijk, H.J.M. van and Geurts, T.G. (1985) Neth. Milk Dairy J. 39, 209-246.
- Wood, G.B., Reid, D.S. and Elvin, R. (1981). J. Dairy Res. 48, 77-83.
- Zoon, P. (1984). M. Sci. Thesis, Agricultural University Wageningen, the Netherlands.

## LIST OF SYMBOLS

A	Hamaker constant	
A	light absorption	
A	Helmholtz energy	J
B	permeability coefficient	$m^2$
D	diffusion coefficient	$m^2 \cdot s^{-1}$
d	particle diameter	m
$\bar{d}$	average particle diameter	m
$D_1$	torsion constant of torsion wire	Nm
$D_2$	torsion constant of strain wire	Nm
E	cylinder constant	$m^3$
$d_{vs}$	volume surface average diameter	m
f	force	N
f'	correction factor	
G	Gibbs energy	J
G	shear modulus	$Nm^{-2}$
G'	storage modulus	$Nm^{-2}$
G''	loss modulus	$Nm^{-2}$
G*	complex shear modulus	$Nm^{-2}$
G(t)*	pseudo-stress relaxation modulus	$Nm^{-2}$
$G_\infty^*$	pseudo-network modulus	$Nm^{-2}$
$G_e$	permanent network modulus	$Nm^{-2}$
$G_e^*$	semi-permanent network modulus	$Nm^{-2}$
$G_s$	modulus of a strand	$Nm^{-2}$
H	length of a casein gel	m
H	enthalpy	J
H	relaxation spectrum	$Nm^{-2}$
$H_0$	strong external magnetic field	Tesla
$H_1$	radio frequency field	Tesla
$\hbar$	$h/2\pi$	Js
h	Planck's constant	Js
h	length of innercylinder	m
h	height of whey level	m
I	moment of inertia	$Nms^2$
I	ionic strength	M
I	intensity of scattered light	

$k$	Boltzmann's constant	$JK^{-1}$
$M_1$	torsion moment exerted by torsion and strain wire	$Nm.rad$
$M_2$	total shear moment	$Nm.rad$
$M_0$	net magnetization of a large number of magnetic moments	
$M_{x_3}(t)$	net magnetization along the $x_3$ -axis	
$M_{x_1x_2}(t)$	net magnetization in the $x_1x_2$ -plane	
$M_{x_1x_2,0}$	net magnetization in the $x_1x_2$ -plane at $t=0$	
$M_{x_1x_2,oi}$	net magnetization in the $x_1x_2$ -plane of the $i^{th}$ phase at $t=0$	
$N$	total number	
$N_u$	number of spins in the spin-up position	
$N_d$	number of spins in the spin-down position	
$P$	pressure	$Pa$
$P_i$	fraction of spins in the $i^{th}$ phase	
$R$	radius	$m$
$R_i$	radius of inner cylinder	$m$
$R_o$	radius of outer cylinder	$m$
$Re$	Reynolds number	
$S$	entropy	$JK^{-1}$
$S$	solubility	
$T$	temperature	$^{\circ}C$ or $K$
$T_m$	temperature of measurement	$^{\circ}C$ or $K$
$T_1$	spin-lattice relaxation time	$s$
$T_2$	spin-spin relaxation time	$s$
$T_{2i}$	spin-spin relaxation time of $i^{th}$ phase	$s$
$t$	time	$s$
$\tan \delta$	loss tangent	
$U$	energy	$J$
$v$	liquid flux	$ms^{-1}$
$v$	voluminosity	$g.g^{-1}$
$x$	direction	
$\gamma$	shear deformation	
$\dot{\gamma}$	shear rate	$s^{-1}$
$\gamma_a$	average maximum shear deformation	

$\gamma$	magnetogyric ratio	$\text{rad.s}^{-1}.\text{Tesla}^{-1}$
$\delta$	diameter	m
$\epsilon$	porosity	
$\epsilon_a$	rotation of driving shaft	rad
$\epsilon_{ao}$	maximum amplitude of rotational oscillation of driving shaft	rad
$\epsilon_c$	rotation of innercylinder	rad
$\epsilon_{co}$	maximum amplitude of rotational oscillation of innercylinder	rad
$\epsilon'_a$	radial displacement of driving shaft	rad
$\epsilon'_c$	radial displacement of innercylinder	rad
$\eta$	viscosity	Pa.s
$\theta$	angle between magnetic moment of nucleus and external magnetic field	
$\lambda$	wave length	$\mu\text{m}$
$\mu$	magnetic moment of a nucleus	
$\mu_{\text{up}}$	magnetic moment parallel to the external magnetic field	
$\mu_{\text{down}}$	magnetic moment anti-parallel to the external magnetic field	
$\rho$	density	$\text{kg.m}^{-3}$
$\sigma$	shear stress	Pa
$\tau$	relaxation time	s
$\tau_c$	correlation time	s
$\phi$	volume fraction	
$\omega$	angular frequency	$\text{rad.s}^{-1}$
$\omega_0$	Larmor precession frequency	$\text{rad.s}^{-1}$

## SUMMARY

Gel formation is involved in the manufacturing of many dairy products such as cheese, quarg and yoghurt, and largely determines the physical structure of them. The structure of such foods is of considerable importance for the perception of taste and texture by the consumer. The aim of this study was to elucidate the structure of acid casein gels, made of skimmilk and sodium caseinate solutions. By structure not only the character, size and spatial distribution of the structural elements is meant, but also the interaction forces between them. These interaction forces determine the nature (strength and life time) of the bonds formed in a gel network.

In chapter 1 a general introduction to the subject is given. The properties of the four different groups of casein molecules are given in some detail, since casein is the main component of acid casein gels. At the end an outline of the study is presented.

In chapter 2 the experimental approach is described. The experiments were carried out with skimmilk and sodium caseinate solutions that were reconstituted from standard powders. The samples were mostly acidified by adding HCl in the cold (0-2 °C) to a pH of about 4.6, i.e. the isoelectrical pH of casein in milk. Gel formation was induced by heating the acidified solutions at rest to temperatures in the range of 20 to 50 °C. The structure of the gels was mainly studied by rheological measurements with a dynamic rheometer, permeametry, electron microscopy and pulse NMR methods.

The formation and spatial arrangement of acid casein gels are discussed in chapter 3. Skimmilk and sodium caseinate solutions give gels with essentially the same properties. Gel formation does not occur below 10 °C and above 10 °C at first very sluggishly; but it is an irreversible process and once a gel is formed, the values of the dynamic moduli ( $G'$  and  $G''$ ) even considerably increase if the temperature is decreased to below 10 °C. The dynamic moduli, after a short lag period tend to increase linearly with the logarithm of the ageing time in the temperature range of 20 to 40 °C. Gelation appears to be subject to an activation Helmholtz energy, which is higher for lower ageing temperatures. A

pronounced contribution to the activation Helmholtz energy arises from the stabilizing effect of the glycomacropeptide part of  $\kappa$ -casein.

Acid casein gels show an inhomogeneous, particulate structure. After acidification in the cold the casein particles in skimmilk or sodium caseinate solutions have approximately the same size distribution as the casein micelles in the original skimmilk; nevertheless their internal structure is different. The inhomogeneous structure of the gel results in part from aggregation existing at different levels: intramolecular, intermolecular between casein molecules of the same particles and intermolecular between casein molecules of different particles. The gel network ultimately formed consists of dense areas of casein particles alternating with large pores. The dense areas are built up of smaller conglomerates and strands of aggregated particles, with small pores inside the conglomerates. The number and diameter of the large pores (between the dense areas) determine the permeability of the gel.

Chapter 4 is concerned with the rheological properties of the gels, which depend on the character and effective number of bonds in the gel network. The effective number of bonds is determined by (a) the number of bonds between adjacent particles and (b) the number of particles which come under stress if the network is deformed. The latter number highly depends on the spatial distribution and is much smaller than the total particle number, because of the inhomogeneity of the gel network. Different interaction forces, particularly hydrophobic bonding and electrostatic interactions (salt bridges), and probably hydrogen bonds and Van der Waals attraction will be involved in bond formation. Moreover steric interactions (e.g. via the conformation of the casein molecules) must also play a part. From variation of experimental conditions, such as ageing and measuring temperature, ionic strength, ionic composition and pH clear conclusions about the relative importance of these interactions cannot be drawn. It was, however, concluded that the internal structure of the casein particles is paramount in determining the number (and possibly life time) of the interparticle bonds. This internal structure results from a subtle balance between the different types of interaction forces.

A considerable proportion of the bonds in an acid casein gel

has a relaxation time in the range of 0.6 to 6000 s. The character of the bonds may be evaluated from the loss tangent  $\tan \delta$  ( $=G''/G'$ ), which parameter is almost independent of the spatial distribution and thus of the number of bonds. In the range from 0.6 to 60 s the character of the bonds did not change drastically with temperature, as it did in the range of 60 to 6000 s, where more bonds were formed with a relaxation time in the order of  $10^3$  s when temperature was decreased; this implies the rheological character becoming more viscous, although both moduli are larger.

Acid casein gels thus become relatively more viscous at longer time scales if temperature is lowered, but they also show distinct elastic behaviour, even at time scales of  $10^4$  s or longer. This followed from the pseudo-stress relaxation modulus, as measured at long time scales; although many bonds relaxed between  $10^3$  and  $10^5$  s, a significant proportion remained longer. The time dependence of this relaxation modulus agreed with the relaxation spectrum as calculated from the dynamic moduli.

When rennet is added to skimmilk acidified in the cold, a gel can be formed in the whole pH range from 4.3 to 6.7 ( $T=20$  °C) and even at 2 °C at pH=4.6. Apparently the glycomacropeptide part of  $\kappa$ -casein, which is split off by rennet, considerably contributes to the stability of the casein particles, even at pH=4.6. Around pH=5.2 a pronounced transition in rheological properties was noticed. Below this pH the gels made with rennet and acid behave like all other casein gels, whereas above this pH they have properties similar to those of normal rennet gels, for instance showing enhanced microsyreresis at higher temperatures. The occurrence of microsyreresis was clearly correlated with the value of  $\tan \delta$ .

The results of chapter 6, on the spin-spin relaxation time ( $T_2$ ) of water protons in casein solutions as a function of pH and temperature, confirm the change of internal structure of the casein particles caused by acidification.  $T_2$  depends almost exclusively on the water-protein interaction inside the casein particles, in which colloidal calcium phosphate, if present, will play a special part.

The most important results and conclusions are summarized and discussed in chapter 7.

## SAMENVATTING

De structuur van een levensmiddel is van groot belang voor de smaakgevaarwording en de beoordeling van het uiterlijk en van de consistentie door de consument. Een produkt waarvan deze eigenschappen niet aan de wensen van de consument voldoen, zal weinig afzet vinden, ook al is de voedingswaarde optimaal. Allerlei melkprodukten zijn gellen, en de structuur daarvan hangt af van de vorming en opbouw van het gel. Beheersing van de gelvorming is dan ook wezenlijk bij het bereidingsproces daarvan.

Dit onderzoek is gericht op de structuur van zure caseïnegelen. Onder structuur wordt hier niet alleen aard, afmetingen en ruimtelijke rangschikking van de bouwstenen van het gelnetwerk verstaan, maar evenzeer het karakter (levensduur en sterkte) van de bindingen tussen deze bouwstenen. Verschillende soorten interactiekrachten, zoals vooral hydrofobe binding en electrostatische interactie, maar ook waterstofbruggen, Van der Waals attractie en sterische interacties kunnen hierbij een rol spelen en bepalen mede sterkte en levensduur van de bindingen in het gelnetwerk.

Caseïne is een verzamelnaam voor 4 verschillende groepen eiwitten, die samen ongeveer 80% van het totale melkeiwit uitmaken. Serumeiwitten spelen bij de hier bestudeerde gellen geen rol van betekenis, aangezien deze alleen door verhitting met de caseïne kunnen reageren en de gebruikte oplossingen niet werden voorverhit.

In dit onderzoek werd gebruik gemaakt van ondermelk en natriumcaseïnaatoplossingen, bereid uit standaardpoeders van constante samenstelling. Zoutzuur werd toegevoegd, bij een zodanig lage temperatuur (0-2 °C) dat geen vlokking optrad, tot een pH van ongeveer 4,6, globaal de isoëlectrische pH van caseïne in ondermelk. Gelvorming werd geïnduceerd door opwarmen tot temperaturen variërend van 20 tot 50 °C. De toegepaste experimentele technieken staan in hoofdstuk 2 beschreven. De voornaamste waren: reologische metingen met een dynamische reometer, permeabiliteitsmetingen, electronenmicroscopie en pulse-NMR onderzoek.

In hoofdstuk 3 wordt ingegaan op de vorming en de ruimtelijke opbouw van zure caseïnegelen. De snelheid van gelvorming bleek af

te hangen van een activerings-Helmholtz-energie, die afneemt met toename van de temperatuur. Deze activeringsenergie kan voor een groot deel toegeschreven worden aan de stabiliserende werking van het glycomacropptide-deel van de  $\kappa$ -caseïne. Gelvorming door opwarmen van een in de kou aangezuurde caseïne-oplossing is een irreversibel proces. Afkoelen van een reeds gevormd gel doet de elasticiteitsmodulus zelfs sterk toenemen. Beide dynamische moduli  $G'$  en  $G''$  blijken na een korte aanloopperiode ongeveer lineair toe te nemen met de logaritme van de tijd.

Een zuur caseïnegel bestaat uit een inhomogeen ruimtelijk netwerk van caseïnedeeftjes. Deze deeltjes, die uit duizenden caseïnemoleculen kunnen bestaan, hebben ongeveer dezelfde diameter (80-300 nm) als de caseïnedeeftjes in de originele ondermelk ("caseïnemicellen"), maar de inwendige structuur van de deeltjes is anders. Het caseïnegel bestaat uit gebieden met een hoge dichtheid aan caseïnedeeftjes, afgewisseld met relatief grote poriën. De eerstgenoemde gebieden zijn weer opgebouwd uit conglomeraten en strengen van geaggregeerde deeltjes, met daartussen relatief kleine poriën.

De permeabiliteit van de gellen is vooral afhankelijk van het aantal en de diameter van de grote poriën, terwijl de reologische eigenschappen (hoofdstuk 4) afhankelijk zijn van het karakter (sterkte en levensduur) en het effectieve aantal bindingen in het gelnetwerk. Het effectieve aantal bindingen wordt bepaald door (a) het aantal bindingen tussen twee met elkaar in aanraking zijnde deeltjes en (b) door het aantal deeltjes dat onder spanning komt te staan als het gel wordt vervormd, m.a.w. het aantal deeltjes dat effectief aan de "sterkte" van het netwerk bijdraagt. Door de onregelmatigheid van het netwerk zal dit laatste aantal slechts een gering deel van het totale aantal deeltjes zijn. De mate van onregelmatigheid is dus een belangrijke factor in de sterkte van het netwerk. Uit metingen onder variabele omstandigheden, zoals vormings- en meettemperatuur, pH, ionsterkte en ion-samenstelling, bleek dat meerdere soorten interactiekrachten in en tussen de caseïnedeeftjes werkzaam zijn. Hydrofobe bindingen en electrostatische interacties (zoutbruggen) spelen in ieder geval een belangrijke rol. De interne structuur van de deeltjes lijkt in hoofdzaak het karakter en het aantal bindingen tussen

naburige deeltjes te bepalen, waarbij bovengenoemde interactiekrachten, Van der Waals-attractie, sterische interacties (o.m. via de conformatie van de caseïnemoleculen) en mogelijk waterstofbruggen een rol zullen spelen. Een kleine verschuiving in het evenwicht tussen deze krachten kan daardoor een groot effect op de structuur van de deeltjes en daarmee op de reologische eigenschappen van het gelnetwerk hebben.

Een aanzienlijk deel van de bindingen heeft een relaxatietijd in de orde van 0,6 tot 6000 s. Ter karakterisering van de bindingen is de verliestangens  $\tan \delta$  ( $=G''/G'$ ) een geschikte parameter, omdat deze vrijwel onafhankelijk is van het effectieve aantal bindingen. In de tijdschaal van 0,6 tot 60 s is  $\tan \delta$  voor alle zure caseïnegelen gelijk en is evenmin afhankelijk van de temperatuur ( $0^\circ\text{C} < T < 50^\circ\text{C}$ ). In de tijdschaal van 60 tot 6000 s is  $\tan \delta$  (en dus het visceuze karakter) groter bij lagere meettemperatuur. Blijkbaar worden bij lagere temperatuur relatief veel bindingen gevormd met een relaxatietijd in de orde van  $10^3$  s, want beide dynamische moduli zijn dan groter.

Hoewel zure caseïnegelen bij langere tijdschaal een meer visceus karakter krijgen, bleken ze toch bij tijdschalen van  $10^4$  s en langer nog steeds duidelijke elastische eigenschappen te hebben. Dit bleek uit metingen van de schijnbare spanningsrelaxatiemodulus bij langdurige vervorming; hoewel veel bindingen relaxeerden in  $10^3$  tot  $10^5$  s, bleek dat een wezenlijk aantal zelfs een nog langere levensduur heeft. Het verloop van de relaxatiemodulus bleek in overeenstemming met het relaxatiespectrum, zoals dat uit de dynamische moduli berekend kan worden.

Wanneer na aanzuren stremsel aan koude ondermelk wordt toegevoegd (hoofdstuk 5), kunnen caseïnegelen gemaakt worden over een veel breder pH- en temperatuurgebied. Het glycomacropptide, d.i. het deel van de  $\kappa$ -caseïne dat door stremsel wordt afgesplitst, bleek bij pH=4,6 nog een belangrijke bijdrage aan de stabiliteit van de caseïnedeeftjes tegen vlokking te leveren. Rond pH=5,2 treedt een scherpe overgang op in de reologische eigenschappen van de aldus bereide gelen. Beneden deze pH hebben de met stremsel en zuur bereide gelen hetzelfde karakter als alle andere zure gelen, terwijl ze boven deze pH globaal het karakter hebben van gelen met stremsel bij de pH van melk gemaakt. Er bleek een goede

correlatie te zijn tussen  $\tan \delta$  en het optreden van microsinerese.

In hoofdstuk 6 wordt de spin-spin relaxatietijd ( $T_2$ ) van waterprotonen in caseïne-oplossingen als functie van pH en temperatuur besproken. De resultaten bevestigen de sterke verandering in de interne structuur van de caseïnedeeltes t.g.v. aanzuren. De gemeten  $T_2$  is vrijwel uitsluitend afhankelijk van de interactie van de watermoleculen met de caseïnemoleculen in de caseïnedeeltes.

De belangrijkste resultaten en conclusies zijn samengevat en aan een discussie onderworpen in hoofdstuk 7.

## CURRICULUM VITAE

Op 9 maart 1956 aanschouwde Bas Roefs het eerste levenslicht op de ouderlijke boerderij in het Brabantse Erp. Aldaar bezocht hij de R.K. lagere jongensschool St. Josef. In de periode 1968-1974 doorliep hij het gymnasium- $\beta$  aan het College van het H. Kruis te Uden. Aansluitend begon hij zijn studie aan de Landbouwhogeschool te Wageningen in de studierichting Moleculaire Wetenschappen. In april 1982 slaagde hij met lof voor het doctoraalexamen, met als hoofdvakken Kolloïdchemie en Moleculaire Fysica, en als bijvakken Bodemscheikunde en Wiskunde. De praktijktijd bracht hij door aan de Ruhruniversität te Bochum (BRD) in de periode mei-oktober 1980.

Per 1 februari 1982 trad hij voor een periode van drie jaar in dienst van de Landbouwhogeschool als wetenschappelijk assistent bij de sectie Zuivel en Levensmideleennatuurkunde van de vakgroep Levensmiddelentechnologie. Gedurende deze tijd verrichtte hij het onderzoek waaruit dit proefschrift is voortgekomen.

Sinds 1 juni 1985 is hij werkzaam bij de afdeling winningsprocessen van het Koninklijke/Shell Exploratie en Produktie Laboratorium te Rijswijk (ZH).

## NAWOORD

Een proefschrift schrijven en het verrichten van de vereiste experimentele arbeid is zelden het werk van een enkel persoon. Ook aan het tot stand komen van dit proefschrift hebben vele mensen een praktische dan wel morele bijdrage geleverd. Op deze laatste bladzijde wil ik iedereen daarvoor oprecht bedanken. Enkele mensen wil ik met name noemen.

Allereerst wil ik mijn ouders bedanken, die mij de gelegenheid gaven om te gaan studeren.

Mijn promotor Albert Prins ben ik erkentelijk voor de vrijheid, die hij mij gaf bij de uitvoering van het onderzoek, en voor de prettige samenwerking bij de afronding van het proefschrift. De dagelijkse begeleiding van co-promotor Ton van Vliet is onontbeerlijk geweest voor het welslagen van dit onderzoek. Zelfs op het ziekbed zette Ton de begeleiding voort. De meestal korte, maar zeer nuttige discussies met Pieter Walstra zullen mij nog lang heugen. De morele en experimentele ondersteuning van Aliza de Groot-Mostert laten zich niet in één zin beschrijven.

In het kader van hun doctoraalonderzoek hebben Frans den Ouden, Frans Durland, Harry Habets, Jan Olde Heuvel, Eric Timmermans, Jenneke Netjes, Martin Warmerdam en Jan Kuil een aanzienlijke bijdrage geleverd.

Het bereidwillig ter beschikking stellen van de NMR apparatuur door de vakgroep Moleculaire Fysica en de hulp van Henk van As bij de interpretatie van de NMR metingen zijn zeer op prijs gesteld.

De elektronenmicroscopische foto's zijn tot stand gekomen met de hulp van El Bouw, Herman Elerie en Bram Broekstein van de afdeling Elektronenmicroscopie van de TFDL.

Aan de vormgeving van het proefschrift is bijgedragen door dhr. C. Rijpma van de tekenkamer, dhr. A. van Baaren en W. van Hof van de afdeling fotografie van het Biotechnion en door mevr. R. Treffers van de afdeling tekstverwerking van de Landbouwhogeschool.

David Horne van het "Hannah Research Institute" te Ayr in Schotland corrigeerde de Engelse tekst op werkelijk voortreffelijke wijze.

Zonder de Brabantse gastvrijheid van Jeanne en Harrie van den Bijgaart zou het veel moeilijker zijn geweest om de afronding van het proefschrift te combineren met een nieuwe baan elders in den lande.

Aan de collega's en doctoraalstudenten van de sectie Zuivel en Levensmiddelen natuurkunde heb ik goede herinneringen vanwege de gezellige sfeer en de goede onderlinge contacten.

En tenslotte een woord van dank aan alle vrienden, vriendinnen en familieleden in Wageningen en in Brabant, wier namen ik hier niet hoef te noemen, maar die ieder voor zich weten hoezeer ik hun betrokkenheid bij dit proefschrift waardeer.